

University of Warwick institutional repository: <http://go.warwick.ac.uk/wrap>

A Thesis Submitted for the Degree of PhD at the University of Warwick

<http://go.warwick.ac.uk/wrap/48973>

This thesis is made available online and is protected by original copyright.

Please scroll down to view the document itself.

Please refer to the repository record for this item for information to help you to cite it. Our policy information is available from the repository home page.

Regulation of juvenility in
Antirrhinum majus

by

Tiziana Sgamma

PhD Plant and Environmental Sciences

University of Warwick

School of Life Sciences

May 2012

Table of Contents

LIST OF FIGURES	VI
LIST OF TABLES.....	IX
ACKNOWLEDGEMENTS.....	X
DECLARATION.....	XI
SUMMARY.....	XII
ABBREVIATIONS.....	XIII
CHAPTER 1. INTRODUCTION	1
1.1 Post-embryonic phases	1
1.2 Juvenile phase	2
1.3 Measuring juvenility.....	6
1.3.1 Photoperiod responsive plants	6
1.3.2 Measuring juvenility in LDPs.....	7
1.4 <i>Arabidopsis</i> flowering pathways.....	9
1.4.1 Vernalization pathway	9
1.4.2 Autonomous pathway	11
1.4.3 Gibberellins and sucrose pathways	11
1.4.4 Photoperiodic pathway.....	13
1.4.5 microRNA pathway	19
1.5 <i>FT</i> and its antagonists and repressors.....	21
1.6 Conservation of <i>Arabidopsis</i> photoperiodic pathway flowering genes in SDP rice and DNP tomato.....	23
1.7 Conservation of <i>Arabidopsis</i> flowering genes in trees	24
1.8 <i>Antirrhinum</i> and resources.....	26
1.9 <i>Olea europaea</i>	27
1.10 Project aims	30
CHAPTER 2. GENERAL MATERIALS AND METHODS	31
2.1 Plant material.....	31
2.1.1 <i>Antirrhinum majus</i>	31

2.1.2	<i>Arabidopsis thaliana</i>	31
2.1.3	<i>Olea europaea</i>	32
2.2	Software tools	32
2.3	Plant growth conditions	33
2.4	<i>Antirrhinum</i> and <i>Arabidopsis</i> transfer experiments	34
2.5	Genomic DNA extraction from <i>Arabidopsis</i>	36
2.6	RNA isolation and cDNA synthesis	37
2.7	Polymerase Chain Reaction (PCR)	38
2.8	Real-time PCR analysis	39
2.9	Agarose gel electrophoresis	40
2.10	Purification of PCR products from gels	40
2.11	Ligation of PCR products into the pGEM-T Easy vector	41
2.12	Electroporation of vector DNA into <i>E.coli</i> and <i>Agrobacterium</i>	41
2.13	Plasmid DNA purification	42
2.14	DNA sequencing	43
	CHAPTER 3. PHOTOPERIOD TRANSFER EXPERIMENTS	44
3.1	Introduction	44
3.2	Materials and Methods	48
3.2.1	<i>Antirrhinum</i> Transfer experiments.....	48
3.2.2	<i>Antirrhinum</i> apex observation and sampling.....	49
3.2.3	Real-time PCR analysis of <i>CEN</i> and <i>FLO</i> expression.....	50
3.2.4	Leaf harvests for <i>AmFT</i> expression analysis.....	50
3.2.5	Real-time PCR analysis of <i>AmFT</i> expression.....	53
3.2.6	<i>Arabidopsis</i> transfer experiment to establish JP length and <i>AtFT</i> and <i>AtCO</i> expression analyses.....	53
3.3	Results	55
3.3.1	Floral initiation.....	55
3.3.2	Determination of juvenile phase length.....	56
3.3.3	Examination of apex morphology throughout development.....	57
3.3.4	Determination of juvenile phase length.....	59

3.3.5	Investigation of <i>AmFT</i> expression throughout development in <i>Antirrhinum</i>	59
3.3.6	Determination of juvenile phase length	61
3.3.7	Analysis of <i>FLO</i> and <i>CEN</i> expression during development	62
3.3.8	<i>AmFT</i> expression during different photoperiods.....	65
3.3.9	Analysis of <i>AtCO</i> expression in <i>Arabidopsis</i>	67
3.4	Discussion	71
CHAPTER 4. ISOLATION AND CHARACTERIZATION OF		
<i>ANTIRRHINUM</i> AND OLIVE TEMPRANILLO ORTHOLOGS.....		75
4.1	Introduction.....	75
4.1.1	Olive.....	79
4.2	Materials and Methods.....	81
4.2.1	<i>Antirrhinum</i> leaf samples	81
4.2.2	Olive leaf samples.....	81
4.2.3	<i>Arabidopsis</i> leaf samples	81
4.2.4	Isolation of a partial <i>TEM</i> like cDNA sequences from <i>Antirrhinum</i> and Olive	82
4.2.5	Acquisition of full length cDNAs representing <i>AmTEM</i> , <i>OeTEM</i> and <i>AtTEM1</i>	87
4.2.6	Amino acid sequence comparisons and phylogenetic analysis	87
4.2.7	Cloning of full length cDNAs into the Gateway binary vector for <i>Agrobacterium</i> -mediated transformation of <i>Arabidopsis</i>	87
4.2.8	Preparation and Transformation of competent <i>Agrobacterium</i> cells	89
4.2.9	<i>Agrobacterium</i> mediated plant transformation of <i>Arabidopsis</i> with <i>AmTEM</i> , <i>AtTEM1</i> and <i>OeTEM</i>	90
4.2.10	PCR screening of transformed plants.....	91
4.2.11	Semi-quantitative PCR.....	91
4.3	Results	93
4.3.1	Screening of RAV sequences.....	93
4.3.2	Acquisition of a full length cDNA representing <i>AmTEM</i>	95
4.3.3	Preliminary analysis of <i>AmTEM</i> expression in juvenile and adult material.....	99
4.3.4	Acquisition of a full length cDNA representing <i>OeTEM</i>	100
4.3.5	Preliminary analysis of <i>OeTEM</i> expression in juvenile and adult material	103

4.3.6	<i>AmTEM</i> and <i>OeTEM</i> phylogenetic analysis.....	104
4.3.7	Acquisition of a full length cDNA representing <i>AtTEM1</i>	105
4.3.8	Functional complementation of the <i>Arabidopsis tem1</i> mutant with <i>AmTEM</i> and <i>OeTEM</i> ...	106
4.4	Discussion	112
CHAPTER 5. <i>AMTEM</i>: ROLE IN JUVENILITY		114
5.1	Introduction.....	114
5.2	Materials and Methods.....	116
5.2.1	Real-time PCR analysis of <i>AmTEM</i> expression.....	116
5.2.2	<i>Arabidopsis</i> transfer experiment	116
5.2.3	Real-time PCR analysis of <i>TEM</i> expression	117
5.3	Results	118
5.3.1	Developmental <i>AmTEM</i> expression during different photoperiods.....	118
5.3.2	Expression of <i>AtFT</i> , <i>AtCO</i> and <i>AtTEM1</i> during development in <i>Arabidopsis</i>	121
5.3.3	<i>AtFT</i> and <i>AtCO</i> expression in <i>TEM</i> mutants	122
5.3.4	Effect of ectopic expression of <i>AmTEM</i> on flowering in the <i>Arabidopsis tem1</i> mutant.....	127
5.3.5	Effect of ectopic expression of <i>AmTEM</i> in the <i>tem1</i> mutant on <i>AtFT</i> and <i>AtCO</i> expression	133
5.3.6	Effect of ectopic expression of <i>AmTEM</i> on juvenile phase length.....	134
5.3.7	Relationship between juvenility and the photoperiodic pathway in <i>tem1</i> plants over-expressing <i>AmTEM</i>	137
5.4	Discussion	139
CHAPTER 6. GENERAL DISCUSSION.....		143
6.1	Discussion	143
6.1.1	Juvenile phase length can be determined in <i>Antirrhinum</i> plants grown in SANYO growth chambers	143
6.1.2	Induction of <i>FT</i> expression linked to end of juvenility	146
6.1.3	<i>TEMPRANILLO</i> , an <i>FT</i> repressor, isolated from <i>Antirrhinum</i> and Olive.....	147
6.1.4	<i>AmTEM</i> and <i>OeTEM</i> regulate flowering time.....	148
6.1.5	<i>TEM</i> regulates JP length through repression of <i>FT</i>	149
6.1.6	How <i>TEM</i> fits into floral initiation pathways.....	151
6.2	Future research	156

6.3 Overall conclusions	161
REFERENCES.....	164
APPENDIX.....	181

LIST OF FIGURES

CHAPTER 1

Figure 1.1 Schematic representation of photoperiod sensitivity determined by reciprocal transfer experiments.....	8
Figure 1.2 Simplified version of the integration of the flowering in <i>Arabidopsis thaliana</i>	9
Figure 1.3 Autonomous and vernalization pathways in <i>Arabidopsis thaliana</i>	10
Figure 1.4 Gibberellins and sucrose pathways in <i>Arabidopsis thaliana</i>	12
Figure 1.5 Photoperiodic pathway in <i>Arabidopsis thaliana</i>	15
Figure 1.6 Simplified representation of the <i>Arabidopsis</i> clock.....	17
Figure 1.7 microRNA pathway in <i>Arabidopsis thaliana</i>	20

CHAPTER 2

Figure 2.1 Schematic representation of the phases of photoperiod sensitivity determined from data obtained from a LD to SD transfer experiment.....	36
Figure 2.2: Map of pGEM®-t Easy transformation vector	41

CHAPTER 3

Figure 3.1 Leaf number during development in Experiment 1.....	55
Figure 3.2 Different phases of photoperiod sensitivity in <i>Antirrhinum</i> in Experiment 1	56
Figure 3.3 Morphological changes at the SAM during development in Experiment 2	58
Figure 3.4 Different phases of photoperiod sensitivity in <i>Antirrhinum</i> in Experiment 2	59
Figure 3.5 Developmental expression of <i>AmFT</i> in leaf material from <i>Antirrhinum</i> plants grown under LD in Experiment 2	60
Figure 3.6 Different phases of photoperiod sensitivity in <i>Antirrhinum</i> in Experiment 3	62
Figure 3.7 Expression of <i>FLO</i> in apex material from plants grown in Experiment 3 under constant LD harvested at ZT15 (A) and constant SD harvested at ZT 7(B).....	63
Figure 3.8 Expression of <i>CEN</i> in apex material from plants grown in Experiment 3 under constant LD harvested at ZT15 (A) and constant SD harvested at ZT 7(B).....	64
Figure 3.9 Relative expression of <i>CEN</i> and <i>FLO</i> throughout development in plants grown under constant LD in Experiment 3	65
Figure 3.10 Developmental expression of <i>AmFT</i> in leaf material from <i>Antirrhinum</i> plants grown under LD at ZT 15 (A) and SD at ZT 7(B) in Experiment 3.....	66
Figure 3.11 Different phases of photoperiod sensitivity in <i>Arabidopsis Col-0</i>	67
Figure 3.12 Developmental expression of <i>AtFT</i> in leaf material from plants grown under LD at ZT 15 (A) and SD at ZT 7(B)	68
Figure 3.13 Developmental expression of <i>AtCO</i> in leaf material from plants grown under LD at ZT 15 (A) and SD at ZT 7(B)	69
Figure 3.14 Developmental expression of <i>AtCO</i> and <i>AtFT</i> at ZT 15 in leaf material from plants grown under LD.....	70

CHAPTER 4

Figure 4.1 Structure of genes belonging to the RAV class I sub-family of the B3 super-family	76
Figure 4.2 Representation of the annealing position of the 10 combinations of degenerate primers used to isolate <i>AmTEM</i> and list of the primers sequences.....	83
Figure 4.3 Map of pDONR 207 vector.....	88
Figure 4.4 Map of the pB2GW7 vector	89

Figure 4.5 Amino acid alignment of 52 RAV and RAV-like protein sequences showing the conserved amino acids WN/RSSQS in the B3 domain.....	93
Figure 4.6 Amino acid alignment of 41 RAV and RAV-like protein sequences showing the conserved APETALA2 (AP2) domain.....	94
Figure 4.7 Phylogenetic analysis of 23 RAV sub-family class I members.	95
Figure 4.8 Gradient PCR products generated using TEM degenerate primers.....	96
Figure 4.9 Amplification of full length <i>AmTEM</i> cDNA.....	97
Figure 4.10 Comparison of protein domain structure in <i>AmTEM</i> , <i>AtTEM1</i> and <i>AmTEM2</i> ...	98
Figure 4.11 Phylogenetic relationship of RAV sub-family class I members	98
Figure 4.12 Amino acid alignment of RAV and RAV-like protein sequences, including <i>AmTEM</i> , showing the conserved amino acids WN/RSSQS in the B3 domain.....	99
Figure 4.13 Semiquantitative analysis of <i>AmTEM</i> and <i>AmFT</i> expression	100
Figure 4.14 Amplification of partial cDNA representing putative <i>OeTEM</i>	101
Figure 4.15 Amplification of full length <i>OeTEM</i>	101
Figure 4.16 Gene structure of <i>OeTEM</i> compared to <i>AtTEM1</i> and <i>AMTEM2</i>	102
Figure 4.17 Amino acid alignment of RAV and RAV-like protein sequences, including <i>OeTEM</i> showing the conserved amino acids WN/RSSQS in the B3 domain.....	103
Figure 4.18 Semi-quantitative analysis of <i>OeTEM</i> expression	104
Figure 4.19 Phylogenetic relationship of RAV members	105
Figure 4.20 Amplification of full length <i>AtTEM1</i>	106
Figure 4.21 Flowering time of Col-0 T ₁ transgenic lines transformed with <i>AtTEM1</i> grown under LD.....	107
Figure 4.22 Flowering time of <i>tem1</i> T ₁ transgenic lines transformed with <i>AmTEM</i> grown under SD	109
Figure 4.23 Phenotype in T ₁ generation	110
Figure 4.24 Flowering time of Col-0 and <i>tem1</i> T ₁ transgenic lines transformed with <i>OeTEM</i> grown under LD.....	111
CHAPTER 5	
Figure 5.1 Developmental expression of <i>AmTEM</i> in leaf material from <i>Antirrhinum</i> plants grown under LD at ZT 15 (A) and SD at ZT 7(B) in Experiment 3	119
Figure 5.2 Real-time PCR analysis of developmental expression of <i>AmTEM</i> and <i>AmFT</i> in the youngest pair full expanded leaves in <i>Antirrhinum</i> plants grown under LD harvested at ZT 15	120
Figure 5.3 Real-time PCR analysis of developmental expression of <i>AtFT</i> , <i>AtCO</i> and <i>AtTEM1</i> in aerial parts in Col-0 plants grown under LD harvested at ZT 15	122
Figure 5.4 Expression of <i>AtTEM1</i> and <i>AtTEM2</i> in the plant aerial parts under LD at ZT 15 in WT, in <i>tem1</i> and in RNAi- <i>tem1/2</i> between day 1 and day 5 after germination	123
Figure 5.5 Real-time PCR analysis of developmental expression of <i>AtFT</i> , <i>AtTEM1</i> and <i>AtTEM2</i> in aerial parts in WT (A), in <i>tem1</i> (B) and RNAi- <i>tem1/2</i> (C) plants grown under LD harvested at ZT 15	124
Figure 5.6 Real-time PCR analysis of developmental expression of <i>AtCO</i> in aerial parts in Col-0, <i>tem1</i> and RNAi- <i>tem1/2</i> plants grown under LD harvested at ZT 15.....	125
Figure 5.7 Different phases of photoperiod sensitivity in <i>Arabidopsis tem1</i>	126
Figure 5.8 Different phases of photoperiod sensitivity in <i>Arabidopsis</i> RNAi- <i>tem1/2</i>	127

Figure 5.9 Leaves present at flowering time of T ₂ generation plants of three lines (2, 75 and 77) engineered to over-express <i>AmTEM</i> in the <i>tem1</i> mutant	129
Figure 5.10 Phenotype of T ₃ transgenic <i>Arabidopsis tem1</i> plants over-expressing <i>AmTEM</i> and the non-transformed <i>tem1</i> mutant	131
Figure 5.11 Real-time PCR analysis of <i>AmTEM</i> expression in aerial parts of WT, <i>tem1</i> mutant and T ₃ transgenic plants from lines 2, 75 and 77 grown under LD harvested at ZT 1	132
Figure 5.12 Real-time PCR analysis of <i>AtFT</i> developmental expression in the <i>tem1</i> mutant and T ₃ generation <i>AmTEM</i> over-expressing <i>tem1</i> plants representing lines 2, 75 and 77....	133
Figure 5.13 Real-time PCR analysis of <i>AtCO</i> developmental expression in the <i>tem1</i> mutant and T ₃ generation <i>AmTEM</i> over-expressing <i>tem1</i> plants representing lines 2, 75 and 77... ..	134
Figure 5.14 Different phases of photoperiod sensitivity in <i>tem1</i> (A), Line 2(B), Line 75(C) and Line 77(D)	136
Figure 5.15 Real-time PCR analysis of developmental expression of <i>AtFT</i> and <i>AtCO</i> in aerial parts in <i>tem1</i> mutant (A), and T ₃ transgenic plants representing Line 2 (B), Line 75 (C) and Line 77(D) grown under LD harvested at ZT 15	138
CHAPTER 6	
Figure 6.1 Simplified representation of the photoperiodic pathway.....	152
Figure 6.2 Simplified representation of the vernalization pathway.....	153
Figure 6.3 Simplified representation of the Gibberellins pathway	154
Figure 6.4 Simplified representation of the miRNAs pathway.....	155
APPENDIX	
Figure A. 1 Light spectrum in the LD cabinet used in <i>Antirrhinum</i> experiment 1.....	181
Figure A. 2 Light spectrum in the SD cabinet used in <i>Antirrhinum</i> experiment 1	181
Figure A. 3 Light spectrum in the LD cabinet used in <i>Antirrhinum</i> experiment 2 and 3 and <i>Arabidopsis</i> experiments during the first 8 hours of the photoperiod	182
Figure A. 4 Light spectrum in the LD cabinet used in <i>Antirrhinum</i> experiment 2 and 3 and <i>Arabidopsis</i> experiments during the last 8 hours of the photoperiod	182
Figure A. 5 Light spectrum in the SD cabinet used in <i>Antirrhinum</i> experiment 2 and 3 and <i>Arabidopsis</i> experiments	183
Figure A. 6 List of 41 amino acid sequences of RAV and RAV-likes used for sequence homology comparisons.....	188
Figure A. 7 Phylogenetic analysis of 41 RAV sub-family members.....	196
Figure A. 8 Position of the 9 degenerate primers used to isolate <i>AmTEM</i>	197
Figure A. 9 Sequence of <i>Antirrhinum TEMPRANILLO</i> Contig CI.....	198
Figure A. 10 Sequence of <i>Olive TEMPRANILLO</i> isotig13527	198
Figure A. 11 Full nucleotide and amino acid sequences of <i>Antirrhinum TEMPRANILLO (AmTEM)</i>	198
Figure A. 12 Full nucleotide and amino acid sequences of olive <i>TEMPRANILLO (OeTEM)</i> ..	199
Figure A. 13 <i>AmFT</i> nucleotide sequence and <i>TEM</i> putative binding sites.....	199
Figure A. 14. Consensus sequences of CAACA and CACCTG motifs deduced from the frequencies of base occurrence at each position	200
Figure A. 15 <i>AtCO</i> nucleotide sequence and putative <i>TEM</i> putative binding sites.....	200

LIST OF TABLES

CHAPTER 3

Table 3.1 Harvest time and sample nomenclature for samples collected during transfer Experiment 2	52
---	----

CHAPTER 4

Table 4.1 RAV gene family table	76
Table 4.2 Primers used for semi-quantitative analysis of <i>AmELFa</i> , <i>AmFT</i> , <i>AmTEM</i> , <i>OeActin</i> and <i>OeTEM</i> expression	92

APPENDIX

Table A. 1 Primers used in the study	184
Table A. 2 Gene specific Primers used for sequencing.	185
Table A. 3 Primers used for semi-quantitative analysis of <i>AmELFa</i> , <i>AmFT</i> , <i>AmTEM</i> , <i>Oe-Actin</i> and <i>OeTEM</i>	185
Table A. 4 Att-primers used for acquisition of full length <i>AmTEM</i> , <i>OeTEM</i> , <i>AtTEM1</i> cDNA.....	186
Table A. 5 Primers used for RACE.	186
Table A. 6 SOC medium recipe.....	187

ACKNOWLEDGEMENTS

Firstly, I would like to thank Prof. Brian Thomas and Dr. Andrea Massiah, my supervisors, for their continuous support, mentoring and guidance, and especially for their sincerity and patience during my PhD.

I would also like to thank Dr. Steve Jackson for his input during lab meetings and Dr. Aaron Abbot, Jemma Taylor, Dr. Ioannis Matsoukas and Dr. Sarah Thornber for their advice; it has been a pleasure sharing the lab with them.

I am also grateful to Dr. Julie Jones for her assistance with the statistical analysis of data. I greatly appreciate the contribution of our collaborators from Professor Rosario Muleo's group at the Università degli studi della Tuscia for the olive material and advice, and Dr Soraya Pelaz Herrero for the provision of *Arabidopsis thaliana* RNAi-*tem1/2* double mutant seeds.

This work was funded by the University of Warwick through a Postgraduate Research Scholarship (WPRS); I very much appreciate the great opportunity that this provided.

A big thank you to all my aunts and uncles, my little cousins Dario, Valentina, Ilaria and my new and old friends for cheering me up, even from far away. I offer a big kiss to those who saw me start this adventure but did not manage to see the end (Zio Mario and Kafai, I miss you).

Last, but not least, I would like to thank my wonderful, caring and ever-supportive parents, papà Achille e mamma Giulia, who always believe and trust in me, my sisters Stefania and Roberta, always there for me, sharing my life, love, thoughts, fears, joys, tears and laughter and to Dean, for his continuous love and dedication.

“Vi amo”

DECLARATION

The material presented in this study is my own work, unless otherwise stated and has not been submitted for a degree at another university.

SUMMARY

Floral initiation is regulated by an elaborate network of signalling pathways, including the photoperiodic pathway. In *Arabidopsis*, flowering is promoted through this pathway by activation of *FLOWERING LOCUS T (FT)* by CONSTANS (CO) in long days. During juvenility plants are incapable of flowering in response to environmental conditions that would normally be favourable.

This project studies the molecular basis of floral incompetence during juvenility in the model annual species, *Antirrhinum majus* and the important commercial tree species, *Olea europaea*, which has an extended juvenile phase.

Photoperiod transfer experiments were used to measure the length of juvenility in plants grown in controlled environment cabinets at different Daily Light Integrals. Analysis of *Antirrhinum FT (AmFT)* expression during development showed that *AmFT* expression is minimal during juvenility and increases in all leaves following the end of the juvenile phase. The photoperiodic pathway was shown to be active during juvenility, suggesting that an additional mechanism involving the repression of *FT* could be involved in the regulation of juvenility.

Full length *Antirrhinum* and Olive cDNAs representing homologues of the *Arabidopsis FT* repressors *TEMPRANILLO 1 (AtTEM1)* and *AtTEM2*, which act antagonistically with CO, were isolated. Molecular and phylogenetic analyses revealed high amino acid identities between *Antirrhinum* (AmTEM) and Olive (OeTEM) TEM-like proteins and AtTEM1 & 2. AmTEM and OeTEM proteins contain AP2 and B3 domains, consistent with AtTEM1 and AtTEM2, and can be classified as Class I members of the RAV sub-family of B3 transcription factors.

AmTEM and *OeTEM* expression levels were shown to be higher during juvenility suggesting a potential role for *TEM* in controlling juvenility. A reciprocal relationship between expression levels of *AmTEM/AtTEM1* and *AmFT/AtFT* was revealed in both *Antirrhinum* and *Arabidopsis*. Analysis of expression across development showed that *AmTEM/AtTEM1* levels decline at around the time juvenility ends corresponding to when *AmFT/AtFT* levels start to increase.

Arabidopsis tem1 mutants over-expressing *AmTEM*, *OeTEM* or *AtTEM1* exhibited delayed flowering compared to the *tem1* mutant, which demonstrated their role in regulating flowering time. Over-expression of *AmTEM* was shown to increase the length of the juvenile phase, delay the induction of *AtCO* and *AtFT* expression and reduce the overall levels of *AtFT* expression. Conversely, the juvenile phases of *tem1* single and *tem1/2* double mutants were shown to be shorter than in wild-type plants, with the induction of *AtCO* and *AtFT* expression occurring earlier.

These findings are consistent with a role for TEM in regulating juvenility, which occurs through the down-regulation of *FT* and *CO*, and results in the inability to proceed to reproductive growth.

ABBREVIATIONS

%	per cent
<	less than
=	equals
>	greater than
°C	degrees Celsius
<i>ABI3/VPI</i>	<i>ABSCISIC ACID INSENSITIVE 3/VPI</i>
<i>AGL42</i>	<i>AGAMOUS-LIKE 42</i>
<i>AGO1</i>	<i>ARGONAUTE1</i>
<i>AmFT</i>	<i>Antirrhinum majus FT</i>
<i>AmTEM</i>	<i>Antirrhinum majus TEM</i>
<i>API</i>	<i>APETALA1</i>
<i>AP2</i>	<i>APETALA2</i>
<i>ARF</i>	<i>AUXIN RESPONSE FACTOR</i>
<i>AtCO</i>	<i>Arabidopsis thaliana CO</i>
<i>AtFT</i>	<i>Arabidopsis thaliana FT</i>
<i>AtTEM1</i>	<i>Arabidopsis thaliana TEM1</i>
<i>AtTEM2</i>	<i>Arabidopsis thaliana TEM2</i>
<i>AVP</i>	<i>adult vegetative phase</i>
bp	base pairs
<i>bri1</i>	<i>BR-insensitive</i>
BR	brassinosteroid
<i>CCA1</i>	<i>CIRCADIAN CLOCK ASSOCIATED 1</i>
<i>CDF1</i>	<i>CYCLING DOF FACTOR 1</i>
CEN	<i>CENTRORADIALIS</i>
<i>CETS</i>	<i>CENTRORADIALIS, TERMINAL FLOWER, SELF PRUNING</i>
cm	centimetre
CNR	National Research Council
<i>CO</i>	<i>CONSTANS</i>
Col-0	Columbia
<i>COPI</i>	<i>CONSTITUTIVE PHOTOMORPHOGENIC 1</i>
CRA	Agricultural Research Council
CRY	cryptochrome
DA	Dolce Agogia
<i>det2</i>	<i>BR-deficient</i>
DLI	daily light integral
DNA	deoxyribonucleic acid
DNPs	day-neutral plants
dNTP	deoxyribonucleotide triphosphate
dsRNA	double-stranded RNA
<i>EBS</i>	<i>EARLY BOLTING IN SHORT DAYS</i>
EDTA	ethylenediaminetetraacetic acid

<i>EF1α</i>	<i>ELONGATION FACTOR 1 ALPHA</i>
<i>FD</i>	<i>FLOWERING LOCUS D</i>
<i>FKF1</i>	<i>FLAVIN-BINDING, KELCH REPEATED</i>
<i>FLC</i>	<i>FLOWERING LOCUS</i>
<i>FLK</i>	<i>FLOWERING LOCUS K</i>
<i>FLO</i>	<i>FLORICAULA</i>
<i>FRI</i>	<i>FRIGIDA</i>
<i>FT</i>	<i>FLOWERING LOCUS T</i>
<i>FUL</i>	<i>FRUITFUL</i>
g	grams
g	relative centrifuge force
GA	gibberellins
GENT	gentamicin
<i>GI</i>	<i>GIGANTEA</i>
HD1	<i>HEADING-DATE1</i>
<i>HD3a</i>	<i>HEADING-DATE 3a</i>
<i>HSI</i>	<i>HIGH-LEVEL EXPRESSION OF SUGAR-INDUCIBLE GENE</i>
<i>HST</i>	<i>HASTY</i>
<i>HYL1</i>	<i>HYPONASTIC LEAVES1</i>
IGA	Institute of Applied Genomics
IPTG	isopropyl/-D- thiogalactoside
<i>JAT</i>	<i>JUVENILE-TO-ADULT-TRANSITION</i>
JP	juvenile phase
LAV	LEAFY COTYLEDON2/ABSCISIC ACID INSENSITIVE3 and HSI/VAL
LB	Luria-Bertani
LD	long days
LDPs	long-day plants
Le	Leccino
<i>LFY</i>	<i>LEAFY</i>
<i>LHY</i>	<i>LATE ELONGATE HYPOCOTIL</i>
M	Molar
MgSO ₄	magnesium sulphate
min	minutes
miR156	microRNA156
miR159	microRNA159
miR172	microRNA172
miRNAs	microRNA
mM	milimolar
NaCl	sodium chloride
NaOH	sodium hydroxide
<i>OeTEM</i>	<i>Olea europaea TEM</i>
OLEA	Olea europaea Advances
PEBP	phosphatidylethanolamine binding protein

<i>PHY</i>	phytochrome
pri-miRNAs	primary transcripts microRNA
<i>PRR</i>	<i>PSEUDO RESPONSE REGULATORS</i>
RACE	Rapid Amplification of cDNA Ends
<i>RAV</i>	<i>RELATED TO ABI3/VP1</i>
<i>REF6</i>	<i>RELATIVE OF EARLY FLOWERING 6</i>
REM	REPRODUCTIVE MERISTEM
RH	relative humidity
RIF	rifampicin
RNA	ribonucleic acid
RNAi	RNA interference
RP	reproductive phase
rpm	revolutions per minute
s	seconds
SAM	shoot apical meristem
SD	short days
SDPs	short-day plants
SDS	sodium dodecyl sulphate
<i>SE</i>	<i>SERRATE</i>
<i>SEP3</i>	<i>SEPALLATA3</i>
<i>SFT</i>	<i>SINGLE FLOWER TRUSS</i>
<i>SMZ</i>	<i>SCHLAFMÜTZE</i>
<i>SNZ</i>	<i>SCHNARCHZAPFEN</i>
<i>SOC1</i>	<i>SUPPRESSOR OF OVEREXPRESSION OF CO1</i>
<i>SP</i>	<i>SELF PRUNING</i>
SPEC	spectinomycin
<i>SPL</i>	<i>SQUAMOSA PROMOTER BINDING PROTEIN LIKE</i>
<i>SQN</i>	<i>SQUINT</i>
<i>TEM1</i>	<i>TEMPRANILLO 1</i>
<i>TEM2</i>	<i>TEMPRANILLO 2</i>
<i>TFL1</i>	<i>TERMINAL FLOWER 1</i>
<i>TFL2</i>	<i>TERMINAL FLOWER 2</i>
<i>TOC1</i>	<i>TIMING OF CAB EXPRESSION 1</i>
<i>TOE1</i>	<i>TARGET OF EAT</i>
<i>TSF</i>	<i>TWIN SISTER OF FT</i>
v/v	volume by volume
<i>VIN</i>	<i>VERNALIZATION INSENSITIVE</i>
<i>VP1</i>	<i>VIVIPAROUS</i>
w/v	weight by volume
WT	wild-type
X-Gal	5-bromo-4-chloro-3-indolyl-beta-D-galactopyranoside
<i>ZIP</i>	<i>ZIPPY</i>
ZT	zeitgeber time
<i>ZTL</i>	<i>ZEITLUPE</i>

μg	micrograms
μl	microlitres
μM	micromolar

CHAPTER 1. INTRODUCTION

Several developmental processes in plants are coordinated by seasonal changes. One of the most important of these is the transition from vegetative growth to flowering. Many angiosperms flower at about the same time every year, despite the fact that they may have started growing at different times. In seasonal regulation of flowering, the shift to a reproductive phase of growth occurs as a response to changes in day-length and temperature. Plants are not sensitive to inductive conditions throughout the course of their post-embryonic development. This study aims to investigate why, identifying genes involved in the shift between vegetative and reproductive phases, that could be used for developing strategies for modify flowering behaviour. This chapter will introduce the necessary background material and review current literature on plant juvenility and flowering pathways, beginning with the three phases of development that plants go through after germination.

1.1 Post-embryonic phases

During post-embryonic development, the shoot meristem passes through three stages: the juvenile phase (JP), in which flowering is absent even when the plant is exposed to inductive conditions, the adult vegetative phase (AVP), in which reproductive competency is established and the plant can respond to inductive conditions, and finally the adult reproductive phase (RP), where the plant is

committed to flower even in non-inductive conditions (Poethig, 2003). The transition from one phase to another is called phase change.

The ability to predict crop development and define the length of each phase is important from both economic and agronomic points of view. Decisions related to the timing of pesticide application or synchronizing flowering of cross-pollinated crops for hybrid seed production are highly influenced by a plant's phase of development (Ritchie, 1993). Also, in woody plants, where the juvenile phase can last many years, this has great economic impact (Hackett, 1985; Meilan, 1997; Robinson and Wareing, 1969). Fruit tree breeders have to wait until the end of juvenility to evaluate fruit quality (Hatsuda *et al.*, 2011; Suarez *et al.*, 2011).

1.2 Juvenile phase

Juvenility has been mostly studied in herbaceous species where it can last for a relatively short time. However, JP length can vary enormously from plant to plant and it can be dramatically extended in woody species, varying from 1 to 20 or more years (Corbesier and Coupland, 2005; Flachowsky *et al.*, 2009; Hackett, 1985; Meilan, 1997; Moreno-Alias *et al.*, 2010; Robinson and Wareing, 1969). In commercial horticulture, being able to determine the length and the timing of the JP is important for meeting market demand. The economic importance of some trees makes it important to have a deeper understanding of the processes involved in the switch from the JP to the AVP (Poethig, 2010; Tan and Swain, 2006). Understanding developmental pathways in woody plants could enable manipulation of the length of juvenility to prevent flowering in trees where wood quality can be

affected by this process; on the other hand being able to shorten juvenility could make the breeding processes and the test of desirable traits easier (Brunner and Nilsson, 2004; Hanke *et al.*, 2007). Studies in *Arabidopsis* have provided information on the main molecular mechanisms involved in vegetative phase change (Poethig, 2010). The JP, measured as difference in trichome distribution on leaves between the JP and the AVP, can be influenced by a wide range of factors like photoperiod, temperature, irradiance and plant hormones (Araki, 2001).

A large number of physiological markers that characterise juvenility have been identified in different species. These features, which include leaf characteristics, leaf arrangement, internode elongation, crown architecture, and rooting ability are not totally reliable, since they are usually species-specific, differ between herbaceous and woody plants and are affected by different factors such as water availability, temperature, photoperiod, light quality and intensity (Brunner and Nilsson, 2004; Kerstetter and Poethig, 1998; Poethig, 2003). In *Arabidopsis*, the main physiological differences between JP and AVP are in leaf morphology. Adult leaves show serrations on their margins, have a more complex venation and have trichomes on the leaf adaxial and abaxial surfaces which are absent on juvenile leaves (Araki, 2001; Chien and Sussex, 1996; Telfer *et al.*, 1997). In olive plants (*Olea europaea* L.), leaf shape and size and internode length can be used as markers to distinguish juvenile from mature plants, but these features may vary between cultivars or due to solar exposure (Garcia *et al.*, 2000; Gucci and Cantini, 2000). Floral incompetence is the most robust physiological marker for the end of juvenility (Poethig, 2003).

A number of biochemical changes are associated with the transition between the JP and AVP. The level of various phytohormones such as auxin, gibberellins,

cytokinin, ethylene, abscisic acid, and brassinosteroids change throughout plant development but they also respond to external stimuli like light and temperature (Chory and Li, 1997).

The molecular mechanisms behind the change between juvenile-to-adult phases are not very clear at present; epigenetic mechanisms like chromatin-mediated control of gene expression could be a key factor involved (Brunner and Nilsson, 2004; Sung, *et al.*, 2003). In *Arabidopsis*, genes like *HASTY* (*HST*), *SERRATE* (*SE*), *ZIPPY* (*ZIP*) and *SQUINT* (*SQN*) are responsible for negatively regulating the transition from vegetative to adult phases (Berardini *et al.*, 2001; Clarke *et al.*, 1999; Hunter *et al.*, 2003; Telfer and Poethig, 1998). The *hst*, *se*, *zip* and *sqn* mutants exhibit adult traits such as accelerated production of abaxial trichomes, complex venation systems and greater serration earlier than wild-type (WT) plants (Berardini *et al.*, 2001; Clarke *et al.*, 1999; Hunter *et al.*, 2003; Telfer and Poethig, 1998). Studies have revealed a link between vegetative phase change genes and RNA silencing pathways (Baurle and Dean, 2006). *SE* is required for the production of a microRNA (miRNAs) starting from longer primary transcripts (pre-miRNAs) and in *se* mutants the reduction of mature miRNAs is responsible for a wide range of morphological imperfections (Dong *et al.*, 2008; Lobbes *et al.*, 2006; Yang *et al.*, 2006). miRNAs are non-coding 21–23 nucleotide-long RNAs, which take part in post-transcriptional regulation of protein through the RNA interference pathway (Bartel and Bartel, 2003). Studies of *sqn* mutants showed that *SQN* is not required for modulating microRNA156 (miR156) levels but it is responsible for miR156 activity, probably by promoting the activity of ARGONAUTE1 (AGO1), a protein responsible for miRNA-directed post-transcriptional silencing in *Arabidopsis* (Smith *et al.*, 2009). Recently, HYPONASTIC LEAVES1 (HYL1), a

nuclear double-stranded RNA (dsRNA)-binding protein required for normal leaf development in *Arabidopsis*, has been shown to be responsible for the accumulation of miR156 in primary leaves and *hyl1* mutants exhibit adult traits in the leaves and vegetative-to-adult transition earlier compared with the WT plants (Li *et al.*, 2012).

In *Arabidopsis*, miRNAs have been shown to play a crucial role in the juvenile-to-adult switch and they are considered a molecular marker for the process (Poethig, 2010). In particular, miR156 has been shown to be extremely important in maintaining juvenility (Wu *et al.*, 2009). Loss of miR156 activity eliminates juvenile traits, which are enhanced if miR156 activity is constitutive (Poethig, 2010). miR156 coordinates the different pathways that control the changes in a number of phase-specific traits such as production of adventitious roots and branches, leaf morphology, flowering time and inflorescence architecture (Poethig, 2010; Wu *et al.*, 2009). Recently, it was shown that miR156 expression is regulated by a factor produced in the leaf primordium and that defoliation increases miR156 expression and delays phase change in both maize and *Nicotiana benthamiana* (Yang *et al.*, 2011). miR156 targets members of the SQUAMOSA PROMOTER BINDING PROTEIN LIKE (SPL) family (Aukerman and Sakai, 2003; Jung *et al.*, 2007; Zhu and Helliwell, 2011). Early in plant development, high levels of miR156 inhibit the production of SPL proteins (Yang *et al.*, 2011). In *Arabidopsis*, high levels of SPL promote juvenile-to-adult phase change by activating the transcription of *SUPPRESSOR OF OVEREXPRESSION OF CO1* (*SOC1*), *LEAFY* (*LFY*), *APETALAI* (*API*) and *FRUITFUL* (*FUL*) and microRNA172 (miR172) (Jarillo and Pineiro, 2011).

Recently, in olive plants, where the juvenile phase can last for 5-6 years (Moreno-Alias *et al.*, 2010), miR156 has been characterised and shown to play a

role in regulating gene expression in JP targeting SPL genes (Donaire *et al.*, 2011). Investigation of vegetative phase transition in olive plants showed different protein content in juvenile and adult plants (Garcia *et al.*, 2000). However, within the same plant, significant differences between juvenile and adult tissues were not evident (Garcia *et al.*, 2000). In olive the *JUVENILE-TO-ADULT-TRANSITION (JAT)* gene has been isolated and studied (Fernández-Ocaña *et al.*, 2010). *JAT* is expressed at a higher level in juvenile tissue than in adult tissue. *JAT* transcripts accumulate mainly in the roots, with lower expression in the leaves and shoot apical meristem. Differences in *JAT* expression level in adult and juvenile branches of the same tree were shown not to be due to their distance from the roots but, instead, to the different developmental stage. In olive plants with a delayed juvenile-adult transition, *JAT* expression levels are lower. This means that higher levels of *JAT* may be required for the juvenile to adult phase transition (Fernández-Ocaña *et al.*, 2010).

1.3 Measuring juvenility

1.3.1 *Photoperiod responsive plants*

Plants can follow the time of the year tracking the day-night length within a 24 hour cycle or photoperiod. On the basis of photoperiod response, plants are considered as obligate short-day plants (SDPs) if they flower only under short days or facultative SDPs if their flowering is accelerated by short days (SD) (Thomas and Vince-Prue, 1997). Obligate long-day plants (LDPs) flower only during long days (LD) whilst facultative LDPs have accelerated flowering during LD (Thomas

and Vince-Prue, 1997). Species that flower irrespective of photoperiod are referred to as day-neutral plants (DNPs) (Thomas and Vince-Prue, 1997). Some plants are not classified in any of the previous categories because they respond to combinations of day lengths (Thomas and Vince-Prue, 1997).

1.3.2 *Measuring juvenility in LDPs*

Plants are not sensitive to photoperiod throughout their entire life time. The photoperiod-sensitive, AVP, is sandwiched between two photoperiod-insensitive phases namely the JP and the RP (Thomas and Vince-Prue, 1997). Expanding the idea of Ellis *et al.* (1992) and Adams (1999), Adams *et al.* (2003) devised a model in *Antirrhinum*, utilising reciprocal transfer experiments to establish the length of these phases. Previous studies used flowering time to estimate the photoperiod sensitive phase, whereas Adams *et al.* (2003) introduced the use of leaf number data as well. The length of different phases of photoperiod sensitivity can be assessed by transferring plants from inductive (LD) to non-inductive (SD) conditions, and *vice versa*, at regular intervals following germination and recording and utilising the flowering times of individual plants (Adams, 1999; Adams *et al.*, 2003; Munir *et al.*, 2010). Flowering time can be recorded as the number of days from germination at first open flower and/or the number of leaves below the first open flower, since no more leaves are formed on the main stem once flower initiation starts. These data are used to generate modelled curves (Figure 1.1) (Adams *et al.*, 2003). Flowering times will be similar between plants transferred from LD to SD before the end of the juvenile phase and plants grown under continuous SD. Flowering times will not be delayed in plants transferred after the end of juvenility due to

experiencing inductive LD whilst adult (Adams *et al.*, 2001; Munir *et al.*, 2010). Plants transferred from LD to SD conditions during the photoperiod sensitive phase show an increasing competence to respond to developmental signals according to the time the plants spend in LD conditions after they ended the juvenile phase (Adams *et al.*, 2003).

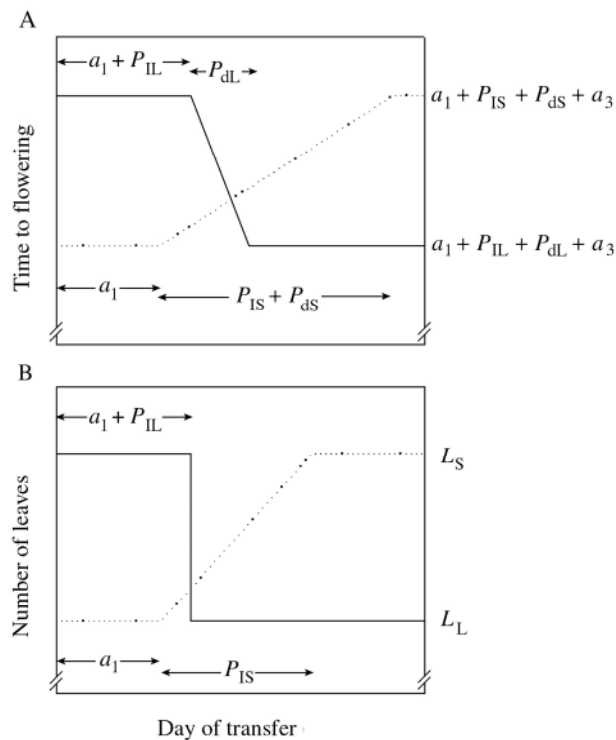


Figure 1.1 Schematic representation of photoperiod sensitivity determined by reciprocal transfer experiments.

Flowering time data expressed as (A) flowering time from seedling emergence and (B) the number of leaves present on the main stem below the inflorescence for LDPs transferred from LD to SD (continuous line) and from SD to LD conditions (broken line) at various times from seedling to emergence. Throughout post embryonic development plants go through a photoperiod-insensitive juvenile phase (a_1), followed by photoperiod-sensitive flower induction and development phases in LD (P_{IL} and P_{dL} , respectively) or SD (P_{IS} and P_{dS} , respectively). The final phase of flower development corresponds to the photoperiod-insensitive flower development phase (a_3). L_L and L_S represent the number of leaves produced under continuous LD and SD conditions, respectively. Figure adapted from Adams *et al.* (2003).

1.4 *Arabidopsis* flowering pathways

In plants, once adult and floral competence is attained, transition to the reproductive phase is regulated by an elaborate network of signalling pathways that converge at the floral pathway integrators. Using molecular genetic approaches in the LDP *Arabidopsis* many components of these pathways have been identified (Boss *et al.*, 2004) (Figure 1.2).

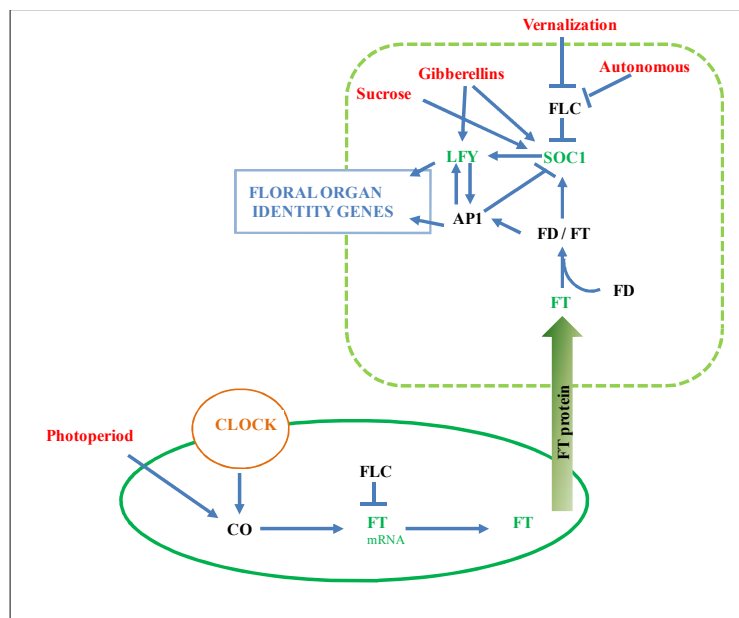


Figure 1.2 Simplified version of the integration of the flowering in *Arabidopsis thaliana*. Schematic representation of the major pathways (in red) regulating flowering time. Arrows indicate activation and T-bars show inhibition. The green oval represents the leaf; the light green square represents the apex. The large green arrow represents FT protein translocation from leaf to apex. Floral pathway integrators are showed in green. The complete nomenclature of the genes can be found in the main text in sections 1.4.1, 1.4.2, 1.4.3, 1.4.4.

1.4.1 Vernalization pathway

To overcome prolonged cold periods, plants adapt their growth habits to ensure reproductive success by flowering after the restrictive weather conditions through vernalization (Kim *et al.*, 2009; Massiah, 2007). In *Arabidopsis* many

isolates require vernalization for early flowering and during vernalization a range of genes show changes in their level of expression (Michaels and Amasino, 2000) (Figure 1.3).

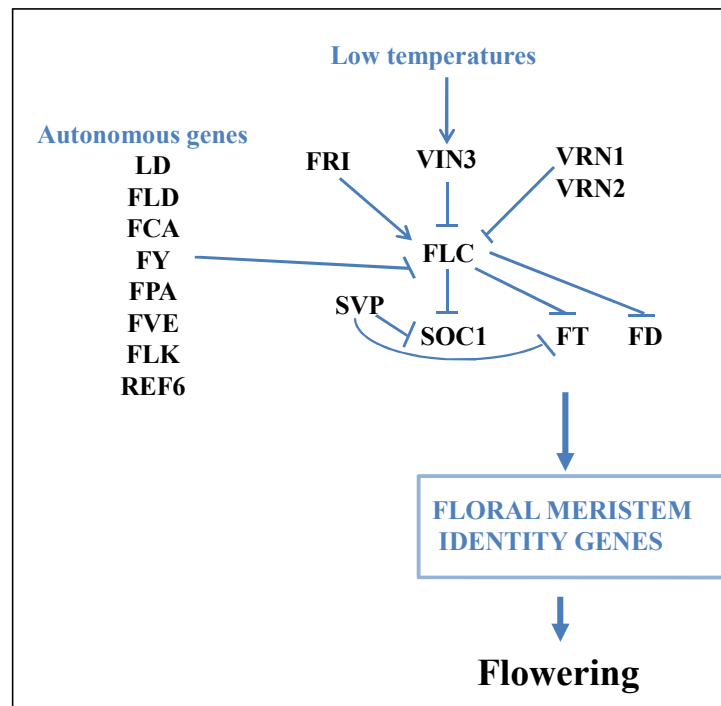


Figure 1.3 *Autonomous and vernalization pathways in Arabidopsis thaliana.* Arrows indicate direct activation and T-bars show inhibition.

FLOWERING LOCUS (FLC), a MADS-box domain transcription factor, is a potent inhibitor of flowering and acts by repressing *FLOWERING LOCUS T (FT)*, *FLOWERING LOCUS D (FD)* and *SOC1* (Boss *et al.*, 2004; Kim *et al.*, 2009; Searle *et al.*, 2006). Plants that have a vernalization requirement have hastened flowering in response to a prolonged period of cold. Cold treatments overcome the up-regulation of *FLC* mRNA by *FRIGIDA (FRI)*, enhance the expression of genes such as *VERNALIZATION INSENSITIVE 3 (VIN3)*, which represses *FLC*, and lead to histone modification of *FLC* chromatin (Boss *et al.*, 2004; Geraldo *et al.*, 2009; Kim *et al.*, 2009; Sung and Amasino, 2004). *FLC* repression is then maintained by

an epigenetic mechanism after the cold treatment by other genes including *VRN1* and *VRN2* (Gendall *et al.*, 2001; Massiah, 2007).

1.4.2 *Autonomous pathway*

Genes classified in the autonomous pathway, *LUMINIDEPENDENS (LD)*, *FLD*, *FCA*, *FY*, *FPA*, *FVE*, *FLOWERING LOCUS K (FLK)* and *RELATIVE OF EARLY FLOWERING 6 (REF6)* suppress *FLC* RNA accumulation independently of environment factors using different mechanisms (Massiah, 2007; Srikanth and Schmid, 2011; Yan *et al.*, 2010) (Figure 1.3).

FCA, *FPA* and *FLK* interact with *FLC* mRNA while *FLD* and *FVE* regulate *FLC* epigenetically, regulating chromatin modification (Simpson, 2004). Some of these genes, such as *FCA* and *FY*, interact to promote *FLC* down-regulation (Simpson *et al.*, 2003). Mutation in the autonomous pathway genes results in *FLC* accumulation and flowering time delay in both LD and SD conditions (Simpson, 2004). The delay in flowering in the autonomous pathway mutants can be overcome if the plants are exposed to cold treatment (Michaels and Amasino, 2001).

1.4.3 *Gibberellins and sucrose pathways*

In 1957, Langridge demonstrated that the administration of exogenous gibberellins (GA) promotes flowering. More recent studies have confirmed this theory using *Arabidopsis* mutants defective in either GA biosynthesis or signalling (Wilson *et al.*, 1992). GAs promote flowering through the indirect activation of *LFY* and *SOC1* expression (Blazquez *et al.*, 1998; Gocal *et al.*, 2001) (Figure 1.4). In

SD, the *gai* mutant, which does not produce the enzyme ent-kaurene synthetase A, shows a reduction in the levels of *LFY* expression and a delay in flowering. The enzyme ent-kaurene synthetase catalyzes the conversion of geranylgeranyl pyrophosphate to copalyl pyrophosphate in the first step of GA biosynthesis (Blazquez *et al.*, 1998; Sun and Kamiya, 1994). In SD, the gibberellin-insensitive *gai-1* mutant shows minimal levels of *SOC1* expression (Moon *et al.*, 2003). It has been proposed that the GA pathway has an additional role in promoting *LFY* expression, also through the up regulation of *SOC1* (Mutasa-Gottgens and Hedden, 2009). In SD, GA indirectly represses microRNA159 (miR159) expression levels through the repression of DELLA proteins. High levels of miR159 cause a reduction of *LFY* expression (Achard *et al.*, 2004). Therefore, in SD, the GA pathway promotes flowering through both *LFY* and *SOC1* expressions.

In the carbohydrate or sucrose pathway, flowering is promoted under SD conditions by induction of *LFY* expression through *SOC1* (Blazquez *et al.*, 1998) (Figure 1.4).

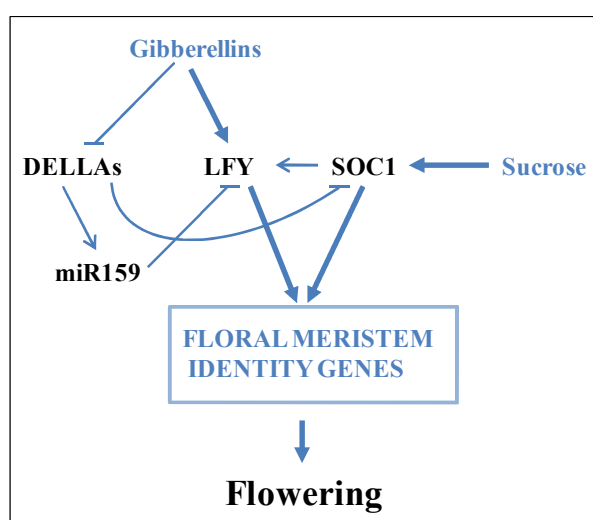


Figure 1.4 Gibberellins and sucrose pathways in *Arabidopsis thaliana*.
The gibberellins pathway and sucrose pathway and their role in flowering through the activation of *LFY* and *SOC1*. Arrows indicate activation and T-bars show inhibition.

1.4.4 *Photoperiodic pathway*

1.4.4.1 The circadian clock and the external/internal coincidence models in plants

Physiological processes within plants fluctuate not only during their development but also during the course of each day. In 1959 Franz Halberg coined the word “circadian” to describe biological phenomena with a frequency of about 24 hours. Circadian processes are present in most eukaryotes and some prokaryotes (Edwards *et al.*, 2010). Environmental stimuli, such as the day/night cycle, can lead to these oscillations (Gardner *et al.*, 2006). Plants are able to anticipate or “remember” periodic changes in the environment due to them having an endogenous circadian clock (Staiger, 2002).

The internal clock continues to run even when conditions are constant and no external cues are present, showing the existence of an internal mechanism. Processes following an endogenous rhythm include stomatal movement, photosynthetic activity and the expression of several genes (Edwards *et al.*, 2010; Millar, 1999). Gene expression can be regulated at the level of transcription, translation and degradation of mRNA (McClung and Gutierrez, 2010; Shu and Lin, 2004).

Several models have been proposed to elucidate how the perception of day length drives developmental responses. The prominent models are the internal and the external coincidence models (Thomas and Vince-Prue, 1997). The external coincidence model proposes that an external signal (light) interacts with the circadian clock to drive a circadian rhythm and the second role of light is to

coincide with a particular phase in the rhythm to drive a periodic response, e.g. flowering. In contrast, the internal coincidence model proposes that the flowering is initiated when two internal rhythms are brought into the same phase under day-lengths that promote flowering. The photoperiodic flowering response in *Arabidopsis* is driven by the external coincidence model as will be shown later.

1.4.4.2 Photoperiodic pathway

The most relevant of the floral pathways for this study is the photoperiodic pathway (Figure 1.5).

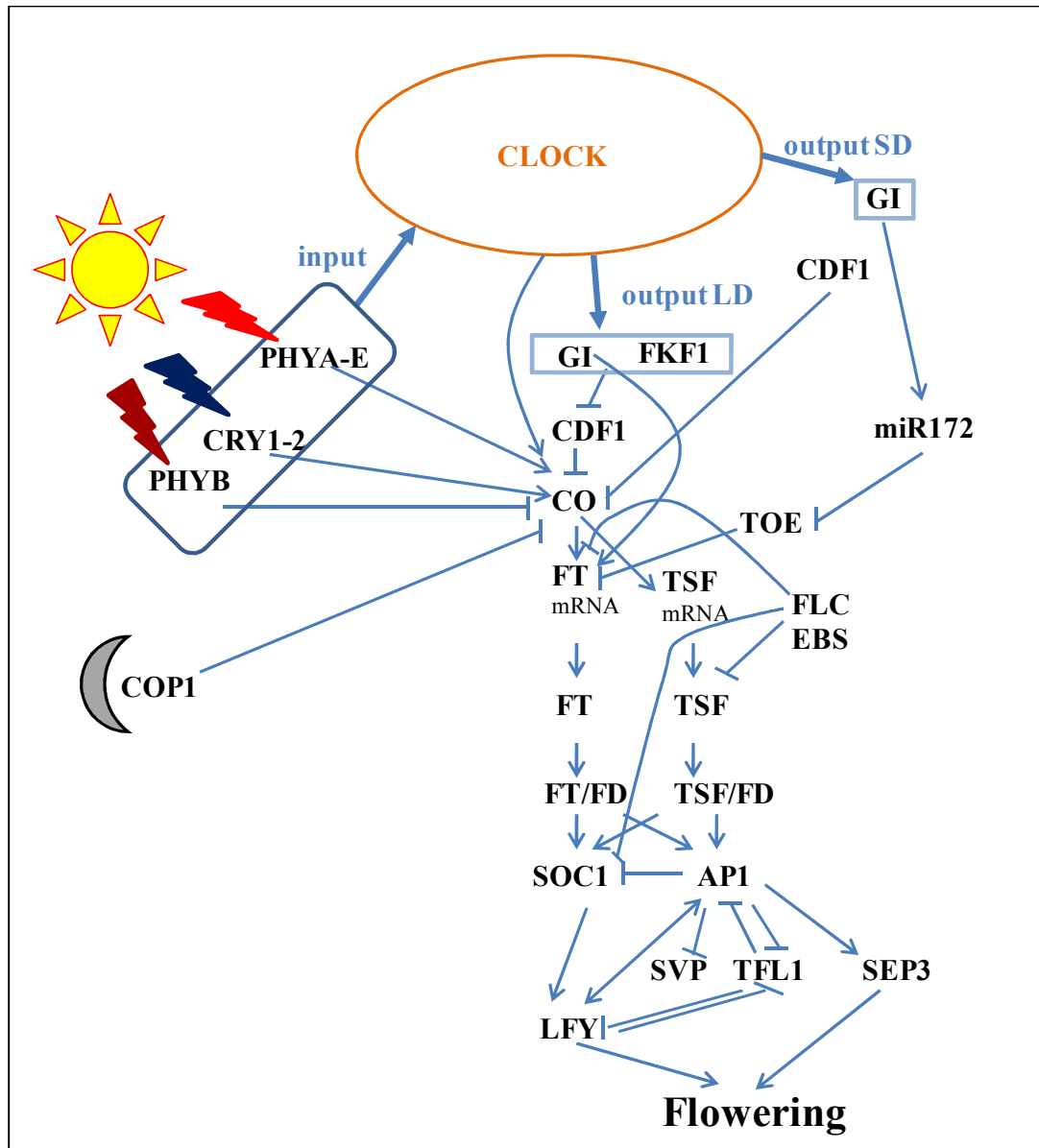


Figure 1.5 Photoperiodic pathway in Arabidopsis thaliana.
Arrows indicate activation and T-bars show inhibition.

This pathway commences in the leaves with the perception of light by the red/far-red light-receptors phytochromes (*PHYA-E*) and the blue/UV-A light-receptors cryptochromes (*CRY1* and *2*) (Clack *et al.*, 1994; Haiyang and Wang, 2002; Lin and Shalitin, 2003; Quail, 2002). Light input to the circadian clock is mediated through these photoreceptors. In plants, the circadian clock regulates a wide range of biological processes and represents the plant's endogenous time keeper (Halliday *et al.*, 2003). A large number of genes have been classified as components of the circadian clock and they show high levels of similarity and functional redundancy (Nakamichi, 2011).

As shown in figure 1.6, TIMING OF CAB EXPRESSION 1 (*TOC1*) is part of the central oscillator and is involved in a negative feedback loop which involves up-regulation of *LATE ELONGATE HYPOCOTIL (LHY)* and *CIRCADIAN CLOCK ASSOCIATED 1 (CCA1)* mRNA expression. In the morning, LHY and CCA1 proteins negatively regulate *TOC1*, binding its promoter (Alabadi *et al.*, 2001). *LHY* and *CCA1* expression decreases during the day allowing *TOC1* expression levels to increase and reactivate indirectly the expression of *LHY* and *CCA1* (de Montaigu *et al.*, 2010). *TOC1* is also negatively regulated at dusk by *ZEITLUPE (ZTL)* which marks *TOC1* protein for proteasome degradation (Mas *et al.*, 2003). In the second loop *PSEUDO RESPONSE REGULATORS 7* and *9 (PRR7* and *PRR9)* repress *LHY* and *CCA1* transcription (de Montaigu *et al.*, 2010). In the third loop *GIGANTEA (GI)* is involved in a negative feedback loop with *TOC1* (Locke *et al.*, 2006). *GI* and *FLAVIN-BINDING, KELCH REPEATED, F-BOX (FKF1)* expression and the complex that they form, are also under clock control (Nakamichi, 2011). In LD, *GI* peaks at 10-12 Zeitgeber (ZT, from German for time giver, in this work the zeitgeber is the light) with *FKF1* and together they form a complex to repress

CYCLING DOF FACTOR 1 (CDF1), which is a repressor of *CONSTANS (CO)*, the first dedicated step of the photoperiodic pathway (Fowler *et al.*, 1999; Paltiel *et al.*, 2006; Sawa *et al.*, 2007). This does not happen in SD because *GI* peaks at 8 ZT, a few hours before *FKF1* and the level of the complex is not high enough to down regulate *CDF1* expression, therefore *CO* remains repressed (Salazar *et al.*, 2009; Sawa *et al.*, 2007). *GI* and *FKF1* have also been shown to promote *CO* expression each by directly binding to its promoter (Mizoguchi *et al.*, 2005; Sawa *et al.*, 2007). In SD, *GI* also regulates *FT* independently of *CO* through regulation of maturation of the non-coding micro miR172 (Jung *et al.*, 2007). miR172 levels increase with the age of the plant and it down-regulates the *FT* repressor *TARGET OF EAT (TOE1)* (Jung *et al.*, 2007).

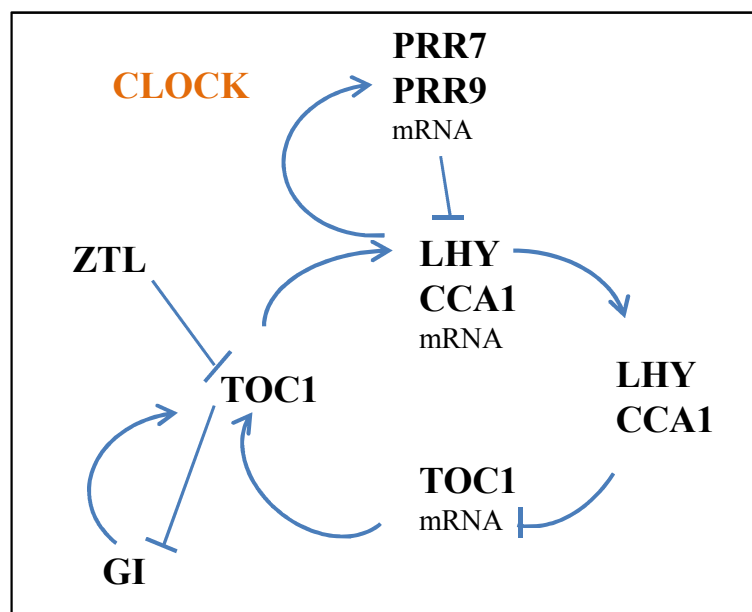


Figure 1.6 Simplified representation of the Arabidopsis clock.
Arrows indicate activation and T-bars show inhibition.

In LD, red light, acting through PHYB, reduces CO abundance during the morning (Valverde *et al.*, 2004). *CO* mRNA peaks at dusk which leads to CO protein accumulation. CO is stabilised by blue and far red light through *PHYA* and *CRY1/2*; the accumulation of CO protein activates the transcription of the floral integrator gene *FT* (Cerdan and Chory, 2003; Samach *et al.*, 2000; Suarez-Lopez *et al.*, 2001; Turck *et al.*, 2008; Valverde *et al.*, 2004). The regulation of *FT* by CO probably occurs through an interaction of CO and the CCAAT-box binding protein factor with the 5' UTR region of *FT* (Ben-Naim *et al.*, 2006). This occurs in long days in LDPs, but not in short days. In SD, *CO* mRNA peaks in the dark and CO protein degradation is facilitated by *CONSTITUTIVE PHOTOMORPHOGENIC 1 (COP1)* (Jang *et al.*, 2008). The accumulation of stable CO protein, in conjunction with light, can be the only limiting factor for flowering which matches the external coincidence model (Turck *et al.*, 2008).

CO is expressed in the phloem companion cells of the leaf where it activates expression of *FT* (An *et al.*, 2004). Studies have confirmed that it is the movement of FT protein through the phloem from the leaf to the apex that leads to flowering though the formation of a complex with FD (Corbesier *et al.*, 2007; Jackson, 2009; Wigge, 2011; Wigge *et al.*, 2005). Earlier study focused on the movement of *FT* mRNA from the leaf to the meristem using a fusion of a promoter from a heat shock inducible gene to *FT*; the publication was later retracted (Bohlenius *et al.*, 2007). Recently, new studies show that *FT* RNA can move and that this movement does not require FT protein. However, it still needs to be proven whether *FT* RNA movement in the phloem has a contribution to the flowering pathway (Li *et al.*, 2009).

FT and its paralog TWIN SISTER OF FT (TSF) are 81.3% identical and they share the capability to communicate long-distance florigenic signal activity (Turck *et al.*, 2008). Expression analyses confirm that, like *FT*, *TSF* responds rapidly to varying levels of *CO* and interacts with FD in the shoot apical meristem (SAM) (Jackson, 2009; Turnbull, 2011; Yamaguchi *et al.*, 2005). *TSF* is repressed by *FLC* and *EARLY BOLTING IN SHORT DAYS (EBS)*. In contrast to *FT*, *TSF* is also expressed in the apical meristem and its contribution to determining flowering time is greater in SD than in LD (Turck *et al.*, 2008; Yamaguchi *et al.*, 2005).

Flowering occurs when the FT/FD or TSF/FD complexes activate *SOC1* and *API*, the flower-meristem-identity genes, which activate the floral organ identity genes (Blazquez *et al.*, 1997). *API* activates *LFY* expression which in turn is also responsible for binding the *API* promoter and controls its expression (Kaufmann *et al.*, 2010). *SEPALLATA3 (SEP3)* expression is up-regulated directly and indirectly by *API* initiating downstream pathways involved in floral organ formation (Kaufmann *et al.*, 2010).

1.4.5 *microRNA pathway*

Recent studies showed miRNAs play important roles in key developmental transitions, which include regulation of flowering (Figure 1.7). miR156 has a role in the juvenile to adult transition and declines over time, as described in section 1.2, but it is also responsible for repressing flowering by down-regulating members of the SPL family in the phloem companion cells (Fornara and Coupland, 2009). SPL3, SPL4 and SPL5 are direct transcriptional activators of the floral promoters *FUL*, *API*, and *LFY* (Yamaguchi *et al.*, 2005), whereas SPL9 promotes the

transcription of the floral promoters *FUL* and *SOC1* (Wang *et al.*, 2009). SPL9 and 10 also regulate flowering by promoting the transcription of miR172 (Wu *et al.*, 2009). miR172 is also up-regulated by *GI* in SD (Jung *et al.*, 2007). miR172 is responsible for repressing the expression of several AP2-like genes, including *TOE1*, *TOE2*, *SCHLAFMÜTZE* (*SMZ*), *SCHNARCHZAPFEN* (*SNZ*) which repress *FT* (Aukerman and Sakai, 2003; Jarillo and Pineiro, 2011; Jung *et al.*, 2007; Zhu and Helliwell, 2011).

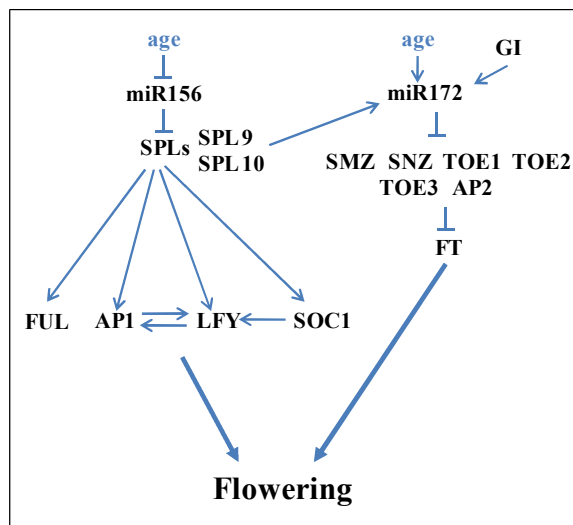


Figure 1.7 microRNA pathway in *Arabidopsis thaliana*.
Arrows indicate activation and T-bars show inhibition.

1.5 *FT* and its antagonists and repressors

FT protein is a component of the CETS family whose members have a role in timing phase change in different species. This family is called CETS because of the first three closely related members, *CENTRORADIALIS* (*CEN*), *TERMINAL FLOWER* (*TFL1*), and *SELF PRUNING* (*SP*), found respectively in *Antirrhinum*, *Arabidopsis* and *Lycopersicon esculentum* (Giakountis and Coupland, 2008; Pnueli *et al.*, 1998). Any gene having a repression role on *FT* can be considered a repressor of flowering.

TFL1 is homologous (defined in this work as genes which share an arbitrary threshold level of similarity, have a common evolutionary origin but may or may not have common activity) to *FT*; they both belong to a multigene family called phosphatidylethanolamine binding proteins (PEBPs) and both play a role in controlling flowering, but act in opposing ways (Figure 1.5) (Ohshima *et al.*, 1997). *TFL1* represses floral meristem identity genes by postponing the change from the vegetative phase to flowering by repressing *LFY* and *API* (Figure 1.5) (Hanzawa *et al.*, 2005; Liljegren *et al.*, 1999). *TFL1* shares 59% identity at the amino acid level with *FT* but the change of a single base can lead to the conversion of *TFL1* function to a floral promoter like *FT* (Hanzawa *et al.*, 2005). *TFL1* has been shown to interact with *FD* and the *TFL1*/*FD* heterodimer antagonizes activation of transcription of floral meristem identity genes by the *FT*/*FD* heterodimer (Figure 1.5) (Giakountis and Coupland, 2008). *TERMINAL FLOWER 2* (*TFL2*) and *EBS*, directly or indirectly reduce *FT* transcription without repressing *CO*. Both *TFL2* and *EBS* repress *FT* by altering its chromatin structure, though a mechanism which is still unclear (Figure 1.5) (Kotake *et al.*, 2003; Pineiro *et al.*, 2003).

In *Arabidopsis*, *FLC* represses flowering through action in both leaves and the shoot apical meristem. In the leaves, *FLC* directly represses *FT* by binding to a putative CArG-box in the first intron of the gene (Helliwell *et al.*, 2006; Searle *et al.*, 2006). In the apex it represses *FD* and *SOC1* (Figure 1.3) (Geraldo *et al.*, 2009; Kim *et al.*, 2009; Michaels and Amasino, 1999; Sheldon *et al.*, 1999).

SVP, a MADS-box domain containing protein, has a role in regulation of flowering in addition to its role in modulating meristem identity. It is strongly expressed in young leaves and in the SAM and weakly expressed in the inflorescence (Fekih *et al.*, 2009). It represses *FT* by binding to the CArG III motif in the *FT* promoter (Figure 1.3) (Fekih *et al.*, 2009; Lee *et al.*, 2007). Its role in the shoot apex during the floral transition is still not clear (Li, D. *et al.*, 2008).

AP2 domain-containing transcription factors are another class of proteins that repress *FT*. These include *AP2*, and the other AP2-like transcription factors such as *TOE1*, *TOE2* and *TOE3*, *SMZ* and *SNZ*, which themselves are down regulated by *API* and *miR172* (Figure 1.7) (Kaufmann *et al.*, 2010; Yant *et al.*, 2009). Defective mutants in these genes present elevated levels of *FT* and the over-expressors show a reduction in *FT* levels. It is still not clear how these proteins repress *FT*. Nevertheless, *CO* does not seem to be involved, since *CO* expression is not influenced by *TOE1* over-expression or in the *toe1* mutant (Jung *et al.*, 2007). Based on this observation, a direct action of AP2-like transcription factors in regulating *FT* has been hypothesised (Yant *et al.*, 2009).

Floral repressors *TEMPRANILLO 1* (*TEM1*) and *TEM2* belong to the RAV (RELATED TO ABI3/VP1) family of transcription factors and contain one AP2 and one B3 binding domain (Castillejo and Pelaz, 2008). They act redundantly to repress *FT*, binding to its 5' untranslated region. Furthermore, the closely

related *RAV* gene, *RAVI*, acts as an inhibitor of growth and development. Hu *et al.* (2004) demonstrated that *Arabidopsis* plants with reduced *RAVI* expression flowered 4.8 days earlier than the WT and 6.6 days earlier than those over-expressing *RAVI*. It is still not clear how this gene regulates plant development.

1.6 Conservation of *Arabidopsis* photoperiodic pathway flowering genes in SDP rice and DNP tomato

Arabidopsis is a facultative long day plant but the photoperiodic pathway is conserved in other flowering plant species although with some differences according to their day-length requirement. In the SDP rice (*Oryza sativa*), the orthologue of *GI* follows a circadian rhythm and promotes the orthologue of *CO* *HEADING-DATE1* (*HDI*) expression in LD. When the *GI* orthologue is over-expressed, this is related with a higher level of *HDI* expression (Hayama *et al.*, 2003). *HDI* follows a circadian rhythm similar to *CO*, peaking at dusk in LD, but it acts as an inhibitor of flowering. *HDI* represses *HEADING-DATE 3a* (*HD3a*), the rice ortholog of the *Arabidopsis* pathway integrator *FT* (Greenup *et al.*, 2009). Expression of *HD3a* is induced in SD and over-expression of *HD3a* promotes flowering (Kojima *et al.*, 2002). In LD, the peak of *HDI* expression coincides with light and PHYB stabilises *HDI* so that it can repress *HD3a*. In SD, *HDI* expression peaks at night, when there is no PHYB to stabilise the protein, and it cannot inhibit *HD3a*, which accumulates in phloem companion cells (Kojima *et al.*, 2002). *HD3a* mRNA then moves to the apical meristem where it promotes flowering (Kojima *et al.*, 2002). Other photoperiodic pathway genes present in *Arabidopsis*, including

CCA1/LHY, *TOC1-like* genes, *ZTL*, *FKF1* and *CDF1* have homologues in rice (Jarillo *et al.*, 2008).

Tomato (*Lycopersicon esculentum*) is a DNP since flowering time is not affected by photoperiod (Lifschitz *et al.*, 2006). Tomato plants show processes that are controlled by the circadian clock, but flowering time is not one of these (Jarillo *et al.*, 2008). Some of the genes responsible for flowering time have been characterized as members of the autonomous pathway (Lozano *et al.*, 2009). *SINGLE FLOWER TRUSS* (*SFT*), the orthologue of *FT* in *Arabidopsis*, plays a similar role in promoting flowering (Lifschitz *et al.*, 2006). *sft* mutants plants show a delay in flowering time and over-expression of this gene in Maryland Mammoth tobacco, which shows a short-day response, in day-neutral tobacco cv. Samsun and in *Arabidopsis* promotes early flowering under non-inductive conditions (Lifschitz *et al.*, 2006). It has been proposed that *SFT* could act as an autonomous pathway gene for flowering regulation (Molinero-Rosales *et al.*, 1999). No evidence of a relationship has been proven to exist with the CO-like genes, which show circadian rhythms but do not promote flowering in tomato (Lozano *et al.*, 2009; Turnbull, 2011).

1.7 Conservation of *Arabidopsis* flowering genes in trees

No many studies have been carried out on woody and fruit trees where the mechanisms involved in the flowering pathways are still not well understood. However, a few studies have demonstrated that the autonomous pathway drives floral initiation in temperate trees while environmental cues drive initiation in

tropical trees as reviewed by Wilkie *et al.* (2008). In trees, after the adult reproductive phase starts, flowering occurs annually, at least in some apical meristems. This suggests that, from a molecular point of view, some mechanisms are shared between annual and perennial plants (Tan and Swain, 2006).

Poplar trees (*Populus trichocarpa*) generally produce the first flowers after 5-10 years (Zhang *et al.*, 2010). Bohlenius *et al.* (2006) isolated *Populus trichocarpa FT* homologue (*PtFT1*), and transgenic *Arabidopsis* plants transformed with *PtFT1* were shown to exhibit early flowering phenotypes (Bohlenius *et al.*, 2006). In poplar, a second *FT* homologue, *PtFT2*, has been isolated. It shares 91% amino acid identity with *PtFT1* (Zhang *et al.*, 2010). *PtFT2* also causes early flowering in transgenic poplar plants when over-expressed (Bohlenius *et al.*, 2006; Hsu *et al.*, 2006). It has been suggested that these genes play a role in phase transition between the JP and AVP and that LD leads to *PtFT1* and *PtFT2* accumulation (Bohlenius *et al.*, 2006).

In apple (*Malus domestica*), juvenility lasts for about 4-8 years (Traenkner *et al.*, 2010). Two apple *CONSTANS-like* genes *MdCOL1* and *MdCOL2* are expressed in leaves (Hattasch *et al.*, 2008; Kotoda *et al.*, 2010; Traenkner *et al.*, 2010). *MdFT1*, *MdCOL1* and *MdCOL2* exhibit circadian expression patterns, peaking at the end of the day (Traenkner *et al.*, 2010). Quantitative analysis of apple *FT-like* genes, *MdFT1* and *MdFT2* show they are differentially expressed in apical buds and reproductive organs. *MdFT1* expression levels are high in apical buds during the adult phase, whereas *MdFT2* expression levels are high in reproductive organs (Kotoda *et al.*, 2010). Furthermore, *MdFT1* expression is low in juvenile seedlings in contrast to *MdFT2* (Kotoda *et al.*, 2010). *MdFT1* was considered to be the gene playing a key role in flowering time regulation, as its mRNA levels were higher in

apical buds in the adult phase than in all the tissue of juvenile seedlings, *MdFT2* was considered to be involved in the development of floral organs. However, both genes, when over-expressed in *Arabidopsis*, led to an earlier flowering phenotype (Kotoda *et al.*, 2010). *MdFT1* expression increases in vegetative meristems before visible morphological changes in the apical meristem while apple *SOCI*-like gene, *MdSOCI* expression levels increase when flower induction is initiated (Hattasch *et al.*, 2008). These results suggest that *MdFT1* could activate *MdSOCI* expression.

1.8 *Antirrhinum* and resources

Antirrhinum majus L., popularly called snapdragon, is native to the Mediterranean region. *Antirrhinum* was initially classified in the *Scrophulariaceae* family, but more recent studies classified it in a larger family, *Plantaginaceae*, based on DNA sequences (Olmstead *et al.*, 2001).

Antirrhinum has been used as an herbaceous model plant in the last 75 years for research involving floral organ identity and leaf and flower asymmetry (Hudson *et al.*, 2008). Besides being used as model plant it also has economic importance, being a popular ornamental plant with a strong and pleasant fragrance, and large bilaterally symmetrical flowers in a range of beautiful colours (Hudson *et al.*, 2008).

Antirrhinum was chosen as a model species to study juvenility for different reasons. It is a quantitative-facultative long-day and seed-raised plant, so its response to photoperiod enables the juvenile phase to be clearly defined (Cockshull, 1985; Cremer *et al.*, 1998). *Antirrhinum* has a relatively short life cycle with an approximate generation time of four months (Adams *et al.*, 2003). The length of the

juvenile phase is long enough to enable both environmental and genetic regulation to be investigated. There is a physiological assay developed to measure stages of development from germination to flowering. Different varieties are present with different characteristics in the market (Hudson *et al.*, 2008). One of such variety is cv. Bells Red which has a dwarf habit and is early flowering. Many genomic resources are available for *Antirrhinum*, including cDNA, genomic and various yeast two-hybrid libraries. An expressed sequence tag (EST) database also exists, containing ~12,000 unique sequences. The first ~2,500 EST sequences have been submitted to the European Molecular Biology Laboratory (EMBL) database (<http://www.antirrhinum.net/blast/blast.html>; <http://www.antirrhinum.net/>).

1.9 *Olea europaea*

Olea europaea L., otherwise known as olive, is one of the most economically important evergreen fruit trees in the Mediterranean area (Diaz-Espejo *et al.*, 2006; Therios, 2009). The fruits and the oil extracted from them have well-known nutritive value and health benefits (Bendini *et al.*, 2007). Furthermore, olive plants have ecological value. Olive trees are resistant to wind and drought and they have the ability to re-sprout after fire (Mulas and Deidda, 1998). Olive plants can easily grow on soil with pH varying from 5.5. to 8.5 (Denney *et al.*, 1985). These characteristics make olive a good candidate for saving areas from desertification and corrosion (Donaire *et al.*, 2011). It is, therefore, very important for this plant to be studied in depth.

In Italy, Università degli Studi della Tuscia has started a project for sequencing the *Olea europaea* genome. Olea europaea Advances (OLEA) involves a total of 15 research units, including Agricultural Research Council (CRA), Italian National Agency for New Technologies, Energy and Sustainable Economic Development (ENEA), National Research Council (CNR), Institute of Applied Genomics (IGA), and six universities. The OLEA group aims to sequence the *Olea europaea* genome in order to deepen essential knowledge for the preservation of olive production and for the identification and selection of clones to use for olive breeding. In particular, the collaborators within this study have research interests in flower development and juvenile-adult phase change.

The transition between these two phases is not just fascinating from a biological perspective but it also has an economic impact. One of the characteristics of olive trees is their almost endless life, but as a consequence their growth is extremely slow. In natural conditions, juvenility in olive can vary between 15-20 years and it is genotype-dependent (El Riachy *et al.*, 2011; Leon and Downey, 2006). This period can be shortened with actions such as cutting, artificial irrigation or additional light (Moreno-Alias *et al.*, 2009). After the end of juvenility, olive plants start to increase their productivity reaching their maximum production after 100 years (Bellini *et al.*, 2008; Suarez *et al.*, 2011). Temperature, but not photoperiod, seems to drive growth and reproduction in olive plants (Denney *et al.*, 1985). Flower buds are set in the late winter and temperature has been shown to be a key factor for blooming response (Perez-Lopez *et al.*, 2008). The ideal temperature for chilling is 7.2°C (Rallo and Martin, 1991). A good vernalization day, for good flowering and fruiting, is expected to have a variation in temperature with a maximum temperature between 12.5°C and 21.1°C and a minimum

temperature between 0°C and 12.5°C (Denney *et al.*, 1985). Typically, olive plants bloom in the spring, flowering starts at the end of May and fruit is mature after 6 months (Lavee, 2007). Generally, fruit yield is influenced by two factors: fruit abscission after the flowering period (just 1-5% of flowers will give fruits) and the biennial reproductive habit characteristic of olive trees (Padula *et al.*, 2008; Perez-Lopez *et al.*, 2008; Suarez *et al.*, 2011). When the plant is about 150 years old production becomes irregular but it can be rejuvenated with cutting (Bellini *et al.*, 2008; Suarez *et al.*, 2011). The end of juvenility is usually marked by the first flower but leaf shape and size and internode length have been indicated as a better and earlier marker (Moreno-Alias *et al.*, 2009). These characteristics may not be good indicators of the end of juvenility since they can differ between cultivars and can be influenced by light exposure or the period of the year in which they were produced (Garcia *et al.*, 2000; Gucci and Cantini, 2000).

1.10 Project aims

The principal aim of this project was to understand the reason for floral incompetence during juvenility in *Antirrhinum majus* and *Olea europaea* (olive) through investigation of the underlying molecular mechanisms. The specific objectives were:

- ❖ To establish the length of the juvenile phase in *Antirrhinum* plants grown under controlled-environment conditions.
- ❖ To investigate *FT* expression in *Antirrhinum* leaves, characterizing *FT* in single leaves at different stages of development.
- ❖ To identify and characterize *Antirrhinum* and *Olea europaea* homologues of *Arabidopsis* genes that reduce or antagonise *FT* expression.
- ❖ To study the regulation of *FT* and *FT* antagonists in juvenile to adult phase transition in *Antirrhinum* and *Olea europaea*.

CHAPTER 2. GENERAL MATERIALS AND METHODS

This chapter describes the general materials and methods that are common to more than one results chapter. Specific protocols and materials will be outlined later in relevant chapters.

2.1 Plant material

2.1.1 *Antirrhinum majus*

F1 seeds of *Antirrhinum majus* (snapdragon), cv. Bells Red, which is dwarf and early-flowering were obtained from Goldsmith Seeds, Inc. (Syngenta Flowers-Gilroy, CA).

2.1.2 *Arabidopsis thaliana*

Seeds of the *Arabidopsis thaliana* Columbia (Col-0) ecotype and *tem1* mutant in the Col-0 background (SALK_097513) were obtained from the Nottingham Arabidopsis Stock Centre (NASC). Seeds of the *Arabidopsis thaliana* *RNAi-tem1/2* double mutant (line 94.9, T5-T6 generations) in the Col-0 background were kindly donated by Dr Soraya Pelaz Herrero (Centre de Recerca Agrigenòmica, SPAIN).

2.1.3 *Olea europaea*

Fresh young leaves were collected from juvenile and adult *Olea europaea* (olive) trees grown in the “Orto Botanico della Tuscia”, the botanical garden operated by Tuscia University in Italy located at about 300 metres above sea level. The juvenile leaves were sampled from a seedling with juvenile characteristics that had never flowered. The seedling was obtained by crossing two highly heterozygous olive cultivars Leccino (female parent) and Dolce Agogia (male parent) (LexDA). Adult leaves were harvested from an adult plant cultivar Leccino (Le).

2.2 Software tools

Primers were designed using Primer3Plus (<http://www.bioinformatics.nl/cgi-bin/primer3plus/primer3plus.cgi>) and synthesised by Invitrogen Ltd and Sigma-Aldrich® (Nasdaq: SIAL).

Data were analysed by Sigma Plot 12® (Systat Software, Chicago, USA) software. Sequences were viewed using SeqBuilder (DNASTAR Lasergene 9, Madison, WI). Chromatogram sequencing files were examined using Chromas 2.23 (Technelysium, Queensland, Australia) and sequence contigs assembled using SeqMan (DNASTAR Lasergene 9, Madison, WI).

National Center for Biotechnology Information (NCBI, National Institutes of Health, Bethesda, MD) Basic Local Alignment Search Tool (BLAST) was used for investigating nucleotide and amino acid sequence homologies.

Phylogenetic analyses were conducted using the MEGA5.05 software package (Tamura *et al.*, 2007). The evolutionary history was inferred with the Maximum Parsimony method using the Close-Neighbor-Interchange algorithm.

2.3 Plant growth conditions

Antirrhinum seeds were sown, one per cell, into Plantpak P40 trays (HSP, Essex, UK) containing Levington F2+Sand (Seed and Modular Compost). Trays were covered with plastic sheets (poly bag 660.4 mm x 1219.2 mm x 50 micron) to keep them moist and put in a SANYO MLR-351H plant growth chamber set at 22°C, 70 ± 2% relative humidity (RH) and short days (SD) (8 h photoperiod). When 50% of seedlings had emerged the plastic was removed and trays placed under the appropriate light conditions as described in section 3.2.1. Plants were fed with Peters excel nutrient 18-10-18 (Scotts International B.V., NL) at a concentration of 0.5 g/l.

Arabidopsis seeds were sown into Plantpak P40 trays containing Levington F2 +Sand compost. Trays were covered with plastic sheets and stratified at 4°C in the dark for 3 days to achieve synchronous germination and then moved to a SANYO MLR-351H plant growth chamber set at 22°C, 70% ± 2% relative humidity (RH) and SD (8 h photoperiod). The plastic was removed when 50% of seedlings emerged and the trays were placed under the appropriate light conditions as described in section 3.2.1 and 5.2.2.

Three *Antirrhinum* transfer experiments were carried out in SANYO cabinets.

For *Antirrhinum* Experiment 1, lighting in the cabinets was provided by fluorescent tubes (General Electric 60W, HU). One of the cabinets was set for long days (LD) (16 h photoperiod) (daily light integral (DLI) = $7.17 \text{ mol}\cdot\text{m}^{-2}\cdot\text{d}^{-1}$) while the other one was set for SD (DLI = $3.53 \text{ mol}\cdot\text{m}^{-2}\cdot\text{d}^{-1}$) with a temperature of 22°C. Spectra are presented in Appendix, Figure A.1-A.5.

During *Antirrhinum* Experiments 2 and 3 lower DLI was used and kept equivalent in SD and LD cabinets. Lighting in SD conditions consisted of 8 h of fluorescent light (DLI = $2.94 \text{ mol}\cdot\text{m}^{-2}\cdot\text{d}^{-1}$). LD conditions were achieved using a combination of 8 h of fluorescent light (DLI = $2.79 \text{ mol}\cdot\text{m}^{-2}\cdot\text{d}^{-1}$) and an extension of 8 h of tungsten light (Philips 32W, NL) (DLI = $0.29 \text{ mol}\cdot\text{m}^{-2}\cdot\text{d}^{-1}$) totalling $3.08 \text{ mol}\cdot\text{m}^{-2}\cdot\text{d}^{-1}$. Light quality and quantity were measured with an EPP 2000 Fiber Optic Spectrometer (StellarNet Inc. USA). Spectra are presented in Appendix, Figure A.1-A.5.

For all the *Arabidopsis* transfer experiments, lighting in the cabinets was provided by fluorescent tubes. One of the cabinets was set for LD (DLI = $7.17 \text{ mol}\cdot\text{m}^{-2}\cdot\text{d}^{-1}$) while the other one was set for SD (DLI = $3.53 \text{ mol}\cdot\text{m}^{-2}\cdot\text{d}^{-1}$) with a temperature of 22°C. Spectra are presented in Appendix, Figure A.1-A.5.

2.4 *Antirrhinum* and *Arabidopsis* transfer experiments

In *Antirrhinum* transfer Experiments 1 and 3, plants were moved from LD to SD every 7 days. In *Antirrhinum* transfer experiments 2 plants were moved from LD to SD every 4 days. For all the experiments, transfer started when 50% of the seedlings germinated (T_0). Plants remained under SD conditions until flowering. In

the *Arabidopsis* transfer experiments plants were moved from LD to SD every day, from 50% of germination (T_0). Flowering time in *Antirrhinum* was measured as the number of true leaves present under the inflorescence. Flowering in *Arabidopsis* was measured as the number of rosette leaves present at the moment when the bolt was at 1 cm length.

Analysis of the flowering time data from the transfer experiments to determine the different phases of photoperiod sensitivity was performed with GenStat (thirteenth edition) (Payne *et al.*, 2009). In Figure 2.1 a schematic representation of a graphic obtained with this software is presented and the juvenile phase (JP), the adult vegetative phase (AVP) and the reproductive phase (RP) are shown. The length of the three phases were calculated based on the number of leaves present on the main stem of the plants at flowering fitting a logistic curve (grey curve), finding the maximum slope (green line) and then fitting the lag time lines (top blue line) and the stationary phase (bottom blue line). These two lines have been calculated from the upper and lower asymptote of the logistic curve. The orange dot lines delimit the three different phases. Vertical error bars denote the standard error of the mean of the number of leaves. Horizontal error bars denote the standard error of the mean of the estimated phase length.

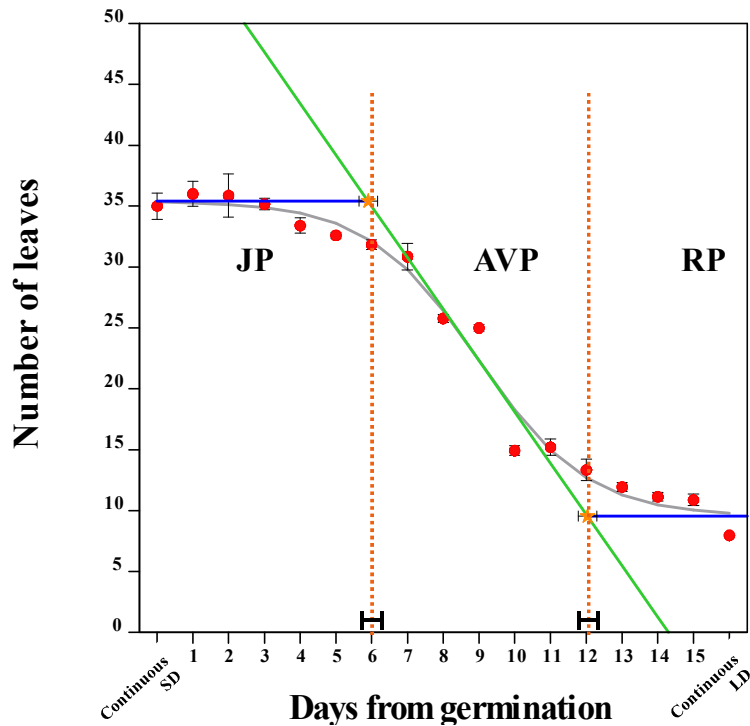


Figure 2.1 Schematic representation of the phases of photoperiod sensitivity determined from data obtained from a LD to SD transfer experiment.

Flowering time, represented by the number of rosette of leaves at 1 cm bolt for *Arabidopsis* plants transferred from LD to SD conditions at various times from germination. The photoperiod-insensitive juvenile phase JP, photoperiod-sensitive adult vegetative phase AVP and the photoperiod-insensitive reproductive phases RP are indicated. SD: short day, LD: long day. Vertical error bars denote the standard error of the mean of the number of leaves. Horizontal error bars denote the standard error of the mean of the estimated phase length. Logistic curve (grey curve), maximum slope (green line), lag time lines (blue lines). The orange dotted lines delimit the three different phases.

2.5 Genomic DNA extraction from *Arabidopsis*

Genomic DNA was extracted from single *Arabidopsis* leaves previously stored at -80°C after harvesting. Frozen leaves were homogenised for 15 s using a Dremel drill (Racine, WI U.S.A) which has an abrasive attachment designed to fit a 2 ml microfuge tube. The protocol used was a modified version of Edwards *et al.* (1991) rapid method for the preparation of plant genomic DNA for PCR analysis. After grinding, 400 μl of extraction buffer (200 mM tris-HCl pH 7.5, 250 mM

NaCl, 25 mM EDTA, 0.5% SDS w/v) was added to the samples. Subsequent to centrifugation at 13,000 rpm for 2 min, the supernatant was transferred to a fresh tube and 300 µl of chloroform:isoamyl alcohol (24:1) added. Samples were centrifuged again for 5 min and the top aqueous layer transferred to a new tube. For DNA precipitation, 35 µl of 3M NaOAc pH 5.2 and 837.5 µl of isopropanol were added to the samples that were incubated for 2 hours at -20°C and subsequently centrifuged for 10 min. After removing the supernatant, the pellet was air-dried and resuspended in 50 µl TE and then treated with 10 µg/ml RNase A for 30 min at 37°C. Samples were then diluted 1:4 with SDW.

2.6 RNA isolation and cDNA synthesis

Total RNA was extracted from leaf material harvested from *Antirrhinum* and *Arabidopsis* plants grown in experiments described in chapter 3 and 5. Samples were homogenised using a Dremel drill and Trizol® reagent (Invitrogen Ltd., Cat. No.15596-026, USA) added. For RNA purification the manufacturer's guidelines were followed with the exception that the chloroform extraction was carried out twice.

RNA quantity was measured with the NanoDrop™ ND-1000 Spectrophotometer (Thermo Scientific) and 1-2 µg of total RNA was run on 1% agarose gel to check quality.

The TURBO DNA-free™ DNase treatment kit (Ambion Inc, Cat. No. AM1907, USA) was used to remove genomic DNA contamination following the manufacturer's guidelines and a PCR, as described in section 2.7, was performed to

prove the lack of DNA contamination using Ant elf-alpha F/Ant elf-alpha R primers for *Antirrhinum* samples and AtActin F/AtActin R primers for *Arabidopsis* samples. Primers sequences and specification can be found in Appendix, Table A.1.

cDNA was synthesised using 3 µg total RNA using Superscript™ II First-Strand Synthesis System (Invitrogen Ltd., Cat. No. 18064-14, USA) for RT-PCR using oligo(dT) following the manufacturer's guidelines and subsequently treated with RNase H (Invitrogen Ltd., Cat. No. 18021-14, USA).

2.7 Polymerase Chain Reaction (PCR)

PCR mixes comprised 1 µl from the cDNA synthesis reaction or 1 µl from a touch from a single bacterial colony dispensed in 40 µl SDW, 0.4 U KOD Hot Start DNA Polymerase (Merck Chemicals, Cat. No. 71086), 1X KOD Hot Start DNA Polymerase reaction buffer, 2 mM MgSO₄, 0.2 mM dNTPs and 0.5 µM of each forward and reverse primer in a total volume of 20 µl made up with SDW. The same reaction, but in a volume of 10 µl was made for gDNA screens using 0.5 µl of template. The amplification consisted of an initial denaturation at 94°C for 2 min, followed by 30 cycles (if not specified otherwise) of denaturation at 94°C for 15 s, annealing (specific primer temperature) for 30 s, and extension at 72°C for 1 min per kb of expected product. A further 10 minutes of extension at 72°C was carried out at the end of the cycles. Primer sequences, annealing temperatures and expected product sizes are presented in the Appendix, Table A.1.

2.8 Real-time PCR analysis

cDNA was synthesised as described in section 2.6. Real-time PCR analysis was conducted using either the ICycler® machine from Bio-Rad using iQ5 software (Bio-Rad Laboratories Ltd., UK) and the LightCycler® 480 Realtime PCR System (Roche Diagnostics Ltd., UK). When using the BioRad machine, each reaction contained 7.5 µl SYBR green (Eurogentec Ltd., Cat. No. RT-SY2X-03+WOUFL), 0.5µl of cDNA, and either 0.2 or 0.04 µM of each primer and 4.6 µl of SDW. When using the Roche machine, each reaction contained 5 µl LightCycler 480 SYBR Green Master (Roche Diagnostics Ltd., Cat. No. 04887352001), 1 µl of cDNA, and 0.5 µM of each primer at the appropriate final concentration and 3 µl of SDW. Details for primers used are presented in the Appendix, Table A.1.

Real-time PCR analysis was performed in three replicates for each sample and data indicated as means and normalized against expression levels of the house keeping genes for each sample.

PCR cycling conditions consisted of an initial cycle (95°C for 5 minutes) followed by 55 cycles of denaturation at 95°C for 15 s and annealing for 1 min (temperature specific for each primer pairs). The melt curve was obtained by performing 80 cycles 55°C for 10 s, increasing the temperature by 0.5°C per cycle after cycle 2.

PCR products were purified as described in section 2.10 and sequenced as described in section 2.14 to confirm that the correct targets were amplified.

2.9 Agarose gel electrophoresis

RNA quality was checked by running 1 μ l of each sample on a 1% (w/v) Agarose gel (Invitrogen Ltd., Cat. No. 15510, USA) prepared with 1x Tris-acetate-EDTA buffer (TAE buffer) (VWR Interbational, Cat. No. 44125D) and 0.2 μ g/ml of ethidium bromide (EtBr) (VWR International, UK).

cDNA was visualized on a 2% (w/v) Agarose gel (Invitrogen Ltd., Cat. No. 15510, USA) prepared with 1x TAE buffer and EtBr.

Orange G (Sigma-Aldrich®, Cat. No. O3756, UK) loading buffer (3 μ l), was added to each 20 μ l sample before loading it on the gel. Electrophoresis was carried out in tanks filled with 1x TAE buffer at 100-120 mA for 40 to 120 min, depending on the sizes of the nucleic acids and the concentration of agarose in the gel. 1Kb Plus DNA ladder (Invitrogen Ltd., Cat. No. 10787, USA) was run alongside the samples in gels. Records of each gel were taken using a G:BOX gel documentation system (Syngene, UK).

2.10 Purification of PCR products from gels

After electrophoresis, nucleic acid containing bands were cut from gels and products isolated using a QIAquick Gel Extraction Kit (QIAGEN, Cat. No. 28704) following the manufacturer's guidelines. Purified products were eluted in 30 μ l of SDW.

2.11 Ligation of PCR products into the pGEM-T Easy vector

An Adenine (A) residue was added to the 3' PCR products by incubating for 30 min at 72°C the PCR fragments with dNTPs and non proofreading TAQ DNA polymerase following initial PCRs. PCR products of the expected lengths were then purified as described in 2.10 section and ligated overnight into the pGEM-T Easy vector (Promega Ltd., Cat. No. A1360, Australia) (Figure 2.2) following the manufacturer's instructions, in 10 µl total volume.

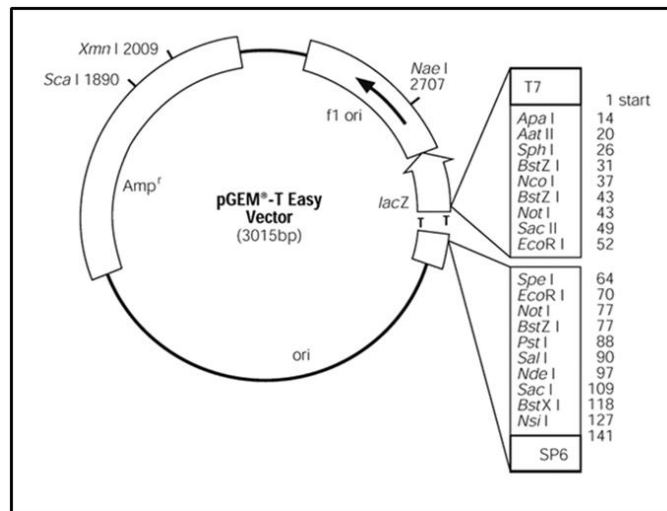


Figure 2.2: Map of pGEM®-t Easy transformation vector

2.12 Electroporation of vector DNA into *E.coli* and *Agrobacterium*

Vector products (2 µl) were added to 20 µl of electrocompetent EC100 *E. coli* cells (Cambio Ltd., Cat. No. EC10005) or electrocompetent *Agrobacterium* cells (AgC58pGV3101) in an electroporation cuvette (Geneflow Ltd., Cat. No. E6-

0050) and electroporated using a Bio-Rad Micropulser, using the bacteria setting at 1.8 kV for 5 ms following the manufacturer's guidelines. After electoporation 1 ml of SOC medium (Appendix, Table A.6) was added and the content transferred to a microcentrifuge tube and shaken at 200 rpm for 1 h at 37°C or 28°C, for *E.coli* or *Agrobacterium* respectively. Aliquots of 10, 50 and 100 µl were plated on LB media (VWR International) containing 100 µg/ml ampicillin, 0.1 M isopropyl/-D-thiogalactoside (IPTG), and 20 mg/ml 5-bromo-4-chloro-3-indolyl-beta-D-galactopyranoside (X-Gal) for *E.coli* selection and 100µg/µl Spectinomycin (SPEC), 25µg/µl Gentamicin (GENT) and 50µg/µl Rifampicin (RIF) for *Agrobacterium* selection and left overnight at 37°C or 28°C, respectively. Colonies were screened by PCR for presence of the expected insert using gene specific primers as described in section 2.7.

2.13 Plasmid DNA purification

A single bacterial colony was used to inoculate 5 ml liquid LB (Luria-Bertani) medium (VWR International, Cat. No. 1.10285, UK) containing the appropriate antibiotics as described in section 2.12 and cultured overnight at 37°C with shaking (250 rpm). Plasmid DNA was extracted following the QIAprep Spin Mini Kit (QIAGEN, Cat. No. 27106) protocol and eluted in 50 µl in SDW.

2.14 DNA sequencing

The Dye® Terminator v.3.1 Cycle Sequencing Kit (Applied Biosystems, Cat No. 4337456) was used to sequence DNA products and the manufacturer's protocol followed. Template was added to 2 µl of Big Dye and 3.2 µM primer concentration in a final volume of 10 µl made up with SDW. Primer details are shown in Appendix, Table A.2. Samples were processed for 25 cycles at 96°C for 10 s, 50°C for 5 s and 60°C for 4 min and sent to Warwick HRI Genomic Resource Centre for sequencing. Results were read with the BioEdit software package and analysed and edited using the EditSeq package of DNASTar Lasergene. Chromatograms were analysed as described in section 2.2.

CHAPTER 3. PHOTOPERIOD TRANSFER EXPERIMENTS

3.1 Introduction

To help the agricultural industry, scientists need to provide tools to predict the developmental stages of plants. Being able to understand and to calculate the growth and development of a crop is important for management decisions related to, for example, the timing of pesticide application or synchronization of flowering. This is the case when the breeder wants two different genotypes ready at the same time for pollination for hybrid seed production or for predictable supply to market. In the current study, experiments have been carried out to determine developmental phase transition timings in plants in relation to photoperiod, one of the most important environmental factors that plays a role in determining the initiation of flowering (Adams, 1999).

The length of the juvenile phase (JP) can be assessed by transfer of plants between inductive long days (LD) and short days (SD) at regular intervals while measuring flowering time and leaf number at flowering (Adams *et al.*, 2003). Plants that undergo the juvenile to adult phase transition prior to transfer are not delayed in flowering. However, plants transferred to SD before the end of their juvenile phase (JP) flower later since they underwent the juvenile to adult phase transition when

exposed to non-inductive SD conditions (Adams *et al.*, 2001). In *Antirrhinum*, the number of leaves present on the main stem can be used as a measure of flowering time. *Antirrhinum* produces a terminal inflorescence and no more leaves are produced on the main stem under the inflorescence once floral initiation has occurred (Adams *et al.*, 2001). The number of days from germination to the first open flower can be used to assess flowering time, as well (Adams *et al.*, 2003).

Developmental stages can be followed by monitoring differentiation of the main stem shoot apex. The arrangement of organs around the axis of growth is termed phyllotaxy. During post-embryonic development, *Antirrhinum* shows three modifications of phyllotaxy (Bradley *et al.*, 1996). On the main stem, during the juvenile phase, a spiral of two leaves is produced at each node (opposite decussate phyllotaxy). During the reproductive phase a single smaller leaf like organ (bract) is produced at each node (spiral phyllotaxy) with shorter internodes. Finally, a flower occurs in the axil of each bract generating four types of organ (sepals, petals, stamens and carpels) in a whorled phyllotaxy (Carpenter *et al.*, 1995). The morphology of the floral meristem can be recognised from the spiral phyllotaxy in the vegetative meristem. The shoot apical meristem (SAM) produces leaves and shoots during the juvenile phase, but after the floral transition, the SAM produces flower primordia. By observing developmental changes in the SAM it is possible to follow flower initiation (Benlloch *et al.*, 2007). At the molecular level, this switch is driven by the activation of the floral meristem identity genes, as described in section 1.4. One of the key genes involved in floral development that is required for determination of floral meristem identity in *Antirrhinum* is *FLORICAULA (FLO)*, the homologue of *LEAFY (LFY)* in *Arabidopsis*. In *flo* mutants, floral meristems turn into shoot meristems, and plants over-expressing *FLO* have shoots that turn

into flowers (Amaya *et al.*, 1999; Coen *et al.*, 1991). *FLO* expression is repressed by *CENTRORADIALIS* (*CEN*), the homologue of *TERMINAL FLOWER1* (*TFL1*) in *Arabidopsis*. *CEN* is required for maintaining an indeterminate shoot identity. In *cen* mutants, the indeterminate inflorescence changes into a terminal flower (Bradley *et al.*, 1996). Amaya *et al.* (1999) suggest that *CEN* expression may be linked to the duration of the vegetative phase.

In previous experiments, *Antirrhinum* plants were germinated in growth rooms and photoperiod transfer experiments were carried out in glasshouses and plants moved into photoperiodic chambers using automated trolleys (Adams *et al.*, 2003; Massiah *et al.*, 2007; Munir *et al.*, 2010; Munir *et al.*, 2004). *Antirrhinum* plants of a recombinant inbred line in the F9 generation called RIL57 were transferred for 10 weeks from SD to LD at weekly intervals from germination and flowering times recorded to assess the length of the juvenile phase. As part of the same experiment, plants were transferred at weekly intervals from SD to LD and were sampled for molecular analysis at the end of the second subjective LD; material was harvested from the youngest expanded pair of leaves only. Expression of the *Antirrhinum* homologue of *FLOWERING LOCUS T* (*AmFT*) was examined throughout development. Expression data showed that *AmFT* expression is significantly lower in juvenile plants than in adult plants (Thomas, 2009).

The study described in this chapter had four aims. The first was to develop an assay for measuring juvenility using controlled environment cabinets that was cheaper and more repeatable than the glasshouse assay used in previous studies. The second was to follow changes at the SAM and gene expression level, using *CEN* and *FLO* as markers. The third aim was to follow the expression of *FT* in all the leaves during *Antirrhinum* development. Additionally, the study aimed to

determine whether the photoperiodic pathway is active during juvenility, using *Arabidopsis* as a model plant.

3.2 Materials and Methods

This section describes the materials and methods specific for this results chapter. Protocols and materials common to more than one chapter are described in chapter 2. All primer details are listed in the Appendix, Table A.1, A.2 and A.3.

3.2.1 *Antirrhinum* Transfer experiments

Antirrhinum majus, cv. Bells Red F1 were grown in two MLR-351 Environmental Test Chamber SANYO cabinets as described in section 2.3. Three transfer experiments were carried out.

Experiment 1 was carried out to determine the length of the JP in *Antirrhinum*. Fifteen plants were moved from the LD ($DLI = 7.17 \text{ mol}\cdot\text{m}^{-2}\cdot\text{d}^{-1}$) cabinet to the SD ($DLI = 3.53 \text{ mol}\cdot\text{m}^{-2}\cdot\text{d}^{-1}$) cabinet weekly for 7 weeks (T_1 - T_7) where they remained until flowering. Five typical plants were selected every week at the time of transfer from the LD cabinet to record leaf number. The number of leaves below the first opened flower was counted in all plants to measure flowering time. Leaf number was assigned starting at the base of the plant. Bracts, but not cotyledons, were considered as leaves in all the analyses. A further 20 plants were grown under constant SD conditions and constant LD condition as controls. The leaf number data were analysed to determine the phases of photoperiod sensitivity at the end of the juvenile phase, as described in section 2.4.

Experiment 2 was carried out using a LD condition at lower light integral, as described in section 2.3, to extend the JP and to provide leaf material for molecular analysis. Apex development was observed as well. Three plants were moved from

the LD (DLI = 3.08 mol·m⁻²·d⁻¹) cabinet to the SD (DLI = 2.79 mol·m⁻²·d⁻¹) cabinet every 4 days for 40 days (T₁-T₁₀) where they remained until flowering. A further 10 plants were grown in constant SD and LD conditions as controls. Leaf number at flowering for each plant transferred from LD to SD was used to determine the length of phases, as described in section 2.4. Five typical plants were selected every 4 days at the time of transfer from the LD cabinet for observation of apex development as explained in section 3.2.2. Leaf material was sampled as explained in section 3.2.4.

Experiment 3 was carried out using the same LD and SD conditions used in Experiment 2. Three plants were moved from the LD cabinet to the SD cabinet every 7 days for 8 weeks (T₁-T₈) where they remained until flowering. A further 10 plants were grown in constant SD and LD conditions as controls. The number of leaves below the first opened flower for each plant transferred from LD to SD was used to determine the length of phases, as described in section 2.4. Ten typical plants were selected every 7 days at the time of transfer from the LD cabinet for collecting apex material as described in section 3.2.2. Leaf material was harvested for molecular analysis as described in section 3.2.4.

3.2.2 *Antirrhinum* apex observation and sampling

Throughout Experiment 2, every 4 days, five plants were dissected under a binocular microscope (magnification 200X) to expose the apical region and the morphology of the meristem studied.

Additionally, throughout Experiment 3, every 7 days, the apices of at least ten plants were harvested for molecular analysis into 5 volumes of RNAlater

solution (Ambion Inc, Cat. No.AM7024, USA) and incubated for 24 hours at room temperature. Plant tissue was then collected by centrifugation at 12,000 xg for 10 min and the RNAlater solution removed before storing at -80°C .

Samples were used for RNA extraction as described in section 2.6 with the final RNA pellet being rehydrated with 100 μl DEPC SDW and the RNA further purified using RNeasy Plant Mini Kit (QIAGEN, Cat. No.74904) following the manufacturer's guidelines. cDNA was synthesised as described in section 2.6.

3.2.3 *Real-time PCR analysis of CEN and FLO expression*

Real-time PCR analysis was conducted using the LightCycler® 480 Realtime PCR System as described in section 2.8 using Ant CEN F/Ant CEN R and Ant FLO F/Ant FLO R primers to detect *CEN* and *FLO* respectively. Ant elf-alpha F/Ant elf-alpha R primers were used to detect the elongation factor housekeeping gene. Primer details, concentrations used at in PCRs and anneal/extension temperatures are provided in the Appendix, Table A.1.

3.2.4 *Leaf harvests for AmFT expression analysis*











Throughout the Experiment 2 and Experiment 3, leaf material was harvested at ZT 15 (zeitgeber time, 15 subjective hours after lights on) every 4 days (T₁-T₁₀) and every 7 days (T₁-T₈), respectively, from plants grown continuously under LD conditions. Additionally, throughout Experiment 3, leaf material was harvested at ZT 7 every 7 days (T₁-T₈) from plants grown continuously under SD conditions.

For each harvest, leaf material was taken from 7 plants. From each plant, the pair of leaves (> 0.5 cm) produced at each node, was harvested separately and then combined with the corresponding pair of leaves from the other 6 plants.

During Experiment 2, a total of 47 samples were collected. Table 3.1 details the leaf collection method and sample nomenclature. For each sample the name was assigned starting from the oldest pair of leaves at the base of the plant. Cotyledons were harvested as well but not included in the leaf number counts and bracts were not included for sampling. For example, at the fifth transfer (T5), there were 2 cotyledons, and 3 pairs of leaves and they were named: T5 cot, T5.1 (oldest leaves), T5.2, T5.3 (youngest leaves). During Experiment 3, the same technique was used to name the samples.

Tissue from both the experiments was frozen directly into liquid nitrogen and stored at -80°C for molecular analysis. Samples were used for RNA extraction and cDNA synthesis as described in section 2.6.

Table 3.1 Harvest time and sample nomenclature for samples collected during transfer Experiment 2

Days from germination		Leaves present and collected											
		Cotyledons	Leaves 1&2	Leaves 3&4	Leaves 5&6	Leaves 7&8	Leaves 9&10	Leaves 11&12	Leaves 13&14	Leaves 15&16	Leaves 17&18		
4 days		T1 cot											
8 days		T2 cot											
12 days		T3 cot	T3.1										
16 days		T4 cot	T4.1	T4.2									
20 days		T5 cot	T5.1	T5.2	T5.3								
24 days		T6 cot	T6.1	T6.2	T6.3	T6.4							
28 days		T7 cot	T7.1	T7.2	T7.3	T7.4	T7.5						
32 days		T8 cot	T8.1	T8.2	T8.3	T8.4	T8.5	T8.6					
36 days		T9 cot	T9.1	T9.2	T9.3	T9.4	T9.5	T9.6	T9.7				
40 days		T10 cot	T10.1	T10.2	T10.3	T10.4	T10.5	T10.6	T10.7	T10.8	T10.9		

3.2.5 *Real-time PCR analysis of AmFT expression*

Real-time PCR analysis was conducted using the BioRad ICycler® machine as described in section 2.8 using Ant put FT F/Ant put FT R primers to detect *AmFT* and Ant elf-alpha F/Ant elf-alpha R primers to detect the elongation factor housekeeping gene. Primer details, concentrations used at in PCRs and anneal/extension temperatures are provided in the Appendix, Table A.1.

3.2.6 *Arabidopsis transfer experiment to establish JP length and AtFT and AtCO expression analyses*

Arabidopsis Col-0 transfer experiments were carried out using SANYO cabinets set up as described in section 2.3. Each day, for 10 consecutive days, 10 seedlings were moved from LD to SD conditions. At each transfer day, at least 10 plantlets were harvested from both LD and SD cabinets at ZT15 and ZT7, respectively. A further 10 plants were grown in constant SD and LD conditions as controls.

Flowering times were assessed by counting rosettes leaves present at 1 cm bolt height for each plant transferred from LD to SD, as described in section 2.4.

Samples were used for RNA extraction and cDNA synthesis as described in section 2.6. Real-time PCR analysis was conducted using the LightCycler® 480 Realtime PCR System as described in section 2.8 using Real-time AtCO F/Real-time AtCO R and Real-time AtFT F/Real-time AtFT R primers to detect *Arabidopsis CO (AtCO)* and *Arabidopsis FT (AtFT)*, respectively. AtActin F/AtActin R primers were used to detect the actin 2 housekeeping gene. Primer

details, concentrations used at in PCRs and anneal/extension temperatures are provided in the Appendix, Table A.1.

3.3 Results

3.3.1 Floral initiation

Experiment 1 was conducted as explained in section 3.2.1 to determine the feasibility of growing *Antirrhinum* plants in SANYO cabinets to assess the length of the juvenile phase. Subsequently, plants were transferred at weekly intervals from LD to SD. The number of leaves present on the main stem at each transfer day is shown in Figure 3.1.

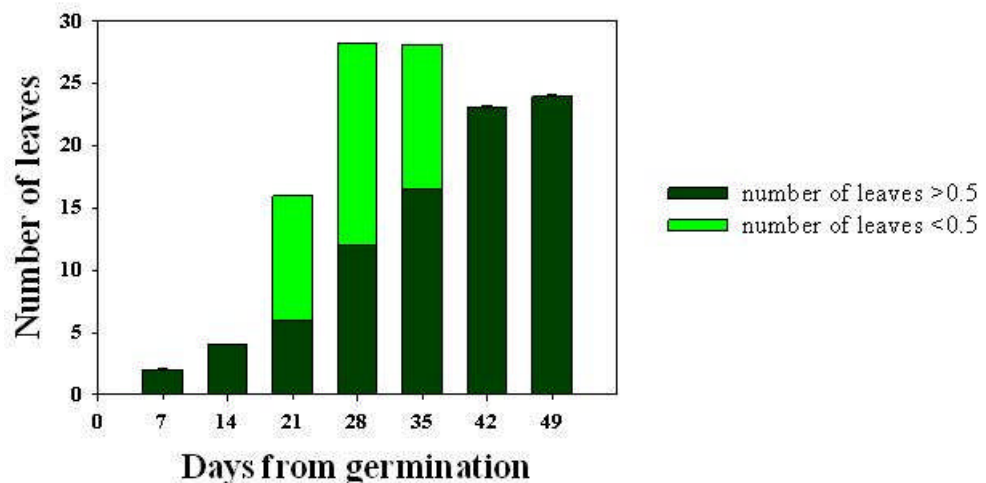


Figure 3.1 Leaf number during development in Experiment 1.

Number of leaves at time of transfer in *Antirrhinum* grown under LD conditions. Data were analysed by general linear model analysis of variance (ANOVA, $p < 0.05$), with subsequent comparison between means using Fisher's least significant difference test. Error bars denote LSD (5% levels) of means of the total number of leaves (LSD = 0.16; d.f. = 36).

The first true leaves were present after 7 days from germination. The number of true leaves, bigger than 0.5 cm, present on the main stem increased gradually reaching a maximum of 24 leaves at 49 days. The total number of leaves reached the maximum at 28 days. After this point no more leaves were produced. Leaves smaller than 0.5 cm were recorded close to the apex between 21 and 35 days.

Flower initiation started between 21-28 days after germination and juvenility must have ended before this time.

The presence of a significant difference in the final number of leaves at 28 and 35 days, compared to the final number of leaves present at 42 and 49 days after germination, was due to the presence of bracts and floral organ primordia that were indistinguishable by visual observation from small leaves at that time.

3.3.2 Determination of juvenile phase length

In order to determine the length of juvenility in *Antirrhinum* plants grown in Experiment 1, as described in section 3.2.1, the number of leaves present at flowering time were counted in plants transferred from LD to SD conditions at weekly intervals (Figure 3.2).

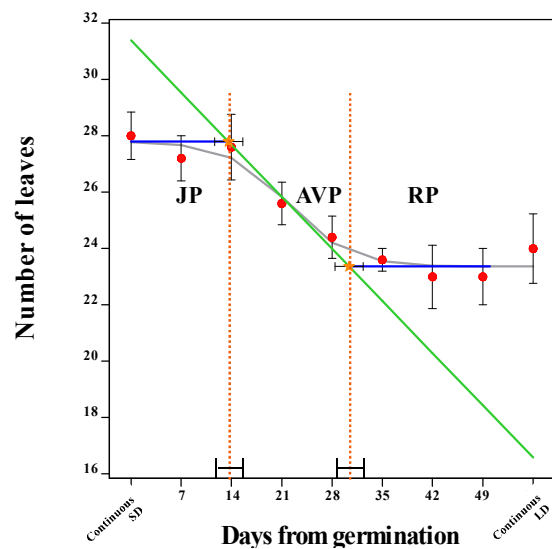


Figure 3.2 Different phases of photoperiod sensitivity in *Antirrhinum* (Bells F1) in Experiment 1. The effect of transferring *Antirrhinum* at weekly intervals (expressed as days from 50% germination) from LD to SD on flowering time. JP: juvenile phase, AVP: adult vegetative phase, RP: reproductive phase, SD: short day, LD: long day. Vertical error bars denote the standard error of the mean of the number of leaves. Horizontal error bars denote the standard error of the mean of the estimated phase length. Logistic curve (grey curve), maximum slope (green line), lag time lines (blue lines). The orange dotted lines delimit the three different phases.

The data indicate that plants were juvenile for $13.6 \text{ d} \pm 1.9 \text{ d}$ after germination. In plants transferred during the reproductive phase, flowering occurred at about the same time as the LD control plants. This is because they had already committed to flower. The AVP lasted for $16.8 \text{ d} \pm 1.9 \text{ d}$.

3.3.3 *Examination of apex morphology throughout development*

Changes in apex morphology were clearly observed throughout development during Experiment 2 (Figure 3.3). Experiment 2 differed from Experiment 1 in that light integrals under LD were lower, as described in section 3.2.1.

From observing apex morphology was revealed that the apex was a dome of undifferentiated cells up to 24 days post emergence (Figure 3.3 A-D). Differentiation into floral meristem occurred from around 28 days (Figure 3.3 E) through to the development of the floral organ primordia (Figure 3.3 E-H). At this point, primordia bracts were also visible and at the end of this stage (Figure 3.3 H), 40 days after germination, sepal primordia were evident.

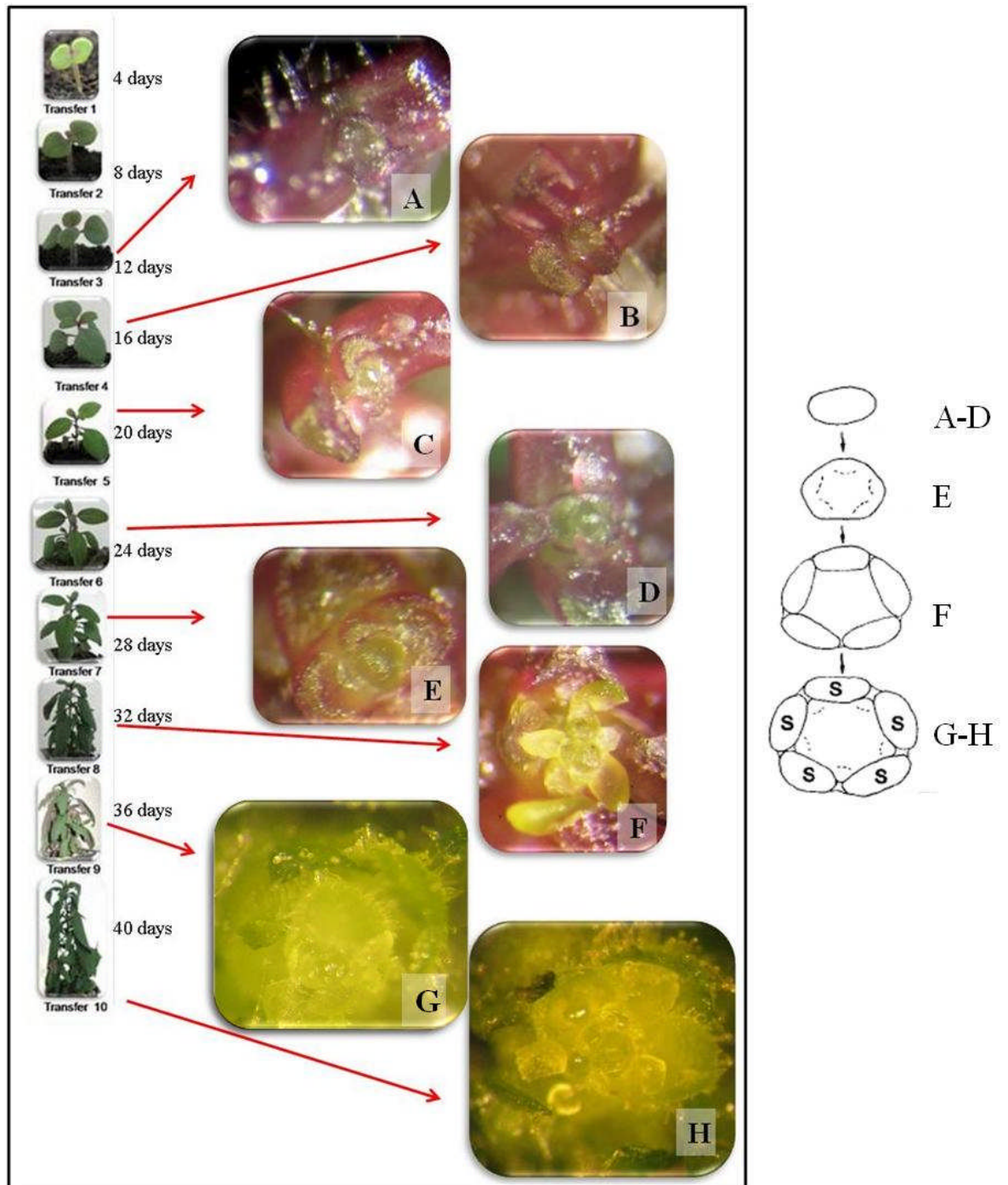


Figure 3.3 Morphological changes at the SAM during development in Experiment 2.

Apex was observed by binocular microscope (magnification 200X). On the left side pictured are the different apex developmental stages at different times from germination. On the right side a diagram of shoot meristem stages modified from (Carpenter et al., 1995) used as guideline for the observation. Dotted lines indicate initiated primordia, S, indicates the sepals.

3.3.4 Determination of juvenile phase length

In Experiment 2, plants were transferred from LD to SD every 4 days as described in section 3.2.1. Juvenility was estimated to end $14.4 \text{ d} \pm 2.7 \text{ d}$ after germination (Figure 3.4), one day longer than in the Experiment 1. Also the AVP was longer, lasting for $20.9 \text{ d} \pm 2.7 \text{ d}$. The data reinforced that it is possible to determine the length of juvenility in plants grown in SANYO cabinets.

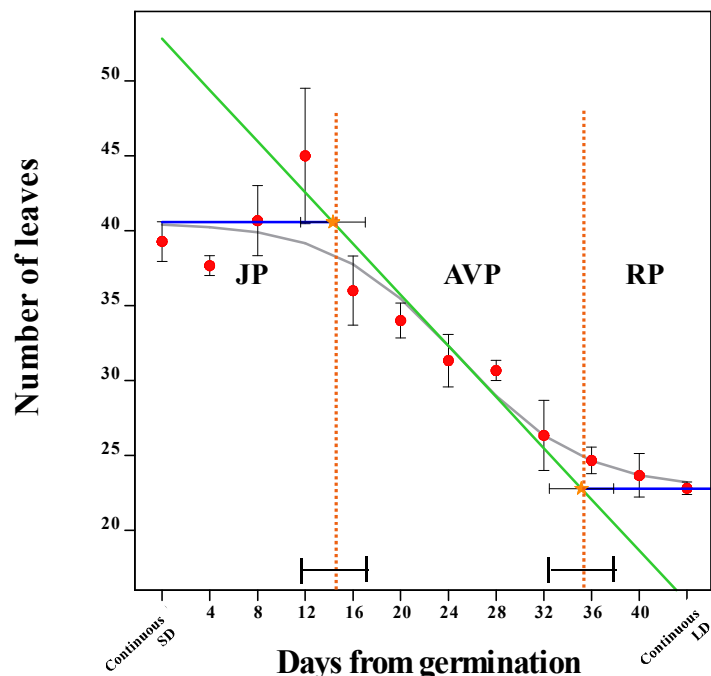


Figure 3.4 Different phases of photoperiod sensitivity in *Antirrhinum* (Bells F1) in Experiment 2. The effect of transferring *Antirrhinum* at weekly intervals (expressed as days from 50% germination) from LD to SD on flowering time. JP: juvenile phase, AVP: adult vegetative phase, RP: reproductive phase, SD: short day, LD: long day. Vertical error bars denote the standard error of the mean of the number of leaves. Horizontal error bars denote the standard error of the mean of the estimated phase length. Logistic curve (grey curve), maximum slope (green line), lag time lines (blue lines). The orange dotted lines delimit the three different phases.

3.3.5 Investigation of *AmFT* expression throughout development in *Antirrhinum*

Expression levels of the *AmFT* were analysed in biological samples harvested from transfer Experiment 2, as described in section 3.2.4.

AmFT expression was analysed across development in each pair of leaves collected from plants grown under constant LD (Figure 3.5).

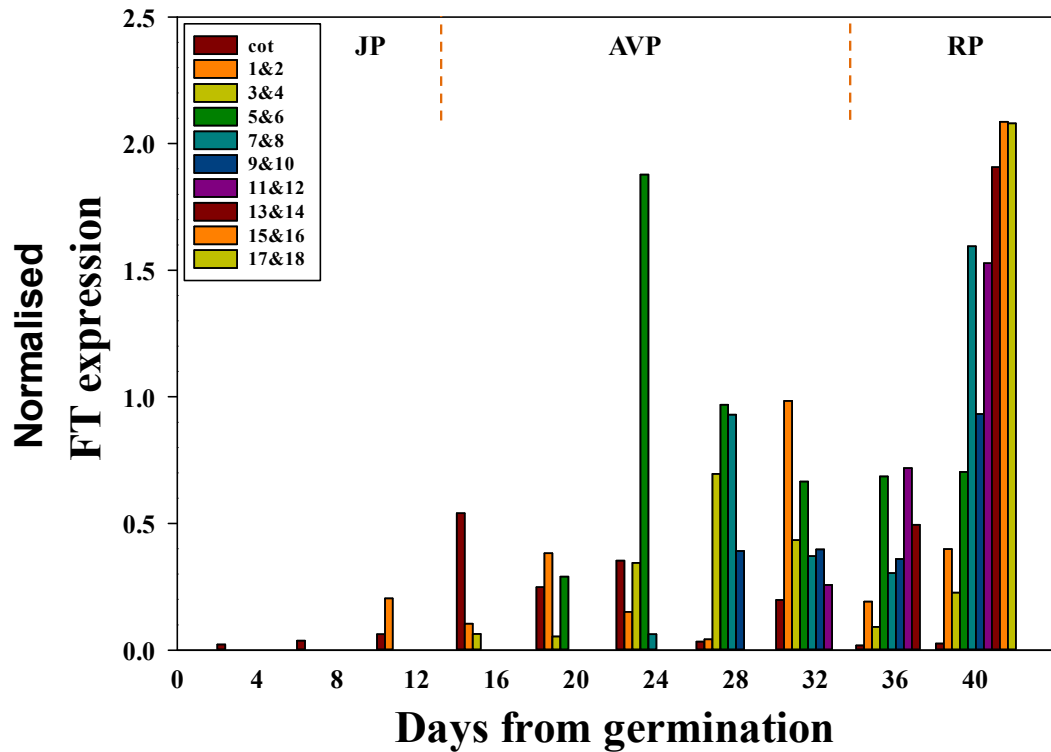


Figure 3.5 Developmental expression of *AmFT* in leaf material from *Antirrhinum* plants grown under LD in Experiment 2. Real-time PCR analysis of the relative expression of *AmFT* normalised to *ELF-alpha*. Expression analysed at ZT 15. JP: juvenile phase, AVP: adult vegetative phase, RP: reproductive phase. The orange dotted lines delimit the three different phases.

Expression of *AmFT* is very low during the first 12 days from germination. This period corresponded to the juvenile phase which ended about 14.5 days after germination. In cotyledons, *AmFT* expression rises and peaks around 16 days from germination, but remains very low thereafter in adult plants, which probably correlates with cotyledon senescence. Following the end of juvenility *AmFT*

progressively increases in all the leaves when plants started to respond to photoperiod.

3.3.6 *Determination of juvenile phase length*

Juvenility length was estimated in Experiment 3 carried out using the same condition of Experiment 2 but plants were transferred every 7 days instead of every 4 days. This experiment was conducted to confirm the reproducibility of growing *Antirrhinum* plant in the SANYO cabinet to assess the JP.

In this experiment juvenility was estimated to end $14.4 \text{ d} \pm 1.6 \text{ d}$ after germination (Figure 3.6). The data confirmed the reproducibility of using the SANYO cabinet for transfer experiments. The AVP lasted for $26.3 \text{ d} \pm 1.6 \text{ d}$. Although Experiment 2 (Figure 3.4) and Experiment 3 (Figure 3.6) showed a similar JP length, the AVP presented more variability, being longer in the Experiment 3.

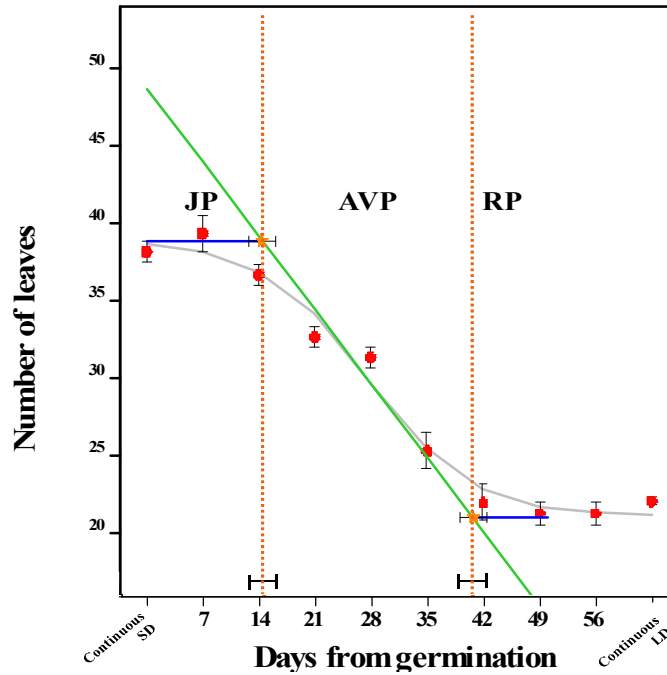


Figure 3.6 Different phases of photoperiod sensitivity in *Antirrhinum* (Bells F1) in Experiment 3. The effect of transferring *Antirrhinum* at weekly intervals (expressed as days from 50% germination) from LD to SD on flowering time. JP: juvenile phase, AVP: adult vegetative phase, RP: reproductive phase, SD: short day, LD: long day. Vertical error bars denote the standard error of the mean of the number of leaves. Horizontal error bars denote the standard error of the mean of the estimated phase length. Logistic curve (grey curve), maximum slope (green line), lag time lines (blue lines). The orange dotted lines delimit the three different phases.

3.3.7 Analysis of *FLO* and *CEN* expression during development

FLO and *CEN* expression was determined by Real-time PCR analyses in apices dissected from plants at various developmental stages grown under constant LD and SD conditions during Experiment 3, as described in sections 3.2.2 and 3.2.3. The same standard curve and cDNA samples were used to analyse expression of all genes, thus relative expression levels can be compared.

The result of *FLO* expression demonstrated that under LD conditions *FLO* expression rises after flower initiation at 28 days (Figure 3.7 A). Apex observations conducted during Experiment 2 revealed that between 32 and 36 days floral organ

primordia started to form. Under SD, *FLO* expression is very weak in comparison to expression observed under LD, approximately five orders of magnitude lower. The rise in expression is delayed and does not appear until 63 days from germination (Figure 3.7 B).

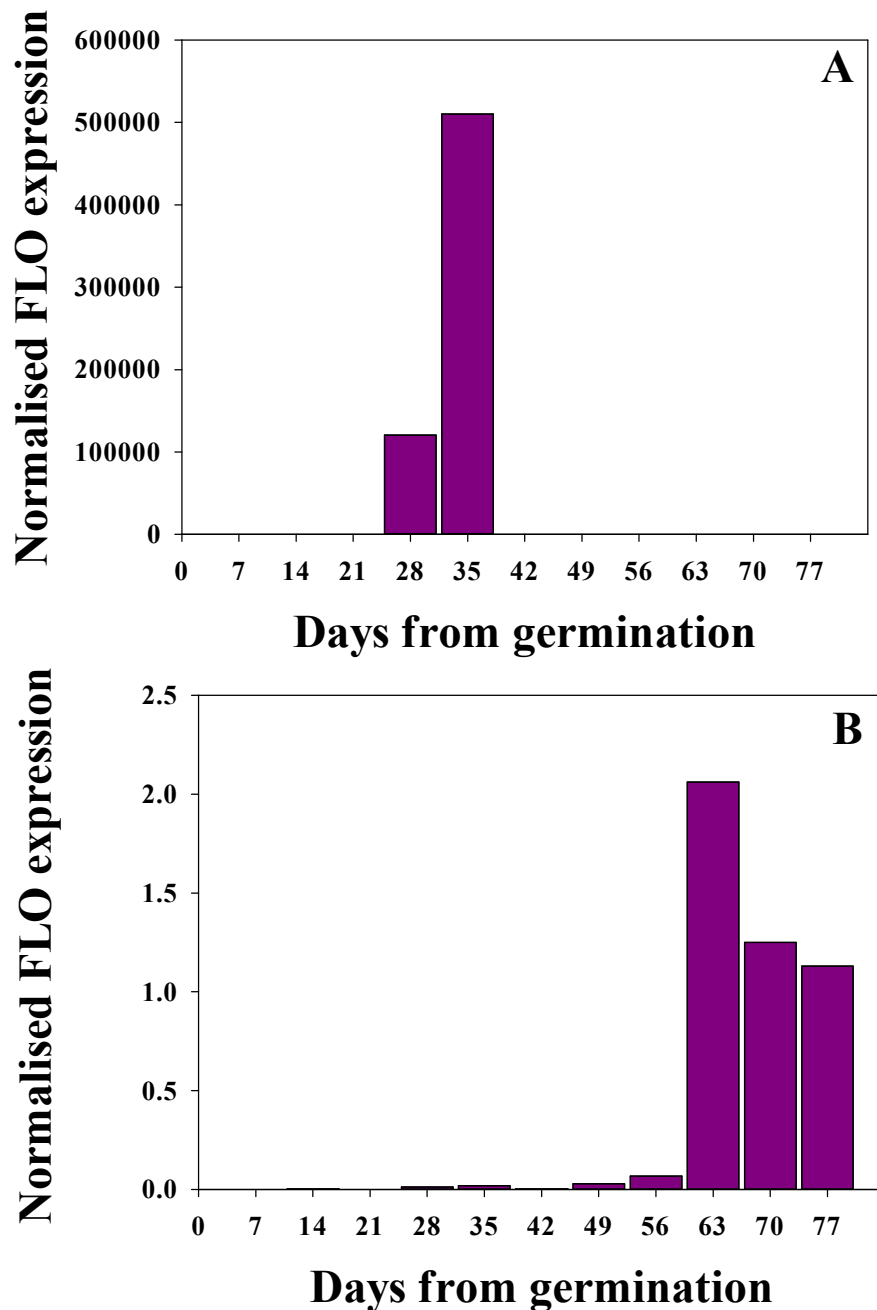


Figure 3.7 Expression of FLO in apex material from plants grown in Experiment 3 under constant LD harvested at ZT15 (A) and constant SD harvested at ZT 7(B). Real-time PCR analysis of the relative expression of FLO normalised against ELF-alpha at each time-point.

Under LD conditions *CEN* is expressed before floral initiation and peaks at 28 days when flower initiation is observed (Figure 3.8 A). *CEN* expression is delayed under SD (Figure 3.8 A). The rise in *CEN* expression levels observed in LD is not evident under SD.

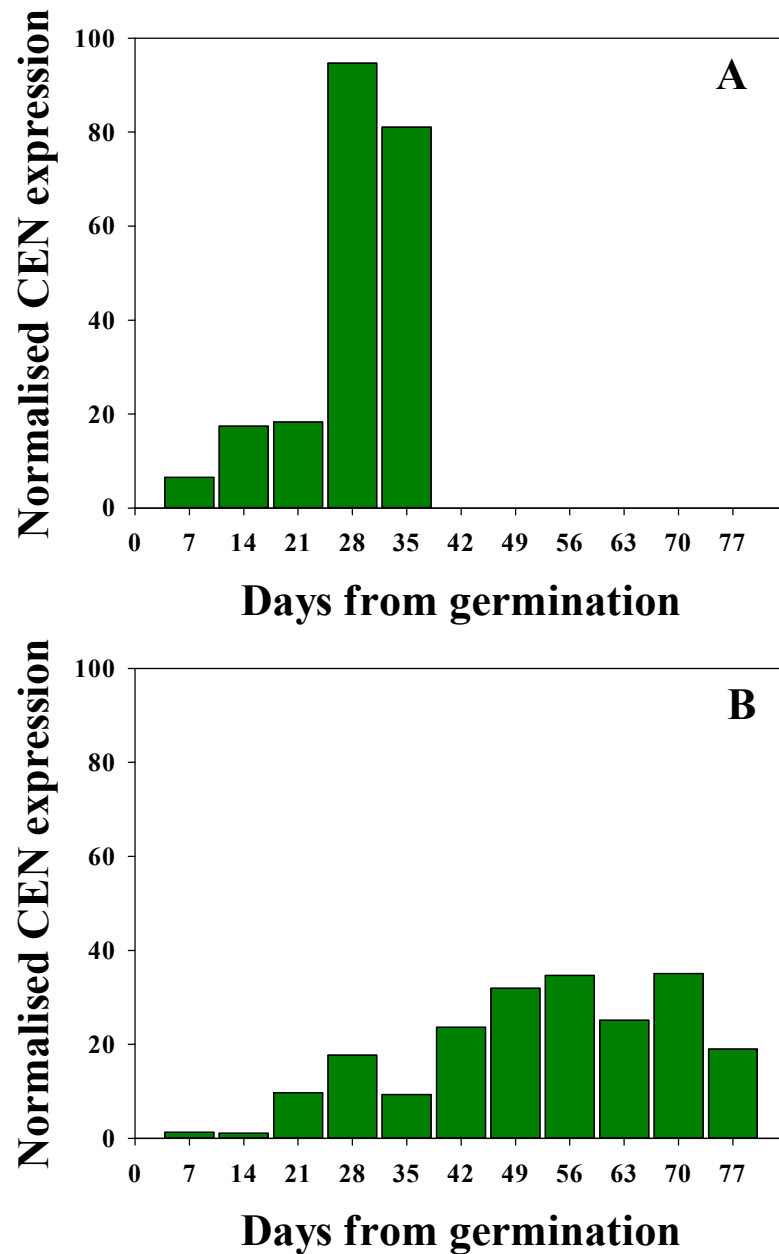


Figure 3.8 Expression of CEN in apex material from plants grown in Experiment 3 under constant LD harvested at ZT15 (A) and constant SD harvested at ZT 7(B). Real-time PCR analysis of the relative expression of CEN normalised against ELF-alpha at each time-point.

When the trends of *CEN* and *FLO* expression under LD are examined together, it is clear that that the rise of *CEN* expression precedes that of *FLO* (Figure 3.9).

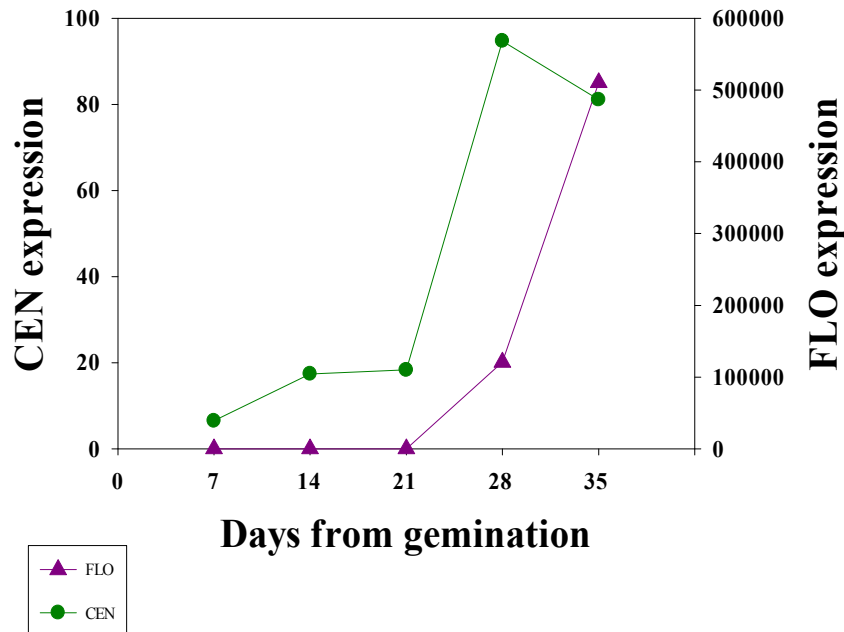


Figure 3.9 Relative expression of *CEN* and *FLO* throughout development in plants grown under constant LD in Experiment 3. *CEN* and *FLO* expression normalised against *ELF-alpha* at each time-point.

3.3.8 *AmFT* expression during different photoperiods

During transfer Experiment 3 new biological samples were collected to study *AmFT* expression in LD grown material as for Experiment 2. In addition, samples were collected from plants grown under constant SD and analysed as described in section 3.2.4 and 3.2.5.

A similar pattern of *AmFT* expression was observed in this experiment (Figure 3.10 A) compared to Experiment 2 (Figure 3.5). *AmFT* expression increases after 14 days and juvenility was estimated to end about 14.5 days after germination.

In cotyledons, *AmFT* expression is very low during the whole development phase. *AmFT* is high in all the true leaves when plants are fully competent after the end of the AVP.

In plants grown under continuous SD conditions, *AmFT* expression is very low during the whole development phase increasing after 56 days (Figure 3.10 B).

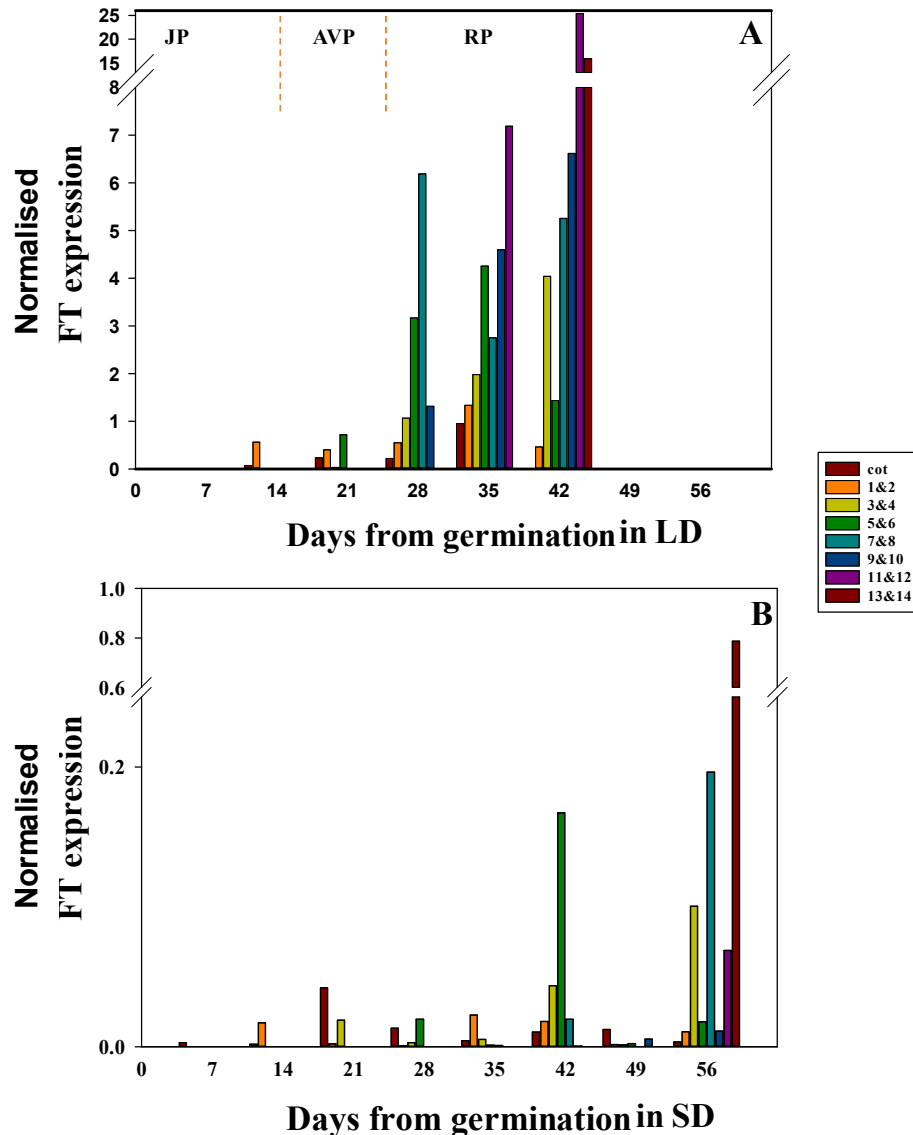


Figure 3.10 Developmental expression of *AmFT* in leaf material from *Antirrhinum* plants grown under LD at ZT 15 (A) and SD at ZT 7(B) in Experiment 3. Real-time PCR analysis of the relative expression of *AmFT* normalised to *ELF-alpha*. Expression analysed at ZT 15. JP: juvenile phase, AVP: adult vegetative phase, RP: reproductive phase. The orange dotted lines delimit the three different phases.

3.3.9 Analysis of *AtCO* expression in *Arabidopsis*

The low level of *AmFT* during juvenility could be due to inactivity of the photoperiodic pathway or to repression of *FT*. Activity of the photoperiodic pathway would ideally be tracked by following expression of *CO*. Since an *Antirrhinum CO* homologue was not available, *Arabidopsis* was used as the experimental system. In order to compare the previous results with *AtFT* expression, the length of juvenility in *Arabidopsis* was investigated. The number of leaves present at flowering time, in plants transferred from LD (DLI = 3.08 mol·m⁻²·d⁻¹) to SD (DLI = 2.79 mol·m⁻²·d⁻¹) daily for 15 days are shown in Figure 3.11. Plants were estimated to have been juvenile for 6.8 d ± 0.2 d after germination. The AVP phase lasted for 4.70 d ± 0.2 d.

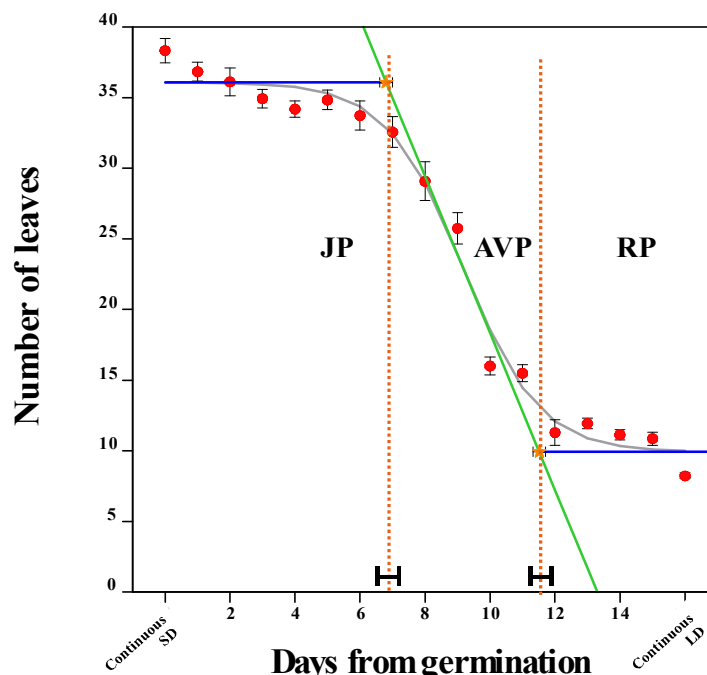


Figure 3.11 Different phases of photoperiod sensitivity in *Arabidopsis Col-0*.

The effect of transferring *Arabidopsis* at weekly intervals (expressed as days from 50% germination) from LD to SD on flowering time. JP: juvenile phase, AVP: adult vegetative phase, RP: reproductive phase, SD: short day, LD: long day. Vertical error bars denote the standard error of the mean of the number of leaves. Horizontal error bars denote the standard error of the mean of the estimated phase length. Logistic curve (grey curve), maximum slope (green line), lag time lines (blue lines). The orange dotted lines delimit the three different phases.

The expression of *AtFT* in was followed in all the rosette leaves present in the plant using Real-time PCR analysis and expression levels increased in plants grown under continuous LD at around 6 days when juvenility was shown to end (Figure 3.12 A).

Figure 3.11 B shows that in plants grown under SD, *AtFT* expression is very low during the assessment period. Although *AtFT* expression increases after the second day from germination the relative amount is too low to be considered, especially if compared to the *AtFT* expression level in plants grown under LD (Figure 3.11 A-B).

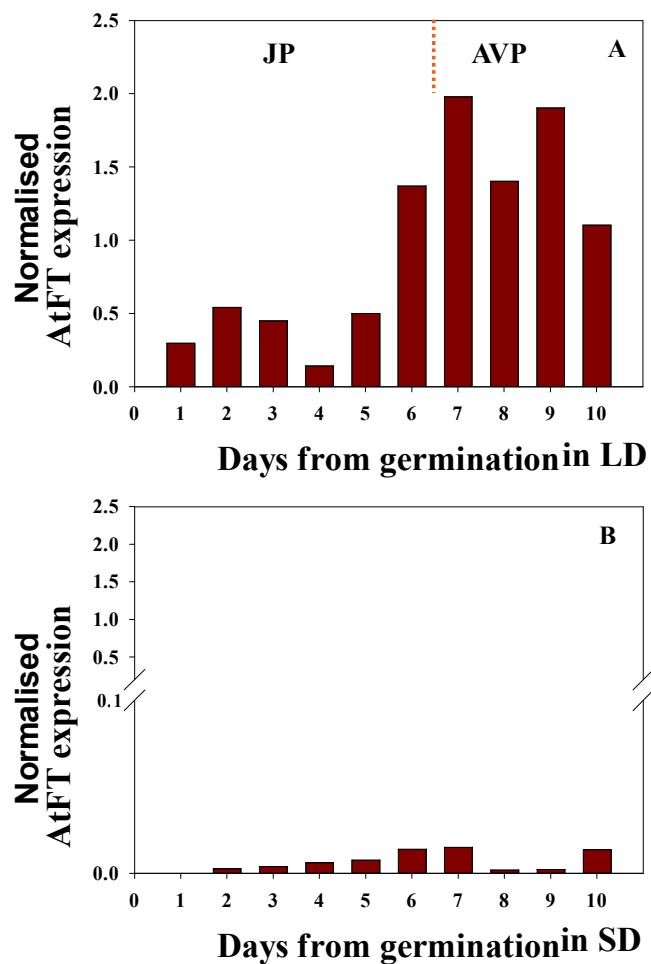


Figure 3.12 Developmental expression of *AtFT* in leaf material from plants grown under LD at ZT 15 (A) and SD at ZT 7(B).

Real-time PCR analysis of the relative expression of *AtFT* normalised to actin at each time point. JP= juvenile phase, AVP= adult vegetative phase. The orange dotted line delimits the phases.

Using Real-time PCR analysis *AtCO* expression was shown to rise from 4 days post germination in plants grown under LD (Figure 3.13 A). This occurs during the JP which ended around 6.8 days post germination. Generally the levels of *AtCO* are 1-2 orders of magnitude higher than *AtFT* levels.

In contrast under SD, *AtCO* expression is lower during the assessment period with an increase occurring at 10 days from germination (Figure 3.13 B).

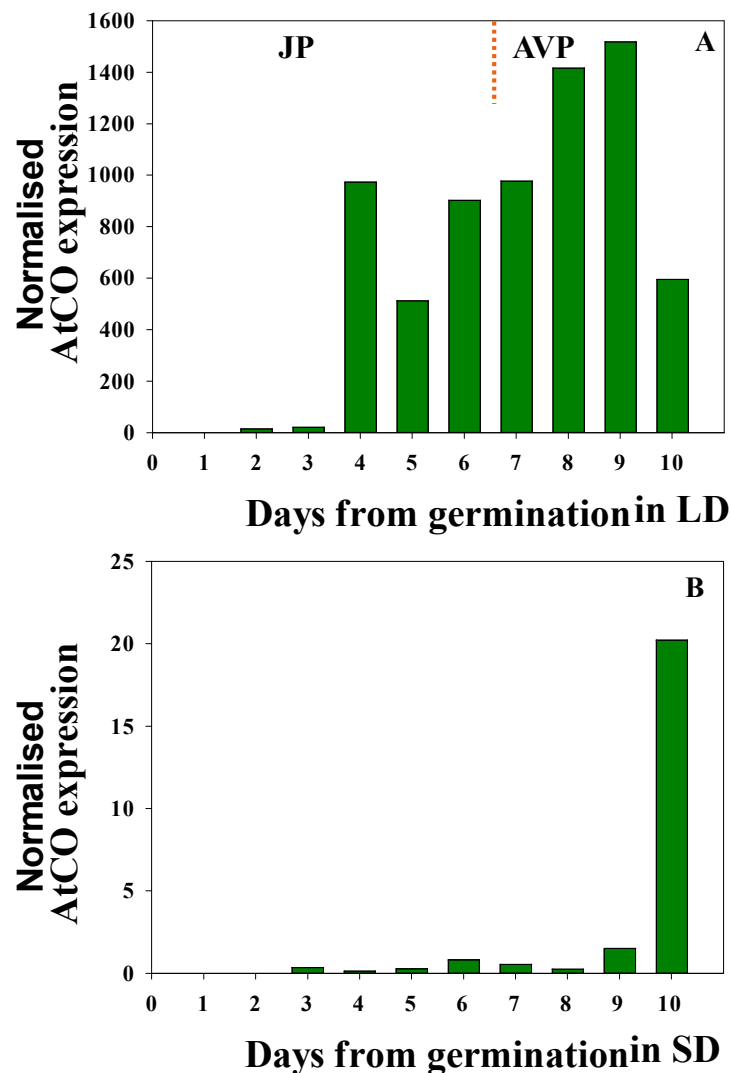


Figure 3.13 Developmental expression of *AtCO* in leaf material from plants grown under LD at ZT 15 (A) and SD at ZT 7(B). Real-time PCR analysis of the relative expression of *AtCO* normalised to actin at each time point. JP= juvenile phase, AVP= adult vegetative phase. The orange dotted line delimits the phases.

Under LD conditions where the photoperiodic pathway is active, whilst the rise in *AtFT* expression coincides with the end of juvenility, *AtCO* levels are high during juvenility and rise prior to the end of juvenility (Figure 3.14). From day 6, changes in *AtCO* were broadly mirrored by changes in *AtFT*. The same standard curve and cDNA samples were used to analyse expression of all genes, thus relative expression levels can be compared.

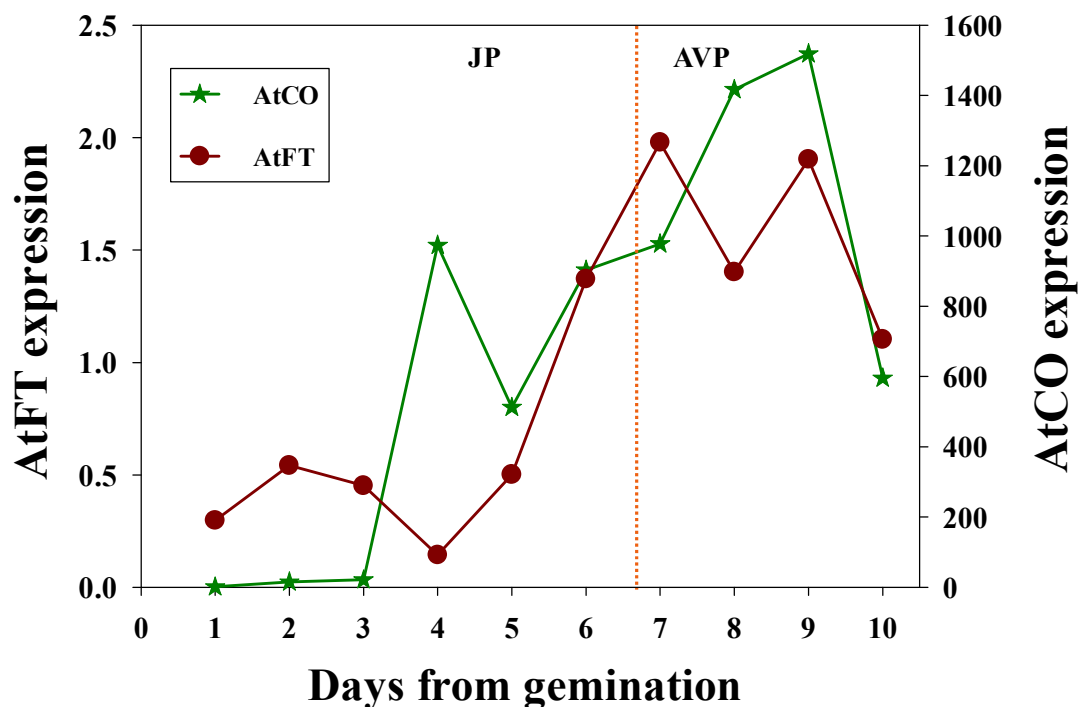


Figure 3.14 Developmental expression of *AtCO* and *AtFT* at ZT 15 in leaf material from plants grown under LD.

Real-time PCR analysis of the relative expression of *AtCO* and *AtFT* normalised to actin at each time point. JP= juvenile phase, AVP= adult vegetative phase. The orange dotted line delimits the phases.

3.4 Discussion

In the current study it has been shown that SANYO MLR-351H cabinets can be used successfully to grow *Antirrhinum* and *Arabidopsis* plants for assessment of juvenility. This represents an advantage over the use of glasshouses from logistic and economic perspectives and most importantly, in achieving reproducibility as shown by the similarity in the estimation of JP length in Experiments 2 and 3.

Under the growth conditions used the juvenile phase length of *Antirrhinum* in Experiment 1 was shown to be around 14 days post emergence, with floral initiation occurring by 28 days post emergence, based on data from the transfer experiment and observation of leaf production.

From apex observation in Experiment 2 and Real-time PCR analyses conducted in Experiment 3, expression of *CEN* and *FLO* was shown to be linked to commitment to floral initiation and not to the end of juvenility. *FLO* was not detectable early in development both in inductive LD and non inductive SD conditions. Under LD, *FLO* expression is induced earlier compared to plants grown under SD where floral induction was delayed. Furthermore, *FLO* expression in plants exposed to SD conditions was very low if compared with the relative amount of *FLO* in LD. This finding was also observed by Bradley *et al.* (1996) in *Antirrhinum*, linking *FLO* expression to floral induction. However, *LEAFY* (*LFY*) in *Arabidopsis* has been shown to be expressed during the vegetative phase rising quickly prior to the initiation of flowering in LD conditions and more slowly in SD (Blazquez *et al.*, 1997). Different roles could be played by *FLO/LFY* in *Antirrhinum* and *Arabidopsis*, respectively.

In LD, *CEN* levels increased after 21 days, which coincides with the time of floral commitment. In SD the expression was lower. *CEN* expression increased earlier compared to *FLO*, but both of them increased after floral initiation takes place. This finding matches with the hypothesis that in *Arabidopsis* TFL1 represses *LFY* in the shoots during the vegetative phase (Bradley *et al.*, 1996; Coen *et al.*, 1990). It is clear that changes in expression of neither gene are associated with the JP to AVP transition.

In Experiment 1 the JP in *Antirrhinum* was estimated to have ended 13.7 days after germination and the AVP lasted for approximately 16.5 days. The experiment was repeated at a reduced light integral in an attempt to extend the JP. In Experiment 2, when light integral was reduced, juvenility was extended by approximately one day and the AVP was prolonged by about 5 days. When Experiment 3 was performed to assess the reproducibility of the assay, similar results were generated for the JP length, while more variability was observed in the AVP length. The results obtained fit with the finding observed in other studies. In a previous study it was demonstrated that the length of juvenility is longer when the plant is exposed to a lower light integral (Adams, 1999). Cremer *et al.* (1998) showed that, for *Antirrhinum*, a higher light integral decreases flowering time and using different shading levels with *Antirrhinum* Munir, *et al.* (2004) concluded that lower levels of light intensity extend flowering time.

FT is one of the key genes in the photoperiodic pathway (Araki *et al.*, 1998; Turck *et al.*, 2008). *FT* is induced in leaves during LD in *Arabidopsis* (Kotake *et al.*, 2003) then it moves through the phloem to the apex to induce flowering (Corbesier *et al.*, 2007). Expression of this gene was analysed throughout plant development.

The current study provides the first description of spatial and temporal *AmFT* gene expression in all the leaves and throughout development. It is shown that *AmFT* expression is lower but not absent during juvenility and increases in all leaves during adulthood in plants grown under LD showing an increase of sensitivity to LD throughout phases. This result complements a previous study in which expression of *FT* was tested in the youngest expanded leaves during *Antirrhinum* development (Thomas, 2009). Other researches demonstrate changes in the expression of *FT* at specific stages of development of several plants. In Poplar two *FT* homologues, *PtFT1* and *PtFT2* have been isolated and it has been suggested that both *PtFT1* and *PtFT2* follow a circadian rhythm and regulate the transition from the JP to the AVP (Bohlenius *et al.*, 2006; Hsu *et al.*, 2006). In apple *FT*-like genes exhibit circadian expression patterns (Traenkner *et al.*, 2010). *MdFT1* expression levels are high in apical buds during the adult phase while *MdFT2* was expressed in reproductive organs, but they both act as floral promoters (Kotoda *et al.*, 2010). *FT*-like genes are also involved in the regulation of the juvenile-to-adult phase transition but they may also play different roles in the same plant.

As described in the introduction, in *Arabidopsis* one of the key genes involved in *FT* regulation is *CO*. *CO* is activated by the circadian clock and *CO* expression peaks at about 16 h ZT (Wigge, 2011). *CO* protein, which activates *FT* expression, is degraded in the dark and stabilised in the light. In the current study *CO* expression was used as a marker for the photoperiodic pathway being active during juvenility. In *Antirrhinum*, the *CO* homologue has not yet been isolated. Using *Arabidopsis* as a model, it was shown that *CO* levels rise before the end of juvenility and *FT* levels rise around the end of juvenility. In the literature, *CO* expression level has been shown to be present throughout development, increasing

during floral transition (Castillejo and Pelaz, 2008). No studies have been published about *CO* expression in the early stages of development or in relation to the JP.

The data presented in the current study showed that in *Arabidopsis* the photoperiodic pathway is active before the end of juvenility. It can be concluded, therefore, that other factors or repressors may repress *FT* transcription during juvenility to avoid premature flowering.

CHAPTER 4. ISOLATION AND CHARACTERIZATION OF *ANTIRRHINUM* AND OLIVE TEMPRANILLO ORTHOLOGS

4.1 Introduction

The switch between vegetative and reproductive growth phases is one of the main transitions plants undergo during post embryonic development. This process is regulated by a complex pathway synchronized by both endogenous and exogenous factors. In *Arabidopsis*, one of the key genes involved in this process is *FLOWERING LOCUS T (FT)*. *FT* expression is rapidly induced by CONSTANS (*CO*) as described in chapter 1. In chapter 3 it was shown that *FT* expression levels rise after the end of juvenility in both *Arabidopsis* and *Antirrhinum*; *CO* expression was shown to be high prior to the end of juvenility. This indicated that mechanisms may be involved to repress *FT* during juvenility hence to avoid premature flowering.

The B3 super-family of transcription factors contains 6 different groups of genes: HSI (HIGH-LEVEL EXPRESSION OF SUGAR-INDUCIBLE GENE), LAV (LEAFY COTYLEDON2/ABSCISIC ACID INSENSITIVE3 and HSI/VAL), ABI3/VPI (ABSCISIC ACID INSENSITIVE 3/VPI), ARF (AUXIN RESPONSE FACTOR), REM (REPRODUCTIVE MERISTEM) and RAV (RELATED TO ABI3/VPI) (Romanel *et al.*, 2009). The B3 domain, a basic domain, was first identified in the maize gene *VIVIPAROUS (VP1)*. VP1 also contains B1 and B2 domains. B3 is a DNA binding domain that can bind to different target sites

according to which sub-family of genes it resides in. Each sub-family of B3 genes contains a defining set of conserved amino acids (Swaminathan *et al.*, 2008).

The RAV sub-family is classified by the conserved WN/RSSQS motif found at amino acid position 245-250 (Swaminathan *et al.*, 2008). In *Arabidopsis*, 13 RAV genes have been classified and these are divided into 2 classes. Class I comprises six members that contain the APETALA2 (AP2) DNA binding domain in addition to the B3 domain (Romanel *et al.*, 2009) (Figure 4.1) and Class II contains 7 other less characterised genes (Table 4.1).

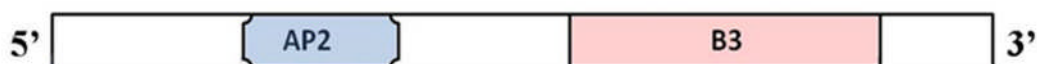


Figure 4.1 Structure of genes belonging to the RAV class I sub-family of the B3 super-family

Table 4.1 RAV gene family table.
Adapted by Romanel *et al.* (2009)

Gene Family	Gene name	Genomic locus	Protein locus
RAV Class I	RAV1	At1g13260	NP_172784
RAV Class I	RAV1-like	At3g25730	NP_189201
RAV Class I	RAV2/TEM2	At1g68840	NP_564947
RAV Class I	TEM1	At1g25560	NP_173927
RAV Class I	RAV-like 4	At1g50680	NP_175483
RAV Class I	RAV-like 5	At1g51120	NP_175524
RAV Class II	RAV-like 3	At5g06250	NP_001119177
RAV Class II	RAV-like 1	At2g36080	NP_850260
RAV Class II	RAV-like 2	At3g11580	NP_850559
RAV Class II	NGA1	At2g46870	NP_566089
RAV Class II	NGA2	At3g61970	NP_191756
RAV Class II	NGA3	At1g01030	NP_171611
RAV Class II	NGA4	At4g01500	NP_192059

The N-terminal AP2 domain recognises the CAACA motif within genes whilst the C-terminal B3 domain recognises the CACCTG sequence, irrespective of their relative orientation on the DNA strands (Kagaya *et al.*, 1999).

RAV1 and *RAV2* (or *TEMPRANILLO2*) were cloned from *Arabidopsis thaliana* by Kagaya *et al.* (1999). Recent work has demonstrated that *RAV1* and *RAV2* expression can change according to various stimuli such as temperature, pathogen attack and steroids (Hu *et al.*, 2004). Brassinosteroids (BRs) are a group of plant steroidal hormones which play an important role in many aspects of plant growth. When the BR-deficient (*det2*) mutants were treated with 24-epibrassinolide, *RAV1* mRNA levels decreased in a dose-dependent manner, which indicated that *RAV1* may be down-regulated by BRs (Hu *et al.*, 2004). Also miRNA172 has been reported to down regulate genes with AP2 domains (Aukerman and Sakai, 2003). Plants can activate RNA silencing if attacked by pathogens and many plant viruses can suppress this process. *RAV2* has been reported to be required for blocking RNA silencing by 2 distinct viral proteins (Endres *et al.*, 2010). Despite the similarity between *RAV1* and *TEMPRANILLO1* (*TEM1*) genes with *RAV2* (*TEM2*), *RAV1* and *TEM1* could not functionally complement the *rav2* mutant (SALK_070847) with respect to suppression of RNA silencing (Endres *et al.*, 2010).

RAV-like genes have been cloned and characterised in other species. *Capsicum annuum*, chilli pepper *CaRAV1* is involved in plant defence responses and shares 69% amino acid identity with *RAV1* and 73% with *RAV2* with an even higher sequence identity in the AP2 and B3 domain (Kim, *et al.*, 2005). In *Galega orientalis*, *GoRAV* is induced by exogenous ABA, low temperature and high-salinity and its expression level decreases if treated with BRs. The overall amino acid sequence identities between *GoRAV* and *Arabidopsis* *RAV1* and 2 and *Glycine*

max RAV-like are 55.13%, 57.61% and 72.24%, respectively (Chen, *et al.*, 2009). In the SDP soybean, *GmRAV* shares 54.8% identity with *Arabidopsis* RAV1, 55.5% identity with *Arabidopsis* RAV2 and 55.1% with *Oryza sativa* RAV2. *GmRAV* expression levels are higher in SD with peaks of expression one and six days after germination. In LD, over-expression of *GmRAV* in tobacco leads to a delay in flowering (Zhao *et al.*, 2008). Hu *et al.* (2004) also transformed *Arabidopsis* with both sense- and anti-sense *RAV1* constructs. Plants with reduced *RAV1* expression flowered 4.8 days earlier than the WT and 6.6 days earlier than those over-expressing *RAV1*, suggesting that RAV1 may act as a repressor of growth and development.

TEM1 and TEM2, have been shown to repress flowering in *Arabidopsis* (Castillejo and Pelaz, 2008). They are proposed to act redundantly to repress *FT*, binding to its 5' untranslated region. Ectopic over-expression of both genes causes late flowering and *TEM1* over-expression almost completely suppresses *FT* expression (Castillejo and Pelaz, 2008). In *Arabidopsis* *TEM1* follows a circadian rhythm, peaking at dusk whilst in *Castanea sativa* *RAV1* (*CsRAV1*), a *TEM1* homologue, peaks at noon (Castillejo and Pelaz, 2008; Moreno-Cortés *et al.*, 2012). In *Arabidopsis* it has been shown that *TEM1* mRNA is abundant in seedlings and declines before the floral transition when *FT* levels peak. Furthermore, *TEM1* and *TEM2* have been proposed to antagonise CO activity by competing for the *FT* binding site (Castillejo and Pelaz, 2008). Additionally, chestnut *CsRAV1* has been shown to induce early formation of sylleptic branches in poplar with no difference in wood anatomy; flowering time was not investigated in the study (Moreno-Cortés *et al.*, 2012).

4.1.1 Olive

Juvenility in olive can last for up to 15-20 years with the length being genotype-dependent (El Riachy *et al.*, 2011; Leon and Downey, 2006). Juvenility can additionally be influenced by the vigor of the seedlings. JP can be shortened by all the factors that increase seedling development like soil solarisation, fertilisation and irrigation management (El Riachy *et al.*, 2011; Gucci and Cantini, 2000). Generally, if an olive plant is vegetatively-produced it may take 2-3 years before the first flowers are produced, with production starting after 7-8 years and full production being reached after 30 years. Morphological traits like leaf shape and size and internode length can be used to distinguish juvenile and mature olive plants, but these characteristics may change between cultivars and, due to solar exposure, they can be visible at the base of the trunk of adult plants (Garcia *et al.*, 2000; Gucci and Cantini, 2000). Achieving predictable flowering in olive is important for planning actions such as pest control treatments (Perez-Lopez *et al.*, 2008). It is also important for breeding projects, where high yields, desirable fruits characteristics and adaptability to different environments are necessary (Bellini *et al.*, 2008).

Since it was hypothesised that *FT* levels are low during juvenility due to repression, having shown that the photoperiodic pathway is active, and armed with the knowledge that TEM binds to the 5' UTR of the *FT* gene and also represses flowering, *TEM* was chosen as a candidate to study in relation to juvenility. The first step in the process was to isolate homologues from other species to enable the study.

The aim of the work in this chapter was to isolate and characterise a *TEM* homologue from *Antirrhinum*. No other *Antirrhinum RAV-like* class I genes in *Antirrhinum* have been identified to date. A further part of this study involved the isolation and characterisation of a *TEM* homologue from *Olea europaea* (Olive). This part of the project involved collaboration with Università degli Studi della Tuscia-Dipartimento di scienze e tecnologie per l'Agricoltura, le Foreste, la Natura e l'Energia (DAFNE) (Italy) who provided plant samples.

4.2 Materials and Methods

This section describes the materials and methods specific for this results chapter. Protocols and materials common to more than one chapter are described in chapter 2. All primer details are listed in the Appendix, Table A.1, A.2, A.3, A.4 and A.5.

4.2.1 *Antirrhinum* leaf samples

Leaf material harvested in *Antirrhinum* during Experiment 2 when plants were 12 days old, hence still juvenile and from 24 day old plants, hence adult, was pooled, total RNA extracted and cDNA synthesised as described in section 2.6.

4.2.2 *Olive* leaf samples

Leaf samples were collected on the 25th of June 2010 at 20:00 (sun rise was at 5:34, sun set was at 20:52), frozen in liquid nitrogen and stored at -80°C until their utilization. Total RNA isolated using RNeasy Plant Mini Kit (Qiagen Inc, Cat. No. 74903, UK) was provided by Prof Rosario Muleo (Universita' degli studi della Tuscia, DAFNE; ITALY). The cDNA was synthesised as described in section 2.6.

4.2.3 *Arabidopsis* leaf samples

Leaf material harvested from *Arabidopsis* at different stages of development (1, 2, 3, 7, 8 and 9 days old plants) was pooled together, total RNA extracted and cDNA synthesised as described in section 2.6.

4.2.4 Isolation of a partial TEM like cDNA sequences from *Antirrhinum* and Olive

4.2.4.1 Isolation of an internal partial sequence of putative *AmTEM*

A partial sequence of *Antirrhinum majus* TEM (*AmTEM*) was isolated by PCR of cDNA using degenerate primers. To aid in the design of degenerate primers the sequences of *Arabidopsis* TEM1, TEM2 and RAVs were obtained from the TAIR database (<http://www.arabidopsis.org/>) and the Basic Local Alignment Search Tool (BLAST) from the National Center for Biotechnology Information (NCBI) GenBank database (<http://www.ncbi.nlm.nih.gov/>) was used to identify other sequences with high sequence homologies. Amino acid sequences used for the alignment were RAVs and RAV-like from different species selected for high homology to the *Arabidopsis* RAV family genes (Table 4.1). A total of 41 amino acid sequences were collected (Appendix, Figure A.6). After initial screening based on phylogenetic analyses (Appendix, Figure A.7) and presence of conserved amino acids in the B3 domain and the presence of the AP2 domain, 23 sequences were aligned using the web-based Multalin software (<http://multalin.toulouse.inra.fr/multalin/multalin.html>) (CORPET) and degenerate primers were designed (Appendix, Figure A.8). To design degenerate primers amino acid sequences were aligned to identify regions of sequences conserved, primers were based on amino acid sequences found in AtTEM1 and AtTEM2 in conserved regions and Codon Usage Database (<http://www.kazusa.or.jp/codon/>) for *Antirrhinum* to determine nucleotides to incorporate into degenerate primers was consulted.

Primers were designed to anneal to different regions of the gene covering almost all the entire *TEM1/2* sequence (Figure 4.2).

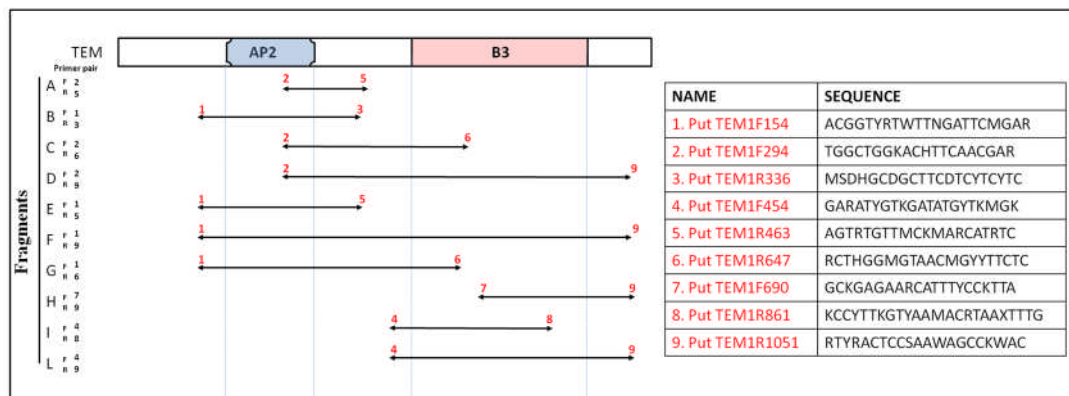


Figure 4.2 Representation of the annealing position of the 10 combinations of degenerate primers used to isolate *AmTEM* and list of the primers sequences.

Antirrhinum cDNA, obtained as described in section 4.2.1, was used as template in the PCR mix, as described in section 2.7 and primers were used at 0.5 μ M. PCR amplification consisted of an initial denaturation at 95°C for 2 min, followed by 35 cycles of denaturation at 94°C for 20 s, gradient annealing temperature from 48°C to 65°C for 10 s, and extension at 70°C for 15 s. A further 10 min of extension at 70°C was carried out at the end of the cycles.

PCR products were visualized on agarose gels as described in section 2.9. Products of the expected lengths were purified as described in section 2.10, using QIAquick® gel Purification Kit (Qiagen, Australia) and ligated into the pGEM-T Easy vector as described in section 2.11.

Ligated vector products (2 μ l) were added to 20 μ l of electrocompetent EC100 *E. coli* cells and electroporated as described in 2.11.

Cells were then plated out on LB/Agar plates containing ampicillin, isopropyl/-D- thiogalactoside (IPTG) and 5-bromo-4-chloro-3-indolyl-beta-D-galactopyranoside (X-Gal) as described in section 2.12. Colony PCR was performed as described in section 2.7 and plasmid DNA isolated from a 5 ml overnight culture in LB medium as described in section 2.12. Plasmid DNA was sequenced as described in section 2.14 using M13 primers.

Contigs were obtained from sequenced fragments, using the Seqman package of DNASTar (DNASTar Inc.). New primers, CI-AmF and CI-AmR specific for the 5'- and 3'- of the contig representing the middle portion of the gene were designed and used in PCR at 0.5 μ M with an annealing temperature of 55°C as described in section 2.7 to isolate the entire contig as a single fragment. Gel isolation, cloning and sequencing using CI-AmF and CI-AmR, were carried out described in sections 2.9-2.14, to confirm the sequence of the contig, called Contig CI (Appendix, Figure A.9).

4.2.4.2 Internal portion of *OeTEM*

A partial putative sequence (isotig13527) of an *Olea europaea TEM* (*OeTEM*) was obtained by Prof. Rosario Muleo from the Università degli Studi della Tuscia (Appendix, Figure A.10). The sequence was found by performing a BLAST search comparing the *Arabidopsis TEM1* and *TEM2* AP2 domains with 448,892 assembled sequenced ESTs of a total of 95578 unigenes, 75388 Singleton and 20170 Tentative Consensus in an Olive floral library (sequenced obtained with 454-Read, Roche) (Prof Rosario Muleo personal communication).

4.2.4.3 5'- and 3'-Rapid amplification of cDNA ends of *AmTEM* and *OeTEM*

To obtain partial cDNAs representing 5'- and 3'- ends of *AmTEM* and *OeTEM*, Rapid Amplification of cDNA Ends (RACE)-PCR was performed on 7 µg of DNase-I treated total RNA from *Antirrhinum* and olive leaf material described in section 4.2.1 and 4.2.2 using the GeneRacer (GeneRacer kit, Invitrogen Ltd. Cat. No. L1500-01, USA) kit 5'- and 3'-RACE protocols following the manufacturer's guidelines.

To obtain the 3'- end, RNA was reverse transcribed, as described in section 2.6, using a GeneRacer Oligo(dT) primer. For the first round of PCR, PCR reactions were set up as described in section 2.7, using either *Antirrhinum* TEM gene specific primer (GSP) Forward or Olive TEM GSP Forward with the GeneRacer reverse primer, GeneRacer™ 3', to amplify *AmTEM* and *OeTEM* 3'-ends respectively. Amplification consisted of an initial denaturation at 94°C for 2 min, followed by 5 cycles of 94°C for 30 s, 72° for 1 min, followed by 30 cycles of 94°C for 30 s, 70° for 1 min. A further 10 min of extension at 72°C was carried out at the end of the cycles.

Nested PCRs were set up as described in section 2.7 using either *Antirrhinum* TEM GSPN Forward or Olive TEM GSPN Forward with the GeneRacer nested reverse primer, GeneRacer™ 3' Nested, to amplify *AmTEM* and *OeTEM* 3'- ends, respectively. Amplification consisted of an initial denaturation at 94°C for 2 min, followed by 30 cycles of 94°C for 30 s, 70° for 1 min. A further 10 min of extension at 72°C was carried out at the end of the cycles.

Products of the expected size were gel-purified and cloned into the pGEM-T Easy vector as described in section 2.10. Plasmid DNA was extracted as described

in section 2.13 and inserts sequenced with M13 primers as described in section 2.14.

The same mRNA templates used to obtain the 3'- end sequence were used for cDNA synthesis to obtain the 5'- end of the cDNA from *AtTEM* and *OeTEM* following the manufacturer's instructions.

For the first round of PCR, PCR reactions were set up as described in section 2.7, using GeneRacer forward primer, GeneRacer™ 5' Primer, with either *Antirrhinum* TEM GSP Reverse or Olive TEM GSP Reverse, to amplify *AmTEM* and *OeTEM* 5'- ends, respectively. Amplification consisted of an initial denaturation at 94°C for 2 min, followed by 5 cycles of 94°C for 30 s, 72° for 1 min, followed by 30 cycles of 94°C for 30 s, 70° for 1 min. A further 10 min of extension at 72°C was carried out at the end of the cycles.

Nested PCRs were set up as described in section 2.7 using GeneRacer nested reverse primer, GeneRacer™ 5' Nested, with either *Antirrhinum* TEM GSPN Reverse or Olive TEM GSPN Reverse with the to amplify *AmTEM* and *OeTEM* 5'- ends, respectively. Amplification consisted of an initial denaturation at 94°C for 2 min, followed by 30 cycles of 94°C for 30 s, 70° for 1 min. A further 10 min of extension at 72°C was carried out at the end of the cycles.

Products of the expected size were gel-purified and ligated into the pGEM-T Easy vector, plasmid DNA extracted as described in section 2.12 and 2.13 and inserts by sequenced with M13 primers as described in section 2.14.

4.2.5 *Acquisition of full length cDNAs representing AmTEM, OeTEM and AtTEM1*

Full length cDNA representing *AmTEM* and *OeTEM* and *AtTEM1* were obtained using PCR conditions and AmTEM1F/AmTEM1072R, OeTEM1F/OeTEM1074R and AtTEM1-F/AtTEM1091-R specific primers, respectively, as specified in section 2.7.

4.2.6 *Amino acid sequence comparisons and phylogenetic analysis*

The nucleotide and deduced amino acid sequences of the *AmTEM* and *OeTEM* cDNA were used for BLAST searches on the NCBI GenBank database. The deduced amino acid sequences were aligned using the Clustal W MegAlign package of DNASTar (DNASTar Inc.). Evolutionary relationships of RAV sub-family members were inferred using the Maximum Parsimony method. Bootstrap values were derived from 500 replicate runs.

4.2.7 *Cloning of full length cDNAs into the Gateway binary vector for Agrobacterium-mediated transformation of Arabidopsis*

Products were sequenced as described in section 2.14 and ligated into the pGEM-T Easy vector as described in section 2.11 and 2.12. Plasmid DNA was isolated, as in section 2.13 and used as template in PCR to attach att-sites at the ends of each cDNA fragment for Gateway cloning.

PCR conditions used were: 1 cycle for 2 min at 95°C; 4 cycles for 20 s at 95°C, 10 s at 55°C, 1 min at 70°C; 20 cycles for 20 s at 95°C, 10 s 63°C (for

AmTEM1F/AmTEM1072R) or 65°C (for OeTEM1F/OeTEM1074R) or 61°C (for AtTEM1-F/AtTEM1091-R), 1 min at 70°C and 1 cycle for 5 min at 70°C. PCR reagents were used at concentration described in section 2.7. Products were gel-purified as in section 2.10 and cloned into Gateway® pDONR™207 vector (Invitrogen Ltd., USA) (Figure 4.3) using a Gateway® BP Clonase® II enzyme mix (Invitrogen, Cat No. 11789-020) following the manufacturer's instructions. The genes were then cloned, using a Gateway® LR Clonase® II (Invitrogen, Cat. No. 11791-043 USA), into a pB2GW7 binary vector (Figure 4.4) (Invitrogen Ltd., USA) to produce the pBAmTEM, pBOeTEM and pBAAtTEM1 vectors. The pB2GW7 vector contains a CaMV 35S promoter and the *bar* gene which confers resistance to the herbicide Glufosinate-ammonium.

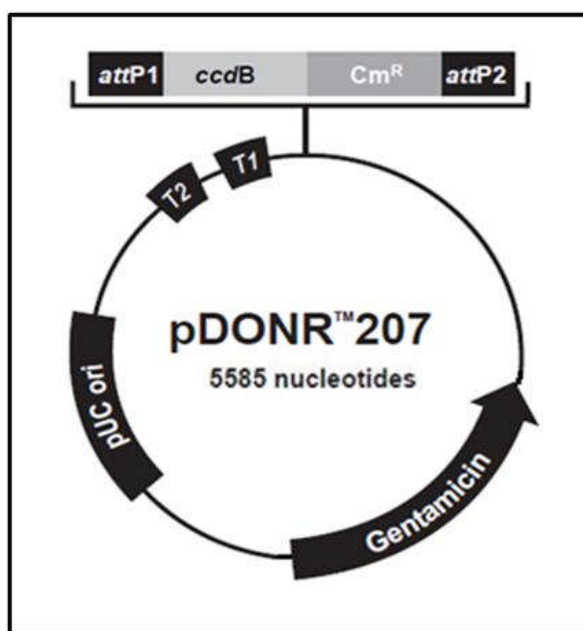


Figure 4.3 Map of pDONR 207 vector

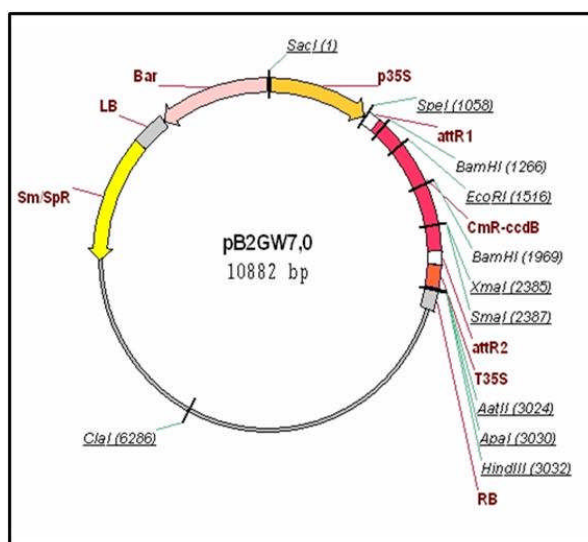


Figure 4.4 Map of the pB2GW7 vector

Plasmid DNA was then isolated as in section 2.12 and the presence of the appropriate gene in the vectors was confirmed by sequencing with gene specific primers seq Amtem F/seq Amtem R (for *Antirrhinum*), seq Oetem F/seq Oetem R (for Olive) and seq Attem1 F/ seq Attem1 R (for *Arabidopsis*), as explained in section 2.14.

4.2.8 Prepararion and Transformation of competent *Agrobacterium* cells

Agrobacterium cells, strain c58pGV3101, were cultured to an O.D. of 0.2-0.4 at 28°C in 200 ml LB media containing Gentamycin (50 µg/ml). The cells were then collected by centrifugation at 3000 rpm at 4°C for 10 min and resuspended in 20 ml ice-cold 1 mM Hepes (pH 7.0). After a further centrifugation the cells were resuspended in 2 ml of ice-cold 10% (v/v) glycerol. This step was repeated again and then the cells were split into 50 µl aliquots and frozen in liquid nitrogen and then stored at -80°C.

The *Agrobacterium* strain c58pGV3101 was then transformed by electroporation as described in 2.12 with pBAmTEM, pBOeTEM and pBAAtTEM1 vectors. *Agrobacterium* plasmid DNA was isolated as described in section 2.13 and the presence of the appropriate genes confirmed using PCR. PCR conditions used were: 1 cycle for 2 min at 95°C; 4 cycles for 20 s at 95°C, 10 s at 55°C, 1 min at 70°C; 20 cycles for 20 s at 95°C, 10 s 63°C (for AmTEM1F/AmTEM1072R) or 65°C (for OeTEM1F/OeTEM1074R) or 61°C (for AtTEM1-F/AtTEM1091-R), 1 min at 70°C and 1 cycle for 5 min at 70°C. PCR reagents were used at concentration described in section 2.7.

4.2.9 *Agrobacterium* mediated plant transformation of *Arabidopsis* with *AmTEM*, *AtTEM1* and *OeTEM*

Agrobacterium harbouring pBAmTEM, pBOeTEM or pBAAtTEM1 vectors was used to transform 10 Col-0, and 10 *tem1 Arabidopsis* plants using the floral dip method (Clough and Bent, 1998). T₀ plants were grown in Sanyo MLR plant growth chambers and T₁ seeds collected. *Arabidopsis* plants transformed with *AmTEM* gene were grown under SD conditions while *Arabidopsis* plants transformed with *OeTEM* and *AtTEM1* genes were grown under LD conditions. T₁ generation seeds were sown, stratified and grown as described in section 2.3 under LD conditions. Plants were sprayed 3 times, every 2 weeks from emergence of the first true leaves, with the BASTA herbicide (Bayer CropScience, Cat. No. 05936136), containing Glufosinate-ammonium at a concentration of 150 mg/l. The resistant plants were allowed to flower. Flowering times were recorded as time to

flowering from germination and number of rosette leaves at 1 cm bolt. T₂ seeds were collected.

4.2.10 *PCR screening of transformed plants*

Genomic DNA from T₁ plants was extracted as in section 2.5 and PCRs performed as described in section 2.7 to confirm the presence of the transgenes using the gene specific primers seq Amtem F/seq Amtem R, seq Oetem F/seq Oetem R and seq Attem1 F/ seq Attem1 R to amplify *AmTEM*, *OeTEM* and *AtTEM1*, respectively. PCR conditions used were: 1 cycle for 2 min at 95°C; 30 cycles for 20 s at 95°C, 10 s 57°C (for seq Amtem F/seq Amtem R) or 63°C (for seq Oetem F/seq Oetem R) or 61°C (for seq Attem1 F/ seq Attem1 R), 1 min at 70°C and 1 cycle for 5 min at 70°C. PCR reagents were used at concentration described in section 2.7.

4.2.11 *Semi-quantitative PCR*

Semi-quantitative PCR to determine differential expression of *AmTEM* and *OeTEM* was performed as described in section 2.7. cDNA templates for *Antirrhinum* were the samples T_{3.1} and T_{6.1}, as explained in Table 3.1 chapter 3, representing a juvenile and an adult sample, respectively. cDNA samples used for the olive analysis represent a juvenile and an adult sample as explained in section 4.2.2. The amplification consisted of an initial denaturation at 94°C for 2 min, denaturation at 94°C for 15 s, annealing for 30 s, and extension at 72°C for 30 s for

a range of cycles, comprising between 15 and 40. Primers, cycle ranges and annealing temperatures used to detect each gene are shown in Table 4.2.

Table 4.2 Primers used for semi-quantitative analysis of *AmELFa*, *AmFT*, *AmTEM*, *OeActin* and *OeTEM* expression.

Organism and gene (GenBank Acc. No.)	Primer name	T _m	Final concentration	Range of cycles tested	Optimum cycle for semi- quantitative analysis
<i>Antirrhinum</i> Elongation factor α (AJ805055)	Ant elf-alpha F	61°C	0.5µM	15-29	25
	Ant elf-alpha R		0.5µM		
<i>Antirrhinum</i> FT (AJ803471)	Ant put FT F	63°C	0.5µM	27-40	36
	Ant put FT R		0.5µM		
<i>Antirrhinum</i> TEM	Ant fragment TEM F	61°C	0.5µM	27-40	35
	Ant fragment TEM R		0.5µM		
Olive actin1 (AY788899)	Oe-Actin F	65°C	0.5µM	20-29	22
	Oe-Actin R		0.5µM		
Olive TEM	Oe fragment TEM F	61°C	0.5µM	25-32	27
	Oe fragment TEM R		0.5µM		

4.3 Results

4.3.1 Screening of RAV sequences

Fifty-two RAV and RAV-like protein sequences were aligned (Figure 4.5). Although 11 of them had been classified in the RAV sub-family, they lack the conserved amino acids WN/RSSQS in the B3 domain (Swaminathan *et al.*, 2008) and were hence excluded from the sequence comparisons.

Species/Abbrv	
1. Arabidopsis thaliana TEM1 NP 173927	--KVMRF RYSYWNSSQS YVLT KGS RFVKEKNLRAGDVVCFERS----
2. Arabidopsis thaliana TEM2 (RAV2) NP 564947	--KVMRF RYSYWNSSQS YVLT KGS RFVKEKNLRAGDVVTFERS----
3. Arabidopsis thaliana RAV1 NP 172784	--KVMRF RYSYWNSSQS YVLT KGS RFVKEKNLRAGDVVFSRS----
4. Arabidopsis thaliana RAV1-like NP 189201	--KVMRF RYSYWNSSQS YVLT KGS RFVKEKNLRAGDVVFSRS----
5. Arabidopsis thaliana RAV-like 4 NP 175483	--RQWKF RYCYWNSSQS FVFT TCGWNSFVKEKNLKEKDI AFYTC DVPNN--
6. Arabidopsis thaliana RAV-like 5 NP 175524	--RQWKF RYCYWNSSQS FVFT TCGWNSFVKEKNLKEKDI AFYTC DVPNN--
7. Vitis vinifera RAV-like XP 002276492	--IPWTF RYSCWESNQS FVFT TCGWNSFVNAKRLKRGETISFYRCGIR---
8. Vitis vinifera RAV-like2 CAN68564	--KVMRF RYSYWNSSQS YVLT KGS RFVKEKNLRAGDVVFSRS----
9. Calceola orientalis RAV-like ACI46678	--KVMRF RYSYWNSSQS YVLT KGS RFVKEKNLRAGDVVFSRS----
10. Nicotiana glauca RAV ACF74549	--KVMRF RYSYWNSSQS YVLT KGS RFVKEKNLRAGDVVFSRS----
11. Populus trichocarpa RAV1 XP 002315958	--KVMRF RYSYWNSSQS YVLT KGS RFVKEKNLRAGDVVFSRS----
12. Populus trichocarpa RAV2 XP 002311438	--KVMRF RYSYWNSSQS YVLT KGS RFVKEKNLRAGDVVFSRS----
13. Populus trichocarpa RAV4 XP 002308395	--KKMR R-----LTNQS YVFT TCGWNSFVKEKNLRAGDVVFSRS----
14. Oryza sativa RAV-like 1 AP2 NP 001041982	--KVMRF RYSYWNSSQS YVLT KGS RFVKEKNLRAGDVVFSRS----
15. Oryza sativa RAV-like 2 NP 001043946	--KVMRF RYSYWNSSQS YVLT KGS RFVKEKNLRAGDVVFSRS----
16. Oryza sativa RAV-like 3 NP 001056237	--KVMRF RYSYWNSSQS YVLT KGS RFVKEKNLRAGDVVFSRS----
17. Camellia sinensis RAV-like ACT33043	--KVMRF RYSYWNSSQS YVLT KGS RFVKEKNLRAGDVVFSRS----
18. Capsicum annuum RAV-like AF478458 1	--KVMRF RYSYWNSSQS YVLT KGS RFVKEKNLRAGDVVFSRS----
19. Glycine max RAV-like NP 001237600	--KVMRF RYSYWNSSQS YVLT KGS RFVKEKNLRAGDVVFSRS----
20. Ricinus communis RAV1 putative XP 002524409	--KVMRF RYSYWNSSQS YVLT KGS RFVKEKNLRAGDVVFSRS----
21. Zea mays RAV1 NP 001151105	--KVMRF RYSYWNSSQS YVLT KGS RFVKEKNLRAGDVVFSRS----
22. Antirrhinum majus RAV like AJ800976	--VLWKF RYCFMSSQS FVFT TCGWNSFVKEKNLRAGDVVFSRS----
23. Solanum lycopersicum RAV2 ABY57635	--KVMRF RYSYWNSSQS YVLT KGS RFVKEKNLRAGDVVFSRS----
24. Malus x domestica AP2 domain ADE41129	--KVMRF RYSYWNSSQS YVLT KGS RFVKEKNLRAGDVVFSRS----
25. Oryza sativa RAV-like 4 RAY75457	--KVMRF RYSYWNSSQS YVLT KGS RFVKEKNLRAGDVVFSRS----
26. Ricinus communis RAV-like XP 002515100	--KVMRF RYSYWNSSQS YVLT KGS RFVKEKNLRAGDVVFSRS----
27. Arabidopsis thaliana NGA3 NP 171611	--KVMRF RYSYWNSSQS YVLT KGS RFVKEKNLRAGDVVFSRS----
28. Arabidopsis thaliana NGA1 NP 566089	--KVMRF RYSYWNSSQS YVLT KGS RFVKEKNLRAGDVVFSRS----
29. Arabidopsis thaliana NGA2 NP 191756	--KVMRF RYSYWNSSQS YVLT KGS RFVKEKNLRAGDVVFSRS----
30. Oryza sativa RAV-like 5 NP 001047754	--KVMRF RYSYWNSSQS YVLT KGS RFVKEKNLRAGDVVFSRS----
31. Oryza sativa RAV-like NP 001174059	--KVMRF RYSYWNSSQS YVLT KGS RFVKEKNLRAGDVVFSRS----
32. Vitis Vinifera ASAPE8 Putative uncharacterized protein CAN73636	--KVMRF RYSYWNSSQS YVLT KGS RFVKEKNLRAGDVVFSRS----
33. Ricinus communis RAV-like XP 002518948	--KVMRF RYSYWNSSQS YVLT KGS RFVKEKNLRAGDVVFSRS----
34. SORGHUM BICOLOR uncharacterized protein XP 002448384	--KVMRF RYSYWNSSQS YVLT KGS RFVKEKNLRAGDVVFSRS----
35. SORGHUM BICOLOR uncharacterized protein XP 002458352	--KVMRF RYSYWNSSQS YVLT KGS RFVKEKNLRAGDVVFSRS----
36. SORGHUM BICOLOR uncharacterized protein XP 002457391	--KVMRF RYSYWNSSQS YVLT KGS RFVKEKNLRAGDVVFSRS----
37. Oryza sativa uncharacterized protein RAY95278	--KVMRF RYSYWNSSQS YVLT KGS RFVKEKNLRAGDVVFSRS----
38. Oryza sativa RAV-putative NP 001065792	--KVMRF RYSYWNSSQS YVLT KGS RFVKEKNLRAGDVVFSRS----
39. SORGHUM BICOLOR uncharacterized protein XP 002452747	--KVMRF RYSYWNSSQS YVLT KGS RFVKEKNLRAGDVVFSRS----
40. Oryza sativa RAV-putative Y1407 ORYSJ	--KVMRF RYSYWNSSQS YVLT KGS RFVKEKNLRAGDVVFSRS----
41. Arabidopsis thaliana RAV-like 1 NP 850260	--KVMRF RYSYWNSSQS YVLT KGS RFVKEKNLRAGDVVFSRS----
42. Arabidopsis thaliana RAV-like 2 NP 850559	--KVMRF RYSYWNSSQS YVLT KGS RFVKEKNLRAGDVVFSRS----
43. Arabidopsis thaliana NGA4 NP 192059	--KVMRF RYSYWNSSQS YVLT KGS RFVKEKNLRAGDVVFSRS----
44. Arabidopsis thaliana RAV-like 3 NP 001119177	--KVMRF RYSYWNSSQS YVLT KGS RFVKEKNLRAGDVVFSRS----
45. Oryza sativa RAV-putative NP 001172942	--KVMRF RYSYWNSSQS YVLT KGS RFVKEKNLRAGDVVFSRS----
46. Oryza sativa RAV-putative RAY85732	--KVMRF RYSYWNSSQS YVLT KGS RFVKEKNLRAGDVVFSRS----
47. Oryza sativa RAV-putative RAG8961	--KVMRF RYSYWNSSQS YVLT KGS RFVKEKNLRAGDVVFSRS----
48. Oryza sativa RAV-putative NP 001048792	--KVMRF RYSYWNSSQS YVLT KGS RFVKEKNLRAGDVVFSRS----
49. Oryza sativa RAV-putative RAY99351	--KVMRF RYSYWNSSQS YVLT KGS RFVKEKNLRAGDVVFSRS----
50. Oryza sativa RAV-putative Y8577 ORYSJ	--KVMRF RYSYWNSSQS YVLT KGS RFVKEKNLRAGDVVFSRS----
51. Oryza sativa RAV-putative Y1071 ORYSJ	--KVMRF RYSYWNSSQS YVLT KGS RFVKEKNLRAGDVVFSRS----
52. Oryza sativa RAV-putative REC68891	--KVMRF RYSYWNSSQS YVLT KGS RFVKEKNLRAGDVVFSRS----

Figure 4.5 Amino acid alignment of 52 RAV and RAV-like protein sequences showing the conserved amino acids WN/RSSQS in the B3 domain (green boxes). Accession numbers are given next to the species name.

Further analysis of the aligned sequences showed that 18 sequences could not be classified in class I of the RAV sub-family because of the absence of the APETALA2 (AP2) domain (Figure 4.6) (Romanel *et al.*, 2009). These were also excluded from further study.

Species/Abbrv	
1. Arabidopsis thaliana TEH1 NP 173927	--KLPSKYNKVVFPQNGRWGAQIYERKQVVLGTFNNEEAAASVDIAVRRFRGDDAVTNFK-----SQVFGNDARSFLD
2. Arabidopsis thaliana TEH2 (RAV2) NP 564947	--KLPSKYNKVVFPQNGRWGAQIYERKQVVLGTFNNEEAAASVDIAACRFRCDDAVTNFK-----NVLE--DCDLAFLE
3. Arabidopsis thaliana RAV1 NP 172784	--KLPSKYNKVVFPQNGRWGAQIYERKQVVLGTFNNEEAAARAYDVAAHFRFRDDAVTNFK-----DVRMDEDVDFLN
4. Arabidopsis thaliana RAV1-like NP 189201	--KLPSKYNKVVFPQNGRWGAQIYERKQVVLGTFNNEEAAARAYDVAAHFRFRDDAVTNFK-----DTTF--EIEVEFLN
5. Arabidopsis thaliana RAV1-like 1 NP 175524	--KTFKPKVVVQNGRWGAQIYERKQVVLGTFNNEEAAASVDIAVRRFRGDDAVTNFK-----PFGDFLHDFDFK
6. Vitis vinifera RAV1-like CAM6954	--KLPSKYNKVVFPQNGRWGAQIYERKQVVLGTFNNEEAAARAYDVAAQFRFRDDAVTNFK-----PLSE--EED--IIRAFLN
7. Galega orientalis RAV1-like AC146676	--KLPSKYNKVVFPQNGRWGAQIYERKQVVLGTFNNEEAAARAYDIAALEFRFRDDAVTNFK-----TLACAGNDNDIETFLN
8. Nicotiana tabacum RAV1 AC74549	--KLPSKYNKVVFPQNGRWGAQIYERKQVVLGTFNNEEAAARAYDVAAQFRFRDDAVTNFK-----PLLENEEDD--MIEAFLN
9. Populus trichocarpa RAV1 XP 002315958	--KLPSKYNKVVFPQNGRWGAQIYERKQVVLGTFNNEEAAARAYDVAAQFRFRDDAVTNFK-----QVN--ETDD--EIEAFLN
10. Populus trichocarpa RAV2 XP 002311438	--KLPSKYNKVVFPQNGRWGAQIYERKQVVLGTFNNEEAAARAYDVAAQFRFRDDAVTNFK-----QVN--ETDD--EIEAFLN
11. Oryza sativa RAV1-like 1 AP2 NP 001041982	--QSSRYKVVFPQNGRWGAQIYERKQVVLGTFNNEEAAARAYDVAAQFRFRDDAVTNFK-----GAA--ASAARLAFLA
12. Oryza sativa RAV1-like 2 NP 001045946	CGKLPSSKFKVVFPQNGRWGAQIYERKQVVLGTFNNEEAAARAYDVAAQFRFRDDAVTNFK-----LAEADPDAARLRFLLA
13. Oryza sativa RAV1-like 3 NP 001056237	--LPSKYNKVVFPQNGRWGAQIYERKQVVLGTFNNEEAAARAYDVAAQFRFRDDAVTNFK-----LAEADPDAARLRFLLA
14. Cassia sinensis RAV1-like ACT33049	--KLPSKYNKVVFPQNGRWGAQIYERKQVVLGTFNNEEAAARAYDVAAQFRFRDDAVTNFK-----PLEHEEQDE--LITFLN
15. Capsicum annuum RAV1-like AF470459 1	--KLPSKYNKVVFPQNGRWGAQIYERKQVVLGTFNNEEAAARAYDVAAQFRFRDDAVTNFK-----PLLEHQEEDD--VEIAFLN
16. Glycine max RAV1-like NP 001237600	--KLPSKYNKVVFPQNGRWGAQIYERKQVVLGTFNNEEAAARAYDIAALEFRFRDDAVTNFK-----PFAAS--DDASDFLN
17. Ricinus communis RAV1 putative XP 002524409	--KLPSKYNKVVFPQNGRWGAQIYERKQVVLGTFNNEEAAARAYDVAAQFRFRDDAVTNFK-----PQATHQSEEDIEITFLN
18. Zea mays RAV1 NP 001151105	--KLPSKYNKVVFPQNGRWGAQIYERKQVVLGTFNNEEAAARAYDVAAQFRFRDDAVTNFK-----LADADPDAARLRFLLA
19. Solanum lycopersicum RAV2 ABY57635	--KLPSKYNKVVFPQNGRWGAQIYERKQVVLGTFNNEEAAARAYDVAAQFRFRDDAVTNFK-----PLLEHQEEDD--MIEAFLN
20. Malus x domestica AP2 domain ADE41129	--KLPSKYNKVVFPQNGRWGAQIYERKQVVLGTFNNEEAAARAYDVAAQFRFRDDAVTNFK-----PSSAEPISSDDEEDD--ARAFLS
21. Oryza sativa RAV1-like 4 RAY75457	--HISKSE-----LKHIERKQVVLGTFNNEEAAARAYDVAAQFRFRDDAVTNFK-----LAEADPDAARLRFLLA
22. Ricinus communis RAV1-like XP 002515100	-----EEEEEEEEETITNTTSLPFPSPSSPSSSATANKYRNFVQHHNSLWLASDHSQDNMTQSSSLNFDKRLDMLDSE
23. Arabidopsis thaliana NGA1 NP 171611	-----DQELTSEIGAS-----
24. Arabidopsis thaliana NGA1 NP 566059	-----DEEARPIAE-----
25. Arabidopsis thaliana NGA2 NP 191756	-----DNE--NPEE-----
26. Oryza sativa RAV1-like 5 NP 001047254	-----EAGC--REIPFMTATAAAPAPTS--SSSPAHHAASASASASAGSTPFR-----
27. Oryza sativa RAV1-like NP 001174059	EEENASPREIIPMTSAAAAATASS--SPTSVSPSATASAAATSSAGGPF-----
28. Vitis Vinifera ASAPES Putative uncharacterized protein CAM73636	-----GKLPFSYSSSSPSSSSSQYR--NLVPLNCCDRWDQIQGWLK-----HQEDGHCYE
29. Ricinus communis RAV1-like XP 002518948	-----GKLPFSYSSSSPSSSSSQYR--NLVPLNCCDRWDQIQGWLK-----SKYDFEQEDA
30. SOBGMH BICOLOR uncharacterized protein XP 002448384	EEDEASPREIIPMTSAAAAATADTGPAA--AASSSPSAAO--ASASASGSAALD-----LADADPDAARLRFLLA
31. SOBGMH BICOLOR uncharacterized protein XP 002458352	--KLPSKYNKVVFPQNGRWGAQIYERKQVVLGTFNNEEAAARAYDVAAQFRFRDDAVTNFK-----LADADPDAARLRFLLA
32. SOBGMH BICOLOR uncharacterized protein XP 002457391	-----GSSPKKVVFPQNGRWGAQIYERKQVVLGTFNNEEAAARAYDVAAQFRFRDDAVTNFK-----GAC--ASAPLRFLLA
33. Oryza sativa uncharacterized protein RAY95278	-----EASPREIIPMTSAAAAATASS--SPTSVSPSATASAAATSSAGGPF-----
34. SOBGMH BICOLOR uncharacterized protein XP 002452747	-----DASMSREIIPMTSAAAAATADTGPAA--AASSSPSAAO--ASASASGSAALD-----LADADPDAARLRFLLA
35. Oryza sativa RAV1-putative Y1407_ORYS2	-----PSSRYKVVFPQNGRWGAQIYERKQVVLGTFNNEEAAARAYDVAAQFRFRDDAVTNFK-----AAEG--ASAGLAFLLA
36. Arabidopsis thaliana RAV1-like 1 NP 850260	-----QQQQQHQDDVVEE-----
37. Arabidopsis thaliana RAV1-like 2 NP 850559	-----LHHHQNDVIAQR-----
38. Arabidopsis thaliana NGA4 NP 192059	-----DQELA--EIRAS-----
39. Arabidopsis thaliana RAV1-like 3 NP 001119177	-----QQRHTIDTSRTTTTATV-----
40. Oryza sativa RAV1-putative NP 001048792	-----MEFITPVRPASAAC-----
41. Oryza sativa RAV1-putative Y1071_ORYS3	-----MEFTP--ISPTTRVAC-----

Figure 4.6 Amino acid alignment of 41 RAV and RAV-like protein sequences showing the conserved APETALA2 (AP2) domain (green boxes). Accession numbers are given to the species name

Phylogenetic analysis showed the similarity between the remaining sequences (Figure 4.7). The sequences share identity ranging from 27.9% between *Arabidopsis thaliana* RAV1-like 5 NP_175524 and *Oryza sativa* RAV-putative Y1407_ORYS2 to 100% between *Populus trichocarpa* RAV2 XP_002311438 and *Populus trichocarpa* RAV1 XP_002315958.

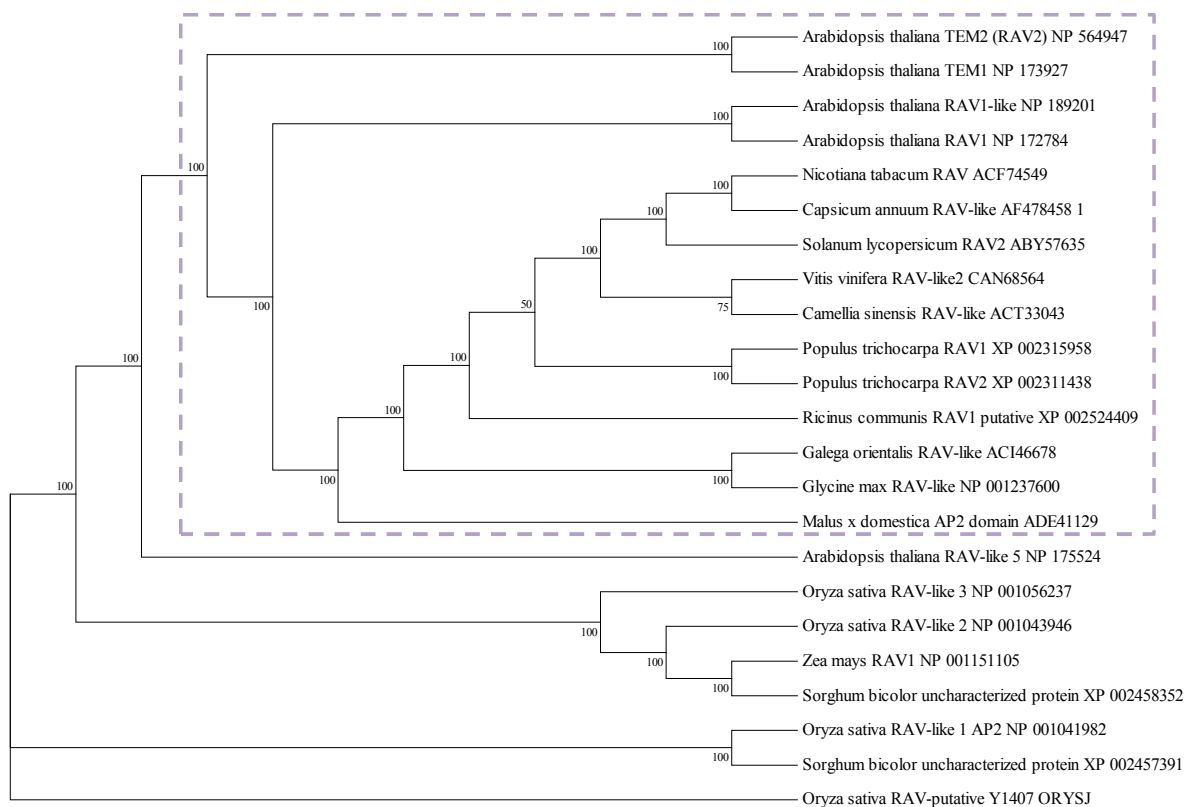


Figure 4.7 Phylogenetic analysis of 23 RAV sub-family class I members.

The evolutionary relationship was inferred using the Maximum Parsimony method. The percentage of parsimonious trees in which the associated taxa clustered together are shown next to the branches. Violet dashed line box shows the sequences with higher similarity to TEM1 and TEM2. Accession numbers are given next to the species name

4.3.2 Acquisition of a full length cDNA representing *AmTEM*

The 8 sequences with highest identity to AtTEM1 and AtTEM2, along with AtTEM1 and AtTEM2, were selected and aligned to design degenerate primers for the isolation of the putative *AmTEM* (Appendix, Figure A.8). An AmRAV-like sequence was also included to show amino acid conservation in the species.

Degenerate primers used in a total of 10 combinations (section 4.2.4.1) generated a number of products using gradient PCR. Whilst many were non-specific, four combinations generated fragments of the expected length inferred from *AtTEM1* and *AtTEM2* gene sequences (Figure 4.8).

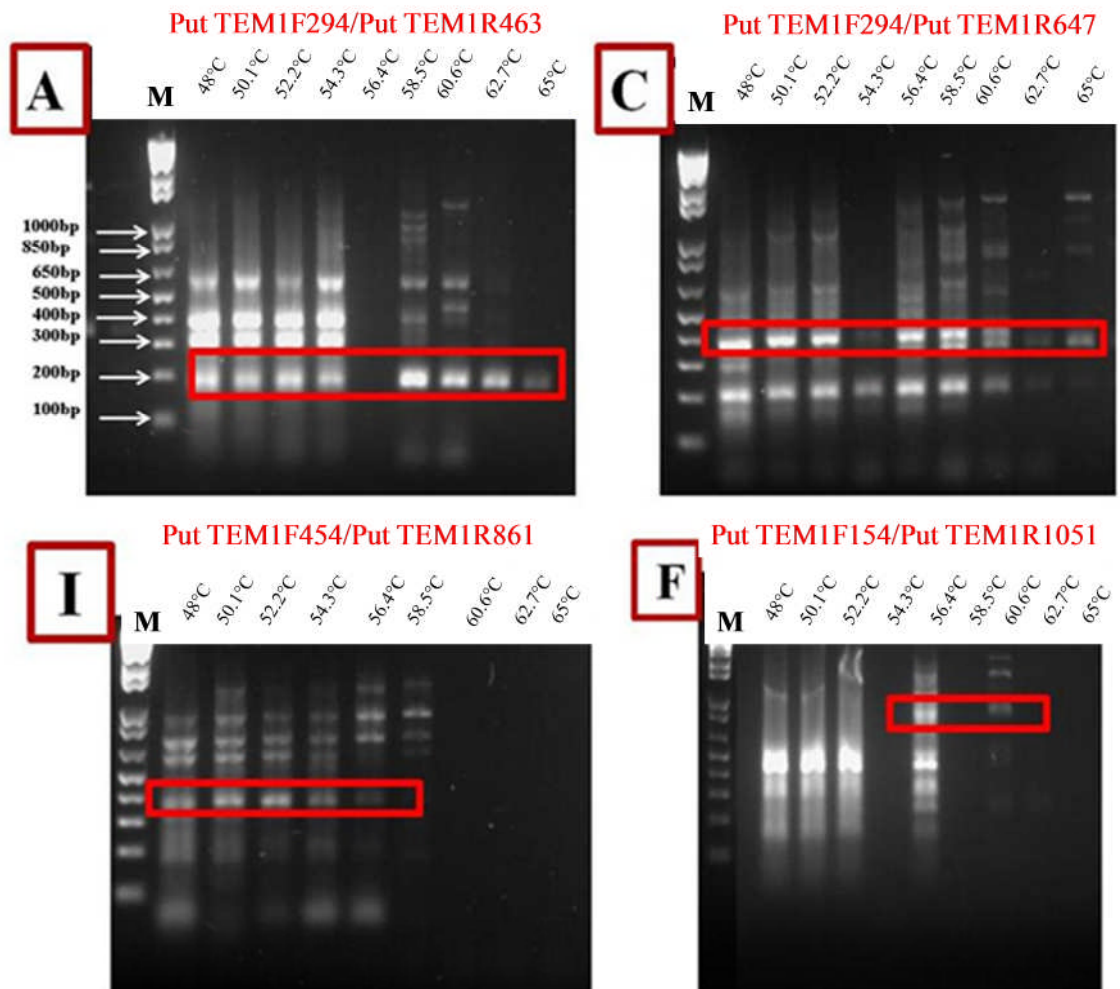


Figure 4.8 Gradient PCR products generated using TEM degenerate primers. Annealing temperature used in PCRs shown above lanes. A, C, I, F = products generated using the primer pairs as shown. Fragments of the expected sizes (for A~ 160 bp; for C~ 350 bp; for I~ 400 bp; for F~ 900 bp) are enclosed within red rectangles. M=1 kb Plus DNA ladder,

Sequencing of all the products revealed A and F to be Glucose-methanol-choline oxidoreductase, magnesium/proton exchanger, phosphatase, or hypothetical proteins. However the C (350 bp) and I (400 bp) products were shown to be RAV-like DNA-binding proteins. The contig of 523 bp called CI was generated by PCR as described in section 4.2.4.1. Sequencing of 15 clones of fragment C, 15 clones of fragment I and 15 clones of contig CI always revealed one unique sequence

although degenerate primers were used in the PCR. Using RACE PCR, as explained in section 4.2.5, to provide the 5' and 3' sequence information, a single cDNA product representing the full length cDNA sequence of *Antirrhinum majus* TEM-like gene (*AmTEM*) was amplified by PCR using primers AmTEM1F/AmTEM1072R (Figure 4.9).

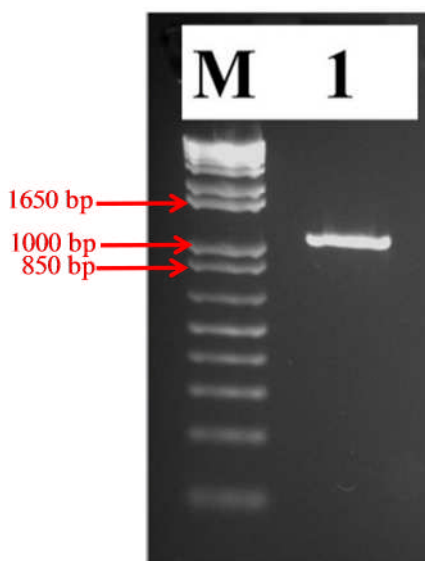


Figure 4.9 Amplification of full length *AmTEM* cDNA.
M=1 kb Plus DNA ladder I= AmTEM 1065bp product representing the full coding sequence

4.3.2.1 *AmTEM* sequence analysis

The *AmTEM* homologue coding sequence contains 1,065 bp and is predicted to encode 354 amino acids (Appendix, Figure A.11). Figure 4.10 illustrates a schematic reconstruction of the possible *AmTEM* protein. *AmTEM* contains an AP2 domain from amino acid 60 to 115 and a B3 domain from amino acid 187 to 297. *AmTEM* shares 68.7% and 68.2% amino acid identity with *AtTEM1* and *AtTEM2* respectively.

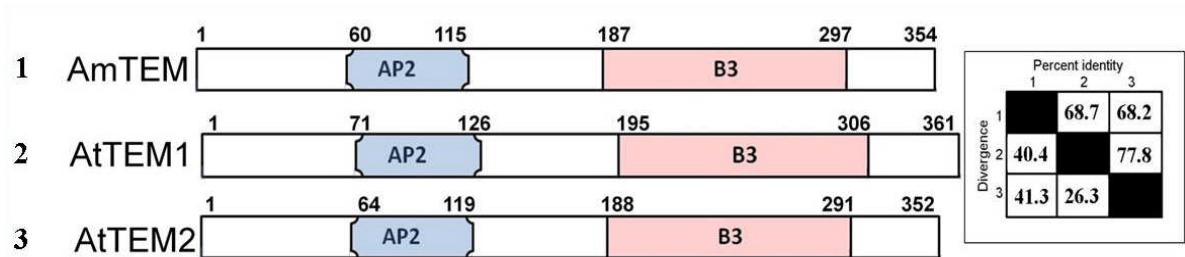


Figure 4.10 Comparison of protein domain structure in *AmTEM*, *AtTEM1* and *AtTEM2*

Phylogenetic analysis of *AmTEM* and other RAV homologues showed that *AmTEM* is closely related to other RAV homologues (Figure 4.11). *AmTEM* is not closely related to *AmRAV*-like due to the lack of AP2 domain in the latter.

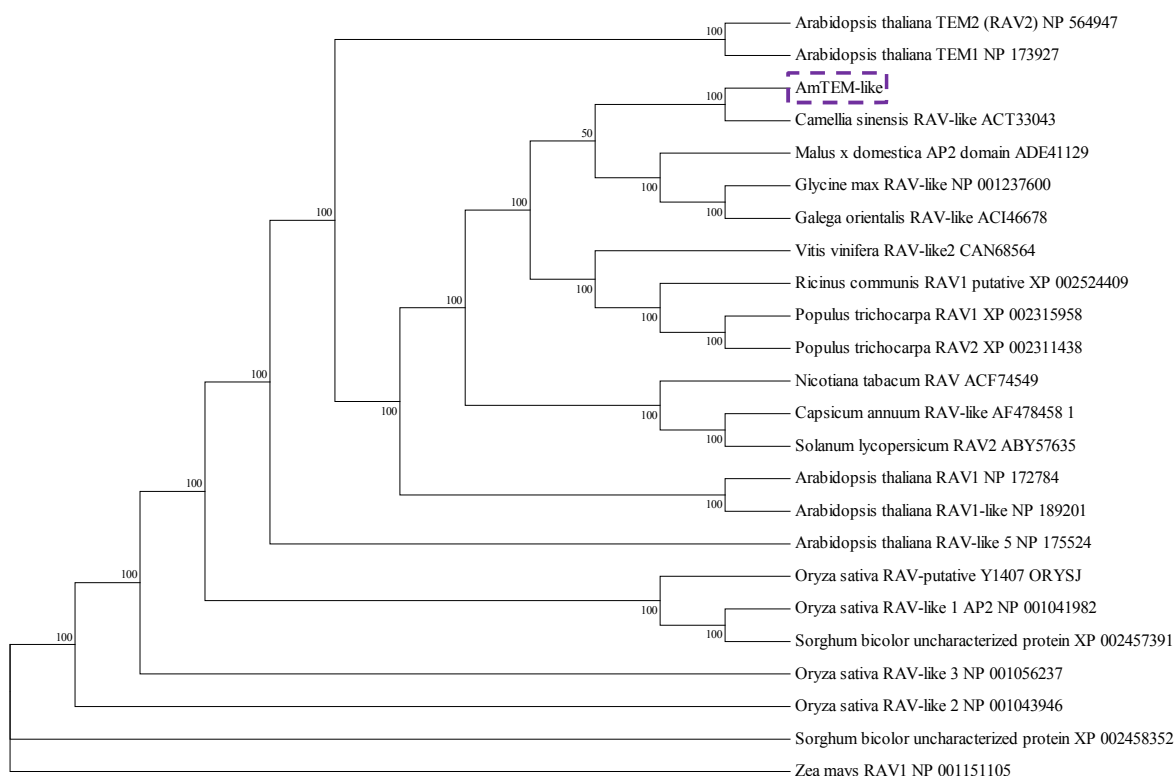


Figure 4.11 Phylogenetic relationship of RAV sub-family class I members.

The evolutionary relationship was inferred using the Maximum Parsimony method. The percentage of parsimonious trees in which the associated taxa clustered together are shown next to the branches. Accession numbers are given next to the species name

shows that the signal from the housekeeping *ELF α* was similar in both samples indicating that similar amounts of cDNA were present in the juvenile and adult samples.

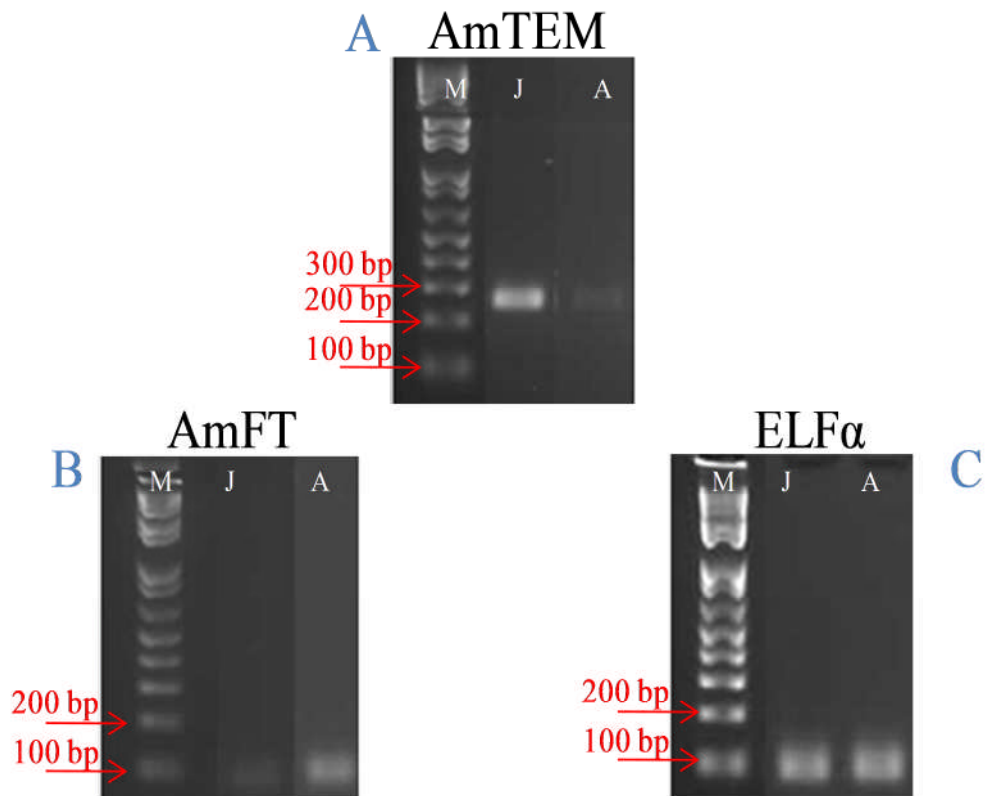


Figure 4.13 Semiquantitative analysis of *AmTEM* and *AmFT* expression. *AmTEM* (263 bp), *AmFT* (78 bp) and *AmELF α* (78 bp) fragments generated using 35, 36 and 24 cycles respectively. J and A refer to Juvenile (12 days from germination) and Adult (24 days after germination) plant material. M=1 kb Plus DNA ladder

4.3.4 Acquisition of a full length cDNA representing *OeTEM*

A fragment representing the partial olive isotig13527 EST sequence was PCR amplified from a pool of juvenile and adult cDNA (section 4.2.2), as described

in section 2.7, using Oe fragment TEM F/Oe fragment TEM R primers (Figure 4.14).

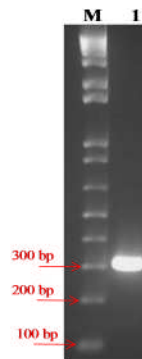


Figure 4.14 Amplification of partial cDNA representing putative *OeTEM*.
*M=1 kb Plus DNA ladder 1= *OeTEM* isotig13527 312bp product*

Sequencing confirmed the identity of the fragment which showed high homology to DNA-binding RAV-like genes.

The 5'- and 3'- end sequences of the putative *Olea europaea TEM-like* gene (*OeTEM*) were obtained by RACE PCR (section 4.2.5) and a fragment representing the full length cDNA generated by PCR using primers *OeTEM1F/OeTEM1074R* (Figure 4.15).

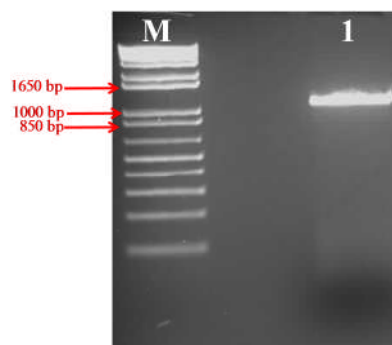


Figure 4.15 Amplification of full length *OeTEM*.
*M=1 kb Plus DNA ladder 1= *OeTEM* 1074bp product*

4.3.4.1 *OeTEM* sequence analysis

Sequence of the full-length *OeTEM* cDNA showed the CDS comprised 1,074 bp that are predicted to encode 357 amino acids (Appendix, Figure A.12). A schematic reconstruction of the possible *OeTEM* protein is presented in Figure 4.16. The *OeTEM* is predicted to contain an AP2 domain from amino acid 63 to 113 and a B3 domain from amino acid 195 to 297. *OeTEM* shares 64.6% and 66.1% amino acid identity with *AtTEM1* and *AtTEM2* respectively.



Figure 4.16 Gene structure of *OeTEM* compared to *AtTEM1* and *AtTEM2*. Amino acid homology comparison.

Amino acid alignment of *OeTEM* with other RAV and RAV-like proteins shows that *OeTEM* contains the characteristic WN/RSSQS motif which distinguished the class I RAV sub-family (Figure 4.17).

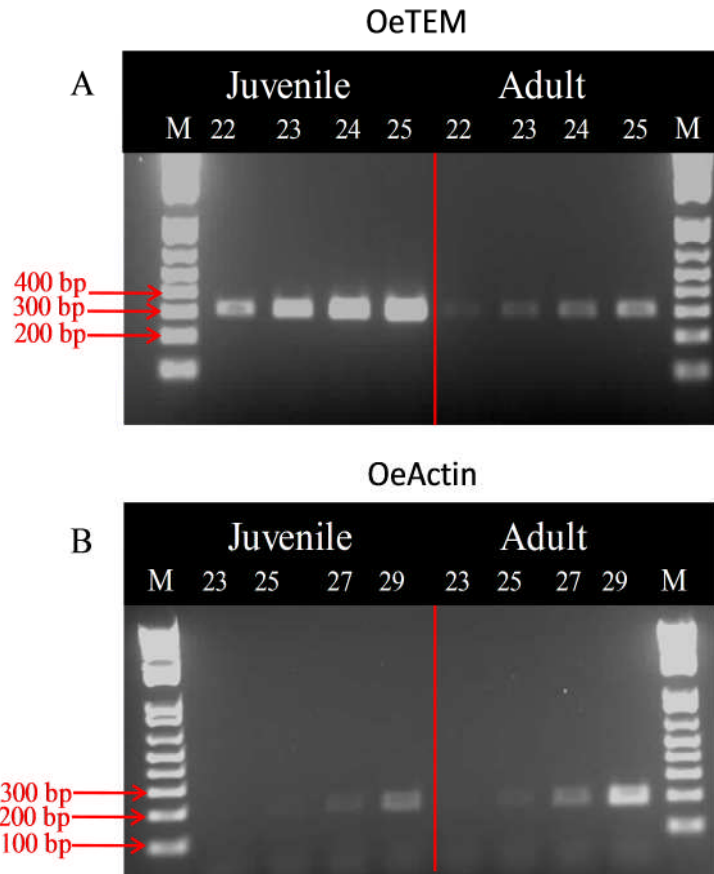


Figure 4.18 Semi-quantitative analysis of *OeTEM* expression.
 Number of cycles used to amplify *OeTEM* (A) and *OeActin* (B) fragments are indicated. M=1 kb
 Plus DNA ladder, Juvenile= juvenile olive leaf, Adult= adult olive leaf

4.3.6 *AmTEM* and *OeTEM* phylogenetic analysis

Phylogenetic analysis, using full length deduced amino acid sequences, shows that *AmTEM* and *OeTEM* proteins are homologous to RAV-like DNA-binding proteins from other organisms (Figure 4.19). Both *OeTEM* and *AmTEM* cluster with *AtTEM1*, *AtTEM2* and *AtRAV1*, *AtTEM1*, *AtTEM2* and *AtRAV1* being more like each other than *AmTEM* and *OeTEM*.

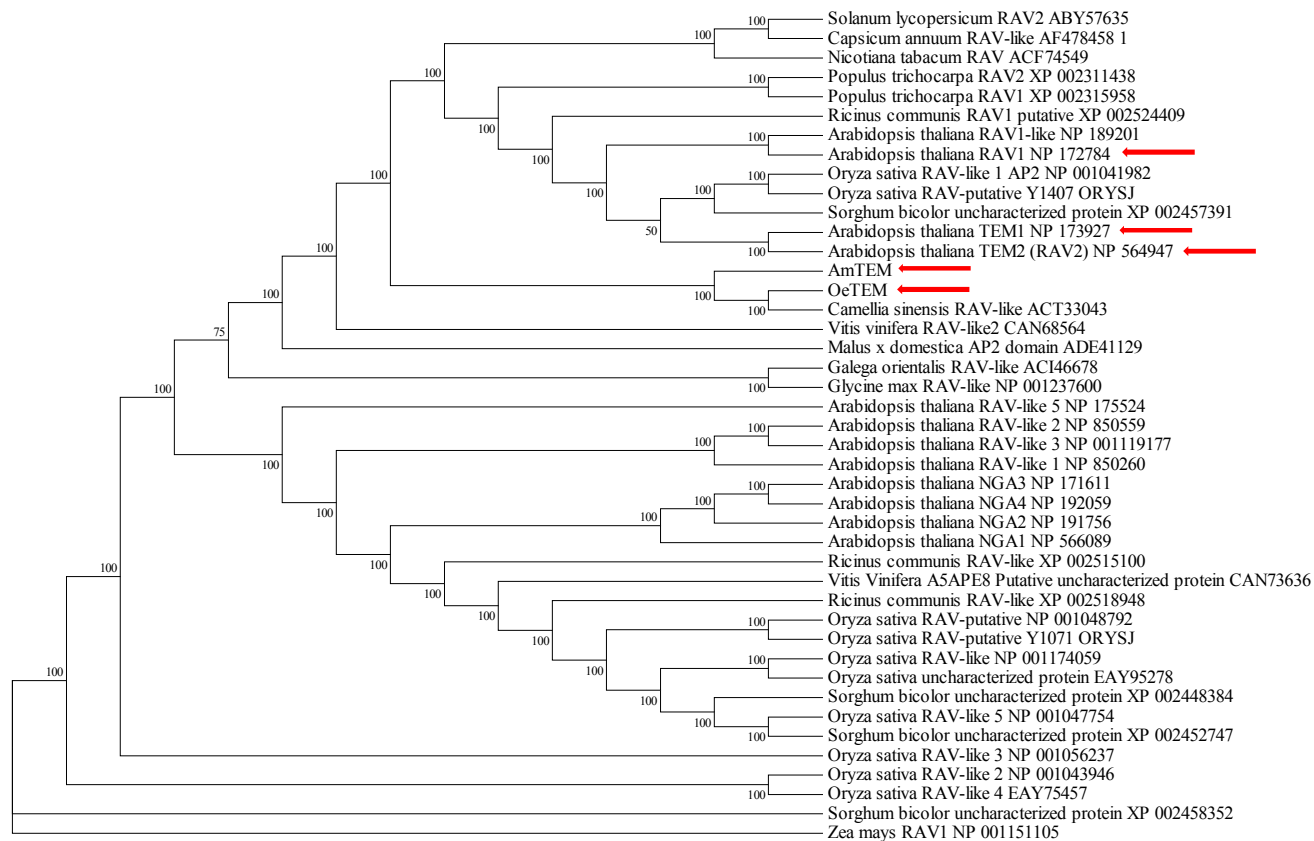


Figure 4.19 Phylogenetic relationship of RAV members.

The evolutionary history was inferred using the Maximum Parsimony method. The percentage of parsimonious trees in which the associated taxa clustered together are shown next to the branches. Accession number is given next to the species name

4.3.7 Acquisition of a full length cDNA representing *AtTEM1*

To study if *OeTEM* and *AmTEM* can perform the same function as *AtTEM1*, complementation experiments were carried out. *Arabidopsis* plants were also transformed with *AtTEM1* as a positive control, as explained in section 4.3.9. To enable this, the full length *AtTEM1* was isolated using primers *AtTEM1-F/AtTEM1091-R* performing a PCR as described in section 2.7. Leaf material from juvenile *Arabidopsis* plants (3 days from germination) was used to generate cDNA

(section 2.6) template. The product obtained as shown in Figure 4.20 was cloned and sequenced as explained in sections 2.11- 2.14.

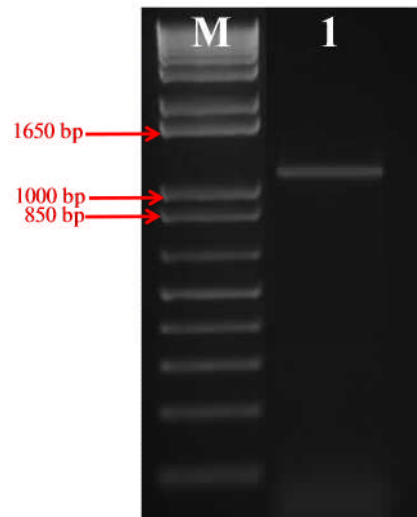


Figure 4.20 Amplification of full length *AtTEM*.
M=1 kb Plus DNA ladder 1=AtTEM 1091bp product

4.3.8 Functional complementation of the *Arabidopsis tem1* mutant with *AmTEM* and *OeTEM*

To investigate a role in flowering time regulation, *Arabidopsis Col-0*, *tem1* and *RNAi-tem1/2* early flowering mutants were transformed with binary vectors engineered to over-express *AmTEM*, *OeTEM* and *AtTEM1* as positive control, as described in sections 4.2.5, 4.2.6 and 4.2.7. Plants were selected with BASTA. None of the transformed double mutant T₁ plants survived BASTA selection.

A total of five *Col-0* and two *tem1* mutant T₁ plants transformed with *AtTEM1* survived BASTA selection. Whilst none of the latter proved transgenic by

PCR screen (section 4.2.7), three of the engineered Col-0 plants were confirmed transgenic. Assessment of flowering times of these T₁ transgenics under LD showed that flowering was delayed in relation to Col-0 WT and the *tem1* mutant (Figure 4.21). Non-transformed WT Col-0 plants flowered in LD with an average of 8.2 (\pm 0.11) leaves, compared to non-transformed *tem1* plants which flowered with an average of 7.2 (\pm 0.12) leaves. Plants ectopically over-expressing *AtTEM1* flowered even later than Col-0 WT showing that the natural level of *AtTEM1* in *Arabidopsis* was not saturating.

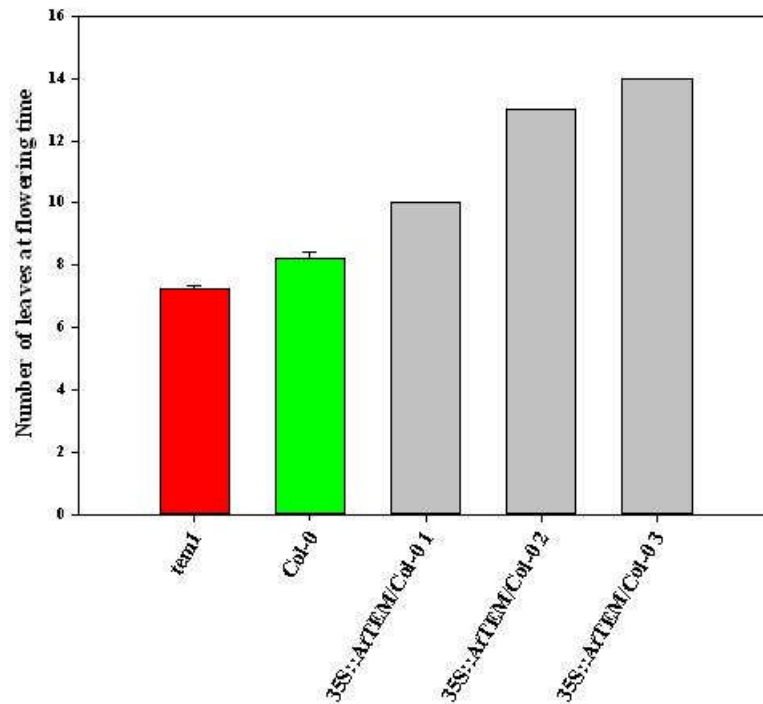


Figure 4.21 Flowering time of Col-0 T₁ transgenic lines transformed with *AtTEM1* grown under LD.

Flowering assessed by number of rosette leaves when the bolt was 1 cm in length. T₁ transformants (grey bars), WT (green bar) and *tem1* mutant (red bar)

A total of 35 *tem1* mutant T₁ plants transformed with *AmTEM* survived BASTA selection and all proved transgenic by PCR screen (section 4.2.7). Assessment of flowering times of these T₁ transgenic lines under SD showed that flowering was delayed in relation to Col-0 WT and the *tem1* mutant (Figure 4.22). Non-transformed WT Col-0 plants flowered with an average of 37.9 (\pm 1.2) leaves, compared to non-transformed *tem1* plants which flowered with an average of 32.4 (\pm 0.9) leaves. *tem1* plants ectopically expressing *AmTEM* flowered generally later than *tem1* and even later than Col-0 WT showing a large degree of variation in the number of leaves at flowering in each line, with an average of 54.6 (\pm 1.8). Among the T₁ plants, 15 of them appeared normal in phenotype, but had altered flowering times. Three independent transgenic lines (35S::*AmTEM/tem1* 2, 35S::*AmTEM/tem1* 75 and 35S::*AmTEM/tem1* 77) were selected for further analysis (Figure 4.23 c-e). These lines however flowered late and were analysed to determine whether *AmTEM* plays a role in determining juvenile phase length as discussed in chapter 5. Among the T₁ generation, some transgenic lines presented severe and moderate alterations in phenotype. Some of the plants presented multiple stems from the base and a high number of small basal leaves (Figure 4.23 f), others, although they bolted, did not flower.

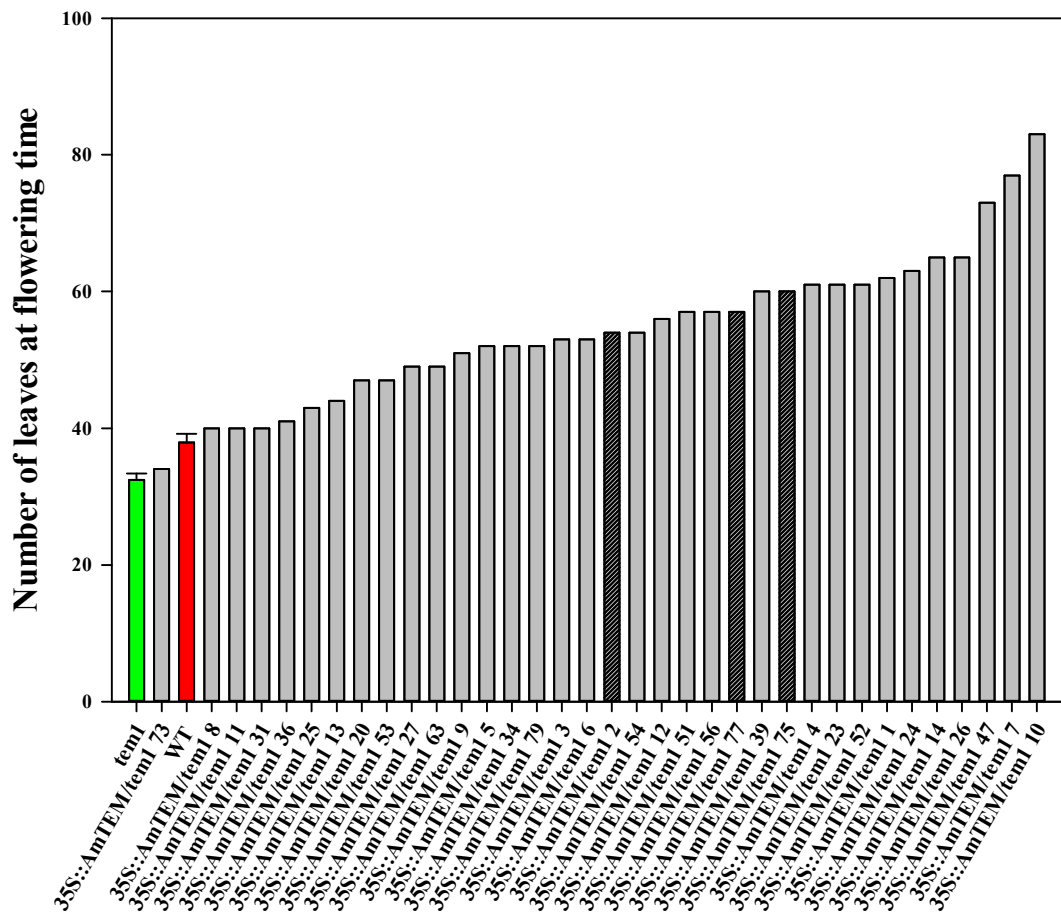


Figure 4.22 Flowering time of *tem1* T_1 transgenic lines transformed with *AmTEM* grown under SD.

Flowering assessed by number of rosette leaves when the bolt was 1 cm in length. T_1 transformants (grey bars), WT (green bar) and *tem1* mutant (red bar). The dark grey bars show the lines selected for further studies. Error bars denote the standard error of number of leaves present at flowering time.

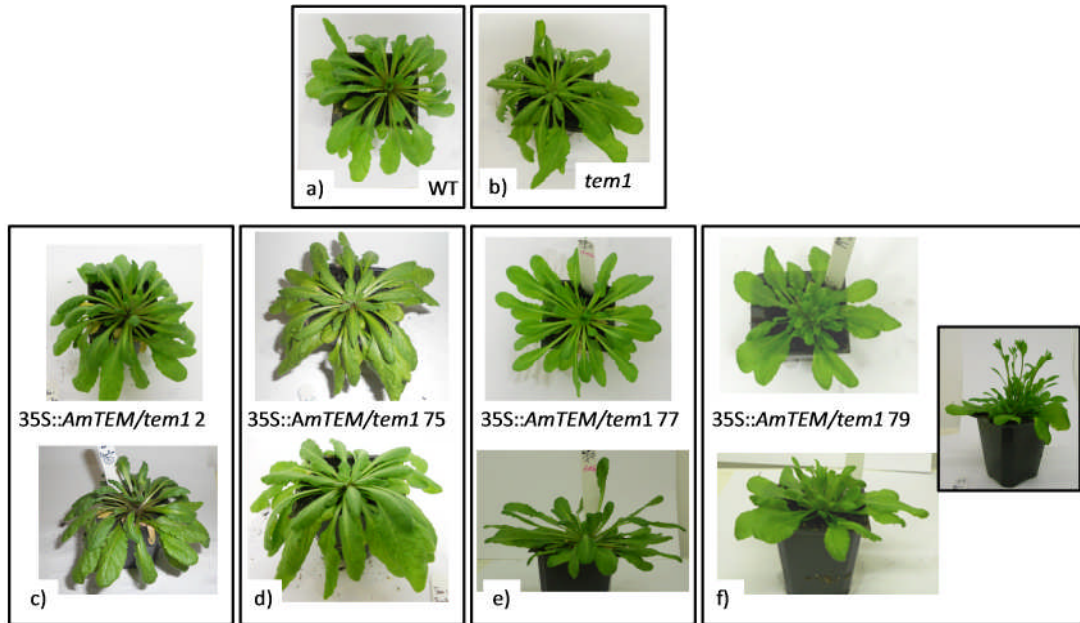


Figure 4.23 Phenotype in T_1 generation.

a-b) Phenotype observed in *Arabidopsis* WT and *tem1* mutant at 40 days from germination c-d-e-f) Phenotype observed in 60 day old plants from T_1 generation of 35S::AmTEM/*tem1* 2, 35S::AmTEM/*tem1* 75 and 35S::AmTEM/*tem1* 77 and 35S::AmTEM/*tem1* 79 lines engineered to over-express AmTEM in the *tem1* mutant grown in SD conditions. On the right side of picture 4.23 f) the 35S::AmTEM/*tem1* 79 after further 10 days is shown.

A total of six Col-0 and one *tem1* mutant T_1 plants transformed with *OeTEM* were obtained that survived BASTA selection and proved transgenic by PCR screen (section 4.2.7). Assessment of flowering times of these T_1 transgenics under LD showed that flowering was delayed in relation to Col-0 WT and the *tem1* mutant (Figure 4.24). *tem1* plants ectopically expressing *OeTEM* flowered later than *tem1* and even later than Col-0 WT.

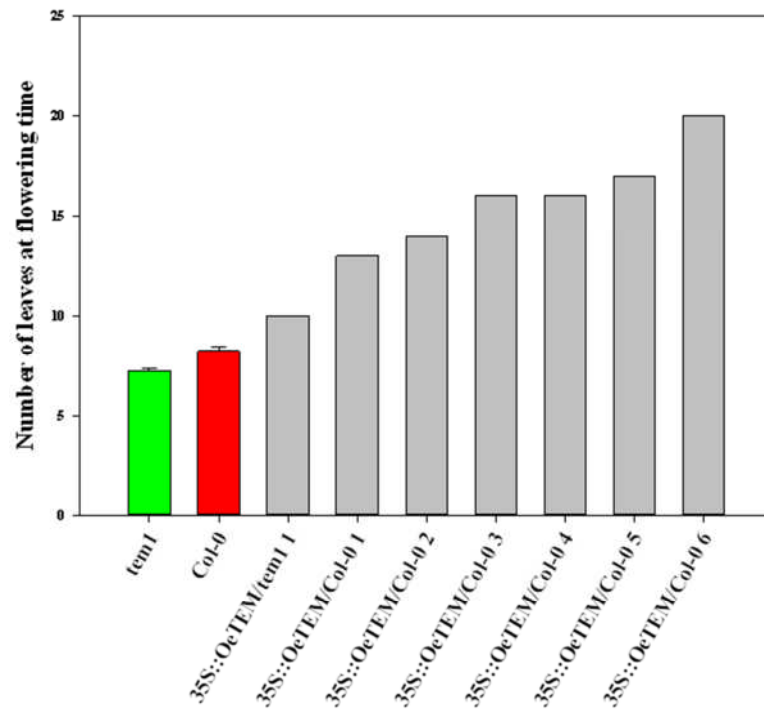


Figure 4.24 Flowering time of Col-0 and tem1 T₁ transgenic lines transformed with OeTEM grown under LD.

Flowering assessed by number of rosette leaves when the bolt was 1 cm in length. T₁ transformants (grey bars), WT (green bar) and tem1 mutant (red bar).

4.4 Discussion

The objective of this chapter was to isolate and characterise orthologues of *AtTEM* from *Antirrhinum* and olive. Evidence from molecular and phylogenetic analyses shows that *Antirrhinum TEM* (*AmTEM*) and Olive *TEM* homologues (*OeTEM*) have been successfully isolated. Since all *AmTEM* PCR fragments cloned and sequenced always represented the same sequence it can be hypothesised that only one *TEM-like* gene is present in *Antirrhinum*. Both *AmTEM* and *OeTEM* can be considered members of the B3 super-family since they contain the B3 domain harbouring the B3 WN/RSSQS motif. Additionally, they can be considered part of the RAV family, Class I as they have the AP2 domain (Romanel *et al.*, 2009).

OeTEM and *AmTEM* were both shown to be expressed more highly in juvenile material compared to adult. In *Arabidopsis TEM1* and *TEM2* expression levels change throughout development and it has been suggested that *FT* is activated when the right equilibrium exists between the activator *CO* and the repressor *TEM1* (Castillejo and Pelaz, 2008).

Experiments in comparative studies have proved that homologues of a gene from one species can play a role in the same pathway in another species, but their function may change (Higgins *et al.*, 2010). An example is the *Arabidopsis CO* equivalent in rice (*Hd1*) which represses the *FT* equivalent (*Hd3a*); this is the opposite to the promotive effect it has on *FT* expression in *Arabidopsis* (Kojima *et al.*, 2002; Turck *et al.*, 2008). The net effect is that in rice *Hd1* represses flowering in LD conditions, whilst in *Arabidopsis CO* promotes flowering in LD. The study of *AmTEM* and *OeTEM* showed that they play a role in flowering time regulation and that their function is conserved. All plants engineered to over-express *AmTEM* and

OeTEM were late flowering. Over expression of both genes led to the rescue of the early flowering phenotype of the *tem1* mutant. These results suggest that *OeTEM* and *AmTEM* can perform the same function as *AtTEM1*, which is validated by the high sequence conservation observed between *AmTEM*, *OeTEM* and *AtTEM1*.

Although in *Arabidopsis*, *TEM1* and *TEM2* have been shown to repress flowering (Castillejo and Pelaz, 2008), *RAV1* may act as a repressor of growth and flowering (Hu *et al.*, 2004). It is possible to assert that the *OeTEM* and *AmTEM* genes isolated are *TEM* genes and not *RAV1* since *RAV1* also plays a role in leaf maturation and senescence (Woo *et al.*, 2010). No signs of premature senescence were visible in any of the transformed plants that were engineered to over-express *OeTEM* and *AmTEM*. Plants engineered to over-express *RAV1* show signs of early senescence (Woo *et al.*, 2010).

Having isolated *AmTEM* and *OeTEM* and proven their role in regulating flowering time, the next task was to determine whether the two genes are involved in regulating juvenility.

CHAPTER 5. *AmTEM*: ROLE IN JUVENILITY

5.1 Introduction

Four members of the RAV (RELATED TO ABI3/VP1) family, RAV1, TEMPRANILLO 1 (TEM1), TEM2 and At3g25730, which all contain the C-terminal RLF_{GV} motif, have been proposed to act as transcription factors (Ikeda and Ohme-Takagi, 2009). TEM1 and TEM2 have been shown to repress flowering acting redundantly to repress *FLOWERING LOCUS T (FT)* early in development through binding to two regions in the *FT* gene 5' untranslated region (Castillejo and Pelaz, 2008). Mutant plants with reduced *TEM1* and *TEM2* activity flower earlier than the single *tem1* mutant, which flower earlier than WT plants. Single mutants lacking *TEM2* do not exhibit early flowering. *TEM1* and *TEM2* over-expressing plants show a late flowering phenotype (Castillejo and Pelaz, 2008). In these plants the late flowering is associated with a decrease in *FT* expression. In WT plants, *TEM1* mRNA is abundant in seedlings and declines before the floral transition. *TEM1* and *TEM2* are down-regulated by APETALA1 (AP1) and GIGANTEA (GI) (Kaufmann *et al.*, 2010; Sawa and Kay, 2011).

Isolation of *TEM* homologues from *Antirrhinum* (*AmTEM*) and olive (*OeTEM*) was reported in the previous chapter. Both were shown to act as floral repressors.

The purpose of the study described in this chapter was to determine whether a relationship exists between patterns of *TEM* and *FT* expression and the juvenile phase (JP) and ultimately whether *TEM* functions in regulating the length of juvenility. To answer these questions both *Antirrhinum* and *Arabidopsis* were used.

5.2 Materials and Methods

This section describes the materials and methods specific for this results chapter. Protocols and materials common to more than one chapter are described in chapter 2. All primer details are listed in the Appendix, Table A.1, A.2, A.3.

5.2.1 *Real-time PCR analysis of AmTEM expression*

The cDNA used for Real-time PCR analysis was generated from leaf material from *Antirrhinum* transfer Experiment 3 (section 3.2.1) which was the same used for previous *Antirrhinum* homologue of *FLOWERING LOCUS T* (*AmFT*) expression analysis (section 3.3.1.3.3). Real-time PCR analysis was conducted using the LightCycler® 480 Realtime PCR System as described in section 2.8 using Real-time AmTEM F/Real-time AmTEM R primers to detect *AmTEM*. Ant elf-alpha F/Ant elf-alpha R primers were used to detect the elongation factor housekeeping gene. Primer details, concentrations used in PCRs and anneal/extension temperatures are provided in the Appendix, Table A.1. The same standard curve and cDNA samples were used to analyse expression of all genes, thus relative expression levels can be compared.

5.2.2 *Arabidopsis transfer experiment*

Arabidopsis Col-0, *tem1* and *RNAi-tem1/2* seeds were sown and grown as described in section 2.3. Transfer experiments were carried out using SANYO cabinets set up as described in section 2.3 and plants transferred as described in

section 3.2.4. Flowering times were assessed by counting rosette leaves present at 1 cm bolt height for each plant transferred from LD to SD, as described in section 2.4.

5.2.3 *Real-time PCR analysis of TEM expression*

At each transfer day (section 5.2.2), at least 10 *Arabidopsis* plantlets were harvested from LD cabinets at ZT15. Samples were used for RNA extraction and cDNA synthesis as described in section 2.6. Real-time PCR analysis was conducted using the LightCycler® 480 Realtime PCR System as described in section 2.8 using Real-time AtCO F/Real-time AtCO R, Real-time AtFT F/Real-time AtFT R, Real-time Tem1 F/ Real-time Tem1 R and Real-time Tem2 F/ Real-time Tem2 R primers to detect *Arabidopsis CONSTANS* (*AtCO*), *Arabidopsis FT* (*AtFT*), *Arabidopsis TEM1* (*AtTEM1*) and *Arabidopsis TEM2* (*AtTEM2*), respectively. AtActin F/AtActin R primers were used to detect the actin 2 housekeeping gene. Primer details, concentrations used at in PCRs and anneal/extension temperatures are provided in the Appendix, Table A.1. The same standard curve and cDNA samples were used to analyse expression of all genes, thus relative expression levels can be compared.

5.3 Results

5.3.1 *Developmental AmTEM expression during different photoperiods*

AmTEM mRNA was detected at high levels in all the true leaves during the first 21 days of growth in *Antirrhinum* plants grown under constant LD (Figure 5.1 A). *AmTEM* expression then decreased in all the leaves after this point. Generally, the expression of *AmTEM* in SD conditions was lower than the expression in LD during the assessed period (Figure 5.1 B). In SD conditions *AmTEM* was expressed for longer compared to LD. After 42 days from germination, when *AmTEM* expression is almost completely absent in LD conditions, *AmTEM* is still detectable in SD, but at very low levels.

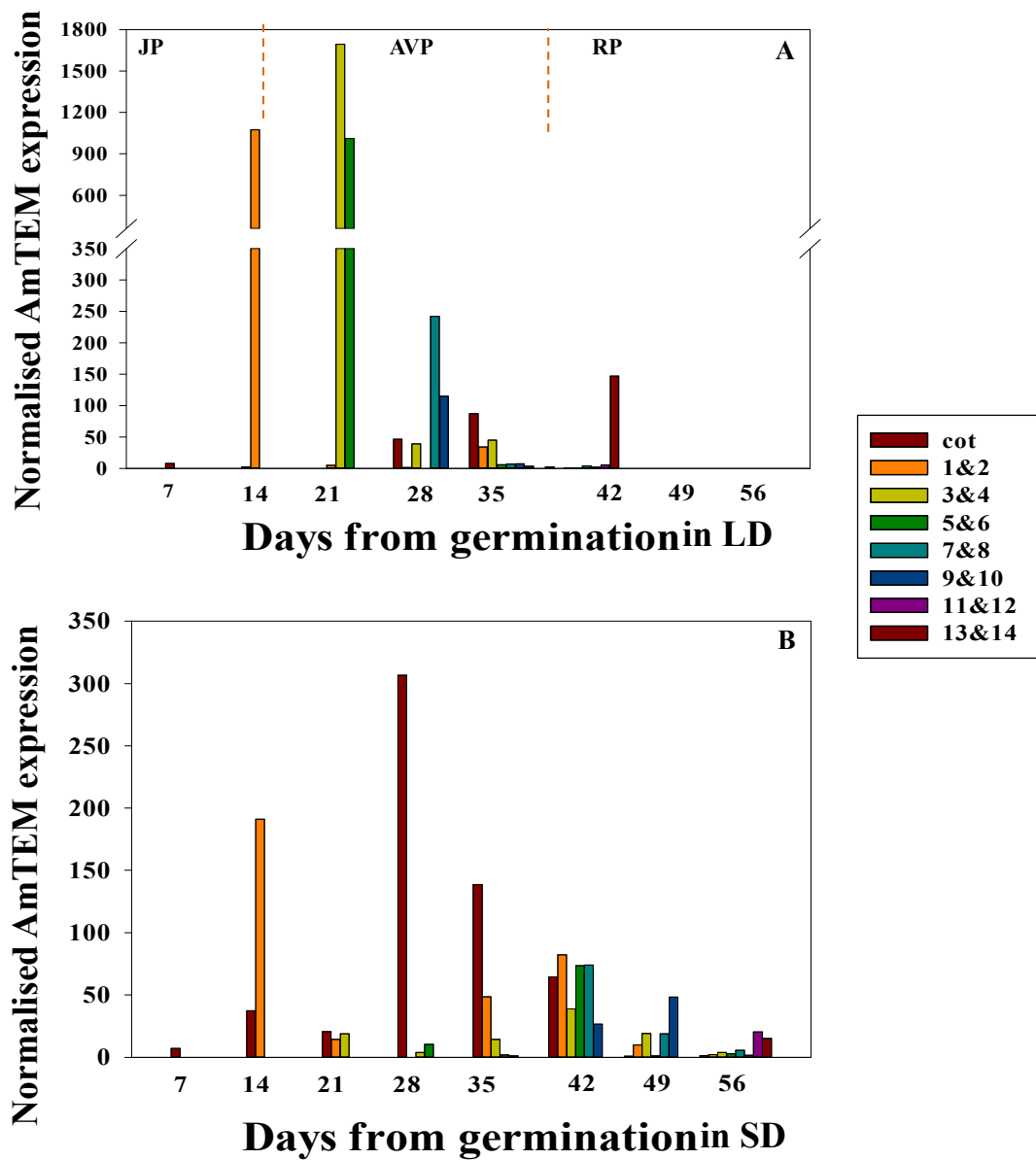


Figure 5.1 Developmental expression of AmTEM in leaf material from *Antirrhinum* plants grown under LD at ZT 15 (A) and SD at ZT 7(B) in Experiment 3.

Real-time PCR analysis of the relative expression of AmTEM normalised to ELF-alpha. Expression analysed at ZT 15. JP: juvenile phase, AVP: adult vegetative phase, RP: reproductive phase. The orange dotted lines delimit the three different phases.

Figure 5.2 shows the expression of *AmTEM* and *AmFT* in the most recent pair of expanded leaves during development. Plants are juvenile for about 14.5 days, as shown in section 3.3.1.3.2 and following the end of juvenility *AmFT* progressively increases while the opposite trend is shown by *AmTEM* expression levels that decrease at the end of juvenility. The pattern is consistent with *AmTEM* repressing *AmFT* expression.

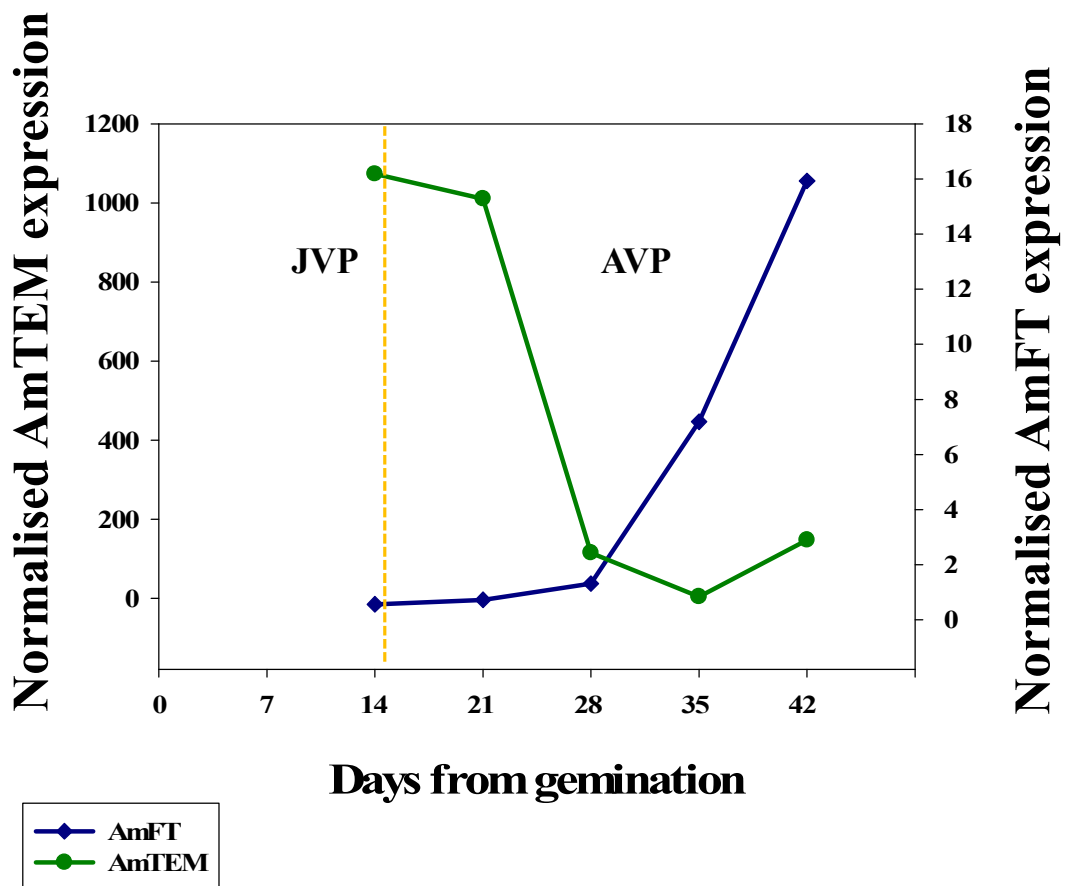


Figure 5.2 Real-time PCR analysis of developmental expression of *AmTEM* and *AmFT* in the youngest pair of fully expanded leaves in *Antirrhinum* plants grown under LD harvested at ZT 15. *AmTEM* and *AmFT* have been normalised to *ELF-alpha* at each timepoint. The JVP and AVP phases are delimited by the orange broken line.

5.3.2 Expression of *AtFT*, *AtCO* and *AtTEM1* during development in *Arabidopsis*

Expression of *CO* was used as a measure of activity of the photoperiodic pathway. Since an *Antirrhinum CO* homologue was not available, to further investigate the activity of the photoperiodic pathway during juvenility and the relationship between *TEM* and *CO* expression, the study was conducted using *Arabidopsis*.

To measure gene expression across development Real-time PCR analysis was carried out in which the same standard curve and cDNA samples were used to analyse expression of all genes. Therefore, the results obtained could be directly compared.

In section 3.3.9, it was shown that the *AtCO* level rises before the end of juvenility (6.8 d \pm 0.2 d after germination) and also before the rise in *FT* level, indicating that the photoperiodic pathway is not completely inactive during the juvenile phase (JP). The level of *AtFT* expression level increases starting from 5 days from germination and reaches the peak at 7 days when plants start to respond to photoperiod (Figure 5.3). *AtTEM1* expression is high until day 4, after this point there is a reduction of the level of expression reaching the lowest level at 7 days from germination. In the previous section it was shown that in *Antirrhinum*, following the end of juvenility, *AmFT* level rises progressively when *AmTEM* level decreases. These observations show that *AtTEM1* and *AtFT* follow the same trend observed for *AmTEM* and *AmFT*. *TEM* may be involved in repressing *FT* transcription during juvenility even though *CO* is present to induce it, to avoid premature flowering.

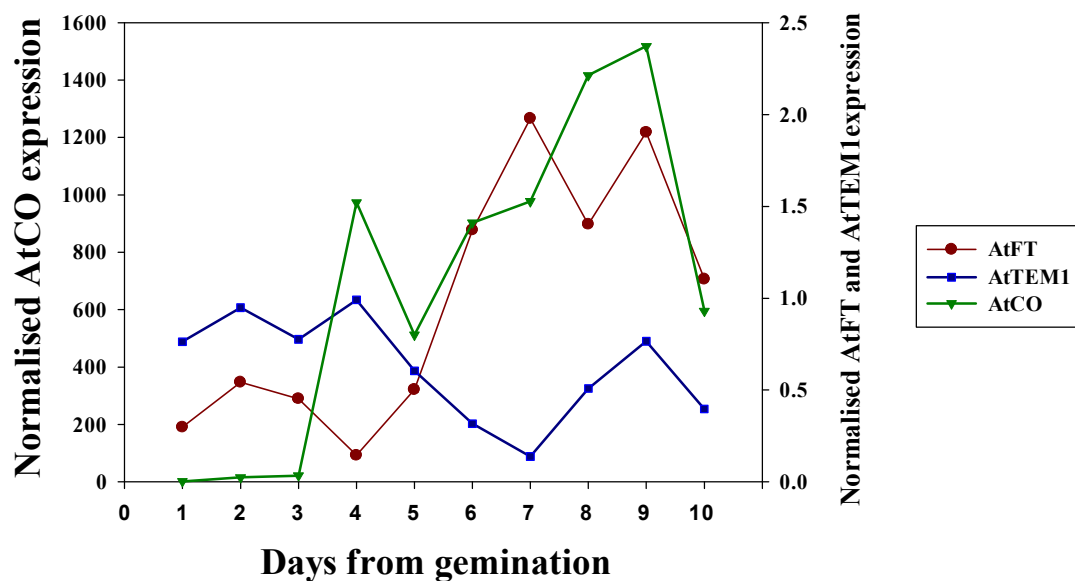


Figure 5.3 Real-time PCR analysis of developmental expression of *AtFT*, *AtCO* and *AtTEM1* in aerial parts in *Col-0* plants grown under LD harvested at ZT 15. *AtFT*, *AtCO* and *AtTEM1* have been normalised to *Actin* at each timepoint.

5.3.3 *AtFT* and *AtCO* expression in *TEM* mutants

To further explore whether *TEM* has a role in determining the length of juvenility through repression of *FT*, *AtFT* and *AtCO* expression was studied in *Arabidopsis tem1* and *RNAi-tem1/2* mutants.

Figure 5.4 shows average levels of *AtTEM1* and *AtTEM2* in the aerial part of plants collected at ZT 15 between day 1 and day 5 from germination. Both *tem1* and *RNAi-tem1/2* showed a significant lower *AtTEM1* expression level compared to WT. *AtTEM2* expression was not significantly lower in the *RNAi-tem1/2* line compared to both WT and the *tem1* single mutant. However, the overall amount of *AtTEM1* and *AtTEM2* in both the mutants was significantly lower than in the WT plants.

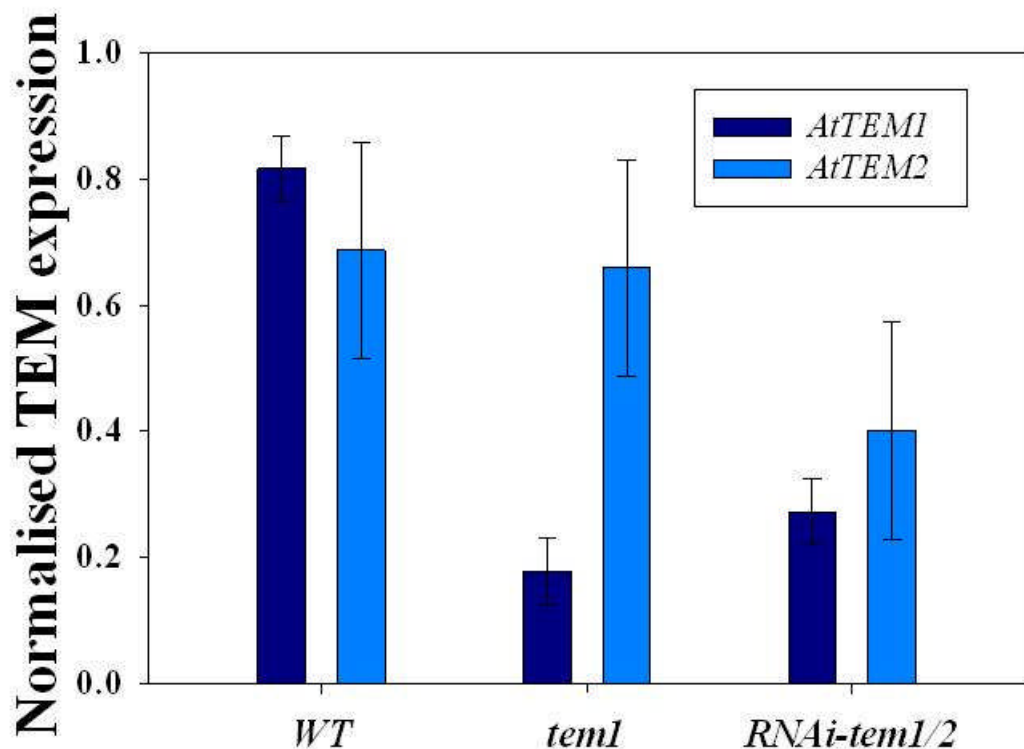


Figure 5.4 Expression of *AtTEM1* and *AtTEM2* in the plant aerial parts under LD at ZT 15 in WT, in *tem1* and in *RNAi-tem1/2* between day 1 and day 5 after germination.

Real-time PCR analysis of the relative expression of *AtTEM1* *AtTEM2* normalised to *Actin*. Material from 5 plants at each sampling day has been collected. Real-time PCR analysis conducted separately for each sampling day and then mean calculated between the 5 days. Data were analysed by general linear model analysis of variance (ANOVA, $p < 0.05$), with subsequent comparison between means using Fisher's least significant difference test. Error bars denote LSD (5% levels) of *AtTEM1* expression levels in WT, *tem1* and *RNAi-tem1/2* (LSD= 0.10; d.f. =8) and of *AtTEM2* expression levels in WT, *tem1* and *RNAi-tem1/2* (LSD= 0.34 d.f. =8).

Differences were observed between developmental patterns of expression of *AtTEM1*, *AtTEM2* and *AtFT* in WT, *tem1* and *RNAi-tem1/2* mutants (Figure 5.5). In *tem1* *AtFT* levels increased at an earlier stage than in the WT (Figure 5.5 A) and a higher level was evident after 4 days (Figure 5.5 B). Furthermore, in *tem1*, *AtTEM2* level increased after 5 days but it did not seem to influence *AtFT* expression. In the *RNAi-tem1/2* plants, where the expression of both *AtTEM1* and *AtTEM2* is low, *AtFT* expression increased after just 2 days (Figure 5.5 C). Moreover, in the first 2 days the relative amount of *AtFT* was higher compared to the same days in WT and

in the single mutant. Therefore, lower *TEM* expression levels correlate with earlier induction and higher *AtFT* expression levels.

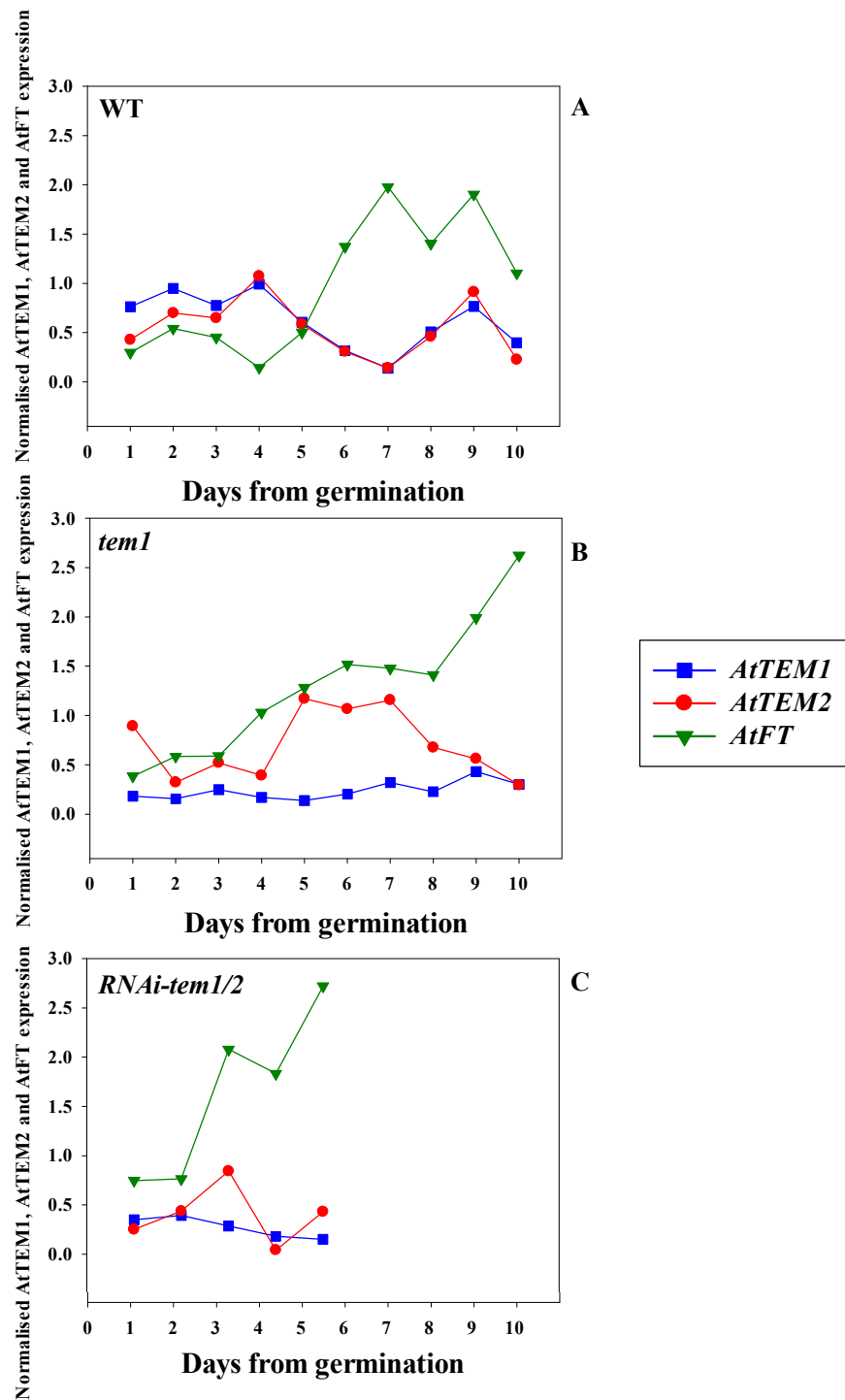


Figure 5.5 Real-time PCR analysis of developmental expression of *AtFT*, *AtTEM1* and *AtTEM2* in aerial parts in WT (A), in *tem1* (B) and *RNAi-tem1/2* (C) plants grown under LD harvested at ZT 15.

AtFT, *AtTEM1* and *AtTEM2* have been normalised to *Actin* at each timepoint.

To further investigate *TEM* effects on the photoperiodic pathway developmental expression of *AtCO* was studied in *Arabidopsis tem1* and *RNAi-tem1/2* mutants (Figure 5.6). *AtCO* transcript levels increased in the *RNAi-tem1/2* line after just 1 day and after 2 days in the *tem1* line. In WT plants *AtCO* level increases after 3 days. The difference in timing of increase of *AtCO* expression in the mutant lines suggests down-regulation of *AtCO* by *TEM*.

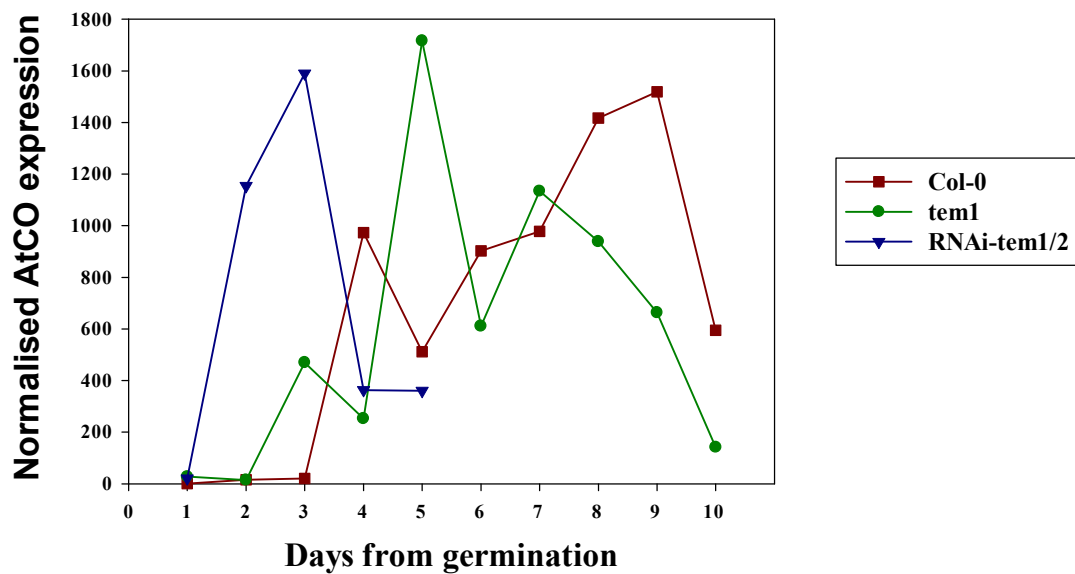


Figure 5.6 Real-time PCR analysis of developmental expression of *AtCO* in aerial parts in *Col-0*, *tem1* and *RNAi-tem1/2* plants grown under LD harvested at ZT 15. *AtCO* has been normalised to *Actin* at each timepoint.

Transfer experiments were conducted using *tem1* and *RNAi-tem1/2* mutant lines in comparison with *Col-0* WT, to determine a role of *TEM* in regulating juvenility.

In section 3.3.9 the length of the juvenile phase in *Col-0* WT plants was calculated to have lasted $6.8 \text{ d} \pm 0.2 \text{ d}$ from germination and the AVP to have lasted for $4.70 \text{ d} \pm 0.2 \text{ d}$. The JP was similarly determined using *tem1* and *RNAi-tem1/2*

mutant plants (Figure 5.7 and 5.8). Under the same growth conditions used for the WT plants, *tem1* plants were shown to be juvenile for $4.06 \text{ d} \pm 0.35 \text{ d}$ following germination, which is approximately 2.5 days shorter than that observed in the WT plants. The AVP was $6.45 \text{ d} \pm 0.35 \text{ d}$, therefore 1.75 days longer than in the WT.

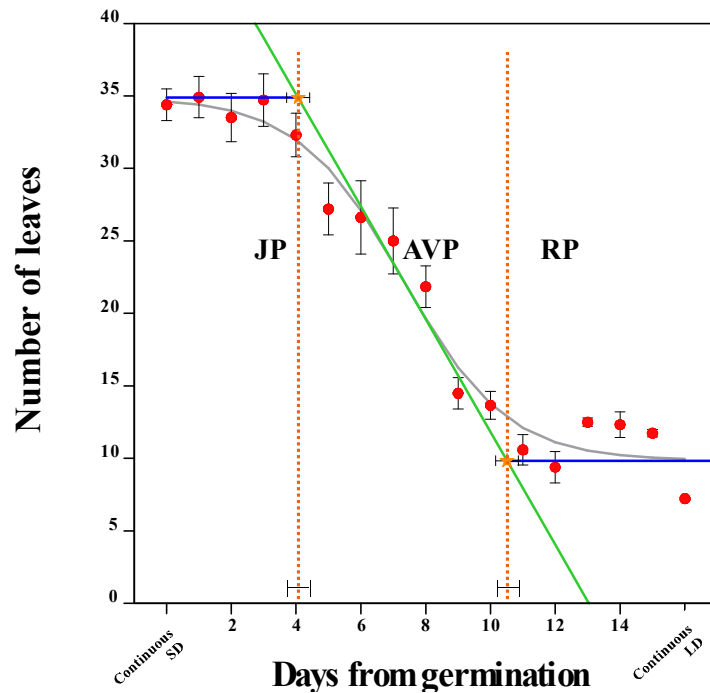


Figure 5.7 Different phases of photoperiod sensitivity in *Arabidopsis tem1*.

The effect of transferring *Arabidopsis* at daily intervals (expressed as days from 50% germination) from LD to SD on flowering time. JP: juvenile phase, AVP: adult vegetative phase, RP: reproductive phase, SD: short day, LD: long day. Vertical error bars denote the standard error of the mean of the number of leaves. Horizontal error bars denote the standard error of the mean of the estimated phase length. Logistic curve (grey curve), maximum slope (green line), lag time (blue lines). The orange dotted lines delimit the three different phases.

RNAi-*tem1/2* plants were juvenile for only $0.009 \text{ d} \pm 0.31 \text{ d}$ after germination indicating that the juvenile phase was extensively abolished in the double mutant. The AVP for the RNAi-*tem1/2* line lasted for $9.71 \text{ d} \pm 0.31 \text{ d}$ (Figure 5.8).

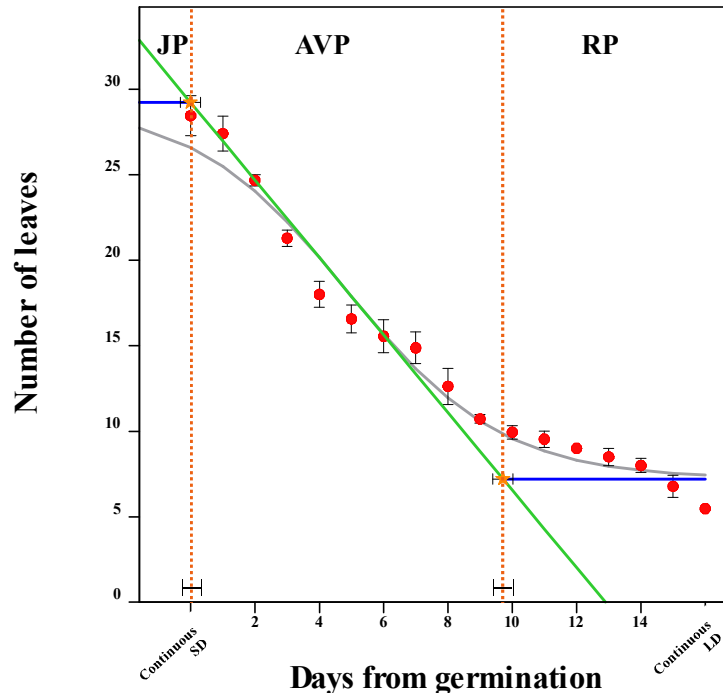


Figure 5.8 Different phases of photoperiod sensitivity in *Arabidopsis RNAi- tem1/2*. The effect of transferring *Arabidopsis* at daily intervals (expressed as days from 50% germination) from LD to SD on flowering time. JP: juvenile phase, AVP: adult vegetative phase, RP: reproductive phase, SD: short day, LD: long day. Vertical error bars denote the standard error of the mean of the number of leaves. Horizontal error bars denote the standard error of the mean of the estimated phase length. Logistic curve (grey curve), maximum slope (green line), lag time (blue lines). The orange dotted lines delimit the three different phases.

5.3.4 Effect of ectopic expression of *AmTEM* on flowering in the *Arabidopsis tem1* mutant

In the absence of *Antirrhinum TEM* knockout lines, to explore the function of *AmTEM* a strategy of over-expression in *Arabidopsis* was used. The CaMV 35S promoter was used to over-express *AmTEM* in the *Arabidopsis tem1* mutant as explained in chapter 4. This was carried out to determine whether *AmTEM* could functionally complement the *tem1* mutant. In addition, the lines were used further to investigate whether *AmTEM* plays a role in regulating juvenility. In chapter 4, 35 independent over-expression lines (35S::*AmTEM/tem1*) that were resistant to BASTA treatment and were PCR positive were described. Among these 3

transgenic lines (35S::*AmTEM/tem1* 2, 35S::*AmTEM/tem1* 75 and 35S::*AmTEM/tem1* 77) were selected for further studies, which are described here after.

T₂ seeds harvested from each T₁ plant were sown and grown under constant LD conditions until flowering and T₃ seed harvested. Late flowering, with respect to *tem1*, was observed in T₂ plants of all three lines (Figure 5.9). A large degree of variation in the number of leaves at flowering in each T₂ plant of each line was observed. There are different reasons why the phenotype would differ between the different lines. All plants shown in Figure 5.9 were PCR positive; therefore, differences in degree of lateness could be due to transgene insertion copy number, WT-like flowering plants could be due to transgene insertion site where the expression is silenced, or due to false positive PCR, and the plant is actually a null segregant. For each transgenic line, T₂ plants were screened by PCR to detect presence of the *AmTEM* transgene (section 4.2.10). Twenty-four, 16 and 40 PCR positive T₂ were generated for lines 2, 75 and 77, respectively. For each line, one T₂ plant was selected to generate T₃ plants for further analysis. These were 35S::*AmTEM/tem1* 2.23 (Line 2), 35S::*AmTEM/tem1* 75.14 (Line 75) and 35S::*AmTEM/tem1* 77.36 (Line 77) which flowered later than WT to varying degrees with 6.77, 8.77 and 9.77 more leaves, respectively.

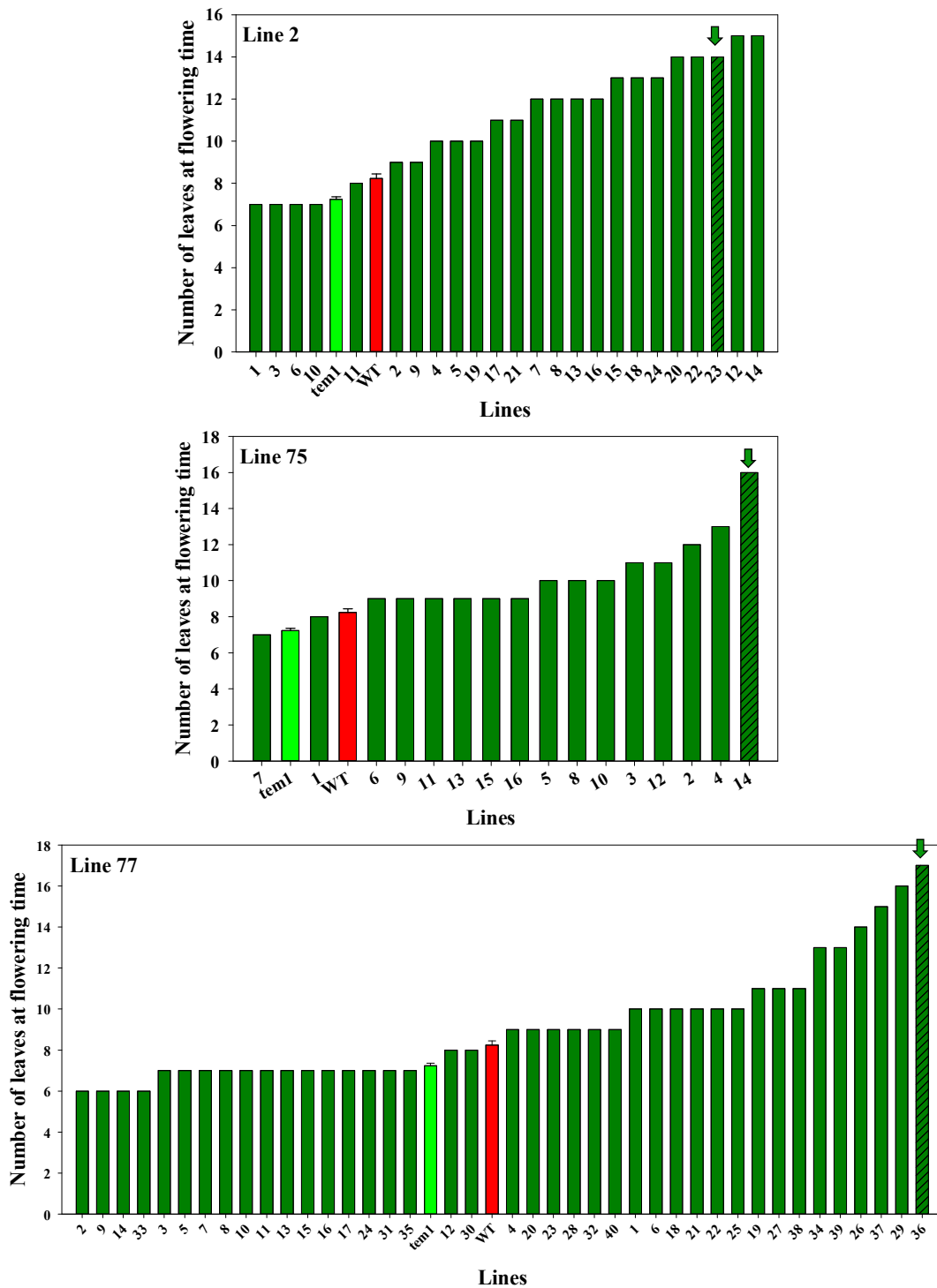


Figure 5.9 Leaves present at flowering time of T_2 generation plants of three lines (2, 75 and 77) engineered to over-express *AmTEM* in the *tem1* mutant. Leaves present at flowering time of WT and *tem1* mutant are shown as comparison. Error bars denote the standard error of number of leaves present at flowering time. Arrows and shaded bars show the plants selected for further analysis.

T₃ plants representing each line were grown and 10 were analysed for the presence of the *AmTEM* transgene by PCR (section 4.2.10). All T₃ plants screened resulted positive and therefore were considered homozygous for the transgene.

Whilst the *tem1* mutant flowered at 26 d following germination, T₃ plants representing the three lines had not flowered at this time (Figure 5.10 A). T₃ plants representing Lines 2, 75 and 77 flowered later than the *tem1* mutant (7.23 leaves) at averages of 9.8 (\pm 0.3), 10.6 (\pm 0.6) and 10.0 (\pm 0.4) leaves respectively (Figure 5.10 B).

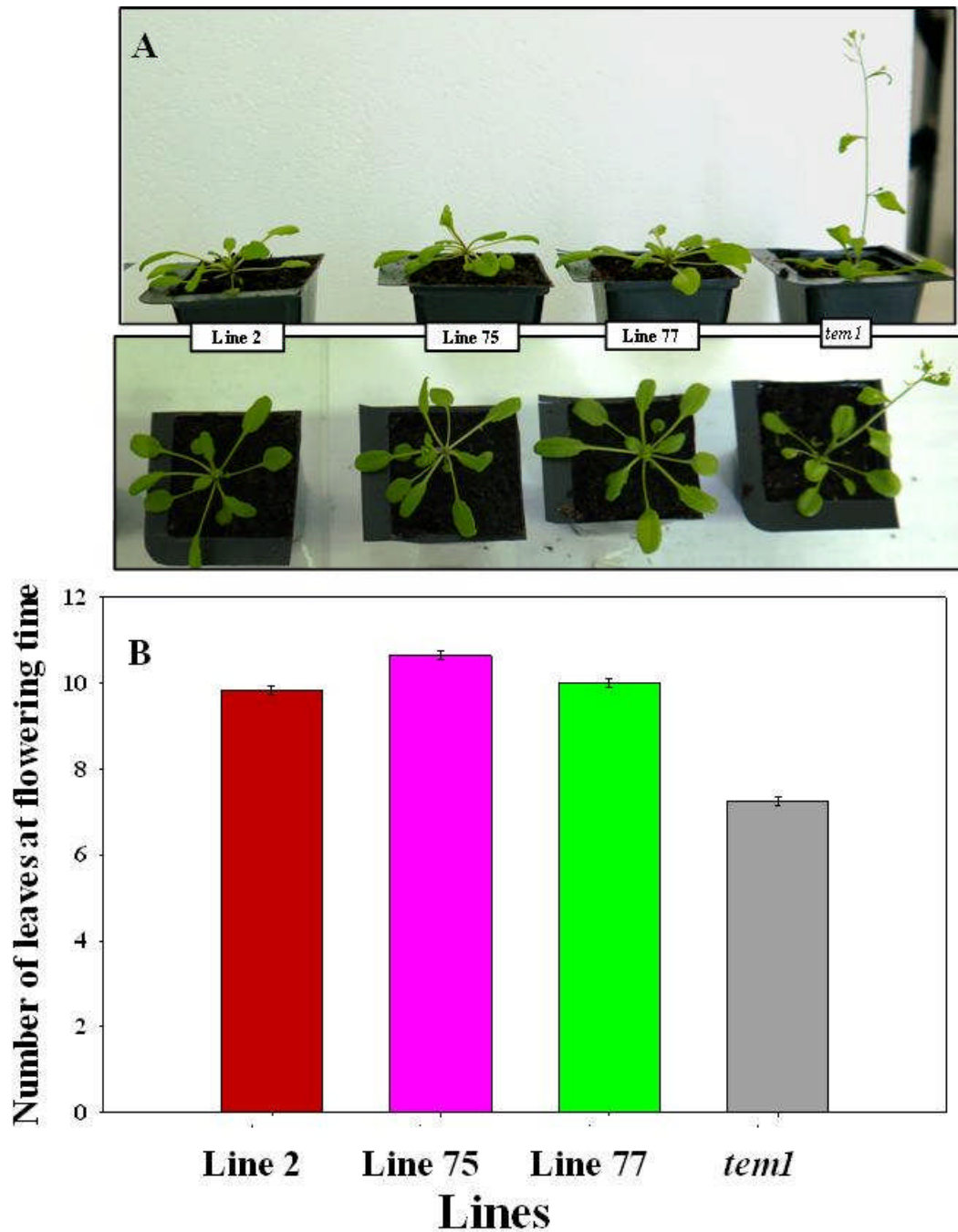


Figure 5.10 Phenotype of T_3 transgenic *Arabidopsis tem1* plants over-expressing *AmTEM* and the non-transformed *tem1* mutant.

A) Transgenic lines at 26 days from germination compared with the *tem1* mutant. B) Number of leaves at flowering time of the transgenic lines and *tem1* mutant under LD conditions. For line 2, $n=11$; for line 75, $n=11$; for line 77, $n=14$; for *tem1* mutant, $n=68$.

Data were analysed by general linear model analysis of variance (ANOVA, $p<0.05$), with subsequent comparison between means using Fisher's least significant difference test. Error bars denote LSD (5% levels) between the lines (LSD= 0.19).

5.3.4.1 Correlation between *AmTEM* expression and flowering in *Arabidopsis tem1*

Real-time PCR analysis was performed to determine a correlation between the delay in flowering and expression level of *AmTEM*. Expression was analysed in samples at daily intervals from germination over the first 10 days. The averaged expression of this time period is shown in Figure 5.11. Expression in WT and the *tem1* mutant was studied as well to verify the specificity of the primers used. Highest *AmTEM* expression was observed in Line 75 with decreasing levels observed in Line 2 and Line 77. Even in Line 77 *AmTEM* expression was sufficient to significantly delay flowering (Figure 5.10 B). No *AmTEM* expression was detected in the *tem1* mutant or in WT.

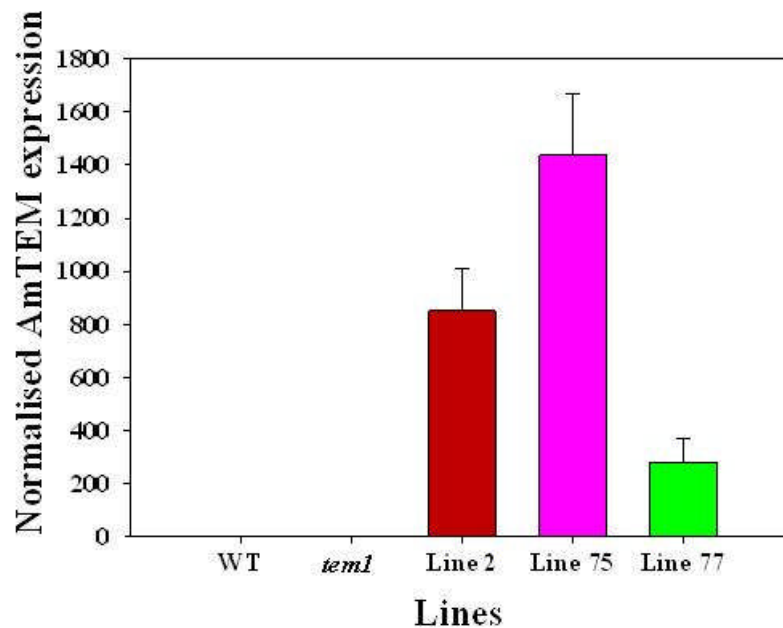


Figure 5.11 Real-time PCR analysis of *AmTEM* expression in aerial parts of WT, *tem1* mutant and T_3 transgenic plants from lines 2, 75 and 77 grown under LD harvested at ZT 15. The average of the first 10 days from germination is presented for each line. *AtTEM1* has been normalised to Actin at each timepoint. Error bars denote the standard error of number of leaves present at flowering time.

5.3.5 Effect of ectopic expression of *AmTEM* in the *tem1* mutant on *AtFT* and *AtCO* expression

Comparison of *AtFT* developmental expression in the *tem1* mutant with the over-expressing lines showed a clear difference (Figure 5.12). Real-time PCR analyses were carried out using the same cDNA samples and standard curve; therefore, the results obtained could be directly compared. All three transgenic lines showed a reduction in *AtFT* expression during all the developmental stages studied compared to *tem1*. In particular there was a delay in the moment at which a rise takes place. In *tem1* *AtFT* expression rose after 3 days from germination, whilst in line 2 and line 77 an increase occurred after 4 days from germination and in line 75 the increase was appreciable after 6 days from germination.

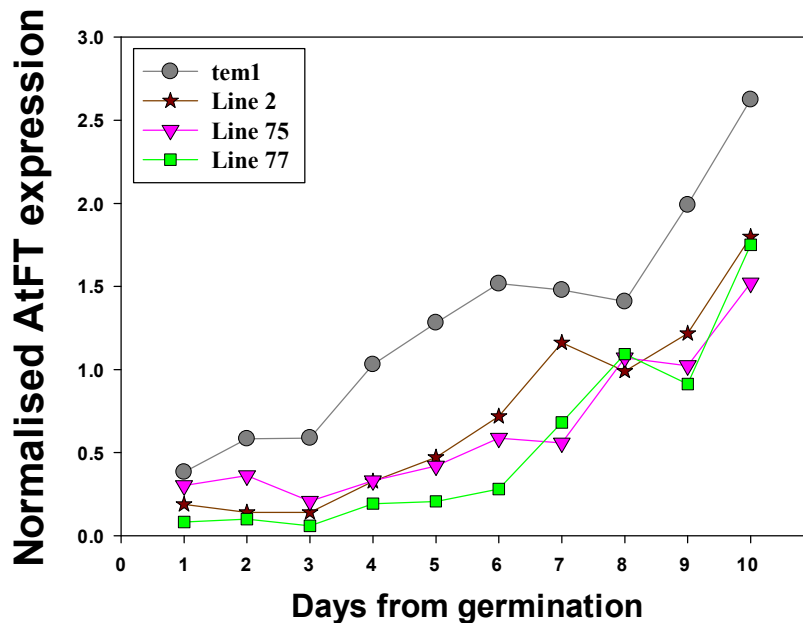


Figure 5.12 Real-time PCR analysis of *AtFT* developmental expression in the *tem1* mutant and T_3 generation *AmTEM* over-expressing *tem1* plants representing lines 2, 75 and 77. Analysis of aerial parts in plants grown under LD harvested at ZT 15. *AtFT* has been normalised to *Actin* at each timepoint.

Ectopic expression of *AmTEM* in the *tem1* mutant also had an effect on *AtCO* expression during development (Figure 5.13). The onset of the induction of

AtCO expression was delayed in the transgenic lines compared with *tem1* to varying degrees. In the *tem1* mutant, *AtCO* expression levels rose after 2 days from germination, peaking 5 days after germination. Line 2 showed a delay of 1 day in *AtCO* expression, rising after 4 days from germination and reaching the maximum level after 6 days from germination. Lines 75 and 77 showed a lower expression of *AtCO* throughout all the development and a delay of 5 and 4 days, reaching *AtCO* maximum levels after 10 and 9 days after germination, respectively.

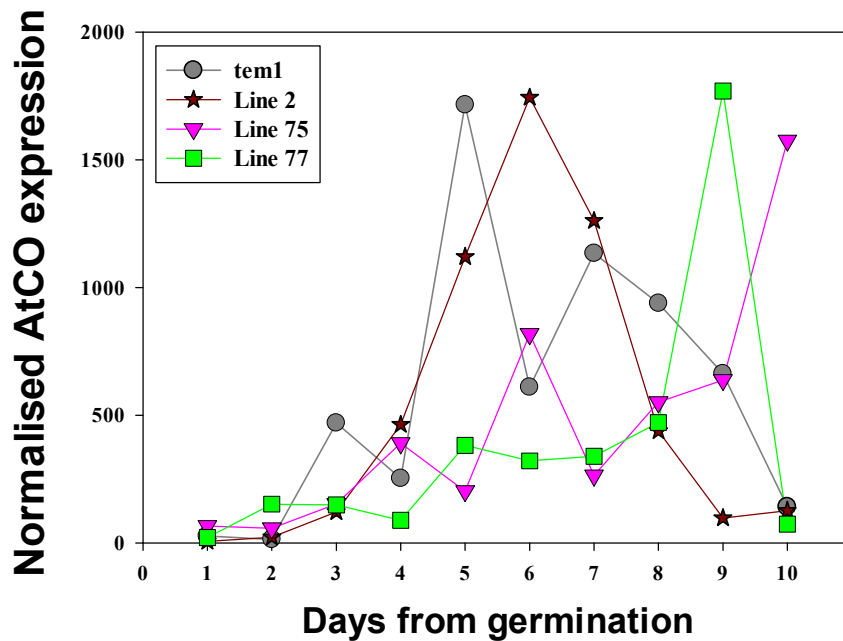


Figure 5.13 Real-time PCR analysis of *AtCO* developmental expression in the *tem1* mutant and T_3 generation *AmTEM* over-expressing *tem1* plants representing lines 2, 75 and 77. Analysis of aerial parts in plants grown under LD harvested at ZT 15. *AtCO* has been normalised to *Actin* at each timepoint.

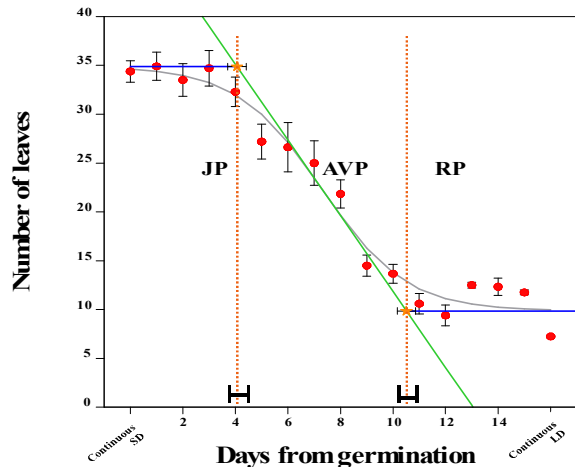
5.3.6 Effect of ectopic expression of *AmTEM* on juvenile phase length

To determine whether over-expression of *AmTEM* affects the length of the juvenile phase, *tem1* and T_3 homozygous plants representing transgenic lines 2, 75 and 77, over-expressing *AmTEM*, were used in transfer experiments from LD (DLI

= $3.08 \text{ mol}\cdot\text{m}^{-2}\cdot\text{d}^{-1}$) to SD (DLI = $2.79 \text{ mol}\cdot\text{m}^{-2}\cdot\text{d}^{-1}$) and the different phases of photoperiod sensitivity determined as described in section 2.4 (Figure 5.14 A-D).

The length of the juvenile phase in *tem1* was calculated as $4.06 \text{ d} \pm 0.35 \text{ d}$ following germination and the AVP as $6.45 \text{ d} \pm 0.35 \text{ d}$ long (Figure 5.14 A). Line 77 exhibited the lowest *AmTEM* mRNA levels (Figure 5.11) and had the shortest juvenile phase amongst the three transgenics, lasting for $7.4 \text{ d} \pm 0.33 \text{ d}$ (Figure 5.14 D). Line 2 had intermediate *AmTEM* mRNA levels (Figure 5.11) and was shown to have a longer juvenile phase, lasting for $8.6 \text{ d} \pm 0.26 \text{ d}$ than the Line 77 (Figure 5.14 B). The highest *AmTEM* mRNA levels were observed in Line 75 (Figure 5.11) and this had a juvenile phase which lasted for $8.9 \text{ d} \pm 0.26 \text{ d}$ (Figure 5.14 C). All the transgenic lines had extended JPs when compared with the *tem1* mutant. The length of JP in the three transgenic lines shows a positive correlation with the different degree of *AmTEM* over-expression.

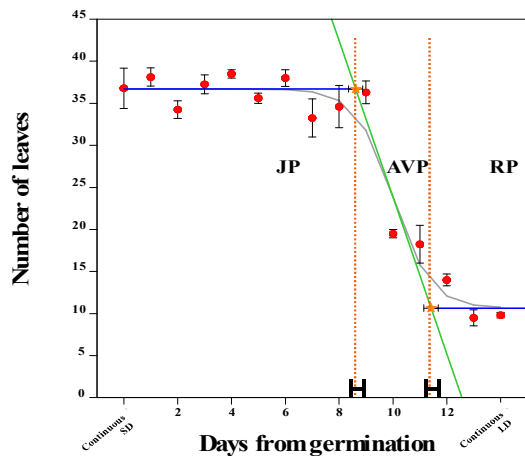
Also influenced by ectopic expression of *AmTEM* in *Arabidopsis tem1* is the length of the adult vegetative phase and onset of the reproductive phase. In the *tem1* mutant the AVP lasted for about 6.5 d and the RP started at about 10.5 d from germination. In the transgenic lines, although the start of the AVP was delayed, it was shorter. The higher the level of *AmTEM* expression the shorter the AVP, lasting for about 2.5, 2.8 and 4.51 d in lines 75, 2 and 77, respectively. Because of the longer JP, the RP is delayed in all the transgenic lines, even if the AVP is shorter.



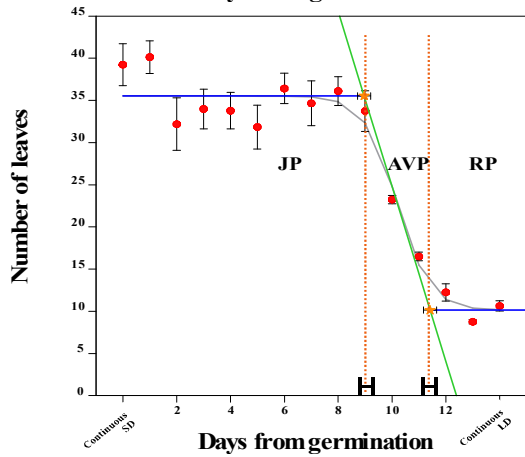
A) *tem1*

Figure 5.14 Different phases of photoperiod sensitivity in *tem1* (A), Line 2(B), Line 75(C) and Line 77(D).

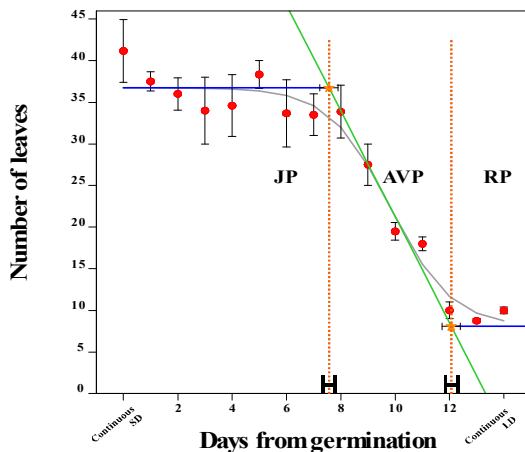
The effect of transferring *Arabidopsis* at daily intervals (expressed as days from 50% germination) from LD to SD on flowering time. JP: juvenile phase, AVP: adult vegetative phase, RP: reproductive phase, SD: short day, LD: long day. Vertical error bars denote the standard error of the mean of the number of leaves. Horizontal error bars denote the standard error of the mean of the estimated phase length. Logistic curve (grey curve), maximum slope (green line), lag time (blue lines). The orange dotted lines delimit the three different phases.



B) Line 2



C) Line 75



D) Line 77

5.3.7 Relationship between juvenility and the photoperiodic pathway in *tem1* plants over-expressing *AmTEM*

In section 5.3.5, it was shown that the presence of *AmTEM* in *tem1* plants alters *AtFT* and *AtCO* expression. In this section, the expression level of these genes is shown in relation to the length of juvenility (Figure 5.15).

In all the transgenic lines over-expressing *AmTEM* and also in the *tem1* mutant, the increase in *AtFT* expression levels matched with the end of juvenility. In the *tem1* mutant and in lines 75 and 77 over-expressing *AmTEM*, *AtCO* was more highly expressed during AVP, after juvenility ended. In Line 2, *AtCO* peaked and was more highly expressed during juvenility. Because of the differences in *AtCO* expression levels in the over-expressing *AmTEM* lines, these data must be interpreted with caution.

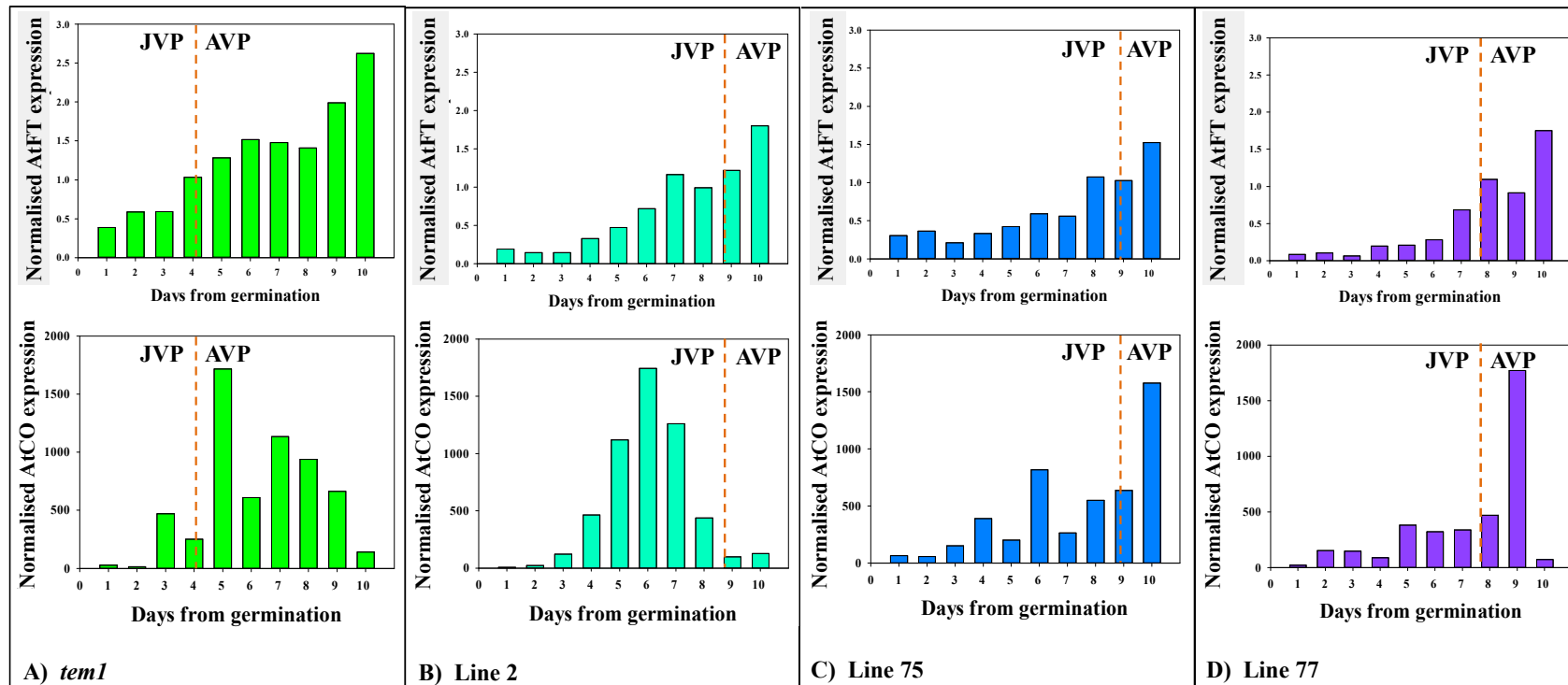


Figure 5.15 Real-time PCR analysis of developmental expression of *AtFT* and *AtCO* in aerial parts in *tem1* mutant (A), and T_3 transgenic plants representing Line 2 (B), Line 75 (C) and Line 77(D) grown under LD harvested at ZT 15.

AtFT and *AtCO* have been normalised to *Actin* at each timepoint. The JVP and AVP phases are delimited by the orange broken line.

5.4 Discussion

In this study the expression pattern of *AmTEM* in *Antirrhinum* throughout development in each pair of leaves present on the plant is reported. *AmTEM* is expressed more highly during the first 21 days from germination and a progressive decrease is notable when juvenility ends. When these data are compared with *AmFT* expression in the youngest, fully expanded leaves the opposite trend is observed. These results are similar to what is reported in *Arabidopsis* where a decrease in *AtTEM1* expression has been hypothesised to be a key factor for induction of *FT* (Castillejo and Pelaz, 2008).

In *Arabidopsis* it has been proposed that the AP2 and B3 domains present in *TEM1* gene, can interact with the 5' UTR region of *FT* by binding to CAACA and CACCTG sequences and thus repress its expression (Castillejo and Pelaz, 2008; Kagaya *et al.*, 1999). These binding sites are close the CAAT sequence, which has been proposed to be the binding site of CO and the CCAAT-box binding protein, which suggests that there could be competition for binding in the *FT* gene 5' UTR (Castillejo and Pelaz, 2008).

Analysis of the *AmFT* 5' UTR reveals that the gene has the binding regions which could be used by *AmTEM* (see Appendix, Figure A.13 for sequence and binding sites). The two binding sites present on *AmFT* are CAACA and GTCCTT which can be considered a variation of the RAV family binding domains as described by Kagaya *et al.*(1999) (Appendix, Figure A.14). The other relevant characteristic is that the motif TAAC, which is bound by CO and the CCAAT-box binding protein (Wenkel *et al.*, 2006), is located between these two sequences in

AmFT. This suggests that this binding mechanism could be conserved in *Antirrhinum* to allow *AmFT* regulation by *AmTEM*.

This chapter also studied the expression of *AtFT*, *AtCO* and *AtTEM* genes in relation to the juvenile phase. In previously published work the length of juvenility was not determined (Castillejo and Pelaz, 2008). The activity of the photoperiodic pathway during juvenility in *Arabidopsis* Col-0 WT plants was established in chapter 3. The photoperiodic pathway activity during juvenility was also studied in the *tem1* and RNAi-*tem1/2* mutants. The overall amount of *AtTEM* present was shown to influence *AtFT* expression and juvenile phase length. The absence of the *AtTEM1* and *AtTEM2* in the mutant plants not only shortened JP length but also prolonged the AVP. In the *tem1* mutant a generally higher level of *AtFT* expression and earlier induction was detected, which corresponded to shorter juvenile phase length. The same trend but with even shorter juvenility and a higher and faster increase in *AtFT* level was observed in the RNAi-*tem1/2* line. These results also demonstrated that *AtTEM2* does not fully compensate *AtTEM1* activity and that they are not entirely functionally redundant in maintaining juvenility.

Although more transgenic lines that over-express *AmTEM* could be used to study the role of *AmTEM* in relation to juvenility, many factors such as the random insertion of the transgene and the number of copies inserted can produce significant differences in transgene expression that can influence phenotype. Nevertheless, it is possible to conclude that *AmTEM* was able to functionally complement the *Arabidopsis tem1* mutant and delay flowering. Plants over-expressing *AmTEM* had an extended juvenile phase compared with the *tem1* plants, with the length of juvenility being proportional to levels of *AmTEM* expression. Also, the delay in flowering time was not determined by an extension of the AVP which, in fact was

shorter than in the *tem1* mutant. At the molecular level the longer JP coincided with delayed and lower *AtFT* expression and a delay in rise of *AtCO* in the over-expressing lines. An opposite trend was observed in the RNAi-*tem1/2* and *tem1* lines where the shorter juvenile phase coincided with higher *AtFT* expression and an earlier increase in *AtCO*. The *AtCO* gene sequence contains two binding regions which could, theoretically, be bound by *AtTEM*. See Appendix, Figure A.15 for the sequence and binding sites. The two binding sites present on *AtCO* are CAACA and ACCCTG. These are variations of the RAV family binding domains, as described by Kagaya *et al.* (1999). For this reason a possible role of *AtTEM1* in the regulation the juvenile phase length through repression of *AtFT* but also in the down regulation of *AtCO* expression can be hypothesised.

Interestingly, in the plants ectopically expressing *AmTEM*, *AtFT* and *AtCO* expression was lower and delayed but not completely absent. As a consequence, flowering was delayed but not repressed. These results lead to the hypothesis of the presence and the action of *TEM* repressors. Therefore, *TEM* may be regulated at both transcriptional and post transcriptional levels.

From data in Figure 5.15 (with the exception of Line 2, which is anomalous), it can be speculated that during juvenility *TEM* is not repressed, therefore *CO* and *FT* levels are low. After juvenility, once adult, *TEM* is repressed, therefore *CO* and *FT* levels are higher. This is consistent with observations of developmental expression of *TEM*.

In LD conditions, GIGANTEA (GI) and FLAVIN-BINDING, KELCH REPEATED, F-BOX (FKF1) repress CYCLING DOF FACTOR 1 (CDF1) which represses *CO* (Fowler *et al.*, 1999; Paltiel *et al.*, 2006; Sawa, *et al.*, 2007). Previous work showed that *TEM1* and *TEM2* are also down-regulated by GI (Sawa and Kay,

2011). So it is possible that *TEM1* could have a similar function to *CDF1* in repressing *CO* expression. In addition, GI also physically binds *FT* at the same binding site of the *FT* repressors *TEM1*, *TEM2*, affecting their activity (Castillejo and Pelaz, 2008; Lee *et al.*, 2007; Sawa and Kay, 2011). Previous studies showed that *TEM1* and *TEM2* are also down-regulated by *APETALA1* (*AP1*) (Kaufmann *et al.*, 2010). Other *AP2-like* genes, such as *TARGET OF EAT1* (*TOE1*) and *TOE2*, have been shown to play a role in repressing flowering (Aukerman and Sakai, 2003). These genes, and other *AP2-like* genes, are targeted by microRNA172 (*miR172*), which increases as plants develop (Aukerman and Sakai, 2003; Jung *et al.*, 2007). High *miR172* levels could also be also responsible for down-regulation of *TEM* during development.

CHAPTER 6. GENERAL DISCUSSION

6.1 Discussion

6.1.1 *Juvenile phase length can be determined in Antirrhinum plants grown in SANYO growth chambers*

Previous studies to determine the juvenile phase (JP) in *Antirrhinum* were carried out in glasshouses, which are expensive and do not give reproducible conditions. In the current study, to obtain more reproducible, uniform and cost-effective conditions, plants were grown in SANYO MLR-351H cabinets. The results obtained here showed that the SANYO MLR-351H cabinets can be used to grow both *Antirrhinum* and *Arabidopsis* plants from seedling to flowering in order to investigate juvenility using a cheaper to run and more controllable environment.

The quantity of light received and used by a plant has a strong impact on its growth, development, yield and quality. Daily light integral (DLI) is a function of light intensity and photoperiod duration and represents the amount of photosynthetically active radiation (PAR) received each day by plants (Faust *et al.*, 2005). The DLI inside a glasshouse can vary with the seasons and it can be crucial for plant development (Faust *et al.*, 2005). A higher DLI increases plant biomass and can also shorten the time to flower, which can be desirable features for crop production (Oh *et al.*, 2009). In *Antirrhinum*, a longer photoperiod leads to earlier

flowering and a reduction in the leaf number (Cremer *et al.*, 1998). Furthermore, a higher DLI has the same effect in reducing time to flower (Cremer *et al.*, 1998).

In the current study, the effect of DLI on JP length was investigated by transferring plants between LD to SD conditions. DLI delivered to the *Antirrhinum* plants in transfer Experiment 1 was 7.17 and 3.53 mol·m⁻²·d⁻¹ in LD and SD, respectively. In the Experiment 2 and Experiment 3 DLI was reduced to 3.08 and 2.94 mol·m⁻²·d⁻¹ in LD and SD, respectively. Although DLI in SD cabinets was similar in the three experiments, the different DLI experienced by plants in LD when they are still juvenile, resulted in a difference in the JP length. Plants grown under LD conditions with the higher DLI had shorter JP than ones grown under lower DLI. Such findings are in accordance with previous experiments conducted in glasshouses using *Antirrhinum* and other plant species such as cyclamen, petunia, marigold and vinca (Adams, 1999; Cremer *et al.*, 1998; Faust *et al.*, 2005; Munir *et al.*, 2004; Oh *et al.*, 2009). Under lower DLI, JP in *Antirrhinum* was the same in both Experiment 2 and Experiment 3, showing that the environmental conditions set in the SANYO cabinet give reproducible results.

Previous studies on *Antirrhinum* in glasshouse experiments have investigated the effects on the JP of different DLI obtained by shading plants during winter and summer experiments. These showed that low DLI (≤ 5 mol·m⁻²·d⁻¹) has a great impact on JP length (Thomas, 2009). In the present study, a reduction of one day on the JP length was observed between *Antirrhinum* experiments of different DLI. The short reduction of the JP length does not fit with the observation of Thomas (2009), where a larger reduction of the JP would be expected through such changes in DLI. One difference between these and previous experiments in glasshouses is that plants received a main light period of 8 h which in the current experiments was extended

to 16 h by a low light extension. Changes in DLI therefore were confined to the main light period, whereas in the glasshouse experiments it was spread evenly over 16 h. This may suggest that the light in the main light period is a critical component of the DLI response. Other studies in progress in the same group of the current study, where plants are grown in SANYO cabinets and then transferred from SD with different DLIs to LD conditions with a high DLI, showed a larger difference in JP length (Piyatida Amnuaykan personal communication). Reducing DLI also prolonged the adult vegetative phase (AVP), suggesting that, although they are competent to respond to the inductive photoperiod, the actual response is delayed. Therefore, the time plants spend in inductive conditions, and the DLI received after the JP, contribute to flowering time in an additive way and during AVP plants are sensitive to DLI. Similar findings were shown in previous *Antirrhinum* studies conducted in glasshouses where plants exposed to a lower light integral had extended AVPs (Adams, 1999). Importantly, differences in JP length in plants grown under different DLIs has been shown not to be caused by differences in growth rate since leaf production rates measured in plants grown under high and low DLI were shown to be the same (Piyatida Amnuaykan personal communication).

Another way of monitoring developmental stages in *Antirrhinum* is by observing phyllotaxy changes at the main stem shoot apical meristem (SAM) (Benlloch *et al.*, 2007; Bradley *et al.*, 1996). Changes here are driven by the activity of a set of key genes. In *Antirrhinum* *FLORICAULA* (*FLO*), the homologue of *Arabidopsis* *LEAFY* (*LFY*), is involved in floral development and its expression is repressed by *CENTRORADIALIS* (*CEN*), the homologue of *Arabidopsis* *TERMINAL FLOWER1* (*TFL1*) (Amaya *et al.*, 1999; Bradley *et al.*, 1996; Bradley

et al., 1996; Coen *et al.*, 1991). It was shown in this study that it is possible to follow plant development through observation of SAM changes. Analysis of *FLO* and *CEN* expression across development linked these genes to commitment to floral initiation. In *Arabidopsis* *LFY* has been shown to be expressed during the vegetative phase and increases before flowering (Blazquez *et al.*, 1997). In *Antirrhinum* *FLO* was shown not to be expressed in SD or LD early in development. This is contrary to the finding in *Arabidopsis* but consistent with the finding of Coen *et al.* (1990) which linked *FLO* expression to the reproductive phase. *CEN* expression increases earlier than *FLO* but still not before flower commitment. In *Arabidopsis* *TFL1* represses *LFY* in the shoots during the vegetative phase (Bradley *et al.*, 1996; Coen *et al.*, 1990). From the results presented in the current study, in *Antirrhinum* this process may be delayed until after the end of the vegetative phase. Neither *FLO* nor *CEN* expression appear linked to the end of juvenility in *Antirrhinum* and thus could not be used as markers for the phase transition.

6.1.2 Induction of *FT* expression linked to end of juvenility

In *Arabidopsis*, *FT* represents one of the key genes involved in the initiation of flowering where most of the floral photoperiodic pathways converge (Araki *et al.*, 1998; Turck *et al.*, 2008). In the current study, expression of the *Antirrhinum* *FT* (*AmFT*) was tested throughout plant development. The study described in this thesis builds on previous work where *AmFT* expression was tested in the youngest expanded leaves during *Antirrhinum* development and shown to be absent during juvenility (Thomas, 2009).

It was shown that *AmFT* expression increases in all leaves across development following the end of juvenility. Notably, during juvenility *AmFT* expression levels were very low under LD condition. These findings led to an investigation to find out whether *AmFT* levels were low during juvenility due to inactivity of the photoperiod pathway or due to repression of *AmFT*. In *Arabidopsis*, as seen in *Antirrhinum*, *Arabidopsis FT (AtFT)* expression was shown to increase around the end of juvenility. However, *Arabidopsis CO (AtCO)* expression was found to be high during juvenility indicating activity of the photoperiodic pathway during this phase. In the light of this finding, repression of *FT* to prevent its accumulation was investigated.

6.1.3 *TEMPRANILLO*, an *FT* repressor, isolated from *Antirrhinum* and Olive

Although the flowering behaviour of woody perennials may be dissimilar to that of herbaceous species, it has been suggested by several previous studies on different plants that some common genetic networks control flowering in annual and perennial plants (Tan and Swain, 2006). One of the aims of the current study was to identify and characterize *Antirrhinum* homologues of *Arabidopsis* genes that reduce or antagonise *FT* expression and to translate the study to the woody plant *Olea europaea*. The targets of this study were the transcription factors, *TEMPRANILLO 1 (TEM1)* and *TEM2*, which in *Arabidopsis* have been shown to repress flowering through repression of *FT* (Castillejo and Pelaz, 2008).

Full length cDNA representing *TEM* homologues from *Antirrhinum* (*AmTEM*) and olive (*OeTEM*) were isolated and characterised. Since all PCR fragments cloned for *AmTEM*, obtained using degenerate primers, corresponded to

one individual sequence, it suggests that only one *TEM-like* gene is present in *Antirrhinum*. Similarly, in *Brachypodium* and rice, only one *TEM-like* gene was identified (Higgins *et al.*, 2010).

Both *AmTEM* and *OeTEM* were classified as members of the B3 superfamily, family RAV, class I. Each possess the B3 domain, which harbours the motif WN/RSSQS that is characteristic of the RAV family and the AP2 domain, that defines Class I genes as defined by Romanel *et al.* (2009). It has been proposed that in *Arabidopsis* the B3 and the AP2 domains are both necessary for inhibition of *FT*, binding to its 5' UTR region, competing with CO for its binding site (Castillejo and Pelaz, 2008; Kagaya *et al.*, 1999). Investigation of the 5' UTR region of *AmFT* showed that it harbours CAACA and GTCCTT regions that could be bound by *AmTEM*. Furthermore, a putative CO binding site is also present in the 5' UTR region of *AmFT*, which lies between the B3 and AP2 putative binding sequences. Thus in *Antirrhinum* a similar competing mechanism could exist for regulation of *AmFT* by *AmCO* and *AmTEM*.

Phylogenetic analysis showed that *AmTEM* and *OeTEM* are closely related to other RAV-like DNA-binding proteins clustering with *AtTEM1* and *AtTEM2* and sharing close homology to the related *AtRAV1*.

6.1.4 *AmTEM* and *OeTEM* regulate flowering time

In *Arabidopsis*, *AtTEM1* expression levels were shown to be high during juvenility and decline after the end of this phase. It was found that the absence of *AtTEM1* and *AtTEM2* in the *tem1* and RNAi-*tem1/2* line mutants shortened JP length. *OeTEM* and *AmTEM* were shown to be expressed more highly in juvenile

material compared to adult. The high levels of *OeTEM* and *AmTEM* expression during juvenility suggest that *OeTEM* and *AmTEM* play a role during early developmental stages. Plants engineered to over-express *AmTEM* and *OeTEM* were late flowering compared to both the *Arabidopsis tem1* single mutant and WT, which demonstrate their role in flowering time regulation. *OeTEM* and *AmTEM* genes isolated in the current study are more likely to be *TEM* genes and not *RAVI* comes from the observation that *AtRAVI* plays a role in leaf senescence (Woo *et al.*, 2010) and no signs of premature senescence were visible in any of the transformed plants that were engineered to over-express *OeTEM* and *AmTEM*, or indeed *AtTEM1*.

6.1.5 *TEM* regulates JP length through repression of FT

A reciprocal relationship between *AmTEM* and *AmFT* was revealed with levels of *AmTEM* being high during early development and decreasing prior to the end of juvenility, after which *AmFT* levels increase. In *Arabidopsis*, following the end of juvenility, *AtFT* level increases as *AtTEM1* level decreases, showing the same trend observed for *AmTEM* and *AmFT*. These observations are in line with findings of Castillejo and Pelaz (2008) in *Arabidopsis* where developmental expression of *AtTEM* and *AtFT* were investigated. Thus a relationship between *TEM* and *FT* expression patterns and juvenility that cuts across plants species was established in the current study.

To investigate the role of *TEM* in determining the length of the JP, the effect of reduced levels or increased levels of *TEM* were investigated in *Arabidopsis*. In both *tem1* and RNAi-*tem1/2* mutants the JP length was shorter compared to the WT, with the RNAi-*tem1/2* line being the shortest. When *AmTEM* was ectopically

expressed in the *tem1* mutants, plants showed a longer JP than in *tem1* plants. Flowering time was also delayed. However, it was found that the delay in flowering time was not caused by a longer AVP. Transgenic lines over-expressing *AmTEM* had shorter AVPs than *tem1*. On the contrary, *tem1* and RNAi-*tem1/2* mutant had longer AVPs than Col-0 WT. Castillejo and Pelaz (2008) proposed functional redundancy between *TEM* genes in regulating *FT* expression. However, the current study showed an additive effect of *AtTEM1* and *AtTEM2* in regulating juvenility and showed that *AtTEM2* cannot fully compensate for the role of *AtTEM1* in maintaining juvenility. The possibility that *AtTEM1* and *AtTEM2* can have independent functions has been shown in a previous study. *TEM2* was proposed as a requirement for blocking RNA silencing by two distinct viral proteins and it was shown that the *tem2* mutant could not be functionally complemented by *AtTEM1* (Endres *et al.*, 2010).

AtFT expression levels were shown to be influenced by overall *TEM* amount. In *tem1*, *AtFT* was more highly expressed than in the RNAi-*tem1/2* line, but still lower than in the WT. *AtFT* expression increased earlier in RNAi-*tem1/2* than in *tem1*, but both of them showed an earlier increase in *AtFT* expression levels compared to the WT. Both mutants showed a higher overall *AtCO* expression and a faster increase than in WT. The three *AmTEM* over-expressing lines showed lower *AtFT* expression, and two of them showed a delay in the rise of *AtCO*. A possible role for *TEM* in repressing *AtCO* expression can now be proposed since analysis of the *AtCO* sequence revealed putative AP2 and B3 binding sites.

6.1.6 How *TEM* fits into floral initiation pathways

The research presented shows that *TEM* acts as a floral repressor and controls juvenility through repression of *FT*. It is possible to devise hypothetical models placing *TEM* in the flowering pathways, as reviewed in chapter 1. These are proposed based on findings from this study on *Antirrhinum* and *Arabidopsis*, in which photoperiod is the main inducer of flowering and, in olive, in which prolonged periods of cold are the main floral trigger.

The first flowering pathway in which *TEM* can be placed is the photoperiodic pathway (Figure 6.1). In both herbaceous and woody plants, *TEM* follows a circadian rhythm, peaking at dusk in *Arabidopsis* and at noon in chestnut (Castillejo and Pelaz, 2008; Moreno-Cortés *et al.*, 2012). In *Arabidopsis*, *TEM* peak of expression is correlated with the diurnal rises in *CO* and *FT* expression levels (Castillejo and Pelaz, 2008; Suarez-Lopez *et al.*, 2001). The correlation in timing is consistent for *TEM* acting as a regulator of both *CO* and *FT*. During juvenility, *TEM* activity inhibits flowering at two different levels, directly down-regulating both *FT* and *CO* expression. After the end of the JP, *GI* represses *TEM*. *GI* is circadian regulated, peaking at 10-12 ZT, a few hours before *TEM* (Fowler *et al.*, 1999). *GI* expression increases throughout development (Fowler *et al.*, 1999). Furthermore, *GI* has been shown to directly down-regulate *TEM* expression and its activity by competing for the same binding site to *FT* 5' UTR region (Kaufmann *et al.*, 2010; Sawa and Kay, 2011). *GI* could have the same role as *CO* in regulating *TEM1* and *TEM2* access to the *FT* promoter. Therefore, whilst plants are juvenile, under inductive photoperiods, *FT* expression cannot be induced because *TEM* expression

is high. Once plants are adult, *TEM* expression decreases and *FT* can be induced by CO.

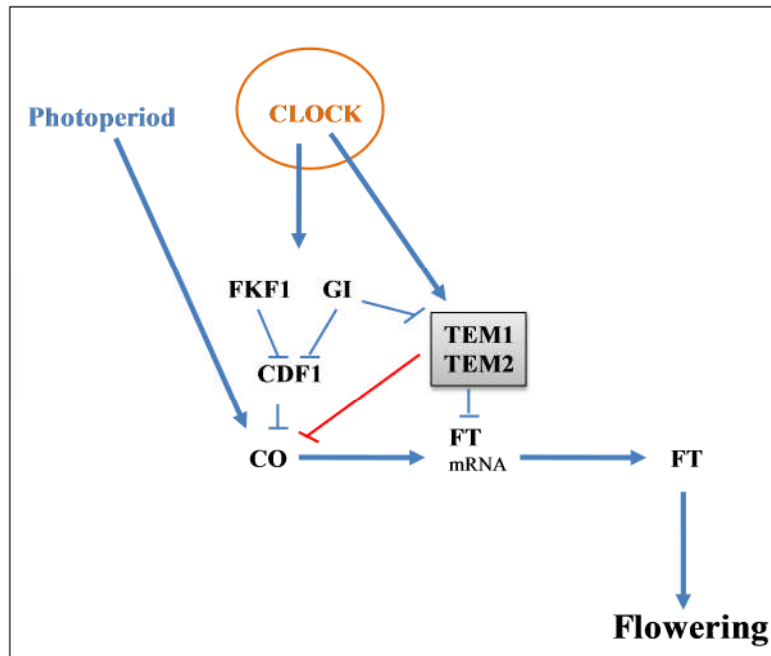


Figure 6.1 Simplified representation of the photoperiodic pathway.
 Schematic representation of the major pathways (in blue) regulating flowering time. Arrows indicate activation and T-bars show inhibition. The red T-bar represents speculative *TEM* regulation. The complete nomenclature of the genes can be found in section 6.1.6 and in chapter 1 where the pathway is shown in detail.

A second pathway, in which *TEM* is probably involved, is the vernalization pathway (Figure 6.2). In biennial and winter-annual plants, vernalization lifts repression of *FT* by *FLC*. In some perennial plants, like olive, although vernalization is required for flowering, low temperature does not lead to flowering after the first winter. In chestnut trees low temperature has been shown to knock down circadian rhythm of the *TEM* but its overall expression is enhanced (Moreno-Cortés *et al.*, 2012). In Brassica, with a vernalization requirement, it was shown that *FT* is not induced following vernalization in juvenile plants, whereas it is in adult

plants (Thomas, 2009). While adult, *TEM* is not present and, during vernalization, the reduction of *FLC* levels lead to an increase of *FT* expression. However, while juvenile, although the vernalization reduces *FLC* expression, high *TEM* expression levels inhibit *FT* expression and thus flowering.

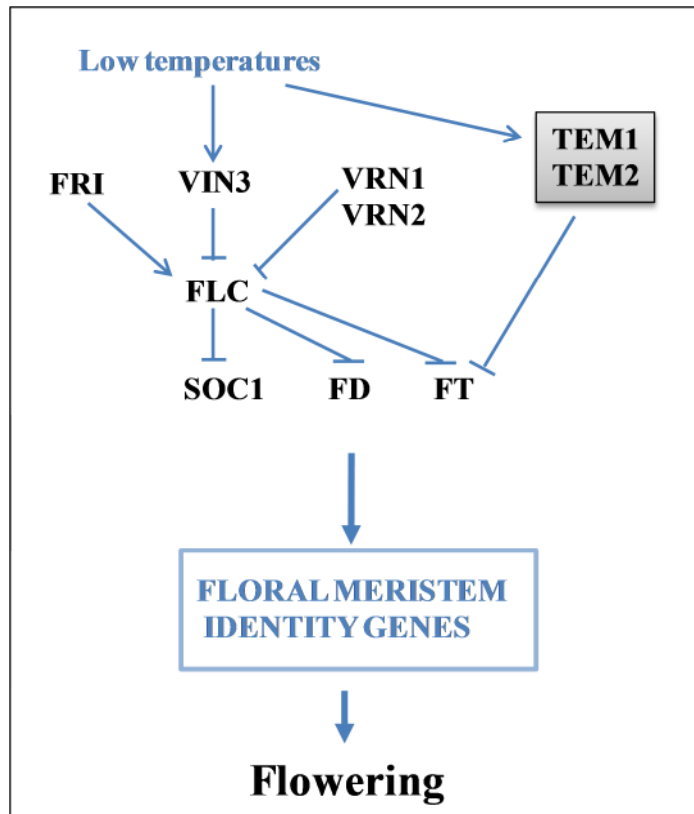


Figure 6.2 Simplified representation of the vernalization pathway
Schematic representation of the major pathways regulating flowering time. Arrows indicate activation and T-bars show inhibition. The complete nomenclature of the genes can be found in section 6.1.6 and in chapter 1 where the pathway is shown in detail.

A role for *TEM* in the gibberellin (GA) pathway can be proposed (Figure 6.3). *DWARF AND DELAYED-FLOWERING 1 (DDF1)*, another AP2-like gene, has been proposed to play a role in repressing the GA pathway and the JP (Magome *et al.*, 2004). In the SAM, *TEM* activity has been proposed to have a role during

apex development in repressing the floral meristem identity gene *LFY* and the floral integrator *SOC1* (Soraya Pelaz Herrero personal communication).

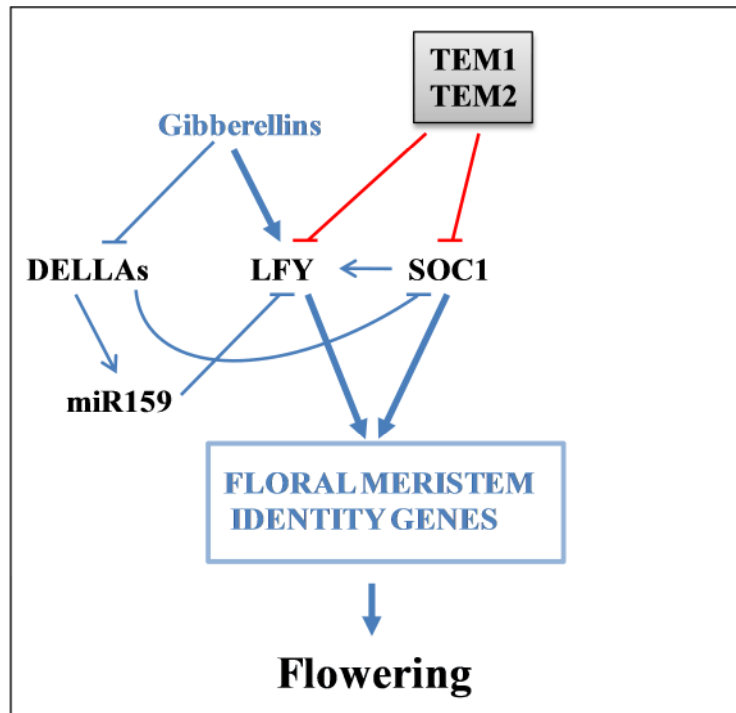


Figure 6.3 Simplified representation of the Gibberellins pathway
 Schematic representation of the major pathways (in blue) regulating flowering time. Arrows indicate activation and T-bars show inhibition. The red T-bar represents speculative *TEM* regulation. The complete nomenclature of the genes can be found in section 6.1.6 and in chapter 1 where the pathway is shown in detail.

Another flowering pathway, in which *TEM* is probably involved, is the miRNA pathway (Figure 6.4). *AP2* has been shown to be involved in the promotion of miR156 in the first stages of plant development and in the repression of miR172 (Yant *et al.*, 2010). Both miRNAs are member of multi-member families and only one member of each, miR156e and miR172b are actually targeted by *AP2* (Yant *et al.*, 2010). *TEM* harbours an AP2 domain and its expression levels are high during the JP in leaves. *TEM* could be responsible for delaying the shift from the JP to

AVP through enhancement of miR156 expression. After the end of juvenility, *TEM* expression in the leaves decreases. miR172 could be responsible for *TEM* repression, as it is for other *AP2-like* genes (Aukerman and Sakai, 2003; Jung *et al.*, 2007; Martin *et al.*, 2010).

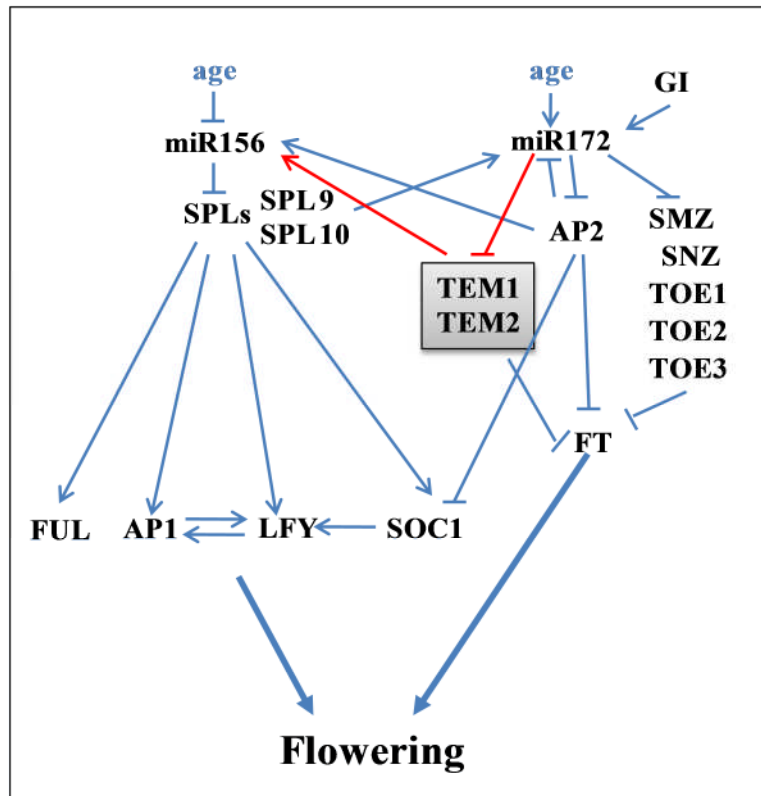


Figure 6.4 Simplified representation of the miRNAs pathway

Schematic representation of the major pathways (in blue) regulating flowering time. Arrows indicate activation and T-bars show inhibition. The red lines represent speculative *TEM* regulation. The complete nomenclature of the genes can be found in section 6.1.6 and in chapter 1 where the pathway is shown in detail.

6.2 Future research

The study of juvenility in plants is of great interest from both academic and economic perspectives. In this study juvenility has been studied in *Arabidopsis* and *Antirrhinum* plants and, in less detail, in olive plants. In olive, prolonged juvenile periods pose particular limitations for breeding and fruit production (Donaire *et al.*, 2011).

In *Arabidopsis*, AP2 expression promotes the expression of miR156 early in plant development which in turn, down-regulates miR172b (Martin *et al.*, 2010; Yant *et al.*, 2010). Furthermore, AP2-like floral repressors are also targeted by miR172 which increases in level during development (Aukerman and Sakai, 2003; Jung *et al.*, 2007). In a recent study in olive small RNAs have been characterised using high-throughput sequencing (Donaire *et al.*, 2011). Among them, miR172 and miR156 were shown to be conserved and to have the same activity as in *Arabidopsis* in targeting AP2-like transcription factors and SPL, respectively (Aukerman and Sakai, 2003; Donaire *et al.*, 2011; Jung *et al.*, 2009). It would be interesting to test whether miR172 had the potential to target and down-regulate olive *OeTEM*. This could be done following the Donaire *et al.* (2011) approach using a computational method where target genes of miRNA can be predicted using online tools. The same approach could also be used to study possible down-regulation of *AmTEM* and *Arabidopsis AtTEM1* and *AtTEM2*. Predictions from computation methods would need to be tested experimentally. The modified RNA ligase-mediated 5' rapid amplification of cDNA ends (RLM-RACE) technique could be used to study directed mRNA cleavage on predicted cDNA targets identifying miRNA binding activity (Donaire *et al.*, 2011; Thomson *et al.*, 2011).

Many other techniques that are able to reveal miRNA binding activity, as recently critically reviewed by Thomson *et al.* (2011) and Chen *et al.* (2010), could be combined together to obtain a picture of miRNA-mediated target binding.

It has been reported that expression of *AtTEM1*, *AtTEM2* and *AtRAV1* are influenced by many factors including temperature, pathogen attack and steroids (Castillejo and Pelaz, 2008; Endres *et al.*, 2010; Hu *et al.*, 2004). In this study it was shown that *AtTEM2* does not fully compensate for *AtTEM1* activity and that they are not fully functionally redundant in maintaining juvenility. This raises the possibility of new and different roles played by TEMs, which could be investigated by studying *TEM* expression in both *Arabidopsis* and *Antirrhinum* plants in different tissues at different developmental stages. For instance, the possibility of TEM genes playing a role in the SAM could be investigated considering that the floral meristem identity gene *LFY* has been shown to be induced earlier in *tem1tem2* (Soraya Pelaz Herrero, personal communication). A similar study could be performed in *Antirrhinum* where the possibility that *AmTEM* could down-regulate *FLORICAULA (FLO)*, the homologue of *Arabidopsis LFY*, could be studied by testing for a relationship between the expression of these genes in the SAM during apex development.

The GA-deficient mutant *dwarf and delayed-flowering 1 (ddf1)* flower later than the WT with shortened hypocotyls and petioles, because of over-expression of a putative *AP2* transcription factor gene named *DDF1* (Magome *et al.*, 2004). The fact that *tem* single and double mutants flower later and have longer hypocotyls, a phenotype observed with elevated levels of GA (Soraya Pelaz Herrero personal communication), justifies an investigation into links between *TEM*, the GA pathway and the JP. This could be investigated by transfer experiments to determine the JP,

and by growing and sampling *tem* single and double mutants and *ddf1* in SD to study expression of key genes such as *LFY* and *SOCI*. If a higher level of *LFY* and *SOCI* expression was detected, a double role of TEM in down-regulating flowering time both in LD and SD conditions through the photoperiodic and the GA pathway respectively, could be assumed.

AtTEM1 has been shown to follow a circadian rhythm, peaking at dusk (Castillejo and Pelaz, 2008). Chestnut *CsRAVI*, an *AtTEM* homologue, has similarly been shown to be circadian regulated, however, it peaks at noon (Moreno-Cortés *et al.*, 2012). It would be interesting to determine whether *AmTEM* and *OeTEM* are circadian clock regulated. The possibility of a different role of this gene in herbaceous and woody plants could result from differences in diurnal regulation.

In chestnut, the circadian rhythm of *CsRAVI* was disrupted when plants were exposed to low temperature, but the overall expression was higher in colder months than in warmer (Moreno-Cortés *et al.*, 2012). In chestnut, other genes involved in the circadian clock like, *CsTOCI* and *CsLHY* presented a disrupted rhythm with an overall higher expression level when exposed to low temperature suggesting a role during dormancy that is typical of woody plants (Ramos *et al.*, 2005). The possibility of a different expression level of *TEM* in response to low temperature could be investigated in olive plants where vernalization plays an important role (Wilkie *et al.*, 2008). In *Arabidopsis*, vernalization overcomes the repression role of *FT* by *FLC* leading to induction of flowering (Kim *et al.*, 2009; Sung and Amasino, 2004). In olive, whilst juvenile, vernalization treatments do not lead to floral induction (El Riachy *et al.*, 2011). By collecting juvenile and adult olive plant material during cold and warm seasons at hourly intervals, it would be possible to investigate whether vernalization during juvenility enhances *OeTEM*

expression in olive with the result of repressing *FT* expression and therefore flowering.

More immediate following up of the present study could be performing a new transfer experiment using a further DLI reduction for further enhancement of the JP length in *Arabidopsis* and *Antirrhinum*. This will enable a more detailed study of the gene expression levels during the switch between JP and AVP. A recent study showed that the over-expression of *CsRAVI* gene induces the formation of sylleptic branches when ectopically expressed in poplar (Moreno-Cortés *et al.*, 2012). For this reason, T₁ lines, like the 35S::*AmTEM/tem1* 79, ectopically expressing *AmTEM* in the *Arabidopsis tem1* mutant (excluded from this current research because they presented multiple stems from the base) could be used for the same study performed and described in chapter 5. It would be also interesting to investigate the relationship and function of *OeTEM* with the JP and *AtFT* in *Arabidopsis* plants ectopically expressing *OeTEM*, as was done for *AmTEM* in chapter 5. Using an olive cDNA library, it could be possible to isolate and characterised other genes such as, *FT*, *FLC* and *CO* involved in the juvenile to adult transition as was done for *OeTEM* (chapter 4). Of course, using the same method described in chapter 4 for characterising new genes can be time consuming. For this reason, high-throughput sequencing technologies could be used to speed up the process and keep the cost of sequencing relatively low. The first olive DNA sequence was published in the NCBI database in 1994 and up to date genomic research on olive has been very limited (Bracci *et al.*, 2011). Although the olive genome is still not fully sequenced, projects like OLAGEN in Spain and OLEA in Italy, are aiming to use new sequencing technologies to fill the gap and identify sequences related to important commercial traits like JP, flower development and

fruit composition (Bracci *et al.*, 2011). 454 pyrosequencing technology has been used to identify genes involved in fruit development (Alagna *et al.*, 2009). This and other low-cost sequencing technologies could be used to characterise genes involved in the JP until the olive genome sequencing process is concluded. This would provide a new insight into juvenility in this tree species and useful information for breeding programs.

The identification of genetic or physiological markers of juvenility would make it easier to make decisions influenced by plant development phases. For this reason further studies are necessary to establish an easy and reproducible developmental stage identification method.

6.3 Overall conclusions

The project aims were set out in section 1.10. The overall aim of this project was to investigate the cause of floral incompetence during juvenility in LDPs plants *Antirrhinum majus* and *Arabidopsis thaliana* and in the tree *Olea europaea* through investigation of the underlying molecular mechanisms.

A brief summary of the conclusions of the project in relation to the original research objectives are presented below:

- ❖ *To establish the length of the juvenile phase in Antirrhinum plants grown under controlled-environment conditions.*

A reproducible, uniform and cost-effective assay was refined for investigating juvenility in plants grown in SANYO MLR-351H cabinets. The length of the JP in *Antirrhinum* under controlled-environment conditions was established using photoperiod transfer experiments. The effect of DLI on this photoperiod insensitive phase was examined and a reciprocal relationship between DLI and juvenility revealed that reducing the DLI resulted in a longer JP.

- ❖ *To investigate FT expression in Antirrhinum leaves, characterizing FT in single leaves at different stages of development.*

A first description of spatial and temporal *AmFT* gene expression throughout the whole plant throughout development was presented. It was shown that in *Antirrhinum* *AmFT* expression increases across development in all leaves following the end of the JP. Using *Arabidopsis*, it was shown that the same

is true for *AtFT* and that FT levels are not low during juvenility due to inactivity of the photoperiodic pathway since *AtCO* levels are high.

- ❖ *To identify and characterize Antirrhinum homologues of Arabidopsis genes that reduce or antagonise FT expression and to study their regulation in juvenile to adult phase transition.*

Full length cDNA representing a *TEM* homologue was isolated and characterised from *Antirrhinum*. *AmTEM* was shown to contain AP2 and B3-like domains characteristic of the RAV family. The CAACA and CACCTG motifs, where AP2 and B3 domains bind to the *AtFT* 5' UTR region were shown also to be present in the *AmFT* 5' UTR region. *AmTEM* expression levels were shown to be higher during juvenility suggesting a potential role for *TEM* in controlling juvenility. Investigation of *AmTEM* over-expressing *Arabidopsis* plants and *tem* single and double mutants, with analysis of JP length and of *AtFT* and *AtCO* expression revealed a role for *TEM* in JP length determination.

- ❖ *To identify and characterize Olea europaea homologues of Arabidopsis genes that reduce or antagonise FT expression and to study their regulation in juvenile to adult phase transition.*

Full length cDNA representing a *TEM* homologue was isolated and characterised from olive. *OeTEM* were shown to contain AP2 and B3-like domains characteristic of the RAV family. In olive, *OeTEM* expression levels were shown to be higher during juvenility than when adult and

OeTEM over-expressing *Arabidopsis* plants showed a delay in flowering revealing a potential role for *OeTEM* in determining JP length in olive.

REFERENCES

- Achard, P., Herr, A., Baulcombe, D. C. and Harberd, N. P.** (2004). Modulation of floral development by a gibberellin-regulated microRNA. *Development*, **131**, 3357-3365.
- Adams, S. R.** (1999). The effects of temperature and light integral on the phases of photoperiod sensitivity in *Petunia x hybrida*. *Annals of Botany*, **83**, 263-269.
- Adams, S. R., Munir, M., Valdes, V. M., Langton, F. A. and Jackson, S. D.** (2003). Using flowering times and leaf numbers to model the phases of photoperiod - Sensitivity in *Antirrhinum majus* L. *Annals of Botany*, **92**, 689-696.
- Adams, S. R., Pearson, S. and Hadley, P.** (2001). Improving quantitative flowering models through a better understanding of the phases of photoperiod sensitivity. *Journal of Experimental Botany*, **52**, 655-662.
- Alabadi, D., Oyama, T., Yanovsky, M. J., Harmon, F. G., Mas, P. and Kay, S. A.** (2001). Reciprocal regulation between *TOC1* and *LHY/CCA1* within the *Arabidopsis* circadian clock. *Science*, **293**, 880-883.
- Alagna, F., D'Agostino, N., Torchia, L., Servili, M., Rao, R., Pietrella, M., Giuliano, G., Chiusano, M. L., Baldoni, L. and Perrotta, G.** (2009). Comparative 454 pyrosequencing of transcripts from two olive genotypes during fruit development. *Bmc Genomics*, **10**.
- Amaya, I., Ratcliffe, O. J. and Bradley, D. J.** (1999). Expression of *CENTRORADIALIS (CEN)* and *CEN*-like genes in tobacco reveals a conserved mechanism controlling phase change in diverse species. *Plant Cell*, **11**, 1405-1417.
- An, H. L., Roussot, C., Suarez-Lopez, P., Corbesler, L., Vincent, C., Pineiro, M., Hepworth, S., Mouradov, A., Justin, S., Turnbull, C. and Coupland, G.** (2004). *CONSTANS* acts in the phloem to regulate a systemic signal that induces photoperiodic flowering of *Arabidopsis*. *Development*, **131**, 3615-3626.
- Araki, T.** (2001). Transition from vegetative to reproductive phase. *Current Opinion in Plant Biology*, **4**, 63-68.
- Araki, T., Kobayashi, Y., Kaya, H. and Iwabuchi, M.** (1998). The flowering-time gene *FT* and regulation of flowering in *Arabidopsis*. *Journal of Plant Research*, **111**, 277-281.
- Aukerman, M. J. and Sakai, H.** (2003). Regulation of flowering time and floral organ identity by a microRNA and its *APETALA2*-like target genes. *Plant Cell*, **15**, 2730-2741.
- Bartel, B. and Bartel, D. P.** (2003). MicroRNAs: At the root of plant development? *Plant Physiology*, **132**, 709-717.

Baurle, I. and Dean, C. (2006). The timing of developmental transitions in plants. *Cell*, **125**, 655-664.

Bellini, E., Giordani, E. and Rosati, A. (2008). Genetic improvement of olive from clonal selection to cross-breeding programs. *Advances in Horticultural Science*, **22**, 73-86.

Bendini, A., Cerretani, L., Carrasco-Pancorbo, A., Gomez-Caravaca, A.M., Segura-Carretero, A., Fernandez-Gutierrez, A., Lercker, G. (2007). Phenolic molecules in virgin olive oils: a survey of their sensory properties, health effects, antioxidant activity and analytical methods. An overview of the last decade. *Molecules*, **12**, 1679-1719.

Ben-Naim, O., Eshed, R., Parnis, A., Teper-Bamnolker, P., Shalit, A., Coupland, G., Samach, A. and Lifschitz, E. (2006). The CCAAT binding factor can mediate interactions between CONSTANS-like proteins and DNA. *Plant Journal*, **46**, 462-476.

Benlloch, R., Berbel, A., Serrano-Mislata, A. and Madueno, F. (2007). Floral initiation and inflorescence architecture: A comparative view. *Annals of Botany*, **100**, 659-676.

Berardini, T. Z., Bollman, K., Sun, H. and Poethig, R. S. (2001). Regulation of vegetative phase change in *Arabidopsis thaliana* by cyclophilin 40. *Science*, **291**, 2405-2407.

Blazquez, M. A., Green, R., Nilsson, O., Sussman, M. R. and Weigel, D. (1998). Gibberellins promote flowering of *Arabidopsis* by activating the *LEAFY* promoter. *Plant Cell*, **10**, 791-800.

Blazquez, M. A., Soowal, L. N., Lee, I. and Weigel, D. (1997). *LEAFY* expression and flower initiation in *Arabidopsis*. *Development*, **124**, 3835-3844.

Bohlenius, H., Eriksson, S., Parcy, F. and Nilsson, O. (2007). The mRNA of the *Arabidopsis* gene *FT* moves from leaf to shoot apex and induces flowering (vol 309, pg 1694, 2005). *Science*, **316**, 367-367.

Bohlenius, H., Huang, T., Charbonnel-Campaa, L., Brunner, A. M., Jansson, S., Strauss, S. H. and Nilsson, O. (2006). *CO/FT* regulatory module controls timing of flowering and seasonal growth cessation in trees. *Science*, **312**, 1040-1043.

Boss, P. K., Bastow, R. M., Mylne, J. S. and Dean, C. (2004). Multiple pathways in the decision to flower: Enabling, promoting, and resetting. *Plant Cell*, **16**, S18-S31.

Bracci, T., Busconi, M., Fogher, C. and Sebastiani, L. (2011). Molecular studies in olive (*Olea europaea* L.): overview on DNA markers applications and recent advances in genome analysis. *Plant Cell Reports*, **30**, 449-462.

Bradley, D., Carpenter, R., Copsey, L., Vincent, C., Rothstein, S. and Coen, E. (1996a). Control of inflorescence architecture in *Antirrhinum*. *Nature*, **379**, 791-797.

Bradley, D., Vincent, C., Carpenter, R. and Coen, E. (1996b). Pathways for inflorescence and floral induction in *Antirrhinum*. *Development*, **122**, 1535-1544.

Brunner, A. M. and Nilsson, O. (2004). Revisiting tree maturation and floral initiation in the poplar functional genomics era. *New Phytologist*, **164**, 43-51.

Carpenter, R., Copsey, L., Vincent, C., Doyle, S., Magrath, R. and Coen, E. (1995). Control of flower development and phyllotaxy by meristem identity genes in *Antirrhinum*. *Plant Cell*, **7**, 2001-2011.

Castillejo, C. and Pelaz, S. (2008). The balance between *CONSTANS* and *TEMPRANILLO* activities determines *FT* expression to trigger flowering. *Current Biology*, **18**, 1338-1343.

Cerdan, P. D. and Chory, J. (2003). Regulation of flowering time by light quality. *Nature*, **423**, 881-885.

Chen, M., Meng, Y., Mao, C., Chen, D. and Wu, P. (2010). Methodological framework for functional characterization of plant microRNAs. *Journal of Experimental Botany*, **61**, 2271-2280.

Chen, X. F., Wang, Z., Wang, X. M., Dong, J., Ren, J. Z. and Gao, H. W. (2009). Isolation and characterization of *GoRAV*, a novel gene encoding a RAV-type protein in *Galega orientalis*. *Genes & Genetic Systems*, **84**, 101-109.

Chien, J. C. and Sussex, I. M. (1996). Differential regulation of trichome formation on the adaxial and abaxial leaf surfaces by Gibberellins and photoperiod in *Arabidopsis thaliana* (L) Heynh. *Plant Physiology*, **111**, 1321-1328.

Chory, J. and Li, J. (1997). Gibberellins, brassinosteroids and light-regulated development. *Plant Cell and Environment*, **20**, 801-806.

Clack, T., Mathews, S. and Sharrock, R. A. (1994). The phytochrome apoprotein family in *Arabidopsis* is encoded by 5 genes - The sequences and expression of *PHYD* and *PHYE*. *Plant Molecular Biology*, **25**, 413-427.

Clarke, J. H., Tack, D., Findlay, K., Van Montagu, M. and Van Lijsebettens, M. (1999). The *SERRATE* locus controls the formation of the early juvenile leaves and phase length in *Arabidopsis*. *Plant Journal*, **20**, 493-501.

Clough, S. J. and Bent, A. F. (1998). Floral dip: a simplified method for *Agrobacterium*-mediated transformation of *Arabidopsis thaliana*. *Plant Journal*, **16**, 735-743.

Cockshull KE. (1985). *Antirrhinum majus*. In: Halevy AH ed. CRC handbook of flowering, Vol. I. Florida: CRC Press, 476–481.

Coen, E. S., Doyle, S., Romero, J. M., Elliott, R., Magrath, R. and Carpenter, R. (1991). Homeotic genes-controlling flower development in *Antirrhinum*. *Development*, 149-&.

Coen, E. S., Romero, J. M., Doyle, S., Elliott, R., Murphy, G. and Carpenter, R. (1990). *FLORICAULA*: a homeotic gene required for flower development in *Antirrhinum majus*. *Cell*, **63**, 1311-1322.

Corbesier, L. and Coupland, G. (2005). Photoperiodic flowering of *Arabidopsis*: integrating genetic and physiological approaches to characterization of the floral stimulus. *Plant Cell and Environment*, **28**, 54-66.

Corbesier, L., Vincent, C., Jang, S. H., Fornara, F., Fan, Q. Z., Searle, I., Giakountis, A., Farrona, S., Gissot, L., Turnbull, C. and Coupland, G. (2007). FT protein movement contributes to long-distance signaling in floral induction of *Arabidopsis*. *Science*, **316**, 1030-1033.

Cremer, F., Havelange, A., Saedler, H. and Huijser, P. (1998). Environmental control of flowering time in *Antirrhinum majus*. *Physiologia Plantarum*, **104**, 345-350.

de Montaigu, A., Toth, R. and Coupland, G. (2010). Plant development goes like clockwork. *Trends in Genetics*, **26**, 296-306.

Denney, J. O., McEachern, G. R. and Griffiths, J. F. (1985). Modeling the thermal adaptability of the olive (*Olea europaea* L.) in Texas. *Agricultural and Forest Meteorology*, **35**, 309-327.

Diaz-Espejo, A., Walcroft, A. S., Fernandez, J. E., Hafidi, B., Palomo, M. J. and Giron, I. F. (2006). Modeling photosynthesis in olive leaves under drought conditions. *Tree Physiology*, **26**, 1445-1456.

Donaire, L., Pedrola, L., de la Rosa, R. and Llave, C. (2011). High-throughput sequencing of RNA silencing-associated small RNAs in olive (*Olea europaea* L.). *PloS one*, **6**, e27916.

Dong, Z., Han, M.-H. and Fedoroff, N. (2008). The RNA-binding proteins *HYL1* and *SE* promote accurate in vitro processing of pri-miRNA by *DCL1*. *Proceedings of the National Academy of Sciences of the United States of America*, **105**, 9970-9975.

Edwards, K., Johnstone, C. and Thompson, C. (1991). A simple and rapid method for the preparation of plant genomic DNA for PCR analysis. *Nucleic Acids Research*, **19**, 1349-1349.

Edwards, K. D., Akman, O. E., Knox, K., Lumsden, P. J., Thomson, A. W., Brown, P. E., Pokhilko, A., Kozma-Bognar, L., Nagy, F., Rand, D. A. and Millar, A. J. (2010). Quantitative analysis of regulatory flexibility under changing environmental conditions. *Molecular Systems Biology*, **6**.

El Riachy, M., Rallo, L., de la Rosa, R. and Leon, L. (2011). May soil solarization reduce the juvenile period in olive? *Hortscience*, **46**, 1241-1244.

Ellis, R. H., Collinson, S. T., Hudson, D. and Patefield, W. M. (1992). The analysis of reciprocal transfer experiments to estimate the durations of the photoperiod-sensitive and photoperiod-insensitive phases of plant development: an example in Soya bean. *Annals of Botany*, **70**, 87-92.

Endres, M. W., Gregory, B. D., Gao, Z. H., Foreman, A. W., Mlotshwa, S., Ge, X., Pruss, G. J., Ecker, J. R., Bowman, L. H. and Vance, V. (2010). Two plant viral suppressors of silencing require the ethylene-inducible host transcription factor *RAV2* to block RNA silencing. *Plos Pathogens*, **6**.

Faust, J. E., Holcombe, V., Rajapakse, N. C. and Layne, D. R. (2005). The effect of daily light integral on bedding plant growth and flowering. *Hortscience*, **40**, 645-649.

Fekih, R., Miyata, K., Yoshida, R., Ezura, H. and Mizoguchi, T. (2009). Isolation of suppressors of late flowering and abnormal flower shape phenotypes caused by overexpression of the *SHORT VEGETATIVE PHASE* gene in *Arabidopsis thaliana*. *Plant Biotechnology*, **26**, 217-224.

Fernández-Ocaña, A., García-López, M. C., Jiménez-Ruiz, J., Saniger, L., Macías, D., Navarro, F., Oya, R., Belaj, A., de la Rosa, R., Corpas, F. J., Barroso, J. B. and Luque, F. (2010). Identification of a gene involved in the juvenile-to-adult transition (*JAT*) in cultivated olive trees. *Tree Genetics & Genomes*.

Flachowsky, H., Hanke, M. V., Peil, A., Strauss, S. H. and Fladung, M. (2009). A review on transgenic approaches to accelerate breeding of woody plants. *Plant Breeding*, **128**, 217-226.

Fornara, F. and Coupland, G. (2009). Plant phase transitions make a SPLash. *Cell*, **138**, 625-627.

Fowler, S., Lee, K., Onouchi, H., Samach, A., Richardson, K., Coupland, G. and Putterill, J. (1999). *GIGANTEA*: a circadian clock-controlled gene that regulates photoperiodic flowering in *Arabidopsis* and encodes a protein with several possible membrane-spanning domains. *Embo Journal*, **18**, 4679-4688.

Garcia, J. L., Avidan, N., Troncoso, A., Sarmiento, R. and Lavee, S. (2000). Possible juvenile-related proteins in olive tree tissues. *Scientia Horticulturae*, **85**, 271-284.

Gardner, M. J., Hubbard, K. E., Hotta, C. T., Dodd, A. N. and Webb, A. A. R. (2006). How plants tell the time. *Biochemical Journal*, **397**, 15-24.

Gendall, A. R., Levy, Y. Y., Wilson, A. and Dean, C. (2001). The *VERNALIZATION 2* gene mediates the epigenetic regulation of vernalization in *Arabidopsis*. *Cell*, **107**, 525-535.

Geraldo, N., Baeurle, I., Kidou, S.-i., Hu, X. and Dean, C. (2009). *FRIGIDA* delays flowering in *Arabidopsis* via a cotranscriptional mechanism involving direct interaction with the nuclear cap-binding complex. *Plant Physiology*, **150**, 1611-1618.

Giakountis, A. and Coupland, G. (2008). Phloem transport of flowering signals. *Current Opinion in Plant Biology*, **11**, 687-694.

Gocal, G. F. W., King, R. W., Blundell, C. A., Schwartz, O. M., Andersen, C. H. and Weigel, D. (2001). Evolution of floral meristem identity genes. Analysis of *Lolium temulentum* genes related to *APETALA1* and *LEAFY* of *Arabidopsis*. *Plant Physiology*, **125**, 1788-1801.

Greenup, A., Peacock, W. J., Dennis, E. S. and Trevaskis, B. (2009). The molecular biology of seasonal flowering-responses in *Arabidopsis* and the cereals. *Annals of Botany*, **103**, 1165-1172.

Gucci, R. and Cantini, C. (2000). Pruning and training systems for modern olive growing, CSIRO, ed.

Hackett, W. (1985). Juvenility, maturation and rejuvenation in woody plants. *Hortic Rev*, 109-155. *Hortic Rev*

Haiyang, W. and Wang, D. X. (2002). Phytochrome signaling mechanism. In *The Arabidopsis Book*. Edited by M. A. S. o. P. B. Rockville: American Society of Plant Biologists, Rockville, MD.

Halberg, F. (1959). Physiologic 24-hour periodicity; general andprocedural considerations with reference to the adrenal cycle. *Z.Vitamin, Hormonu. Fermentforsch.* 10: 225-296

Halliday, K. J., Salter, M. G., Thingnaes, E. and Whitelam, G. C. (2003). Phytochrome control of flowering is temperature sensitive and correlates with expression of the floral integrator *FT*. *Plant Journal*, **33**, 875-885.

Hanke, M., Flachowsky, H., Peil, A. and Hättasch, C. (2007). No flower no fruit–Genetic potentials to trigger fowering in fruit trees. *Genes, Genomes and Genomics*.

Hanzawa, Y., Money, T. and Bradley, D. (2005). A single amino acid converts a repressor to an activator of flowering. *Proceedings of the National Academy of Sciences of the United States of America*, **102**, 7748-7753.

- Hatsuda, Y., Nishio, S., Komori, S., Nishiyama, M., Kanahama, K. and Kanayama, Y.** (2011). Relationship between *MdMADS11* gene expression and juvenility in apple. *Journal of the Japanese Society for Horticultural Science*, **80**, 396-403.
- Hattasch, C., Flachowsky, H., Kapturska, D. and Hanke, M. V.** (2008). Isolation of flowering genes and seasonal changes in their transcript levels related to flower induction and initiation in apple (*Malus domestica*). *Tree Physiology*, **28**, 1459-1466.
- Hayama, R., Yokoi, S., Tamaki, S., Yano, M. and Shimamoto, K.** (2003). Adaptation of photoperiodic control pathways produces short-day flowering in rice. *Nature*, **422**, 719-722.
- Helliwell, C. A., Wood, C. C., Robertson, M., Peacock, W. J. and Dennis, E. S.** (2006). The *Arabidopsis* *FLC* protein interacts directly in vivo with *SOC1* and *FT* chromatin and is part of a high-molecular-weight protein complex. *Plant Journal*, **46**, 183-192.
- Higgins, J. A., Bailey, P. C. and Laurie, D. A.** (2010). Comparative genomics of flowering time pathways using *Brachypodium distachyon* as a model for the temperate grasses. *Plos One*, **5**.
- Hsu, C.-Y., Liu, Y., Luthe, D. S. and Yuceer, C.** (2006). Poplar *FT2* shortens the juvenile phase and promotes seasonal flowering. *Plant Cell*, **18**, 1846-1861.
- Hu, Y. X., Wang, Y. H., Liu, X. F. and Li, J. Y.** (2004). *Arabidopsis* *RAVI* is down-regulated by brassinosteroid and may act as a negative regulator during plant development. *Cell Research*, **14**, 8-15.
- Hudson, A., Critchley, J. and Erasmus, Y.** (2008). The genus *Antirrhinum* (snapdragon): a flowering plant model for evolution and development. *CSH protocols*, **2008**.
- Hunter, C., Sun, H. and Poethig, R. S.** (2003). The *Arabidopsis* heterochronic gene *ZIPPY* is an *ARGONAUTE* family member. *Current Biology*, **13**, 1734-1739.
- Ikeda, M. and Ohme-Takagi, M.** (2009). A novel group of transcriptional repressors in *Arabidopsis*. *Plant and Cell Physiology*, **50**, 970-975.
- Jackson, S. D.** (2009). Plant responses to photoperiod. *New Phytologist*, **181**, 517-531.
- Jang, S., Marchal, V., Panigrahi, K. C. S., Wenkel, S., Soppe, W., Deng, X. W., Valverde, F. and Coupland, G.** (2008). *Arabidopsis* *COPI* shapes the temporal pattern of CO accumulation conferring a photoperiodic flowering response. *Embo Journal*, **27**, 1277-1288.

Jarillo, J. A., del Olmo, I., Gomez-Zambrano, A., Lazaro, A., Lopez-Gonzalez, L., Miguel, E., Narro-Diego, L., Saez, D. and Pineiro, M. (2008). Photoperiodic control of flowering time. *Spanish Journal of Agricultural Research*, **6**, 221-244.

Jarillo, J. A. and Pineiro, M. (2011). Timing is everything in plant development. The central role of floral repressors. *Plant Science*, **181**, 364-378.

Jung, J.-H., Seo, P. J. and Park, C.-M. (2009). MicroRNA biogenesis and function in higher plants. *Plant Biotechnology Reports*, **3**, 111-126.

Jung, J.-H., Seo, Y.-H., Seo, P. J., Reyes, J. L., Yun, J., Chua, N.-H. and Park, C.-M. (2007). The *GIGANTEA*-regulated microRNA172 mediates photoperiodic flowering independent of *CONSTANS* in *Arabidopsis*. *Plant Cell*, **19**, 2736-2748.

Kagaya, Y., Ohmiya, K. and Hattori, T. (1999). *RAVI*, a novel DNA-binding protein, binds to bipartite recognition sequence through two distinct DNA-binding domains uniquely found in higher plants. *Nucleic Acids Research*, **27**, 470-478.

Kaufmann, K., Wellmer, F., Muino, J. M., Ferrier, T., Wuest, S. E., Kumar, V., Serrano-Mislata, A., Madueno, F., Krajewski, P., Meyerowitz, E. M., Angenent, G. C. and Riechmann, J. L. (2010). Orchestration of floral initiation by *APETALA1*. *Science*, **328**, 85-89.

Kerstetter, R. A. and Poethig, R. S. (1998). The specification of leaf identity during shoot development. *Annual Review of Cell and Developmental Biology*, **14**, 373-398.

Kim, D. H., Doyle, M. R., Sung, S. and Amasino, R. M. (2009). Vernalization: winter and the timing of flowering in plants. *Annual Review of Cell and Developmental Biology*, **25**, 277-299.

Kim, S. Y., Kim, Y. C., Lee, J. H., Oh, S. K., Chung, E., Lee, S., Lee, Y. H., Choi, D. and Park, J. M. (2005). Identification of a *CaRAVI* possessing an AP2/ERF and B3 DNA-binding domain from pepper leaves infected with *Xanthomonas axonopodis* pv. *glycines* 8ra by differential display. *Biochimica Et Biophysica Acta-Gene Structure and Expression*, **1729**, 141-146.

Kojima, S., Takahashi, Y., Kobayashi, Y., Monna, L., Sasaki, T., Araki, T. and Yano, M. (2002). *Hd3a*, a rice ortholog of the *Arabidopsis FT* gene, promotes transition to flowering downstream of *Hdl* under short-day conditions. *Plant and Cell Physiology*, **43**, 1096-1105.

Kotake, T., Takada, S., Nakahigashi, K., Ohto, M. and Goto, K. (2003). *Arabidopsis TERMINAL FLOWER 2* gene encodes a heterochromatin protein 1 homolog and represses both *FLOWERING LOCUS T* to regulate flowering time and several floral homeotic genes. *Plant and Cell Physiology*, **44**, 555-564.

Kotoda, N., Hayashi, H., Suzuki, M., Igarashi, M., Hatsuyama, Y., Kidou, S., Igasaki, T., Nishiguchi, M., Yano, K., Shimizu, T., Takahashi, S., Iwanami, H.,

- Moriya, S. and Abe, K.** (2010). Molecular characterization of *FLOWERING LOCUS T*-like genes of apple (*Malus domestica* Borkh.). *Plant and Cell Physiology*, **51**, 561-575.
- Langridge J.** (1957). Effect of day-length and gibberellic acid on the flowering of *Arabidopsis*. *Nature*;180:36–37
- Lavee, S.** (2007). Biennial bearing in olive (*Olea europaea*). *Annales Series Historia Naturalis*, **17**, 101-112.
- Lee, J. H., Yoo, S. J., Park, S. H., Hwang, I., Lee, J. S. and Ahn, J. H.** (2007). Role of *SVP* in the control of flowering time by ambient temperature in *Arabidopsis*. *Genes & Development*, **21**, 397-402.
- Leon, L. and Downey, G.** (2006). Preliminary studies by visible and near-infrared reflectance spectroscopy of juvenile and adult olive (*Olea europaea* L.) leaves. *Journal of the Science of Food and Agriculture*, **86**, 999-1004.
- Li, C. Y., Zhang, K., Zeng, X. W., Jackson, S., Zhou, Y. and Hong, Y. G.** (2009). A cis element within *FLOWERING LOCUS T* mRNA determines its mobility and facilitates trafficking of heterologous viral RNA. *Journal of Virology*, **83**, 3540-3548.
- Li, D., Liu, C., Shen, L., Wu, Y., Chen, H., Robertson, M., Helliwell, C. A., Ito, T., Meyerowitz, E. and Yu, H.** (2008). A repressor complex governs the integration of flowering signals in *Arabidopsis*. *Developmental Cell*, **15**, 110-120.
- Li, S., Yang, X., Wu, F. and He, Y.** (2012). *HYL1* controls the miR156-mediated juvenile phase of vegetative growth. *Journal of Experimental Botany*.
- Lifschitz, E., Eviatar, T., Rozman, A., Shalit, A., Goldshmidt, A., Amsellem, Z., Alvarez, J. P. and Eshed, Y.** (2006). The tomato *FT* ortholog triggers systemic signals that regulate growth and flowering and substitute for diverse environmental stimuli. *Proceedings of the National Academy of Sciences of the United States of America*, **103**, 6398-6403.
- Liljegren, S. J., Gustafson-Brown, C., Pinyopich, A., Ditta, G. S. and Yanofsky, M. F.** (1999). Interactions among *APETALA1*, *LEAFY*, and *TERMINAL FLOWER1* specify meristem fate. *Plant Cell*, **11**, 1007-1018.
- Lin, C. T. and Shalitin, D.** (2003). Cryptochrome structure and signal transduction. *Annual Review of Plant Biology*, **54**, 469-496.
- Lobbes, D., Rallapalli, G., Schmidt, D. D., Martin, C. and Clarke, J.** (2006). *SERRATE*: a new player on the plant microRNA scene. *Embo Reports*, **7**, 1052-1058.
- Locke, J. C. W., Kozma-Bognar, L., Gould, P. D., Feher, B., Kevei, E., Nagy, F., Turner, M. S., Hall, A. and Millar, A. J.** (2006). Experimental validation of a

predicted feedback loop in the multi-oscillator clock of *Arabidopsis thaliana*. *Molecular Systems Biology*, **2**, 6.

Lozano, R., Gimenez, E., Cara, B., Capel, J. and Angosto, T. (2009). Genetic analysis of reproductive development in tomato. *International Journal of Developmental Biology*, **53**, 1635-1648.

Magome, H., Yamaguchi, S., Hanada, A., Kamiya, Y. and Oda, K. (2004). *dwarf* and *delayed-flowering 1*, a novel *Arabidopsis* mutant deficient in gibberellin biosynthesis because of overexpression of a putative AP2 transcription factor. *Plant Journal*, **37**, 720-729.

Martin, R. C., Asahina, M., Liu, P.-P., Kristof, J. R., Coppersmith, J. L., Pluskota, W. E., Bassel, G. W., Goloviznina, N. A., Nguyen, T. T., Martinez-Andujar, C., Kumar, M. B. A., Pupel, P. and Nonogaki, H. (2010). The *microRNA156* and *microRNA172* gene regulation cascades at post-germinative stages in *Arabidopsis*. *Seed Science Research*, **20**, 79-87.

Mas, P., Kim, W. Y., Somers, D. E. and Kay, S. A. (2003). Targeted degradation of TOC1 by *ZTL* modulates circadian function in *Arabidopsis thaliana*. *Nature*, **426**, 567-570.

Massiah, A., Adams, S., Jackson, A., Valdes, V., Morris, K. and Thomas, B. (2007). Physiological and genetic control of the juvenile phase in *Antirrhinum*. *Comparative Biochemistry and Physiology a-Molecular & Integrative Physiology*, **146**, DOI 10.1016/j.cbpa.2007.01.511|19.

Massiah, A. J. (2007). Understanding flowering time. **In:** 2, CAB Reviews: *Perspectives in Agriculture, Veterinary Science, Nutrition and Natural Resources*.

McClung, C. R. and Gutierrez, R. A. (2010). Network news: prime time for systems biology of the plant circadian clock. *Current Opinion in Genetics & Development*, **20**, 588-598.

Meilan, R. (1997). Floral induction in woody angiosperms. *New Forests*, **14**, 179-202.

Michaels, S. D. and Amasino, R. M. (1999). *FLOWERING LOCUS C* encodes a novel MADS domain protein that acts as a repressor of flowering. *Plant Cell*, **11**, 949-956.

Michaels, S. D. and Amasino, R. M. (2001). Loss of *FLOWERING LOCUS C* activity eliminates the late-flowering phenotype of *FRIGIDA* and autonomous pathway mutations but not responsiveness to vernalization. *Plant Cell*, **13**, 935-941.

Michaels, S. D. and Amasino, R. M. (2000). Memories of winter: vernalization and the competence to flower. *Plant Cell and Environment*, **23**, 1145-1153.

Millar, A. J. (1999). Tansley review no. 103 - Biological clocks in *Arabidopsis thaliana*. *New Phytologist*, **141**, 175-197.

Mizoguchi, T., Wright, L., Fujiwara, S., Cremer, F., Lee, K., Onouchi, H., Mouradov, A., Fowler, S., Kamada, H., Putterill, J. and Coupland, G. (2005). Distinct roles of *GIGANTEA* in promoting flowering and regulating circadian rhythms in *Arabidopsis*. *Plant Cell*, **17**, 2255-2270.

Molinero-Rosales, N., Jamilena, M., Zurita, S., Gomez, P., Capel, J. and Lozano, R. (1999). *FALSIFLORA*, the tomato orthologue of *FLORICAULA* and *LEAFY*, controls flowering time and floral meristem identity. *Plant Journal*, **20**, 685-693.

Moon, J., Suh, S. S., Lee, H., Choi, K. R., Hong, C. B., Paek, N. C., Kim, S. G. and Lee, I. (2003). The *SOC1* MADS-box gene integrates vernalization and gibberellin signals for flowering in *Arabidopsis*. *Plant Journal*, **35**, 613-623.

Moreno-Alias, I., Leon, L., de la Rosa, R. and Rapoport, H. F. (2009). Morphological and anatomical evaluation of adult and juvenile leaves of olive plants. *Trees-Structure and Function*, **23**, 181-187.

Moreno-Alias, I., Rapoport, H. F., Leon, L. and de la Rosa, R. (2010). Olive seedling first-flowering position and management. *Scientia Horticulturae*, **124**, 74-77.

Moreno-Cortés, A., Hernández-Verdeja, T., Sánchez-Jiménez, P., González-Melendi, P., Aragoncillo, C. and Allona, I. (2012). *CsRAV1* induces sylleptic branching in hybrid poplar. *New Phytologist*, **194**: 83–90.

Mulas, M. and Deidda, P. (1998). Domestication of woody plants from Mediterranean maquis to promote new crops for mountain lands. *Symposium on Plant Biotechnology as a Tool for the Exploitation of Mountain Lands*, 295-301.

Munir, M., Hadley, P., Carew, J., Zubair, M., Adams, S., Hussain, S. B., Baloch, J. U. D., Hussain, N. and Amanullah, M. (2010). An appraisal of the use of reciprocal transfer experiments: assessing the stages of photoperiod sensitivity in *Antirrhinum majus* L. *Pakistan Journal of Botany*, **42**, 1931-1940.

Munir, M., Jamil, M., Baloch, J. and Khattak, K. (2004). Impact of light intensity on flowering time and plant quality of *Antirrhinum majus* L. cultivar Chimes White. *J Zhejiang Univ Sci*, **5**, 400-5.

Mutasa-Gottgens, E. and Hedden, P. (2009). Gibberellin as a factor in floral regulatory networks. *Journal of Experimental Botany*, **60**, 1979-1989.

Nakamichi, N. (2011). Molecular mechanisms underlying the *Arabidopsis* circadian clock. *Plant and Cell Physiology*, **52**, 1709-1718.

Oh, W., Cheon, I. H., Kim, K. S. and Runkle, E. S. (2009). Photosynthetic daily light integral influences flowering time and crop characteristics of *Cyclamen persicum*. *Hortscience*, **44**, 341-344.

Ohshima, S., Murata, M., Sakamoto, W., Ogura, Y. and Motoyoshi, F. (1997). Cloning and molecular analysis of the *Arabidopsis* gene *TERMINAL FLOWER 1*. *Molecular & General Genetics*, **254**, 186-194.

Olmstead, R. G., DePamphilis, C. W., Wolfe, A. D., Young, N. D., Elisons, W. J. and Reeves, P. A. (2001). Disintegration of the Scrophulariaceae. *American Journal of Botany*, **88**, 348-361.

Padula, G., Giordani, E., Bellini, E., Rosati, A., Pandolfi, S., Paoletti, A., Pannelli, G., Ripa, V., De Rose, F., Perri, E., Buccoliero, A. and Mennone, C. (2008). Field evaluation of new olive (*Olea europaea* L.) selections and effects of genotype and environment on productivity and fruit characteristics. *Advances in Horticultural Science*, **22**, 87-94.

Paltiel, J., Amin, R., Gover, A., Ori, N. and Samach, A. (2006). Novel roles for *GIGANTEA* revealed under environmental conditions that modify its expression in *Arabidopsis* and *Medicago truncatula*. *Planta*, **224**, 1255-1268.

Payne, R. W., Murray, D. A., Harding, S. A., Baird, D. B. and Soutar, D. M. (2009). GenStat for Windows (12th Edition) Introduction. VSN International, Hemel Hempstead.

Perez-Lopez, D., Ribas, F., Moriana, A., Rapoport, H. F. and De Juan, A. (2008). Influence of temperature on the growth and development of olive (*Olea europaea* L.) trees. *Journal of Horticultural Science & Biotechnology*, **83**, 171-176.

Pineiro, M., Gomez-Mena, C., Schaffer, R., Martinez-Zapater, J. M. and Coupland, G. (2003). *EARLY BOLTING IN SHORT DAYS* is related to chromatin remodeling factors and regulates flowering in *Arabidopsis* by repressing *FT*. *Plant Cell*, **15**, 1552-1562.

Pnueli, L., Carmel-Goren, L., Hareven, D., Gutfinger, T., Alvarez, J., Ganai, M., Zamir, D. and Lifschitz, E. (1998). The *SELF-PRUNING* gene of tomato regulates vegetative to reproductive switching of sympodial meristems and is the ortholog of *CEN* and *TFL1*. *Development*, **125**, 1979-1989.

Poethig, R. S. (2003). Phase change and the regulation of developmental timing in plants. *Science*, **301**, 334-336.

Poethig, R. S. (2010). The past, present, and future of vegetative phase change. *Plant Physiology*, **154**, 541-544.

Quail, P. H. (2002). Phytochrome photosensory signalling networks. *Nature Reviews Molecular Cell Biology*, **3**, 85-93.

Rallo, L. and Martin, G. C. (1991). The role of chilling in releasing olive floral buds from dormancy. *Journal of the American Society for Horticultural Science*, **116**, 1058-1062.

Ramos, A., Perez-Solis, E., Ibanez, C., Casado, R., Collada, C., Gomez, L., Aragoncillo, C. and Allona, I. (2005). Winter disruption of the circadian clock in chestnut. *Proceedings of the National Academy of Sciences of the United States of America*, **102**, 7037-7042.

Ritchie, J. T. (1993). Genetic specific data for crop modeling. *Systems Approaches for Agricultural Development*, **2**, 77-93.

Robinson, L. W. and Wareing, P. F. (1969). Experiments on Juvenile-Adult phase change in some woody species. *New Phytologist*, **68**, 67-&.

Romanel, E. A. C., Schrago, C. G., Counago, R. M., Russo, C. A. M. and Alves-Ferreira, M. (2009). Evolution of the B3 DNA binding superfamily: new insights into REM family gene diversification. *Plos One*, **4**.

Salazar, J. D., Saithong, T., Brown, P. E., Foreman, J., Locke, J. C. W., Halliday, K. J., Carre, I. A., Rand, D. A. and Millar, A. J. (2009). Prediction of photoperiodic regulators from quantitative gene circuit models. *Cell*, **139**, 1170-1179.

Samach, A., Onouchi, H., Gold, S. E., Ditta, G. S., Schwarz-Sommer, Z., Yanofsky, M. F. and Coupland, G. (2000). Distinct roles of *CONSTANS* target genes in reproductive development of *Arabidopsis*. *Science*, **288**, 1613-1616.

Sawa, M. and Kay, S. A. (2011). *GIGANTEA* directly activates *FLOWERING LOCUS T* in *Arabidopsis thaliana*. *Proceedings of the National Academy of Sciences of the United States of America*, **108**, 11698-11703.

Sawa, M., Nusinow, D. A., Kay, S. A. and Imaizumi, T. (2007). *FKF1* and *GIGANTEA* complex formation is required for day-length measurement in *Arabidopsis*. *Science*, **318**, 261-265.

Searle, I., He, Y. H., Turck, F., Vincent, C., Fornara, F., Krober, S., Amasino, R. A. and Coupland, G. (2006). The transcription factor *FLC* confers a flowering response to vernalization by repressing meristem competence and systemic signaling in *Arabidopsis*. *Genes & Development*, **20**, 898-912.

Sheldon, C. C., Burn, J. E., Perez, P. P., Metzger, J., Edwards, J. A., Peacock, W. J. and Dennis, E. S. (1999). The *FLF* MADS box gene: A repressor of flowering in *Arabidopsis* regulated by vernalization and methylation. *Plant Cell*, **11**, 445-458.

Shu, Y. and Lin, H.-h. (2004). Transcription, translation, degradation, and circadian clock. *Biochemical and Biophysical Research Communications*, **321**, 1-6.

Simpson, G. G. (2004). The autonomous pathway: epigenetic and post-transcriptional gene regulation in the control of *Arabidopsis* flowering time. *Current Opinion in Plant Biology*, **7**, 570-574.

Simpson, G. G., Dijkwel, P. P., Quesada, V., Henderson, I. and Dean, C. (2003). *FY* is an RNA 3'end-processing factor that interacts with *FCA* to control the *Arabidopsis* floral transition. *Cell*, **113**, 777-787.

Sinelli, N., Casiraghi, E., Tura, D. and Downey, G. (2008). Characterisation and classification of Italian virgin olive oils by near- and mid-infrared spectroscopy. *Journal of near Infrared Spectroscopy*, **16**, 335-342.

Smith, M. R., Willmann, M. R., Wu, G., Berardini, T. Z., Moller, B., Weijers, D. and Poethig, R. S. (2009). Cyclophilin 40 is required for microRNA activity in *Arabidopsis*. *Proceedings of the National Academy of Sciences of the United States of America*, **106**, 5424-5429.

Srikanth, A. and Schmid, M. (2011). Regulation of flowering time: all roads lead to Rome. *Cellular and Molecular Life Sciences*, **68**, 2013-2037.

Staiger, D. (2002). Circadian rhythms in *Arabidopsis*: time for nuclear proteins. *Planta*, **214**, 334-344.

Suarez, M. P., Casanova, L., Jimenez, R., Morales-Sillero, A., Ordovas, J. and Rallo, P. (2011). Variability of first flower to ground distance in olive seedlings and its relationship with the length of the juvenile period and the parent genotype. *Scientia Horticulturae*, **129**, 747-751.

Suarez-Lopez, P., Wheatley, K., Robson, F., Onouchi, H., Valverde, F. and Coupland, G. (2001). *CONSTANS* mediates between the circadian clock and the control of flowering in *Arabidopsis*. *Nature*, **410**, 1116-1120.

Sun, T. P. and Kamiya, Y. (1994). The *Arabidopsis GAI* locus encodes the cyclase ent-kaurene synthetase-a of gibberellin biosynthesis. *Plant Cell*, **6**, 1509-1518.

Sung, S. B. and Amasino, R. M. (2004). Vernalization in *Arabidopsis thaliana* is mediated by the PHD finger protein *VIN3*. *Nature*, **427**, 159-164.

Sung, Z. R., Chen, L. J., Moon, Y. H. and Lertpiriyapong, K. (2003). Mechanisms of floral repression in *Arabidopsis*. *Current Opinion in Plant Biology*, **6**, 29-35.

Swaminathan, K., Peterson, K. and Jack, T. (2008). The plant B3 superfamily. *Trends in Plant Science*, **13**, 647-655.

Tamura, K., Dudley, J., Nei, M. and Kumar, S. (2007). MEGA4: Molecular evolutionary genetics analysis (MEGA) software version 4.0. *Molecular Biology and Evolution*, **24**, 1596-1599.

Tan, F.-C. and Swain, S. M. (2006). Genetics of flower initiation and development in annual and perennial plants. *Physiologia Plantarum*, **128**, 8-17.

Telfer, A., Bollman, K. M. and Poethig, R. S. (1997). Phase change and the regulation of trichome distribution in *Arabidopsis thaliana*. *Development*, **124**, 645-654.

Telfer, A. and Poethig, R. S. (1998). *HASTY*: a gene that regulates the timing of shoot maturation in *Arabidopsis thaliana*. *Development*, **125**, 1889-1898.

Thomas, B. (2009). Defra project: HH3728SX Developing tools for growers and breeders to enable the predictable manipulation of flowering. End of project report. Warwick University.

Thomas, B. and Vince-Prue, D. (1997). Photoperiodism in plants, Second Edition Edition.

Thomson, D. W., Bracken, C. P. and Goodall, G. J. (2011). Experimental strategies for microRNA target identification. *Nucleic Acids Research*, **39**, 6845-6853.

Traenkner, C., Lehmann, S., Hoenicka, H., Hanke, M.-V., Fladung, M., Lenhardt, D., Dunemann, F., Gau, A., Schlangen, K., Malnoy, M. and Flachowsky, H. (2010). Over-expression of an *FT*-homologous gene of apple induces early flowering in annual and perennial plants. *Planta*, **232**, 1309-1324.

Turck, F., Fornara, F. and Coupland, G. (2008). Regulation and identity of florigen: FLOWERING LOCUS T moves center stage. *Annual Review of Plant Biology*, **59**, 573-594.

Turnbull, C. (2011). Long-distance regulation of flowering time. *Journal of Experimental Botany*, **62**, 4399-4413.

Valverde, F., Mouradov, A., Soppe, W., Ravenscroft, D., Samach, A. and Coupland, G. (2004). Photoreceptor regulation of CONSTANS protein in photoperiodic flowering. *Science*, **303**, 1003-1006.

Wang J.W., Czech B., Weigel D. (2009). miR156-Regulated *SPL* transcription factors define an endogenous flowering pathway in *Arabidopsis thaliana*. *Cell* - **138**, Issue 4, 738-749

Wenkel, S., Turck, F., Singer, K., Gissot, L., Le Gourrierec, J., Samach, A. and Coupland, G. (2006). *CONSTANS* and the CCAAT box binding complex share a functionally important domain and interact to regulate flowering of *Arabidopsis*. *Plant Cell*, **18**, 2971-2984.

Wigge, P. A. (2011). FT, A mobile developmental signal in plants. *Current Biology*, **21**, R374-R378.

- Wigge, P. A., Kim, M. C., Jaeger, K. E., Busch, W., Schmid, M., Lohmann, J. U. and Weigel, D.** (2005). Integration of spatial and temporal information during floral induction in *Arabidopsis*. *Science*, **309**, 1056-1059.
- Wilkie, J. D., Sedgley, M. and Olesen, T.** (2008). Regulation of floral initiation in horticultural trees. *Journal of Experimental Botany*, **59**, 3215-3228.
- Wilson, R. N., Heckman, J. W. and Somerville, C. R.** (1992). Gibberellin is required for flowering in *Arabidopsis thaliana* under short days. *Plant Physiology*, **100**, 403-408.
- Woo, H. R., Kim, J. H., Kim, J., Lee, U., Song, I. J., Lee, H. Y., Nam, H. G. and Lim, P. O.** (2010). The *RAVI* transcription factor positively regulates leaf senescence in *Arabidopsis*. *Journal of Experimental Botany*, **61**, 3947-3957.
- Wu, G., Park, M. Y., Conway, S. R., Wang, J. W., Weigel, D. and Poethig, R. S.** (2009). The sequential action of miR156 and miR172 regulates developmental timing in *Arabidopsis*. *Cell*, **138**, 750-759.
- Yamaguchi, A., Kobayashi, Y., Goto, K., Abe, M. and Araki, T.** (2005). *TWIN SISTER OF FT (TSF)* acts as a floral pathway integrator redundantly with *FT*. *Plant and Cell Physiology*, **46**, 1175-1189.
- Yan, Z., Liang, D., Liu, H. and Zheng, G.** (2010). *FLC*: A key regulator of flowering time in *Arabidopsis*. *Russian Journal of Plant Physiology*, **57**, 166-174.
- Yang, L., Conway, S. R. and Poethig, R. S.** (2011). Vegetative phase change is mediated by a leaf-derived signal that represses the transcription of miR156. *Development*, **138**, 245-249.
- Yang, L., Liu, Z., Lu, F., Dong, A. and Huang, H.** (2006). *SERRATE* is a novel nuclear regulator in primary microRNA processing in *Arabidopsis*. *Plant Journal*, **47**, 841-850.
- Yant, L., Mathieu, J., Dinh, T. T., Ott, F., Lanz, C., Wollmann, H., Chen, X. M. and Schmid, M.** (2010). Orchestration of the floral transition and floral development in *Arabidopsis* by the bifunctional transcription factor *APETALA2*. *Plant Cell*, **22**, 2156-2170.
- Yant, L., Mathieu, J. and Schmid, M.** (2009). Just say no: floral repressors help *Arabidopsis* bide the time. *Current Opinion in Plant Biology*, **12**, 580-586.
- Zhang, H., Harry, D. E., Ma, C., Yuceer, C., Hsu, C.-Y., Vikram, V., Shevchenko, O., Etherington, E. and Strauss, S. H.** (2010). Precocious flowering in trees: the *FLOWERING LOCUS T* gene as a research and breeding tool in *Populus*. *Journal of Experimental Botany*, **61**, 2549-2560.

Zhao, L., Luo, Q. L., Yang, C. L., Han, Y. P. and Li, W. B. (2008). A *RAV*-like transcription factor controls photosynthesis and senescence in soybean. *Planta*, **227**, 1389-1399.

Zhu, Q.-H. and Helliwell, C. A. (2011). Regulation of flowering time and floral patterning by miR172. *Journal of Experimental Botany*, **62**, 487-495.

APPENDIX

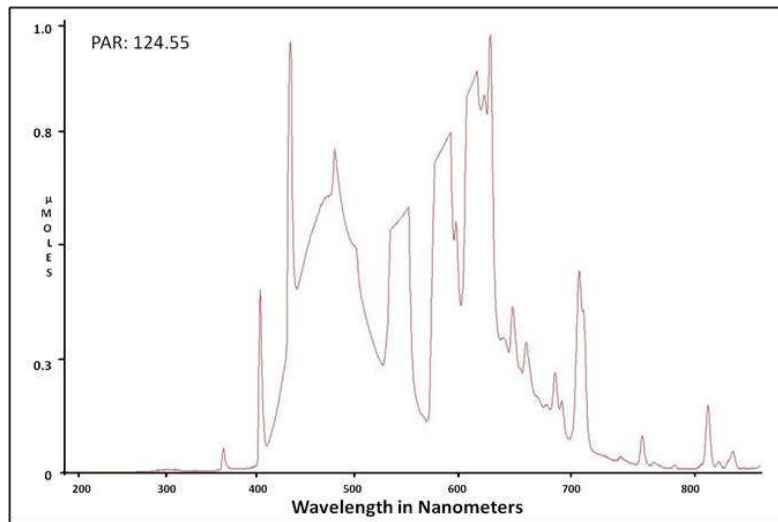


Figure A. 1 Light spectrum in the LD cabinet used in *Antirrhinum* experiment 1. Spectrum obtained from fluorescent tubes. Spectrum is shown as the relative spectral irradiance in the wavelength range of 300-800 nm.

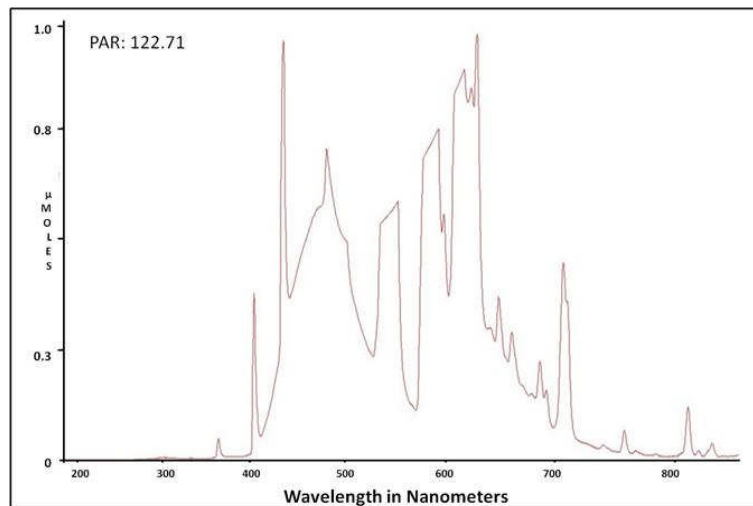


Figure A. 2 Light spectrum in the SD cabinet used in *Antirrhinum* experiment 1. Spectrum obtained from fluorescent tubes. Spectrum is shown as the relative spectral irradiance in the wavelength range of 300-800 nm.

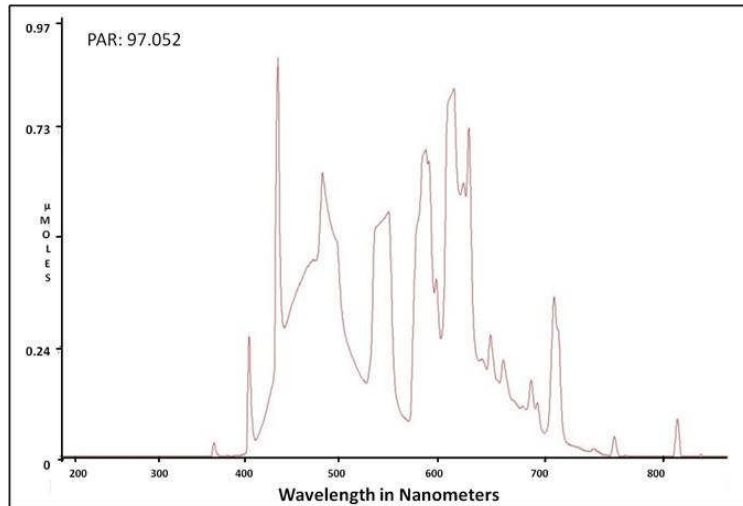


Figure A. 3 Light spectrum in the LD cabinet used in *Antirrhinum* experiment 2 and 3 and *Arabidopsis* experiments during the first 8 hours of the photoperiod. Spectrum obtained from fluorescent tubes. Spectrum is shown as the relative spectral irradiance in the wavelength range of 300-800 nm.

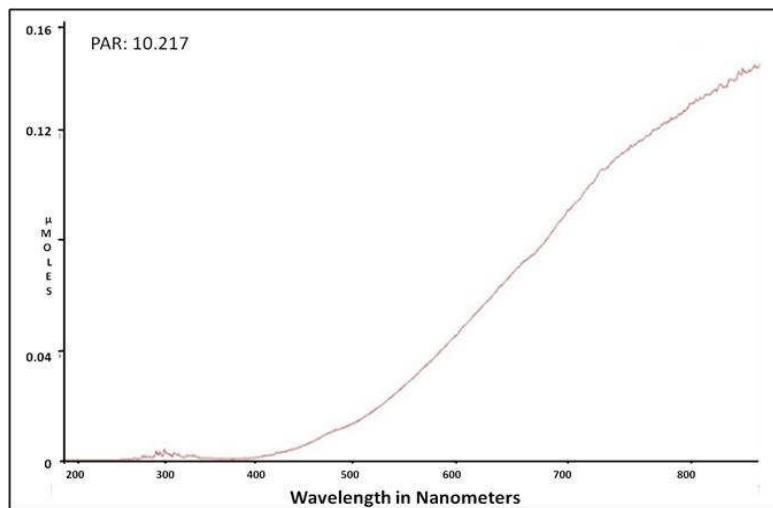


Figure A. 4 Light spectrum in the LD cabinet used in *Antirrhinum* experiment 2 and 3 and *Arabidopsis* experiments during the last 8 hours of the photoperiod. Spectrum obtained from tungsten tubes. Spectrum is shown as the relative spectral irradiance in the wavelength range of 300-800 nm.

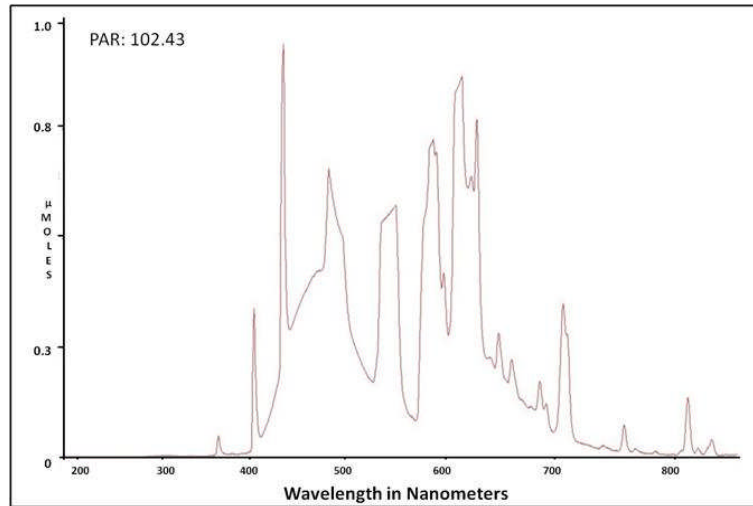


Figure A. 5 Light spectrum in the SD cabinet used in *Antirrhinum* experiment 2 and 3 and *Arabidopsis* experiments.

Spectrum obtained from fluorescent tubes. Spectrum is shown as the relative spectral irradiance in the wavelength range of 300-800 nm.

Table A. 1 Primers used in the study.

In Real-time PCR analysis, 2-step cycling was performed and annealing and extension were carried out at the annealing temperatures shown

Organism and gene (GenBank Acc. No.)	Primer name	Sequence (5'-3')	Annealing temperature	Product size (bp)	Final concentration for standard PCR	Final concentration for Real-time PCR
<i>Antirrhinum</i> <i>Elongation factor α</i> (AJ805055)	Ant elf-alpha F	GAGTACCCACCTCTGGACGTT	61°C	92	0.5 μM	0.2 μM
	Ant elf-alpha R	CTGGGGTCTTTCTTCTCAACAC			0.5 μM	0.2 μM
<i>Antirrhinum</i> <i>FT</i> (AJ803471)	Ant put FT F	GCCAGAATTCAACACGAGAGAC	63°C	78	0.5 μM	0.2 μM
	Ant put FT R	GGCAATTGAAGTAGACAGCAGCA			0.5 μM	0.2 μM
<i>Antirrhinum</i> <i>TEM-like</i>	AmTEM1F	ATGGACGGAAGCTGCATAGAC	63 °C	1072	0.5 μM	
	AmTEM1072R	CTAAATGTTACAAAGCATCAATCACC			0.5 μM	
<i>Antirrhinum</i> <i>TEM-like</i>	Real-time AmTEM F	AATCTGAAAAGCGGGCGATGTTGTA	65°C	100		0.2 μM
	Real-time AmTEM R	CCGACCCATTACCATTACTCCTCA				0.2 μM
<i>Antirrhinum</i> <i>CEN</i> (AJ251993)	Ant CEN F	GAGTCCCTACGTCTGCTACCA	61°C	103		0.04 μM
	Ant CEN R	TTCCCATTTCTCCATCTTTTCCTT				0.04 μM
<i>Antirrhinum</i> <i>FLO</i> (AJ801751)	Ant FLO F	GCATTCAAGGAGCGTGGTGAGA	65°C	141		0.04 μM
	Ant FLO R	GGGACATAACCAGATCGAGAGACG				0.04 μM
<i>Arabidopsis</i> <i>Actin 2</i> (BE038458)	AtActin F	TGTCGCCATCCAAGCTGTTCTCT	63°C	cDNA 85 gDNA 163	0.5 μM	0.2 μM
	AtActin R	GTGAGACACACCATCACCAGAAT			0.5 μM	0.2 μM
<i>Arabidopsis</i> <i>FT</i> (NM_105222)	Real-time AtFT F	GGCCTTCTCAGGTTCAAAAACA	55°C	119	0.5 μM	0.2 μM
	Real-time AtFT R	TCGGAGGTGAGGGTTGCTA			0.5 μM	0.2 μM
<i>Arabidopsis</i> <i>TEM1</i> (NM_102367)	Real-time Tem1 F	CTGGAACAGCAGTCAAAGTTACGTGT	67°C	100		0.2 μM
	Real-time Tem1 R	TGATCTCTCGAAACAAACCACATCAC				0.2 μM
<i>Arabidopsis</i> <i>TEM1</i> (NM_102367)	AtTEM1-F	ATGGAATACAGCTGTGTAGACGA	61°C	1091	0.5 μM	
	AtTEM1091-R	ATTTGTCACAAGATGTTGATAATCG			0.5 μM	
<i>Arabidopsis</i> <i>TEM2</i> (NM_105558)	Real-time Tem2 F	GCCGTTTGCGGTGGAAAAGAGAT	61°C	104		0.2 μM
	Real-time Tem2 R	GAAAAGGAAATATGTCACAAAGCAT				0.2 μM
<i>Arabidopsis</i> <i>CO</i> (NM_001036810)	Real-time AtCO F	GAGAAATCGAAGCCGAGGAGCA	61°C	80		0.2 μM
	Real-time AtCO R	TCAGAATGAAGGAACAATCCCATATA				0.2 μM
<i>Olive actin1</i> (AY788899)	Oe-Actin F	TCCTGAGGTTCTTTACCAGCCTTC	65°C	191	0.5 μM	
	Oe-Actin R	CTAGCGCTGTAATTTCTTGCTCA			0.5 μM	
<i>Olive</i> <i>TEM-like</i>	OeTEM1F	ATGGATACTAGTCAATAGGTGAAAGC	65 °C	1074	0.5 μM	
	OeTEM1074R	TTACAAAGCATCAATAACCCTCTGTT			0.5 μM	
<i>Olive</i> <i>TEM-like</i>	Oe fragment TEM F	CAAAGCTACGTGTTAACAAAAGGAT	61°C	312	0.5 μM	
	Oe fragment TEM R	TACAAAGCATCAATAACCCTCTG			0.5 μM	

Table A. 2 Gene specific Primers used for sequencing.

Organism and gene	Primer name	Sequence (5'-3')	Final concentration
<i>Antirrhinum</i> <i>TEM-like</i>	Seq Amtem F or CI-Am F	CGGAAACGGAACACGATGACG	3.2 μ M
	Seq Amtem R or CI-Am R	CGACAAAACGAACGGACACGAT	3.2 μ M
<i>Arabidopsis</i> <i>TEM1</i> (NM 102367)	Seq Attem1 F	ATGGAATACAGCTGTGTAGACGA	3.2 μ M
	Seq Attem1 R	ATTTGTGCACAAGATGTTGATAATCG	3.2 μ M
<i>Arabidopsis</i> <i>TEM2</i> (NM 105558)	Seq Attem2 F	ATGGATTCTAGTTGCATAGACGAG	3.2 μ M
	Seq Attem1 R	GAAAAGGAAATATGTCACAAAAGCAT	3.2 μ M
<i>Olive</i> <i>TEM-like</i>	Seq Oetem F	CAAAGCTACGTGTTAACAAAAGGAT	3.2 μ M
	Seq Oetem R	TACAAAAGCATCAATAACCCTCTG	3.2 μ M
<i>E.Coli</i> <i>M13</i>	M13F	TGTAACACGACGGCCAGT	3.2 μ M
	M13R	GAAACAGCTATGACCATG	3.2 μ M

Table A. 3 Primers used for semi-quantitative analysis of *AmELF α* , *AmFT*, *AmTEM*, *Oe-Actin* and *OeTEM*.

Organism and gene (GenBank Acc. No.)	Primer name	Sequence (5'-3')	Tm	Final concentration	Product size
<i>Antirrhinum</i> <i>Elongation factor α</i> (AJ805055)	Ant elf- α F	GAGTACCCACCTCTTGGACGTT	61°C	0.5 μ M	92bp
	Ant elf- α R	CTGGGGTCTTTCTTCTCAACAC		0.5 μ M	
<i>Antirrhinum</i> <i>FT</i> (AJ803471)	Ant put FT F	GCCAGAATTCAACACGAGAGAC	63°C	0.5 μ M	78bp
	Ant put FT R	GGCAATTGAAGTAGACAGCAGCA		0.5 μ M	
<i>Antirrhinum</i> <i>TEM-like</i>	Ant fragment TEM F	ACGCGGTCSCGAACTTCA	61°C	0.5 μ M	263bp
	Ant fragment TEM R	CACATCGCTCGGAGTAACC		0.5 μ M	
<i>Olive</i> <i>actin1</i> (AY788899)	Oe-Actin F	TCCTGAGGTTCTTTACCAGCCTTC	65°C	0.5 μ M	191bp
	Oe-Actin R	CTAGCGCTGTAATTCCTTGCTCA		0.5 μ M	
<i>Olive</i> <i>TEM-like</i>	Oe fragment TEM F	CAAAGCTACGTGTTAACAAAAGGAT	61°C	0.5 μ M	312bp
	Oe fragment TEM R	TTACAAAAGCATCAATAACCCTCTG		0.5 μ M	

Table A. 4 Att-primers used for acquisition of full length AmTEM, OeTEM, AtTEM1 cDNA.

Organism	Primer name	Sequence (5'-3')	Final concentration used
<i>Antirrhinum</i>	Am tem att-site F	GGGGACAAGTTTGTACAAAAAAGCAGGCTATGGACGGAAGCTGCATAGACG	0.5µM
	Am tem att-site R	GGGGACCACTTTGTACAAGAAAGCTGGGTCTAAATGTTACAAAGCATCAATCACC	0.5µM
Olive	Oe tem att-site F	GGGGACAAGTTTGTACAAAAAAGCAGGCTATGGATACTAGTTCAATAGGTGAAAGC	0.5µM
	Oe tem att-site R	GGGGACCACTTTGTACAAGAAAGCTGGGTTTACAAAGCATCAATAACCCCTCTGTT	0.5µM
<i>Arabidopsis</i>	At tem att-site F	GGGGACAAGTTTGTACAAAAAAGCAGGCTATGGAATACAGCTGTGTAGACGA	0.5µM
	At tem att-site R	GGGGACCACTTTGTACAAGAAAGCTGGGTATTGTGACAAGATGTTGATAATCG	0.5µM

Table A. 5 Primers used for RACE.

NAME	Sequence (5'-3')
Antirrhinum TEM GSP Forward	GAAGCCGCCAGAGCCTACGACAC
Olive TEM GSP Forward	CAACACGCCGAGAAACACTTCCCTTT
Antirrhinum TEM GSPN Forward	ACTCCCCGACAAAACGAACGGACAC
Olive TEM GSPN Forward	GACTGGAAACCGAGGAACGGATCAA
Antirrhinum TEM GPS Reverse	AACCTCCACACTTTACCCCCAACAC
Olive TEM GPS Reverse	GCCAAAAGCTCCATTTCCCTCCCTCATCC
Antirrhinum TEM GPSN Reverse	CACACTTTACCCCCAACATCCTCAAAA
Olive TEM GPSN Reverse	GCACCCCTTTGGAATTGTTCCCACT
GeneRacer Oligo(dT) primer	GCTGTCAACGATACGCTACGTAACGGCATGACAGTG(T) ₂₄
GeneRacer™ 3'	GCTGTCAACGATACGCTACGTAACG
GeneRacer™ 3' Nested	CGCTACGTAACGGCATGACAGTG
GeneRacer™ 5' Primer	CGACTGGAGCACGAGGACACTGA
GeneRacer™ 5' Nested	GGACACTGACATGGACTGAAGGAGTA

Table A. 6 SOC medium recipe.

SOC medium recipe:	
0.5 % (w/v)	Yeast Extract
2 % (w/v)	Tryptone
10 mM	NaCl
2.5 mM	KCl
10 mM	MgCL2
10 mM	MgSO4
20 mM	Glucose

Figure A. 6 List of 41 amino acid sequences of RAV and RAV-likes used for sequence homology comparisons.

```
>Arabidopsis thaliana TEM1 NP_173927
MEYSCVDDSTTSESLSISTTPKPTTTTEKKLSSPPATSMRLYRMGSGGS
SVVLDSSENGVETESRKLPSKSKYKGVVPPQNGRWGAQIYEKHKQVWLGTFN
EEEEAASSYDIAVRRFRGRDAVTNFKSQVDGNDAESAFLEDAHSKAEIVDM
LRKHTYADEFEQSRKRFVNGDGKRSGLLETATYGNDAVLRAREVLFKTVT
PSDVGKLNRLVIPKQHAEKHFPLPAMTTAMGMNPSPTKGVLINLEDRTGK
VWFRFRYSYWNSSQSYVLTGKWSRFVKEKNLRAGDVVCFERSTGPDRLYI
HWKVRSSPVQTVVRLFGVNI FNVSNNEKPNDAVECVGKKRSREDDLFSLG
CSKKQAIINIL
>Arabidopsis thaliana TEM2 (RAV2) NP_564947
MDSSCIDEISSSTSESFSATTAKKLSPPPAALRLYRMGSGGSSVVLDP
NGLETESRKLPSKSKYKGVVPPQNGRWGAQIYEKHKQVWLGTFNQEEAAR
SYDIAACRFRGRDAVVNFKNVLEDGDLAFLEAHSKAEIVDMLRKHTYADE
LEQNNKRQLFLSVDANGKRNGSSTTQNDKVLKTREVLFEKAVTPSDVGKL
NRLVIPKQHAEKHFPLPSPSPAVTKGVLINFEDVNGKVVWFRFRYSYWNSSQ
SYVLTGKWSRFVKEKNLRAGDVVTFERSTGLERQLYIDWKVRSRGPENPV
QVVVRLFGVDIFNVTTVVKPNDVAVCGGKRSRDVDDMFALRCSKKQAIIN
AL
>Arabidopsis thaliana RAV1 NP_172784
MESSVDESTTSTGSICETPAITPAKKSSVGNLYRMGSGSSVVLDSSENGV
EAESRKLPSKSKYKGVVPPQNGRWGAQIYEKHKQVWLGTFNDEEAARAYD
VAVHRFRRRDAVTNFKDVKMDEDEVDFLNSHSHKSEIVDMLRKHTYNEELE
QSKRRRNGNGNMTRTLLTSGLSNDGVSTTGFRSAEALFEKAVTPSDVGKL
NRLVIPKHHAEKHFPLPSSNVSVKGVLLNFEDVNGKVVWFRFRYSYWNSSQS
YVLTGKWSRFVKEKNLRAGDVVSFSRSNGDQQLYIGWKSRSRSGDL DAGR
VLRLFGVNI SPESRNDVVGKRVNDTEMLSLVCSKKQRI FHAS
>Arabidopsis thaliana RAV1-like NP_189201
MDAMSSVDESSTTTDSIPARKSSSPASLLYRMGSGTSSVVLDSSENGVEVEV
EAESRKLPSRFRKGVVPPQNGRWGAQIYEKHKQVWLGTFNDEEAARAYD
VAAHRFRGRDAVTNFKDITTFEEEEVEFLNAHSKSEIVDMLRKHTYKEELDQ
RKRNRDNGKETTAFALASMVVMTGFKTAELLFEKTVTPSDVGKLNRLVI
PKHQAEKHFPLPLGNMNVSVKGMLLNFEDVNGKVVWFRFRYSYWNSSQSYVL
TKGWSRFVKEKNLRAGDLISFKRSNDQDQKFFIGWKSRSRSGDLLETGRVMR
LFGVDISLNAVVVVKETTTEVLMSSLRCKKQVRL
>Arabidopsis thaliana RAV-like 4 NP_175483
MRLDDEPENALVVSSPKTVVAGSNVYKGVVQQQNGHWGAQIYADHKRI
WLGTFKSADEAATAYDSASIKLRSFDANSHRNPWSTITLNEPDFQNCYT
TETVLNMIRDGSYQHKFRDFLRIRSQIVASINIGGPKQARGEVNQESDKC
FSCTQLFQKELTPSDVGKLNRLVIPKKYAVKYPFISADQSEKEEGEIVG
SVEDVEVVVFYDRAMRQWKFRYCYWKSQS FVFTRGWNSFVKEKNLKEKDV
IAFYTCVDPNPKTLEGRKNFLMIDVHCFSDNGSVVAEEVSM TVHDSV
QVKKTENLVSSMLEDKETKSEENKGGFMLFGVRIECP
>Arabidopsis thaliana RAV-like 5 NP_175524
MDEMSNAKTTTETSGLTDSVLSLTKRMKPTEVTTTTPKALSNTTKFKGV
VQQQNGHWGAQIYADHRRIWLGTFKSAHEAAAAYDSASIKLRSFDANSHR
NFPWSDFTLHEPDFQECYTTEAVLNMIRDGSYQHKFRDFLRIRSQIVANI
NIVGSKQVLGGGEGGQESNKCFSCCTQLFQKELTPSDVGKLNRLVIPKKYA
VKYMPFISDDQSEKETSEGVEDVEVVVFYDRAMRQWKFRYCYWRSSQS FV
TRGWNGFVKEKNLKEKDIIVFYTCVDPNPKTLEGRSKTFLMIDVHHFSG
NGFVVPEEVNKTVHEISDEEMKTETLFTSKVEEETKSEEKKGFFMLFGVR
IQ
>Vitis vinifera RAV-like XP_002276492
MELEMDSTISYSRAGMVAERSFSNSFSLSQPNDHRSSRFRGVVLLHSGN
WGARISIQYQLVWLGTFTAEEAAAAYDTAALKLHKGDSFLNFPWSDHSPQ
EIMFQSYYSIGEIFKMIKDKSYSSNLATFIADQSLIMNYASDPMCEQGIY
QLLFKKALTPRDVAKHPRLLIPKEYALMYFPPITGDVESVQLMFYDKDGI
PWTFRYSWESNQSFVFTTGWKQFVNAKRLKRGETISFYRCGIEEEFEDS
```

AFFMIDVDRGDWESDAIGEHEMGEIISVGGNSNNGMDADDKEKEAADKGFV
LFGVKLG

>*Vitis vinifera* RAV-like2 CAN68564

MDGSCIDESTTSDSISTSLPALSALPATKSPESLCRVGSGT SVILDSESS
IEAESRKLPSRFKGVVPPQNGRWGAQIYEKQHRVWLGT FNEEEEAAKAY
DIAAQRFRRDAVTNFKPLSETEEDDIEAAFLNSHSHKAEIVDMLRKHTYN
DELEQSKRNYGLDANGKRSRAEGLMTPFGSDRVTKSREQLFEKTVTPSDV
GKLNRLVIPKQHAEKHFPLQTGTTSKGVLLNFEDMGGKVWRFRYSYWNSS
QSYVLTGWSRFVKEKNL KAGDIVSFQRSTGGDKQLYIDWKARNGPTNQI
NPVEPVEMVRLFGVNI FKVVPVNSSVVVANNGSWTGKRMIEMELLSFECSK
KQRMVVKGYDKKI

>*Galega orientalis* RAV-like ACI46678

MEGGSCIDETTTTSDSLSVSIFPAKLSPPPTNTLSRVGSGASAI F DPEI
CAGSGEAE SRKLPS SKYKGVVPPQNGRWGAQIYEKQHRVWLGT FN EEEDEA
ARAYDIAALRFRRGKDAVTNSKTLAGAGNDNDEAE TEFLNSHSHKSEIVDML
RKHTYDDEL RQSMRDT CGGRQRRNGESSAAA SRGACDSNAREQLFEKTVT
PSDVGKLNRLVIPKQHAEKHFPLGAVAAAVSVAVDGISPAVSAAGLLLN
FEDIGKLVWRFRYSYWNSSQSYVLTGWSRFVKEKNL RAGDAVQFCRSTG
PDRQLYIDCKARSVS VVGIGNTYTDNLFIPVRPVVEPVQMVRLFGVNL
LKLPGSDGVGGSCNGKRKEMDLFTLECTKKPKIIGAL

>*Nicotiana tabacum* RAV ACF74549

MEGSSSIDESTTSDSLSIAPAISTSTLPVMKSPESLCRMGSGT SVIIDAE
NGVEAESRKLPSRYEGVVPQNGRWGAQIYEKQHRVWLGT FN EENEAAAR
AYDVAQRFRGRDAVTNFKPLLENEENDDMEIAFLNSHSHKAEIVDMLRKH
TYIDELEQSKKNYGF SKDGKRTYCTKDGLMSSFFSSVDKVNKAREQLFEK
AVTPSDVGKLNRLVIPKQHAEKHFPLQNGNTSKGVLLNFEDLNGKVWRFR
YSYWNSSQSYVLTGWSRFVKEKNL KAGDIVSFQRSTGEDKQLYIDFKAR
NATPTISPTVASQVQVQVQVQVQVRLFGVNI CKVPAVNNVV INNNNNNNN
DNNMTSCSGKRRIEMELLTFESCRKKQRVIIINAL

>*Populus trichocarpa* RAV1 XP_002315958

MDGSCIDESTTSSADNSISITPTSLPPFPPTATTTKSPESLCRVRS GNS
SVILDSESGVEAESRKLPS SKYKGVVPPQNGRWGAQIYEKQHRVWLGT FN
EENEAAARAYDIAAQRFRRGKDAVTNFKQVNETEDDEIEAAFLNAHSHKAEIV
DMLRKHTYSDELEQSKRNHR SNNGGNGKQYKNTANYENNSYDHGCGRVLK
AREQLFEKAVTPSDVGKLNRLVIPKQHAEKHFPLQSTSSNSTKGVLLNLE
DVSGKLVWRFRYSYWNSSQSYVLTGWSRFVKEKNL KAGDIVCFQRSTGPD
NQLYIDWKARCGSNQVQVQVQVQVRLFGVNI FNVPGMENGC DGKRSIRDMEL
LSIDRQYSKKQRIIGAL

>*Populus trichocarpa* RAV2 XP_002311438

MDGSCVDESTTSSSTDNSISITPTSLTPSPPPATTTKSPESLCRVGSGNS
VILDLELGVAE SRKLPS SKYKGVVPPQNGRWGAQIYEKQHRVWLGT FN E
EDEAARAYDTAAQRFRGRDAVTNFKQVNETEDDEIEAAFLITHSHKAEIVD
MLRKHTYSDELEQSKRNQRSNNGVNGKQYKNTANYESNSYDHGCGRVLKA
REQLFEKAVTPSDVGKLNRLVIPKQHAEKHFPLQSTSSCSTKGVLLNLED
MSGKVWRFRYSYWNSSQSYVLTGWSRFVKEKSLKAGDIVCFQRSTGPDK
QLYIDWKARSGSNQVQVQVQVQVQVRLFGVNI FNVPGMENGCNGKRSVREM
ELLSLDHQYSKKQRIIGAL

>*Populus trichocarpa* RAV4 XP_002308395

MEEETVSLILNAETS VIEELSDSNSSTHPFPNKRARSGSNVSASRFKGV
VPQPNGHWGCQIYANHQR IWLGT FKSEREAA MAYDSAAIKLRSGDSRRNF
PPTDITVQEPKFQSYYSIEVVLAMIKDGT YQSKFADFIRTCSQSVETALS
LKLMPQSSEGLTCKQLFRKELTPSDVGKLNRLVIPKYYA I KYFPNTKAL
KKMRLTNQSYVFTRGWNR FVKEKLLKANDSIVFWLCESGETVDSAAQTF
QMIDVSN CENISNIAESSNQSIASKVELQLLQGPGIARDSTVKKNVEEDR
MVRADKPTHDAVKTGFKLFGIQIM

>*Oryza sativa* RAV-like 1 AP2 NP_001041982

MGVVSFSSTSSGASTATTESGGAVRMSPEPVVAVAAAAQQLPVVKGVDSA
DEVVTSRPA AAAAQSSRYKGVVPPQNGRWGAQIYERHARVWLGT FPD E E
AAARAYDVAALRYRGRDAATNFPGAAA SAAELAF LAHSHKAEIVDMLRKH
TYADELRQLRRGRGMGARAQPTPSWAREPLFEKAVTPSDVGKLNRLVVP

KQHAEKHFPLRRAASSDSASAAATGKGVLLNFEDGEGKVWRFVFRYSYWNSS
QSYVLTGWSRFRVREKGLRAGDTIVF'SRSAYGPKLLFIDCKKNNAAAAT
TTCAGDERPTTSGAEPRVRLFGVDIAGGDCRKRERAVEMGQEVFLLKRQ
CVVHQRTPALGALLL

>*Oryza sativa* RAV-like 2 NP_001043946
MDSSSCLVDDTNSGGSSTDKLRALAAAAAETAPLERMGSASAVVDAEEP
GAEADSGSGGRVCGGGGGGAGGAGGKLPSSKFKGVVPPQPNGRWGAQIYER
HQRVWLGTTFAGEDDAARAYDVAAQRFRGRDAVTNFRPLAEADPDAAAEELR
FLATRСКАEVDMLRKHTYFDELAQSKRTFAASTPSAATTTASLSNGHLS
SPRSPFAPAAARDHLFDKTVTPSDVGKLNRLVIPKQHAEKHFPLQLPSAG
GESKGVLLNFEDAAGKVWRFVFRYSYWNSSQSYVLTGWSRFRVKEKGLHAGD
VVGFYRSAASAGDDGKLFIDCKLVRSTGAALASPADQPAPSPVKAVRFLG
VDLLTAPAPVEQMAGCKRARDLAATTPPQAAAFKKQCIELALV

>*Oryza sativa* RAV-like 3 NP_001056237
MDSTSCLLDDASSGASTGKKAASAAAASKALQRVGSGASAVMDAAEPGAEA
DSGGERRGGGGKLPSSKYKGVVPPQPNGRWGAQIYERHQRVWLGTFTGAEA
EAARAYDVAAQRFRGRDAVTNFRPLAESDPEAAVELRFLASRСКАEVDMD
LRKHTYLEELTQNKRAFAAISPPPPKHPASSPTSSSAAREHLFDKTVTPS
DVGKLNRLVIPKQHAEKHFPLQLPPPTTSSVAAAADAAAGGDCKGVLL
NFEDAAGKVWFRYSYWNSSQSYVLTGWSRFRVKEKGLHAGDAVGFYRAA
GKNAQLFIDCKVRAKPTTAAAAAFLSAVAAAAAPPVAVKAIIRLFGVDLL
TAAAPQLDAGGAAMTKSKRAMDAMAESQAHVVFKKQCIELALT

>*Camellia sinensis* RAV-like ACT33043
MDGSCIDESTTSDLSIALASASTSILLATKTKASSPKSLCRVGSSTSAI
LDSLEGGAEAESRKLPSRFRKGVVPPQPNGRWGAQIYEKQRVWLGTFNEE
DEAARAYDIAAQRFRGRDAVTNFKPLSENEEQDELETFLNSHSHKSEIVD
MLRKHTYNDPEQSRKNYIGGFINNNGNKKACCNEKSTTNYKNNVKATEQ
LFEKAVTPSDVGKLNRLVIPKQHAEKHFPLQSETTSKGVLLNFKDVGAKV
WRFVFRYSYWNSSQSYVLTGWSRFRVKEKSLKAGDIVSFYRSTGSDNQLFID
WKPRNGSNPVVQPVQMVRLFGVNIQVPIISGGLDSNCGGKRMREMELLAL
ECSKKVRVIGAL

>*Capsicum annuum* RAV-like AF478458_1
MEGTSSIDQESTTSDLSIAPMTTTPPESLCRMGSSTSSVIIDGENGVE
AESRKLPSKYKGVVPPQPNGRWGAQIYEKQRVWLGTFNEEAARAYDV
AAQRFRGRDAVTNFKPLLENQESDDDDVEIAFLNSHSHKAEIVDMLRKHTYI
DELEQSKKLFYTKDGTMAKNKDGLIDISSFFGGGGTIDKVNKNVREQLF
EKAVTPSDVGKLNRLVIPKQHAEKHFPLQNGNNSKGVLLNFEDLNGKVWR
FRYSYWNSSQSYVLTGWSRFRVKEKNLKAGDIVSFQRSTSGDKQLYIDFK
ARNMPTNPVVTNQVQAQVQVPRVQMMRLFGVNIQVPIINNVVDDNNNN
NNNNMANCSGGKRMMEMLLTFESCRKKQRVIIDAL

>*Glycine max* RAV-like NP_001237600
MDGGCVTDETTTSSDLSVPPPSRVGSAVAVVDPDGCCVSGEAEERKLP
SSKYKGVVPPQPNGRWGAQIYEKQRVWLGTFNEEAARAYDIAALRFRG
PDAVTNFKPPAASDDAESEFLNSHSHKFEIVDMLRKHTYDDELQQSTRGGR
RRLDADTASSGVFDAKAREQLFEKTVTPSDVGKLNRLVIPKQHAEKHFPL
SGSGDESSPCVAGASAAKGMLLNFEDVGGKVWRFVFRYSYWNSSQSYVLTGK
WSRFRVKEKNLRAGDAVQFFKSTGPDRLYIDCKARSGEVNNAAGLFPVPI
GPVVEPVQMVRLFGVNLKLPVPGSDGVGKRKEMELFAFECCKKLKVIGA
L

>*Ricinus communis* RAV1 putative XP_002524409
MDGSCIDESTTSDSISITPTSNISSPSSNPLPSKSPESPLCRVGSSTSVVL
DSESGIEAESRKLPSKYKGVVPPQPNGRWGAQIYEKQRVWLGTFNEEDE
AAKAYDIAAQRFRGRDAITNFKPQATDHQSEDEIETAFLNSHSHKAEIVD
MLRKHTYNDLEQSKRNYTSNNGRGDKFQNRNMMNNVGLSGSERIIMKAR
EQLFEKAVTPSDVGKLNRLVIPKQHAEKHFPLQSGSNSTKGVLLNFEDIT
GKVWRFVFRYSYWNSSQSYVLTGWSRFRVKEKNLKAGDIVRFLKSTGPKQL
YIDWKVRTLTPTVSNPVVCSVQPVQMVRLFGVNIQVPIGNSHIEGCNGKR
IREMELLSLDCIKKQRVIGAL

>*Zea mays* RAV1 NP_001151105

MDSASSLVDDTSSGGGGGGASTDKLRALAVFAAASGTPLERMGSGASAV
VDAEAPGAEADSGSGAAAVSVGGKLPSSRYKGVVPPQNGRWGAQIYERHQ
RVWLGTFFAGEADAARAYDVAAQRFRGRDAVTNFRPLADADPDAEAELRFL
ASRSKAEVVDMRLKHTYFDELAQNKRAFAAASAATASSLANNPSSYASLS
PATATAAAAAAREHLFDKTVTPSDVGKLNRLVIPKQHAEKHFPLQLPSAG
GESKGVLLNLEDAAGKVWFRFRYSYWNSSQSYVLTGWSRFVKEKGLQAGD
VVGFYRSAAGADTKLFDCKLRPNVVAASTAGPSPRAPVAKAVRLFVGD
LLTAPATAAAAPAEAVAVAGCKRARDLGSPPQAAFKKQLVELALV
>Antirrhinum majus RAV like AJ800976
MVSTSEAKAGQSVQLQLFQSRFSLVEILNMIKTGSYPMKFNNYLISEVQG
ISRSPLYLQCALGTGLRLLFQKELTPSDVSKLNRLVIPKKYAVEYFPVISE
MEGENSGTCDAELEFFDRSMVLWKFYCFWKSSQSFFVTRGWNRFKAKEK
GLRAKDQVIFSTYESGDRGTEARRIIDVAYTGEAMVAPVARAIVNNGLES
ESEEMDEDVNEKYGETSENVGNFVGAEMRKSVRLEFGVEIFG
>Solanum lycopersicum RAV2 ABY57635
MEGSISSIDQESTTSDLSIAPAASSSTMIKSSSTTIKLPPEGLCRMGS
TSVVIDAENGVEAESKLLPSSRYKGVVPPQNGRWGAQIYEKHQVWLGT
NEENEAAARAYDIAAQRFRGRDAVTNFKPLENQEESDDMEIAFLNSHSAE
IVDVLKHTYIDELEQSKRLFGFTKDGMIKRDGLVISSFFGSTNDKVC
KAREQLFEKVVTPSDVGKLNRLVIPKQHAEKHFPLQNGNNSKGVLLNFED
LNGKVWFRFRYSYWNSSQSYVLTGWSRFVKEKNLKAGDIVSFQRSTSGDK
QLYIDFKAKNVGNTSMVVTNQVQAVQVPLVQMVRLFVNICVVPANVSN
VVIDNNNNNNNNNMTSWGGGKRRMEMELLTFESCRKKQRVIDAL
>Malus x domestica AP2 domain ADE41129
MDGISSTEESTSSDSISIIYPLQHIVARVDPFAKSAPQVASLCRIGSGASS
VILDPELSSSGGTGGVEAESRKLPSRYKGVVPPQNGRWGAQIYEKHQV
WLGTFFNEEADAARAYDVAAQRFRGRDAVTNFKPSSAEPISDDEENDDAE
AAFLSCHSKSEIVDMRLKHTYNDELEQSKRNNSAYGKRSRNSGSLGLFGT
DNSGVPKAREQLFEKAVTPSDVGKLNRLVIPKQHAEKHFPLQSGSAATLT
VSASTACKGVLLNFEDVGGKVWFRFRYSYWNSSQSYVLTGWSRFVKEKNL
MAGDIVSFQRSTGPDQKLYIDWKARMSVNTNNGSSPVQVGPVPMVRLF
GVNIFKIPGSSGPGSADAAAAAIGGGCANNIGKRMREMELELEFGKKP
RIIGAL
>Oryza sativa RAV-like 4 EAY75457
MAGRSDNGDGALTKCVNQEELHHDEHFSFIYKWKNKISSAGNARLYYHYG
YNFGMISSKSELRKIYERHQVWLGTFFAGEDDAARAYDVAAQRFRGRDAV
TNFRPLAEADPDAEAELRFLATRSKAEVVDMRLKHTYFDELAQSKRTFAA
STPSAATTTASLSNGHLSSPRSPFAPAAARDHLFDKTVTPSDVGKLNRLV
IPKQHAEKHFPLQLPSAGGESKGVLLNFEDAAGKVWFRFRYSYWNSSQSYV
LTKGWSRFVKEKGLHAGDVVGFYRSAASAGDDGKLFIDCKLVRSTGAALA
SPADQPAPSPVKAVRLFVGDLLTAPAPVEQMAGCKRARDLAATTPPQAAA
FKKQCIELALV
>Ricinus communis RAV-like XP_002515100
MNFVEQEREYCDKGEEQEEEEEEEEEEEEETIMTTTSMLEPFPSPSSPSS
ATAKYRNFPLQHHNSLWLASSDHSQQDNKTQESSLNFDKLDLMDLSLGN
DNRTLNTSTSTAGASSGSIEREHMF'DKVVTTPSDVGKLNRLVIPKQHAEKY
FPLDSSSNEKGLLLNFEDRNGKLRFRYSYWNSSQSYVMTKGWSRFVKEK
KLDAGDIVSFQRGVGESGKHRLYIDWRRRPNAPDPTSFTHLELQNLHFP
QSVRWGRLYSLPQLSVPRVPFEQSQFHHLNYTIQPYIHNHHDHYYHHHQ
QQQVTSYGNAAAPQYYLRPSPPPPLPSPGTVRIGAVHHHHHPQQQEEG
GDKGSMVIDSIPIVNGRSAGKRLRLFGVNMECPTQDDQYSSSSDNLPHGS
TVLSSFFPHLASHSRPPSSSGASMPTSRQADAHHEFPKKGKTSLSFDLDI
>Arabidopsis thaliana NGA3 NP_171611
MDLSLAPTITTTSSDQEQDRDQELTSNIGASSSSGPGSNNNNLPMMPPPP
EKEHMF'DKVVTTPSDVGKLNRLVIPKQHAERYFPLDSSNNQNGTLLNFQDR
NGKMWRFRYSYWNSSQSYVMTKGWSRFVKEKLDAGDIVSFQRGIGDESE
RSKLYIDWRHRPDMSLVQAHQFGNFGFNFPPTTSQYSNRHFHPLPEYNSV
PIHRGLNIGNHQRSYYNTQRQEFVGYGYGNLAGRCYYTGSPLDHRNIVGS
EPLVIDSVVPPVGRLLTPVMLPPLPPPPSTAGKRLRLFGVNMECGNDYNQQ

EESWLVPERGEIGASSSSSSALRLNLSTDHDDDDNDDGDDGDDDDQFAKKGKS
SLSLNFP

>Arabidopsis thaliana NGA1 NP_566089

MMTDLSLTRDEDEEEAKPLAEEEGAREVADREHMFDKVVTPSDVGKLNRL
VIPKQHAERFFPLDSSSNEKGLLLNFEDLTGKSWRFRYSYWNSSQSYVMT
KGWSRFVVKDKKLDAGDIVSFQRCVGDSDGRDSRLFIDWRRRPKVPDHPHFA
AGAMFPRFYSFPSTNYSLYNHQQQRHHHSGGGYNYHQIPREFGYGYFVRS
VDQRNNPAAAVADPLVIESVPMVMHGRANQELVGTAGKRLRFLGVDMCEG
ESGMTNSTEEESSSSGGSLPRGGGGGASSSSFFQLRLGSSSEDDHFTKKG
KSSLSFDLDQ

>Arabidopsis thaliana NGA2 NP_191756

MNQEDKEKPIEEASSSMERHMFDKVVTPSDVGKLNRLVIPKQHAERYFP
LDNSTTNDNSNKGLLLNFEDRSGNSWRFRYSYWNSSQSYVMTKGWSRFVKD
KKLDAGDIVSFQRDSCNKDKLYIDWRRRPKIPDHHHQFAGAMFPRFYTF
PHPQMPTNYETHNLYHRFHQRDLGIGYYVRSMEERSHPTAVIESVPMVMQR
RAQVASMASRGEKRLRFLGVDMCEGGGGGSVNSTEEESSSSGGSI PRGRV
SMVGAGSLLQLRLVSSDDESLVAMEAASLEDHFFFTKKGKPSLSFDLDR

>Oryza sativa RAV-like 5 NP_001047754

MEFTTSSRFSKEEEDEEQDEAGRREIPFMTATAEAAPAPTSSSSSPAHHA
ASASASASASGSSTPFRSDDGAGASGSGGGGGGGGEAEVVEKEHMFDKVV
TPSDVGKLNRLVIPKQYAEKYFPLDAAANEKGLLLNFEDRAGKPWRFRYS
YWNSSQSYVMTKGWSRFVKEKRLDAGDTSVSRGIGDEAARHRLFIDWKR
RADTRDPLRLPRGLPLPMLTSHYAPWIGGGGGFFVQSPPATLYEHRL
RQGLDFRAFNPAAMGRQVLLFGSARIPQAPLLARAPSPHHHYTLQPS
GDGVRAAGSPVVLDSVPVIESPTTAAKRVRLFGVNLNPHAGGGGGAAAG
ESSNHGNALSLQTPAWMRRDPTLRLELPPHHHGAESSAASSPSSSSSS
KRDAHSALDLDL

>Oryza sativa RAV-like NP_001174059

MEFATTSSRFSKEEEEEEGEQEMEQEDEEEEEAEASPREIPFMTSAAA
AATASSSSPTSVPSPATASAAASTSASGSPFRSSDGAGASGSGGGGGED
VEVIEKEHMFDKVVTPSDVGKLNRLVIPKQHAEKYFPLDSAANEKGLLLS
FEDRTGKLWRFRYSYWNSSQSYVMTKGWSRFVKEKRLDAGDTSVFCRGAA
EATRDRFLIDWKRRADVRDPHRFQRLPLPMTSPYGPWGGGAGASSCRPRR
PPRSTSITAFARASTSATSTPLCRRGSSSSSAPQGRGFISTRPCHRRRRH
LRLLTNSTLRCTTRAP

>Vitis Vinifera A5APE8 Putative uncharacterized protein CAN73636

MDLLPDRDVVCEQEQVIRGKQLPFSYSSSSPSSSSSQYRNLVPLPNGGD
RWDAQIQRGWLGHQEDGMRCFEGGAASKLELMDTSPNDEDDVDDVRR
RDSQALEREHMFDKVVTPSDVGKLNRLVIPKQHAEKYFPLDSSANEKGLL
LNFEEDRSGKPWRFRYSYWNSSQSYVMTKGWSRFVKEKLDAGDIVSFQRG
VGESGKDRLYIDWRRRPDAPEPSSLAHHFFHRSVPWSPFLFQAPVAGGAV
SMGRQQVQLAQPNYMSHLGGRNPYSGAYSYNNAVNPCSGSVFYLRPTAP
QQVGMVQVQQGGVEPMVFNVPVVGKAAAKRLRFLGVNMECPISSEDEC
DILSSTSIPHAAVASQPPHLSSPSSHHHPLQLRLYNAEIEGMQRLEKKKE
KVVRSLGQLIGYGCHHEGLRKGTMQVQVWLNKEDGDYEIPVLGVVVLVAA
SLGTPAGIAEKVAELYMDAYLIIIFVSSKEELYMLENFPMGDSNEADLT
NHDMN

> Ricinus communis RAV-like XP_002518948

MEIGSAAGIISTEEEQMSK GKHL PFSYSSSSSPSSSSSQHKPHLLALSQ
IYDKNHHPQVGSWLGSKYDPEQEDAGSAAGIFEEEEGSGECECGVVIQKE
HMFDKVVTPSDVGKLNRLVIPKQHAEKYFPLDSSSTNDKGLLLNFEDKTGK
AMFRKYSYWNSSQSYVMTKGWSRFVVKDKKLDAGDIVSFQRGVGEAAKDRL
YIDWRRRPDGP HHQP THRHQHHLSSIPWSPLLMRPPVPRDHFHLSNP
YINSSGGGGASAYGFGYGNSSNNYNSNVGSSNSGTI IYMRSPQQAG
MVQWQQAAAASSGFMFEPVVFESVPPVQKAAAKRLRFLGVNMDCPISDSD
HECDKLSTSTPIPAMAAALQQPSHHPLQLRLYNGTPLPSPQFLHKGKSSM
SLDLDI

>SORGHUM BICOLOR uncharacterized protein

XP_002448384

MEFASSSSRFSKEEDEEEEGEEDEEASPREIPFMTAAAATADTGPAAS
SSSPSAAAGASASASGSAAALRSGDGAGASGSGGGGGSDVEVIEKEHMF
DKVVTPSDVGKLNRLVIPKQHAKEYFPLDAAANEKGLLLSFEDRAGKLWR
FRYSYWNSSQSYVMTKGWSRFVKEKRLDAGDTVSFRCRAGEAARDRLFID
WKRRADSRDPRHRPRLPLPMPVSPYGLGPWGGGAGGFFMPPAPPATLY
EHHRFRQALDFRNINAAAAAPARQLLFFGSQGMPPRASMPLOQQQPQPQPS
LPPPPPLHSIMMVQPGSPAVTHGLPMLVDSVPLVNSPTAAAKRVRLFV
NLDNPQQGSSAESSQDANALSLRMPGWQRPGPLRFFESPQRGAAESSAAS
SPSSSSSSKREAHSSLDL

>SORGHUM BICOLOR uncharacterized protein
XP_002458352

MD\$ASSLVDDTSSGSGGGGASTDKLRALAVAAAAAGPPLERMGSASAV
LDAAEPGAEADSAAAAAPGAVGVGGKLPSSRYKGVVPPQNGRWGAQIYER
HQRVWLGTFADEADAARAYDVAAQRFRGRDAVTNFRPLADADPDAEAELR
FLASRSKAEVVDMLRKHTYFDELAQNKRAFAAAAAAASSAATTTASSLA
NNNNNHSSLASPSPATAREHLFDKTVTPSDVGKLNRLVIPKQHAEKHFPL
QLPSAGGESKGVLLNLEDAAGKVWRFYRYSYWNSSQSYVLTKGWSRFVKEK
GLQAGDVVGFYRSSAVGAGADTKLFDCKLRPNVATASTTTGPAVGSPP
PAPAPAPVATKAVRLFVVDLLTAPAATAAAPAEAMAAGCKRARDLASPPQ
AAFKKQLVELALV

>SORGHUM BICOLOR uncharacterized protein
XP_002457391

MGIESMSPTAAPAEDSSSSSRFSAASTATTESGAAQPRAASAAPGGGAV
VVGRDASLADEQAVTSQPLAASTAAVAQSSRFKGVVPPQNGRWGAQIY
ERHARVWLGTFADEEAAAARAYDVAALRYRGREAAATNFPGAGASAPELTFL
AAHSKAEIVDMLRKHTYADELRQGLRRGRMGARAQPTPAWARSLLFEKA
VTPSDVGKLNRLVVPKQHAEKHFPLKRAPEASAAAATTKGVLLNFEDGE
GKVWRFYRYSYWNSSQSYVLTKGWSRFVREKGLRAGDTIVF\$HSTYSSEKQ
LFIDCKKTKTTT\$VATTDGAPVPAPAEKPKSEARVVRLFVVDIAGDGCQKR
ARPVEIAFEHGPQQLLKKKQCVGVAHHRSPALGAFLL

>Oryza sativa uncharacterized protein EAY95278

MEQEQDEEEEAASPREIPFMTSAAAAATASSSSPTSVSPSATASAAAS
TSASGSPFRSSDGAGASGSGGGGGEDVEVIEKEHMF\$DKVVTPSDVGKLN
RLVIPKQHAKEYFPLDSAANEKGLLLSFEDRTGKLWRFYRYSYWNSSQSYV
MTKGWSRFVKEKRLDAGDTVSFRCRGAQA\$TRDRLFIDWKRRADVRDPRHF
RQLPLPMTSPYGPWGGGAGAFFMPPAPPATLYEHHRFRQGFDFRNINPAV
PARQLVFFGSPGTGIHQHPPLPPPPPPPPHQLHITVHHPSPVVTAGLP
MVVDSVPHVNNPAAASKRVRLFVGNLDNPHPDGGQSSSGHDANALSLRMP
GWQRPAPLRSLELPPHPAGAAGAESSAASSPSSSSSSKREAHSSLDL

>Oryza sativa RAV-putative NP_001065792

MAMNHPLFSQEQPQSWPWGVAMYANFHYHHH\$YEKEHMF\$EKPLTPSDVGKL
NRLVIPKQHAERYFPLGAGDAADKGLILSFEDEAGAPWRFYRYSYWTSSQS
YVLTKGWSRYVKEKRLDAGDVVHFERVRSFGVGDRLFICRRRGDAAAA
QTPAPPPAVRVAPAAQ\$NAGEQQPWS\$PMCYSTSGGGSYPTSPANSYAYRRA
ADHDHGDMMHADESPRDT\$PSFSAGSAPSRRLRLFVGNLDCGPEPEADT
TAAATMYGYMHQ\$SSYAAMSAVPSYWGNS

>SORGHUM BICOLOR uncharacterized protein XP_002452747

MDQFAASGRFSREEEADEEHEDASNSMREISFMPAAAAAGTAPSSSAAAS
AASTSASASAASGSSSATAPFRSASGDAAGASGSGGGGGAAADVEAVEKE
HMF\$DKVVTPSDVGKLNRLVIPKQYAEKYFPLDAAANEKGLLLSFEDSAGK
HWRFRYSYWNSSQSYVMTKGWSRFVKEKRLVAGDTV\$FSRAAAEDARHRL
FIDWKRRVDTRGLRFSGLALPMLASHYGP\$HYS\$PWGFGIGVGGGGGGG
GGFFMPPSPATLYEHRLRQGLDFRSMTNYPAPT\$VGRQQLLFFGSARMPP
HHAPAPQPRPLSLPLH\$FTVQPSAAAGVTAASRPVVDL\$V\$VIESPTTAA
KRVRLFVGNL\$DNNPLSEPDGGVGEASHQGNALSLQMPGWQ\$QRTTPTLRL
ELPRHGAAESSAASSPSSSSSSKREARSALDL

>Oryza sativa RAV-putative Y1407_ORYSJ

MEQEAAMVVFSCNSGSGSSSTTDSKQEEEEEEELAA\$EDEL\$IHVVQAA
ELRLPSSTTATR\$PSSRYKGVVPPQNGRWGAQIYERHARVWLGT\$FPDEEAA
ARAYDVAALRFRGRDAVTN\$RAPAAEGASAGELAF\$LAH\$SKAEVVDMLRKH

TYDDELQOGLRRGSRAQPTPRWAREPLFEKAVTPSDVGKLNRLVVPKQQA
 ERHFPPFLRRHSSDAAGKGVLLNFEDGDGKVVFRFRYSYWNSSQSYVLTGK
 WSRFVREKGLRPGDVTVAFSRSAAAAGWTEKHLLDCKKMERNNLATVDDDA
 RVVVKLFGVDIAGDKTR
 >Arabidopsis thaliana RAV-like 1 NP_850260
 MSINQYSSDFHYHSLMWQQQQQQHONDVVEEKEALFEKPLTPSDVGKL
 NRLVIPKQHAERYFPLAAAAADAVEKGLLLCFEDEEGKPWRFRYSYWNSS
 QSYVLTGKWSRYVKEKHLDAGDVVLFHRHRSDGGRFFIGWRRRGDSSSSS
 DSYRHHVQSNASLQYYPHAGAQAQAVESQRGNSKTLRLFGVNMECQLDSWSE
 PSTPDGSNTYTTNHDQFHYPQQQHYPPPYMDISFTGDMNRTS
 >Arabidopsis thaliana RAV-like 2 NP_850559
 MSVNHYHNTLSLHHHHQNDVAIAQRESLFEKSLTPSDVGKLNRLVIPKQH
 AEKYFPLNNNNNGSGDDVATTEKGMLLSFEDESGBKWKFRRYSYWNSSQ
 SYVLTGKWSRYVVKDKHLDAGDVVFFQRHRFDLHRLFIGWRRRGEASSSPA
 VSVVSQEALVNTTAYWSGLTTPYRQVHASTTYPNIHQEYSHYGKFKPFIS
 SFVFSFSLIYMSDLYSSLFSFKICLFHKNR
 >Arabidopsis thaliana NGA4 NP_192059
 MNLDQELAEIRASSSDHTNYFYSSERREHMFDKVLTTPSDVGKLNRLVIPK
 QHAENFFPLEDNQNGTVLDFQDKNGKMWRFRYSYWNSSQSYVMTKGWSRF
 VKEKFLFAGDVTVSFYRGYIPDDNAQPERRRKIMFIDWRPRAEINFVHNIN
 NHNFVFGSPTYPTARFYPTPEYSMPYRSFPPFYQNFQEREYLGYYGR
 VVNGNGVRYAGSPLDQHHQWNLGRSEPLVYDSVPVFPAGRVPSPAPPQP
 STTKLRLFGVDVEESSSSGDTRGEMGVAGYSSSSPVVIRDDDQSFWRSP
 RGEMASSSSAMQLSDDEEYKRKGSLEL
 >Arabidopsis thaliana RAV-like 3 NP_001119177
 MSVNHYSTDHHTLLWQQQHRHTTDTSETTTTATWLHDDLKESLFEKSL
 TTPSDVGKLNRLVIPKQHAKEYFPLNAVLSAAADTSSEKGMLLSFEDE
 SGKSWRFRYSYWNSSQSYVLTGKWSRFVKDKQLDPGDVFFQRHRSDSR
 LFIGWRRRGQSSSSVAATNSAVNTSSMGALSYHQIHATSNYSNPPSHSE
 YSHYGAAVATAAETHSTPSSSVVGSRTVRLFGVNLECMDENDGDDSSVA
 VATTVESPDGYYGQNMYYYYSHPHNMVILTLL
 >Oryza sativa RAV-putative NP_001172942
 MAASLPLSAAIVGAEEESVDKEVLEMEYLFKFLMPSDLCSNTEWLGIPPE
 HVRKFLGMMLEDRDGYSVIFFQDGVVPGKLVCFRYWKSNGVHGLTKGWRFC
 VREKGLKAGDTISFFRGSACGRLFICCRGLGTHATFASSSTLHHGFSMPPP
 PARPLVGLQSGMLARDVPSLQARLHDGNQDGGGAPSRHVPSSGRRVEAQ
 LSRVSSRRQRRTMKHSIPEPTIETPPILESMFLIAAPPVAVKCLRLFGVNI
 YVLPVSSSGQPKQESSP
 >Oryza sativa RAV-putative EAY85732
 MAASPPLPTSIDGGQVLDDMEVEMKYLFGKVLMPSDVSWDTEQLVIPDE
 HVGKLLDMVMMNRPEGGFVVVVVEDGEVTGKLWLFYWKRRDDVHCLTKGW
 GCYAREKGLRAGDTVSFFHSTACGRFFICCRCTCMSFLSLPTTSHRIHGS
 SVLPQPRAAQEAHHPFSGHATLCLGNKASDHAPARHATASLGAAAQPP
 QVPPTPTPRRRRRSMMVHPEPPEHTTDGMPVILESMALVSTPPVAKRVRL
 FGVYIDVPPPLRPGGEATQDFNP
 >Oryza sativa RAV-putative BAG89861
 MEPIREGEGPPRRRHSLRLGLVWPRQAALHRLQEEQHGGGHRRRREANYK
 RRSNTRREAVRHGHRRRRRLPEAGEGGGNGARGVLDEEAMRGSSAYSSCP
 WCPAVITSNQFIYTS
 >Oryza sativa RAV-putative NP_001048792
 MEFITPIVRPASAAAGGGEVQESGGRSLAAVEKEHMFDKVVTPSDVGKLN
 RLVIPKQHAKEYFPLDAASNEKGLLLSFEDRTGKWRFRYSYWNSSQSYV
 MTKGWSRFLVKEKRLDAGDVTVSFGRGVGEAARGRLFIDWRRRPDVVAALQP
 PTHRFAHHLPSIPFAPWAHHHGHGAAAAAAAAAAGARFLLPSSSTPIYDH
 HRRHAHAVGYDAYAAATSRQVLFYRPLPPQQQHHPAVVLESVPVRMTAGH
 AEPPSAPSKRVRLFGVNLDCANSEQDHAGVVGKTAPPPLPSPSSSSSSSS
 GKARCSLNLDL
 >Oryza sativa RAV-putative EAY99351
 MATIVAWESRNLQLOGGGGGHGGGGGGGERREYMFKVVTPSDVGKLN
 RLVVPKHAYAEKYFPLGPAARTSPAGTVLCFEDARGGDSTWRFRYSYWSSS

QSYVITKGWSRYVRDKRLAAGDTVSVFCRAGARLFIDCRKRAASVSSSSLV
PPALIKVQLPPSRPVVDEEEAACGRRCLRLFGVDLQLRADASPALDLQL
>Oryza sativa RAV-putative Y8577_ORYSJ
MYMDLTLGGALLQVEEATEEEEEEEEEEEQALGQEPAPAAAAAALVLGRRH
GVVVGSGGGGVVVAAREHMFDPKVVTPSDVGKLNRLVVPKQHAERFFPAA
AAGTQLCFEDRAGTPWRFRYSYWGSSQSYVMTKGWSRFVRAARLSAGDTV
SFSRAADGRYFIDYRHCHRHGGRDISFASAATAMPAAAWPLFGRVQTAAP
VSYGGGHGSAAAATMFLDTPVAPVAAAGGHRGEVGPSPGQRSFRLFGVNVEC
GGDVDAAAEEEDADDDVDDGDHRRGEEMELVMWNTNHR
>Oryza sativa RAV-putative Y1071_ORYSJ
MEFTPIPPTRVAGGEEDSERGAAAWAVEKEHMFVKVVTTPSDVGKLNRL
VIPKQHAERYFPLDAAAGAGGGGGGGGGGGKGLVLSFEDRTGKAWRFR
YSYWNSSQSYVMTKGWSRFVKEKRLGAGDTVSVFGRGLGDAARGRLFIDFR
RRRQDAGSFMFPPTAAPPSSHSHHHHQRHHPPLPSVPLCPWRDYTTAYGGG
YGYGGGGSTPASSRHVFLRFPQVPAAVVLKSPVHVAATSAVQEAATTT
RPKRVRLFGVNLDCPAAMDDDDDIAGAASRTAASSLLQLPSPSSSTSSST
AGKKMCSLDLGL
>Oryza sativa RAV-putative EEC68891
MAMHPLAQGHPQAWPWGVAMYTNLHYHHHYEREHLFEKPLTPSDVGKLNRL
LVIPKQHAERYFPLGGGDSGEKGLLLSFEDESGKPWRFRYSYWTSSQSYV
LTKGWSRYVKEKRLDAGDVVHFERVRGLGAADRLFIGCRRRGESAPAPP
AVRVTPQPPALNGGEQQPWSPMCYSTSGSSYDPTSPANSYAYHRSVDQDH
SDILHAGESQREADAKSSSAASAPPPSRRLRLFGVNLDCGPEPEADQATA
MYGYMHHSQSPYAAVSTVPNYWSVFFQF

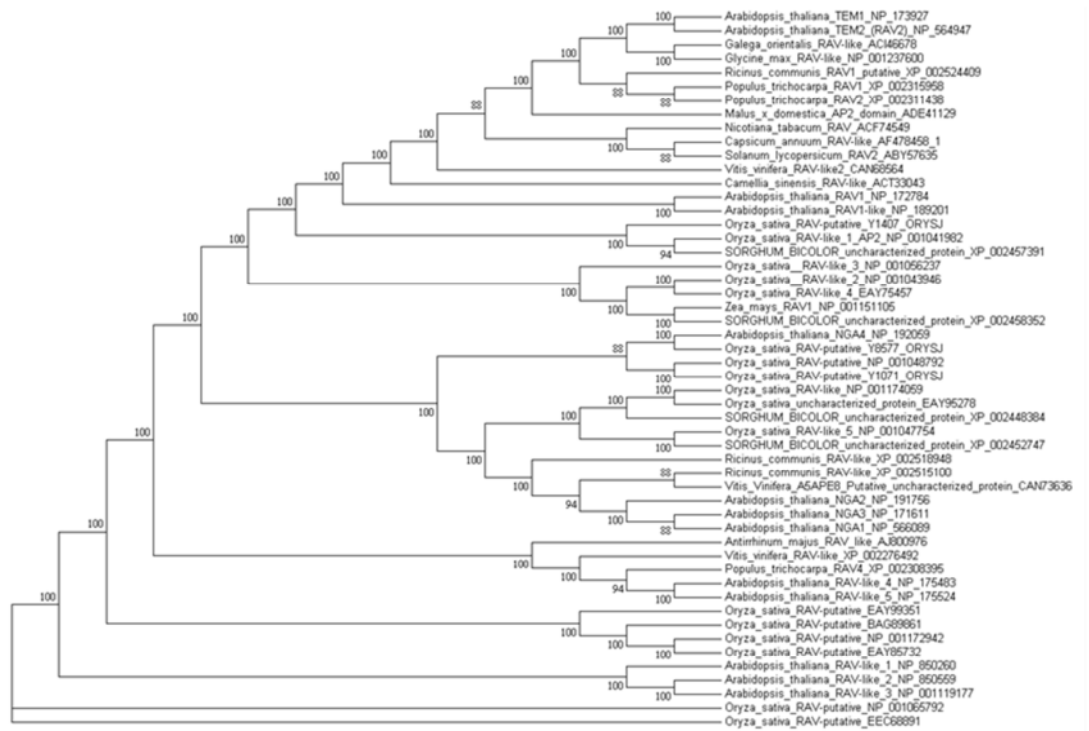


Figure A. 7 Phylogenetic analysis of 41 RAV sub-family members.

The evolutionary relationship was inferred using the Maximum Parsimony method. The percentage of parsimonious trees in which the associated taxa clustered together are shown next to the branches. Accession number can be found close to the species name in the figure.

```

1
AtTEM1 MEYSKVVDD-S STTSESLIS TTPKPTTTE KKLSPAPPATS MRLYRMGSSG SSVLVDSENG VE----TESR KLPSKYYKGV VPQPNRWGA QIYEKHQVW LGTFNEDDEA ASSYDIAVRR FRGRDAVNF 130
AtRAV2/TEM2 MDSSCIDIEIS SSTSESFSS-----ATTA KKLSPAPPAAA LRLYRMGSSG SSVLVDSENG LE----TESR KLPSKYYKGV VPQPNRWGA QIYEKHQVW LGTFNEDDEA ARSYDIAACR FRGRDAVNF
AtRAV1 MESSSVDES TTSTGSI--- -----CETP AITPAKSSV GNLYRMGSSG SSVLVDSENG VE----AESR KLPSKYYKGV VPQPNRWGA QIYEKHQVW LGTFNEDDEA ARSYDVAVHR FRGRDAVNF
AtRAV1-like MDAMSSVDES STTTDSI--- -----PARK SSSPASL--- --LYRMGSSG SSVLVDSENG GVEVEVEAESR KLPSKYYKGV VPQPNRWGA QIYEKHQVW LGTFNEDDEA ARSYDVAHR FRGRDAVNF
GoRAV-like MEGGSCIDET TTTSDSL--- -----SVSIF PAKLSPPTT- NTLRVRGSSG AALFDFEIC AG-SGEAESR KLPSKYYKGV VPQPNRWGA QIYEKHQVW LGTFNEDDEA ARSYDIAALR FRGRDAVNF
NtRAV MEGSSIDES TTSDLSLSI--- -----APAIS TSTLPVPMKSG ESLCRMSGG- TQVIIDAE- -N-GVEAESR KLPSKYYKGV VPQPNRWGA QIYEKHQVW LGTFNEDDEA ARSYDVAQR FRGRDAVNF
AtRAV-like 4 MRLDD ERENALVVS SP---KTVV ASGNVYKGV VQVQNGHWGA QIYADHKRIM LGTFKSDDEA ATAYDSASIK LRSFDANSHR
AtRAV-like 5 MDEM SNVAKTTTET SGLTDSVLSL TTRMKPTEVT TT---TKPA SNTTKFKGV VQVQNGHWGA QIYADHKRIM LGTFKSDHEA AAAYDSASIK LRSFDANSHR
PtRAV4 MEEE TVSLILNAET SVIEELSDSN STHFPFPMK RA---RSGS NVSASRFKGV VPQPNRWGA QIYANHQRIW LGTFKSDHEA AAAYDSAAIK LRSFD--SRR
VvRAV-like MELE MDSTISYSRA GMVAERSFSS NAFSLSQPH D----- -RSSRFRGV VLLHSGNWGA RISIQYQLWV LGTFKSDHEA ARSYDTAALK LHKGD--SFL
AmRAV-like
Consensus ..... 1 ..... 130
131
AtTEM1 KSVQ---DG NDAESAFLEDA HSKAEIVDML RKHTYADEFE QSRRK---FVN GDGK---RSG LETATYGNDA V--LRAREVL FRKVTTPSDV GKLNRLVIPK QHAEKHFPLE AMTTAMGM-- ----NPSP
AtRAV2/TEM2 KNVL---E- -DGDLEAFLEA HSKAEIVDML RKHTYADEFE QNNKRQLFSL VDAN---GKR NGSSTTQNDK V--LKTREVL FRKAVTPSDV GKLNRLVIPK QHAEKHFPLE SPS-----PAVT
AtRAV1 KDVK---M- DEDEVDFLNS HSKAEIVDML RKHTYADEFE QSKRRRNGNG NMTR---TLL TSLGSDNGVS TTGFSAEAL FRKAVTPSDV GKLNRLVIPK QHAEKHFPLE --S-----SNVSV
AtRAV1-like KDIT---F- EE-EVEFLNA HSKAEIVDML RKHTYADEFE QSKRRRNGNG KETT---AFA LASM---VV MTGFKTAEAL FRKVTTPSDV GKLNRLVIPK QHAEKHFPLE LGN-----MNVSV
GoRAV-like KTLAGAGNDN DEAEIETFLNS HSKAEIVDML RKHTYADEFE QSMRDTCCGR Q---RRN GESSAASRG ACSDNAREAL FRKVTTPSDV GKLNRLVIPK QHAEKHFPLE AVAAAVSVAV DGISPAVSA
NtRAV PLL-EENEEN DDMEIETFLNS HSKAEIVDML RKHTYADEFE QSKKNYGFSK DGKRTYCTDK GLMSFFSVS DKVKNAREAL FRKAVTPSDV GKLNRLVIPK QHAEKHFPLE -----QNGTNS
AtRAV-like 4NFPW---STI TLNEPFDQNC YTTETVLMKI RIGSYQHFKR DFILRISQIV ASIINIGPKQ ARG-EVNGQE SDKCFSTCL FRKELTPSDV GKLNRLVIPK KYAVKYPFI SADQSEKEEG EIVG----SV
AtRAV-like 5NFPW---SDF TLHEPFDQEC YTTETVLMKI RIGSYQHFKR DFILRISQIV ANINIVGSKV VLGSGEGGQE SNKCFSTCL FRKELTPSDV GKLNRLVIPK KYAVKYPFI SDDQSEKETS E-----GV
PtRAV4 NFPW---TDI TVQEPKQSY YSIEVLMKI RIGSYQHFKR DFILRISQIV -----ET ALSLKLMPQ SSEGLTCKAL FRKELTPSDV GKLNRLVIPK KYAVKYPFI KALKMRRRL-----
VvRAV-like FWP---SDH SPQEIFQSY YSIEVLMKI RIGSYQHFKR DFILRISQIV -----NYASDEM CEQGISYQL FRKELTPSDV AKHPRLLIPK EYAVKYPFI TGDVESVQL-----
AmRAV-like VSTSEAKAGQ SVQLQLQSR FSLVEILMI KIGSYPMKFN NYLISEVQGI -----SRSPYLQ CALGTGLRLL FRKELTPSDV SKLNRLVIPK KYAVKYPFI SEMEGE-----NGSGT
Consensus .....e..Fg...s..ST..MI..F..TY...l...r..... 131
260
AtTEM1 KGVLINLEDR TGKWRFRYS YWNSDSYVL TKG SRVFKV KNLKAGDVV FERSTGPRQ LYIHWKVR- ----- --SPVQTVR LFGVNIENVE NEK-----PNDVAV
AtRAV2/TEM2 KGVLINLEDR TGKWRFRYS YWNSDSYVL TKG SRVFKV KNLKAGDVV FERSTGPRQ LYIDWKVRSR PR----- -ENPVQVVR LFGVDIFNVE TVK-----PNDVAV
AtRAV1 KGVLINLEDR TGKWRFRYS YWNSDSYVL TKG SRVFKV KNLKAGDVV FERSTGPRQ LYIGWKSRSR -S----- -DLAAGRVL LFGVNIENVE SR-----NDVV-
AtRAV1-like KGMLINLEDR TGKWRFRYS YWNSDSYVL TKG SRVFKV KNLKAGDVV FERSTGPRQ FFIWKSRSR -L----- -DLETGRVM LFGVDIS- -L-----NAVV-
GoRAV-like KGLLLNFEDI GKWWRFRYS YWNSDSYVL TKG SRVFKV KNLKAGDVV FERSTGPRQ LYIDCKARV SVVGVGIGNT YTDNLFIPVR PVVEPVQMR LFGVNLKLP G-----SDGVGG
NtRAV KGVLINLEDR TGKWRFRYS YWNSDSYVL TKG SRVFKV KNLKAGDVV FERSTGPRQ LYIDFKARV TP-----T ISPTVASQV VQVQVQMR LFGVNIENVE AVNNVNNNN NNNNNNMT
AtRAV-like 4EDVEVVFYDR AMRQWFRYS YWNSDSYVL TKG SRVFKV KNLKAGDVV FRTCDVFNV KTLGQKRFN LMI----- DVHCFSDNGS VVAEVSMTV HDSVQVKK-----TENLVS
AtRAV-like 5EDVEVVFYDR AMRQWFRYS YWNSDSYVL TKG SRVFKV KNLKAGDVV FRTCDVFNV KTLGQKRFN LMI----- DVHCFSDNGS VVPEVVKTV HEISDEEMK-----TETLFT
PtRAV4 -----MFYDK DGIPWTFRYS CWSNSDSYVL TKG SRVFKV KNLKAGDVV FRTCDVFNV KTLGQKRFN LMI----- DVHCFSDNGS VVPEVVKTV HEISDEEMK-----TETLFT
VvRAV-like -----MFYDK DGIPWTFRYS CWSNSDSYVL TKG SRVFKV KNLKAGDVV FRTCDVFNV KTLGQKRFN LMI----- DVHCFSDNGS VVPEVVKTV HEISDEEMK-----TETLFT
AmRAV-like QDALEEFDR SMVLMKFRYS FWSNSDSYVL TKG SRVFKV KNLKAGDVV FRTCDVFNV KTLGQKRFN LMI----- DVHCFSDNGS VVPEVVKTV HEISDEEMK-----TETLFT
Consensus .....f.d...g..w.frys yw.ssQSsVF T.GW.rFvke KNL.ag#.l. F.r.....d..... 260
390
AtTEM1 ECYVGGKRSRE DDLFSLG-CS KKQA-I INIL 423
AtRAV2/TEM2 VCGGKRSRDV DDMFALR-CS KKQA-I INAL
AtRAV1 ---GNKRVDN TMLSLV-CS KKQR-I FHAS
AtRAV1-like ---VVKETTE VLMSSLR-C- KKQR-VL
GoRAV-like SCNG--KRKE MDLFTLE-CT KKPK-I GAL
NtRAV SCSGGKRRIE MELLTFESCR KKQRVI INAL
AtRAV-like 4SMLEDKETKS EEN-----K GGFMLFGVRI ECP
AtRAV-like 5SKVEE-ETKS EK-----K GGFMLFGVRI Q
PtRAV4 KNVEEDRMVR ADKPTHDAVK TGFKLPFIQI M
VvRAV-like ADDKEEA ADK-----G FVLPFGVKL G
AmRAV-like KYYGETSENV GNFSVGAEMR KSVRLFGVEI FG
Consensus ...g.k....#. .... k...lfg... 390

```

Figure A. 8 Position of the 9 degenerate primers used to isolate AmTEM.

AtTEM1=Arabidopsis thaliana TEM1 (NP_173927); AtRAV2/TEM2=Arabidopsis thaliana RAV2/TEM2 (NP_564947); AtRAV1=Arabidopsis thaliana RAV1 (NP_172784); AtRAV1-like=Arabidopsis thaliana RAV1-like (NP_189201); AtRAV-like 4=Arabidopsis thaliana RAV-like4 (NP_175483); AtRAV-like 5=Arabidopsis thaliana RAV-like5 (NP_175524); GoRAV-like=Galega orientalis RAV-like (ACI46678); NtRAV=Nicotiana tabacum RAV (ACF74549); PtRAV4=Populus trichocarpa RAV4 (XP_002308395); VvRAV-like=Vitis vinifera RAV-like (XP_002276492); AmRAV-like=Antirrhinum majus RAV-like (AJ800976). Black boxes denote where degenerate primers were designed. Red dotted box delimits the AP2 domain, the green dotted box delimits the B3 domain

Figure A. 9 Sequence of *Antirrhinum TEMPRANILLO* Contig CI.

```
>Antirrhinum majus contig CI
TCGGGACATTCAACGAGGAGTCGGAAGCCGCCAGAGCCTACGACACTGCCGCACAACGGT
TCCGCGGTTCGGGACGCGGTACGAACTTCAAACCTGTTGTTCGGAAACCGGAACACGATGACG
TGGAGGCTTCTTCTTGAATTTCGATTCCTCAAGTCCGAGATCGTGGACATGCTGAGGAAGC
ACACGTACAATGACGAACTCGAGCAGAGCAGGAAGAAGCTTTAGTAACAACAGCGGGGTTA
ATAAATCGTGTCCGTTTCGTTTTGTTCGGGGAGTGC GGATGCGAAGGCGGAGCGCGAGAAC
AGCTTTTTTGAGAAAGCGGTTACTCCGAGCGATGTGGGGAAATTTGAACAGGCTTGTATAC
CGAAGCAACATGCTGAAAAGCATTTTCCGTTACAAAATAATGGGAATAATGGGAATAGTA
GTAGTACGTCGAAGGGTGT TTTGTTGAATTTTGAGGATGTTGGGGGTAAAGTGTGGAGGT
TTAGTACTCGTATTGGAATAGTAGTCAAAGTTACGTGTTAAC
```

Figure A. 10 Sequence of *Olive TEMPRANILLO* isotig13527.

```
>Olea europaea isotig13527 gene=isogroup06587 length=600
numContigs=1
TATTCCAAACAACACGCCGAGAAACACTTCCCTTTAAAAAGTGGGAACAATTCCAAAGG
GGTGC TTTTAAATTTTCGAAAGATATGGGTGGAAAAGTATGGAGATTTTCGATATTCATACTG
GAACAGTAGCCAAAGCTACGTGTTAACAAAAGGATGGAGTAGATTTGTGAAGGAAAAGAA
CTTGAAGGCCGGTGACATTTGTGAGCTTTCAACGATCGACTGGGCCGGACAATCAACTCTA
CATCGACTGGAAACCGAGGAACGGATCAAATGTTGTGGGGCTACCAGTCCC GGCCAGCC
TATTCGATGGTAAGACTATTCGGAGTGAACATATTCGAGGTACCAAGTAATGAAAGTTG
CAGTACTGGAAAAAGGATGAGGGAAAATGGAGCTTTTGGCATTAGAATGTACCAAAAAACA
GAGGTTTATTGATGCTTTGTAACATTTGTATTTTAATAATTTGTTTTTGTGGAGGGGG
AATGTTGTTGTTGCAAGTTGCAAAAAGTTAAATTTGTATAGTTTTTTTTAGTGATTA AATG
CTGAAGAGCTGGAAGTATTAGGTGAGAGAAATATGGAAATACAAAACCTTGTCAATTTGT
```

Figure A. 11 Full nucleotide and amino acid sequences of *Antirrhinum TEMPRANILLO* (*AmTEM*).

```
>AmTEM-like
ATGGACGGAAGCTGCATAGACGAGAGCACGACCAGCTCCGACACCGTCCAGCAGCGACTCCAGCAC
CACAACCTCCCCCTCCCGACAAGCTCTGCCGTGTCGGGAGCGGCACCAGCGTGATCCTCGACGCCGC
AGAATGCGGCGTCGAGGCCGAGTCCCGCAAACCTCCCTCCTCTCGATTCAAAGCGTGGTCCCACAG
CCCAACGGCCGCTGGGGCGCACAGATTTACGAGAAGCACCAGCGCGTGTGGCTCGGAACGTTCAACG
AGGAGTCCGGAAGCCGCCAGAGCCTACGACACTGCCGCACAACGGTTCCGCGGTTCGGGACGCGGTCAC
GAACTTCAAACCTGTTGTTCGAAACCGGAACACGATGACGTGGAGGCTTCTTTCTTGAATTCGCATTC
AAGTCCGAGATCGTGGACATGCTGAGGAAGCACACGTACAATGACGAACTCGAGCAGAGCAGGAAGA
ACTTTAGTAACAACAGCGGGGTTAATAAATCGTGTCCGTTTCGTTTTGTTCGGGGAGTGC GGATGCGAA
GGCGCGAGCGCGAGAACAGCTTTTTTGAGAAAGCGGTTACTCCGAGCGATGTGGGGAAATTTGAACAGG
CTTGTTATACCGAAGCAACATGCTGAAAAGCATTTTCCGTTACAAAATAATGGGAATAATGGGAATA
GTAGTAGTACGTCGAAGGGTGT TTTGTTGAATTTTGAGGATGTTGGGGGTAAAGTGTGGAGGTTTAG
GTACTCGTATTGGAATAGTAGTCAAAGCTATGTGTTGACTAAAAGGTTGGAGCAGATTCGTTAAGGAG
AAGAATCTGAAAGCGGGCGATGTTGTAAC TTTTCAAAGGTCGACTGGGGTCGATAAGCAGCTATACA
TTGATTGGAAAGTGAGGAGTAATGGTAATGGGTTCGGATCAGGTGACCGGGTTAACGGGTTCGGGTTCA
GATGGTGAGGTTGTTTGGTGTGAACATATTTGAGGTGCCAATGAATAATGATGGGAAGAGGATTAGG
GAGATTGAGATGTTAGAATTAGAGTGTAGCAAGAAACAAAGGGTGATTGATGCTTTGTAA
>AmTEM-like
MDGSCIDESTTSSDVTVTATPAPQPPPPDKLCRVSGTSVILDAECCGVEAESRKLPPSRF
KGVVPQPNGRWGAQIYEKQHVWLGTFFNEESEAARAYDTAAQRFRRGRDAVTNFKLLSETEH
DDVEASFLNSHSEIIVDMLRKHTYNDELEQSRKNFSNNSGVNKSFCFVLSGSADAKARAR
EQLFEKAVTPSDVGLNRLVIPKQHAEKHFPLQNNGNNGNSSSTSKGVLLNFEDVGGKVWR
FRYSYWNSSQSYVLTKGWSRFVKEKNLKGADVVTQFQSTGVQDKQLYIDWKVRSNNGSDQV
TGLTGRVQMVRLFGVNI FEVPMNNDGKRIREIEMLELECSKKQRVIDAL
```


Figure A. 12 Full nucleotide and amino acid sequences of olive TEMPRANILLO (OeTEM).

```
>OeTEM-like
ATGGATACTAGTTCAATAGGTGAAAAGCACAAACCAGTGATTCTATATCTATGGCACC AATYT
CCGCCGCCTCGRCTTTGCCGGTGACAAAGTCGCCGGAGAGTCTTTGCCGTGTCGGAAGTGG
CAGCAGTGCATTATAGATGCGGAGGTCCGGTGTGAAGCTGAGTCTAGGAAAGTCCCTTCT
TCAAGATTCAAAGGTGTAGTCCCCAACCTAATGGCAGGTGGGGTGCACAAATCTATGAAA
AGCACCAAAGGGTTTGGTTAGGCACTTTCAATGAAGAAGATGAGGCAGCCAAGGCGTACGA
TATCGCGGCCCAAAGATTTTCGAGGCCGAGATGCAGTCACAACTTTAAACCATTGTTCGGAA
ACTGAAGAAGATGACGTTGAAACAGCCTTCTTGAATTCTCATTTCAAGGCTGAGATTGTTCG
ACATGTTAAGGAAACATACATACAGTGATGAACTCGAACAAAGCAGGAAGAACTACGGCTT
GTTTCGACGGCAGTGGCCAAAGGATCATGAATAAAGACGGCCTTTTCAGCTCATTTGGTGGC
GGCGATAGGGCAGTGAAATCCCGAGAACAGCTCTTCGAGAAGGCGGTAACCTCCTAGCGACG
TGGGGAAGCTCAACCGCCTGGTTATTCCAAAACAACACGCCGAGAAAACACTTCCCTTTAAA
AAGTGGGAACAATTCCAAAGGGGTGCTTTTAAATTTTGAAGATATGGGTGGAAAAGTATGG
AGATTTTCGATATTCATACTGGAACAGTAGCCAAAGCTACGTGTTAACAAAAGGATGGAGTA
GATTTGTGAAGGAAAAGAAGCTTGAAGGCCGGTGACATTGTGAGCTTCAACGATCGACTGG
GCCGGAACAATCAACTCTACATCGACTGGAACCGGAGGAACGATCAAATGTTGTGGGGCTA
CCAGTCCCAGCCAGCCTATTCCGATGGTAAGACTATTTCGGAGTGAACATATTCGAGGTAC
CAAGTAATGAAAGTTGCAGTACTGGAAAAAAAAAAAAAAAAAAAAAAAAAACTTTTGGCATTAGA
ATGTACCAAAAAACAGAGGGTTATTGATGCTTTGTAA
>OeTEM
MDTSSIGESTTSDSISMXPXSAASXLPVTKSPESLCRVGSGSSAIIIDAEVGV EAESRKL PSS
RFKGVVPPQPNGRWGAQIYEKHQRVWLGT FNEEDEAAKAYDIAAQFRFRGRDAVTNFKPLSETE
EDDVETAFLNSHSAEIVDMLRKHTYSDELEQSRKNYGLFDGSGQRIMNKDGLFSSFGGGDR
AVKSREQLFEKAVTPSDVGLNRLV I PKQHA EKHFPLKSGNNSKGVLLNFEDMGGKVWRFRY
SYWNSSQSYVLTKGWSRFVKEKNL KAGDIVSFQRSTGPDNQLYIDWKPRNGSNVVGLPVPAQ
PIPMVRLFGVNI FEVPSNES CSTGKKKKKKKLLALECTKKQRVIDAL
```

Figure A. 13 AmFT nucleotide sequence and TEM putative binding sites.
ATG is marked in red. The TEM putative binding sites, present in 5' UTR region, are highlighted in yellow. In green is highlighted the binding site of CO and the CCAAT-box binding protein.

```
> Antirrhinum majus AmFT (EM:AJ803471)
GAAA CAACATAAC TTGTCCTT CTATATAGTATTTTTCATATAAAAATTATAC
ATTTATATATCTTTCTTATCGTCATTAATTATAATTTAGACAAAAA
ATG CCTAGAGATAGGGATCCACTGGTGGTGGGAAGAGTGATAGGAGAAGT
ATTGGAGCCTTTCACGAGATCAATAGGGCTGAGAGTGATCTATAACAACA
GAGAAGTAAGCAATGGTTGTGATTTAAGGCCCTCTCAAGTTGTCAACCAA
CCTAGGGTTGAGATTGGAGGGGATGATCTCCGCACCTTCTACACTTTGGT
TATGGTGGACCCTGATGCTCCAAGTCTTAGTGACCCGAGTCTTAGGGAAT
ACTTACACTGGTTGGTGACTGATATCCCAGCAACCACCGGAACAACTTC
GGTCAAGAGATTGTGTGTTATGAGAATCCACGGCCGTCGATGGGGATTCA
CCGCTTTGTTTTACACTATTCCGCCAGTTGGGGCGGCAACGGTGTACC
CTCCGGGTTGGCGCCAGAATTTCAACACGAGAGACTTTGCTGAGCTATAC
AACCTTGGCGCCCCAGTTGCTGCTGTCTACTTCAATTGCCAGAGGGAGAG
TGGTACCGGCGGGAGACGACGATAACGTCGAATTCGATCTCAATAATAGA
TCGATAAATAAAAATCATTTGATGGAATGTCAGTTTCGATTTTATCAATA
GTTGATCAAGTAGGAATCTTCATGCTTTG
```

CAACA motif											CACCTG motif														
	-3	-2	-1	1	2	3	4	5	6	7	8	9		-2	-1	1	2	3	4	5	6	7	8	9	10
				C	A	A	C	A					C	A	C	C	T	G							
A	14	16	7	0	47	62	0	69	9	41	34	27	A	22	13	8	40	1	0	0	0	24	12	12	8
C	17	11	14	62	12	4	69	0	7	4	6	9	C	12	15	49	6	56	65	0	0	7	15	14	20
G	12	10	35	0	9	3	0	0	32	4	10	17	G	10	8	1	8	3	0	0	58	19	18	16	5
T	6	14	1	0	0	0	0	0	21	20	19	16	T	18	28	7	11	5	0	65	0	5	9	10	13
total	49	51	57	62	68	69	69	69	69	69	69	69	total	62	64	65	65	65	65	65	58	55	54	52	46
consensus g C a A C A g/t a/t													consensus c a C C T G a/g												

Figure A. 14. Consensus sequences of CAACA and CACCTG motifs deduced from the frequencies of base occurrence at each position. The numbers of sequences with the indicated bases at each position are shown. (Kagaya et al., 1999).

Figure A. 15 *AtCO* nucleotide sequence and putative TEM putative binding sites. ATG is marked in red. The TEM putative binding sites, present in 5' UTR region, are highlighted in yellow.

```

>gi|79327898|ref|NM_001036810.1| Arabidopsis thaliana zinc
finger protein CONSTANS (CO) mRNA, complete cds
AGCTCCCACACCATCAAACCTTACTACATCTGAGTTATTATGTTGAAACAA
GAGAGTAACGACATAGGTAGTGGAGAGAACAACAGGGCACGACCCTGTGA
CACATGCCGGTCAAAACGCCTGCACCGTGTATTGCCATGCAGATTCTGCCT
ACTTGTGCATGAGCTGTGATGCTCAAGTTCCTCTGCCAATCGCGTTGCT
TCCCGCCATAAACGTGTCCGGTCTGCGAGTCATGTGAGCGTGCTCCGGC
TGCTTTTTTGTGTGAGGCAGATGATGCCTCTCTATGCACAGCCTGTGATT
CAGAGGTTTCATTCTGCAAACCCACTTGCTAGACGCCATCAGCGAGTTCCA
ATTCTACCAATTTCTGGAACTCTTTCAGCTCCATGACCACTACTCACCA
CCAAAGCGAGAAAACAATGACCGATCCAGAGAAGAGACTGGTGGTGGATC
AAGAGGAAGGTGAAGAAGGTGATAAGGATGCCAAGGAGGTTGCTTCGTGG
CTGTTCCCTAATTCAGACAAAAATAACAATAACCAAAAACAATGGGTTATT
GTTTAGTGATGAGTATCTAAACCTTGTGGATTACAACCTCGAGTATGGACT
ACAAATTCACAGGTGAATACAGTCAACACCAACAAAACCTGCAGCGTACCA
CAGACGAGCTACGGGGGAGATAGAGTTGTTCCGCTTAAACTTGAAGAATC
AAGGGGCCACCAGTGCCATAACCAACAGAATTTTCAGTTCAATATCAAAAT
ATGGCTCCTCAGGGACTCACTACAACGACAATGGTTCATTAACCATAAC
GTAAGGCTTTTGTATATTTGTTACCCCTTCAATTTAGCATCTTCCATAA
CCACAGGGGTGAATTTCTTTCATCATAACACAAAATCCACTGATCCACTG
CCAACAGTTGATCTATAGCACATAGAAAATTTACCAGAAGTCTATAATAA
AAACAATATATGCTTCCCTTTGTCATCGACTCTCTTTAGTCCCTTACCAG
GGGGATTGAGAATGTCTTTGTTTCTGTCATTAGGCATACATTTTCATCCAT
GGAAACTGGTGTGTGTCGGAGTCAACAGCATGTGTCCACAACAGCTTCAC
ACCCAAGAACGCCAAAGGGACAGTAGAGCAACAACCTGACCTGCAAGC
CAGATGATAACAGTAACACAACCTCAGTCCAATGGACAGAGAAGCCAGGGT
CCTGAGATACAGAGAGAAGAGGAAGACAAGGAAATTTGAGAAGACAATAA
GGTATGCTTCGAGGAAGGCATATGCAGAGATAAGACCGGGTCAATGGC
CGGTTCCGAAAGAGAGAAAATCGAAGCCGAGGAGCAAGGGTCAACACGAT
GCTAATGTACAACACAGGATATGGGATTGTTCCCTTCATTCTGATACTCCT
GTGGCAAAAAGAAAACCTAGATTGCAAGCTGTAAATTAATTTAGTTTGA
GATTATGTTAGGTTTGGTGAAATTTCTAGCTTCAAGAAGTATTACTACTG
TTGTGCAAAATGGGTTTGTAGTTTTGGCTAATTAACCTATAGTATTTCTTC
TTT

```